Master's thesis

NTNU
Norwegian University of Science and Technology
Faculty of Natural Sciences
Department of Materials Science and Engineering

Benjamin Dale Hosum

Reduction Rate of SiMn Slags With Different Carbon Materials

Master's thesis in Materials Science and Engineering

Supervisor: Merete Tangstad, IMA

June 2020

NTNU
Norwegian University of
Science and Technology

Benjamin Dale Hosum

Reduction Rate of SiMn Slags With Different Carbon Materials

Master's thesis in Materials Science and Engineering
Supervisor: Merete Tangstad, IMA
June 2020

Norwegian University of Science and Technology
Faculty of Natural Sciences
Department of Materials Science and Engineering

NTNU
Norwegian University of
Science and Technology

Preface

This master thesis investigates the reduction rate of MnO and SiO_2 from slag from the production of SiMn. The present thesis and experimental work are submitted to the Norwegian University of Science and Technology (NTNU), Department of Materials Science and Engineering spring 2020 and is a part of TMT4920 Materials Technology, Master's Thesis. The work has been funded by SFI Metal Production, a Centre for Research-based Innovation.

First of all, I wish to thank my supervisor Professor Merete Tangstad for all the guidance through this last year. I am very grateful for all the knowledge she has shared and I have learned much about the ferroalloy production, which will definitely be used throughout my carrier after this master's degree. I would also like to thank my co-supervisor Vincent Canaguier (NTNU) for much appreciated assistance and good discussions. In addition, I would also like to thank Leif Sigurd Storlien for his help and many good and helpful pointers on much of the experimental work.

I also wish to thank Sarina Bao (SINTEF) for much appreciated help on the sessile drop furnace. In addition to Ingrid Hansen (SINTEF) which helped by performing the last needed experiments which could not be done by me due to the situation regarding Covid-19. I would also like to thank Morten Peder Raanes for performing the analysis on the EPMA. Finally, I would like to thank Berit Kramer and Ivar Andre Ødegård for training and helping me with equipment and assistance with the experimental work.

My fellow students also needs mentioning for making the last 5 years a time to always remember. Finally, I wish to thank my fiancee Marte for supporting and encouraging me through the ups and downs when writing this thesis.

Benjamin Dale Hosum
Trondheim, June 2020

Abstract

When producing silicomanganese (SiMn) carbon is needed as the reducing agent. In the industry today, a material called coke is mostly used as the carbon source. However, coke comes from fossil sources, and if CO_2-emissions are to be reduced in the future other sources of carbon may be used. For this purpose, charcoal may be a suitable alternative to coke in the process. In this study, the reduction rate of slag from SiMn production is investigated. The difference between coke and charcoal as a reducing agent has been investigated, where the materials have been pelletized with different load. This has been compared to coke and charcoal particles, also called green materials. Lastly, the influence of sulfur in the slag was studied as there was performed experiments with two different slags with and without sulfur.

The coke and charcoal were crushed and then pressed into pellets using a uni-axial press. The load used on the press was 500 kg, 1000 kg and 2000 kg when making the coke/charcoal pellets, where 1000 kg is used on most of the experiments. To make the slag pellets, different oxide powder was mixed and then pressed into a pellet. The experiments are performed in a sessile drop furnace, and after the experiments in the furnace, the samples are analysed in the EPMA. Also, the coke and charcoal materials have been analysed where the porosity and density are analysed. Lastly, the surface roughness of the pellets is analysed.

During the experiments in the sessile drop furnace, there are several photos taken continuously. These pictures are analysed to find the relative volume of the slag droplet throughout the experiment. The wetting angle and contact area between the slag and the substrate are also measured. From the relative volume, there was no significant difference between many of the experiments, except for when charcoal is used with the slag without sulfur. From this combination, there is very little reaction compared to the other combinations, which is coke with and without sulfur and charcoal and slag with sulfur. In materials with sulfur, like e.g. coke, the difference between slags with and without sulfur is not so large. However, for materials almost without sulfur, like charcoal and graphite, very little reduction will occur when the slag is not containing any sulfur. This is both noticed in the chemical analyses, the volume change during the experiment and change in wettability.

From the chemical analysis, the results found from the relative volume and wetting angle was confirmed. There could be seen that there is a very little reduction when charcoal is used with the slag without sulfur. It can also be seen that the slag containing sulfur has in general a higher reduction rate compared to slag without. From these results it can be concluded with that sulfur in a SiMn slag will increase the reduction rate, and especially if charcoal is used as the carbon source. From the experiments with green particles, it was found that there was a higher reduction rate of MnO and SiO_2 for pelletized coke compared to green coke. However, for the experiments with charcoal there could not be found any significant difference in the reduction of MnO, but somewhat more reduced SiO_2 for the pelletized charcoal.

Sammendrag

I produksjonen av silikomangan (SiMn) er det behov for karbon som reduseringsmiddel, og i dagens industri brukes materialet koks for det meste. Koks har opphav fra fossile kilder, og dersom CO_2 utslippet skal reduseres i fremtiden vil det være hensiktsmessig å bruke en annen kilde til karbon. Et alternativ til koks vil være trekull. I denne studien skal reduksjonsraten for slagg fra produksjonen av SiMn undersøkes. Det er undersøkt forskjellene mellom trekull og koks, hvor materialene er pelletert med forskjellig trykk på pressen i tillegg til grønne partikler av materialene. Til slutt ble påvirkningen av svovel i slaggen undersøkt. Det er utført eksperimenter med to forskjellige typer slagg, hvor en inneholder svovel og den andre gjør ikke det.

Gjennom studiet har koks og trekull blitt knust og presset til pellets ved hjelp av en enakset presse. Trykket som ble brukt på pressen var 500 kg, 1000 kg og 2000 kg, hvor 1000 kg ble brukt for de fleste eksperiementene. For å lage slagg-pelletene ble forskjellige oksidpulver blandet sammen og deretter presset sammen til en pellet. Eksperimentene ble gjennomført i en fuktningsovn, og deretter ble prøvene analysert i en EPMA.

Samtidig som eksperimentet i fuktningsovnen pågår, er det et kamera som tar kontinuerlig bilder av prosessen. Bildene har blitt analysert for å finne det relative volumet av slaggen gjennom hele eksperimentet. Fuktningsvinkelen og kontaktflaten mellom slaggen og substratet er også målt. Funnene fra målingene av relativt volum viser til dels mye likheter mellom flere av eksperimentene, sett bort fra der hvor trekull brukes sammen med slagg uten svovel. Ved denne kombinasjonen genereres det lite gass og av den grunn blir det lav reduksjonsrate av oksidene. Denne forskjellen mellom trekull og slagg uten svovel, og i de andre eksperimentene, ble også sett på målingene av fuktningsvinkelen og kontaktflaten mellom substratet og slagg. Omtrent alle eksperimentene hadde en fuktningsvinkel rundt 120° i starten og som avtok over tid. Derimot viste kombinasjonen trekull og slagg uten svovel at vinkelen er omtrentlig konstant gjennom hele eksperimentet.

Den kjemiske analysen gjort på EPMA viser at resultatene sett fra det relative volumet og fuktningsvinkelen ble bekreftet. Analysen viste at det var lite reduksjon av oksider når trekull og slagg uten svovel ble brukt sammenlignet med de andre eksperimentene. Analysen viste også at eksperimentene som ble gjort med slagg som inneholdt svovel hadde generelt en høyere reduksjonsrate sammenlignet med eksperimentene gjort med slagg uten svovel. Videre viser analysen at forskjellen i reduksjonsraten er større for trekull enn koks, om det er svovel i slagget eller ikke. En årsak til det kan være at koks har et høyere askeinnhold, og et høyere innhold av svovel enn trekull. Det vil da være alltid noe svovel til stede i prosessen når koks brukes. Med disse resultatene kan det konkluderes med at svovel i slagg fra produksjonen av SiMn vil øke reduksjonshastigheten av MnO og SiO_2, og spesielt dersom trekull brukes som karbonkilde. Fra eksperimentene med grønne materialer ble det funnet at reduksjonsraten av MnO og SiO_2 er høyere for pelletert koks sammenlignet med grønn koks. Det var også ingen signifikante forskjeller på reduksjonen av MnO for eksperimentene med grønt trekull, men en høyere reduksjonsrate av SiO_2 ble funnet for pelletert trekull sammenlignet med grønn trekull.

Contents

List of Figures

List of Tables

1 Introduction

In the last several years the problems regarding the climate and global warming has been a large issue and talking point for different industries, scientists/researcher and people in general. This is a problem that needs to be solved, and somewhat quickly. Furthermore, this is something (almost) every country agrees on and in 2015 the Paris Agreement was signed by almost 200 countries around the world. The aim of the Paris Agreement is to limit the rise in temperature to below 2 °C at the end of this century, compared to pre-industrial times. The agreement requires that all countries put their best effort in reducing emissions [1, 2].

In Norway, around 70 % of all emissions comes from burning of fossil fuel and cement production. The largest onshore industry in Norway is the metal production industry. Hence, this industry is a large contributor to these emissions. When producing metals (and alloys) large quantities of energy and raw material is needed. When producing ferroalloys, carbon is needed as the reducing agent and coke is largely used as the source of carbon. The problem with this is that carbon comes from coal, which is a fossil source. If the ferroalloy industry are going to reduce emissions the use of fossil sources must be removed or limited. This entails that other sources of carbon can/must be used. Green carbon/biocarbon/charcoal may be a good alternative instead of coke [3].

If coke is to be substituted with charcoal, more knowledge is needed on how charcoal interacts with slag from the silicomanganese process. In this study the differences between coke and charcoal is to be investigated in a sessile drop furnace. One main advantage with this furnace is that there is a camera taking continuously pictures of the process. From these pictures the slag droplet is analysed, where the relative volume, wetting angle and contact area between the slag and substrate will be measured. It is important to understand how the slag interacts with the different carbon materials. Another aspect of this study is to investigate how the addition of sulfur in a slag from the SiMn process would affect the reduction rate of MnO and SiO_2. Two different slags will be made, where one contains sulfur and one does not, and the other compounds will be the same in both slags. After the experiments in the furnace, the samples will be analysed in an EPMA, so that the chemical composition can be found to see if any reduction has occured. The carbon pellets itself will also be further investigated where the porosity and density is analysed, in addition to the surface roughness of the carbon pellets. The main objective of this thesis is to investigate the differences between coke and charcoal, and how these materials interacts with a slag from the SiMn production. The reduction of MnO and SiO_2 is focused on in this study, and the amount reduced of these oxides will be compared if coke or charcoal is used as the carbon source (substrate) and if the slag contains sulfur or not.

1.1 Manganese ferroalloys

Manganese (Mn) ferroalloys are produced by a carbothermic reduction of manganese ores. The reduction occurs in a submerged arc furnace (SAF). Electric furnaces are typically circular and have three electrodes, which are connected to a separate electrical phase. There are many different types of manganese ferroalloys, and they vary in composition.

The main elements are Mn, iron (Fe), carbon (C) and silicon (Si). The two most common alloys are ferromanganese (FeMn) and silicomanganese (SiMn). These two are generally divided by the silicon content. FeMn has less than 2 % Si (but most often less than 0.5 %) and SiMn has typically between 16-30 % Si. These two alloys can again be divided into more alloys dependent on the carbon content, which can be seen in Figure 1.1 [4, 5, 6].

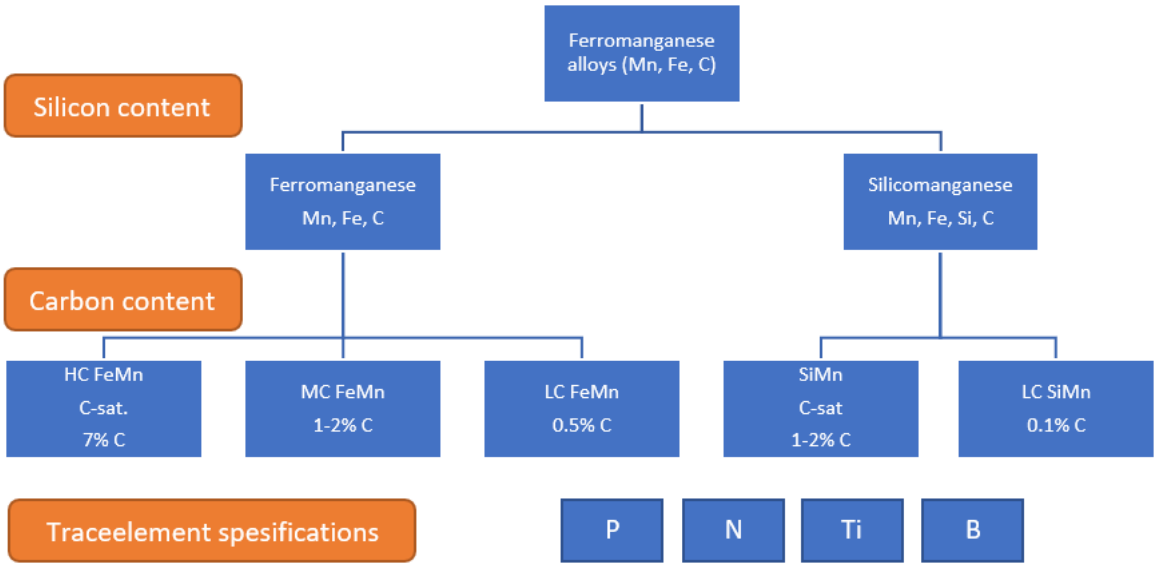

Figure 1.1: Overview of the manganese ferroalloys (after [4])

The production of FeMn are quite similar to the production of SiMn but one does not need quartz as a raw material and the temperatures are about 200 °C lower [7]. Since the goal of this project is the investigation of SiMn slag, only the SiMn process will be described in the following chapters.

1.1.1 Production of silicomanganese

As mentioned earlier, SiMn are produced in a submerged arc furnace (SAF). The furnace is normally circular with three electrodes inside. The electrodes are submerged into to the raw materials, and the tip of the electrode is in a bed of carbon materials, which consists mostly of coke, i.e. coke bed. Heat will be generated from the resistivity in the coke bed, which will melt and reduce the oxides into liquid metal. Figure 1.2 shows a sketch of a SAF. The figure shows that the raw materials enter from the top and the liquid alloy is tapped from the bottom. Furthermore, it shows clearly a coke bed around the electrode and the raw materials being reduced as they descend in the furnace [4, 5, 6].

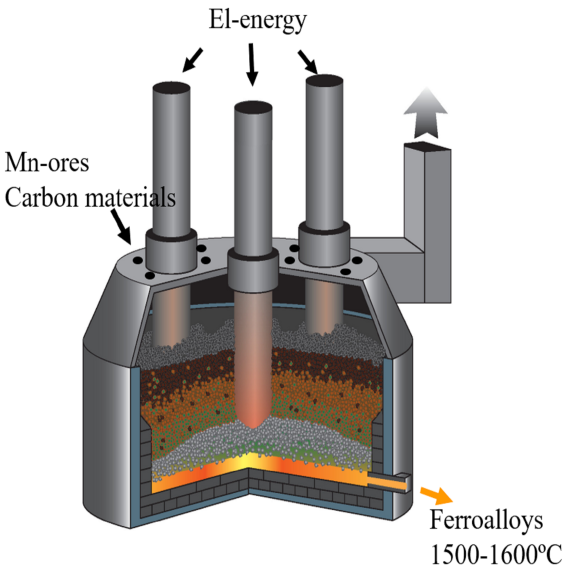

Figure 1.2: Sketch of a submerged arc furnace [8]

In addition to ore, quartz and carbon materials there is also fluxes in the raw materials mix. Fluxes are oxides which will end up in the slag phase. The fluxes that are normally used in the production of SiMn are limestone ($CaCO_3$) and dolomite ($(Mg,Ca)CO_3$). Fluxes are added to improve the physical properties of the slag phase [6]. Slag can also be used as a raw material for the SiMn production. Slag from the FeMn production has a high concentration of MnO, and can therefore be used in the SiMn process. The production of FeMn and SiMn can therefore be seen as a duplex process. Furthermore, the mixture of different raw materials is used to obtain the wanted composition of the alloy [5].

As mentioned, the raw materials enter the furnace at the top and the temperature will be low and the materials will be in its solid form. When the materials descend further down in the furnace they will be reduced (and heated) with CO gas. The reactions are shown in Figure 1.3. The furnace can be divided into two main zones; the pre-reduction zone and the coke bed zone. They can also be termed the low temperature zone and high temperature zone. The green line in Figure 1.3 separates the pre-reduction zone and the coke bed zone. Inside the furnace the coke bed starts at approximately the tip of the electrodes. It can be added more or less coke in the charge to increase or decrease the size of the coke bed. Two of the most important tasks of the coke bed is that it is the reducing agent, and also the heating element. It is generated heat when the electric current runs through the coke bed and then ohmic energy will be produced. Hence, the coke bed will then determine the energy and temperature distribution in the furnace. The parameters of the coke bed will therefore influence the production rate, quality of product and the stability of the process in general. It is hence crucial to control the addition and consumption of carbon, and is one of the most important tasks for the operator controlling the furnace [5].

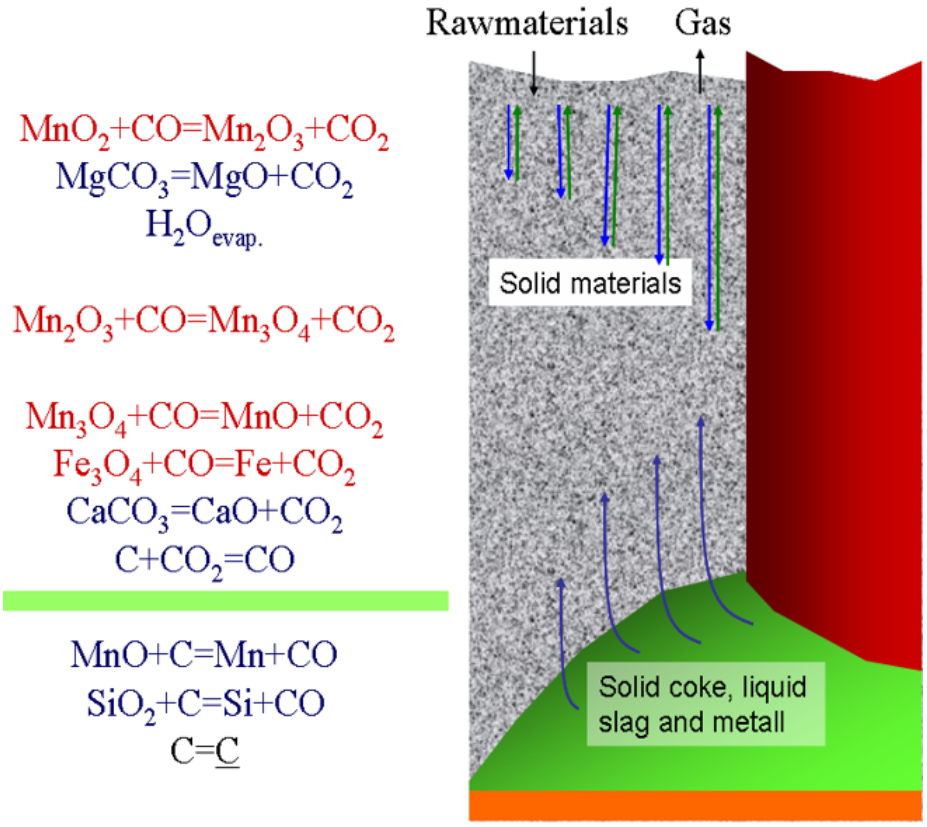

Figure 1.3: Sketch of mass transfer and chemical reactions inside the furnace. The blue reactions are endothermic and the red reactions are exothermic. The green line separates the pre-reduction zone and the coke bed zone [5].

As seen in Figure 1.3, the raw materials (MnO_2) and the flux is added at the top and is reduced by CO gas. MnO_2 are first reduced to Mn_2O_3 from Equation 1. Equation 2 and 3 shows the different Mn-oxides being reduced to MnO [5].

$$MnO_2 + {}^1/_2\,CO \rightleftharpoons {}^1/_2\,Mn_2O_3 + {}^1/_2\,CO_2 \qquad \Delta H^o_{298} = -99.9\,\text{kJ} \tag{1}$$

$${}^1/_2\,Mn_2O_3 + {}^1/_6\,CO \rightleftharpoons {}^1/_3\,Mn_3O_4 + {}^1/_6\,CO_2 \qquad \Delta H^o_{298} = -31.3\,\text{kJ} \tag{2}$$

$${}^1/_3\,Mn_3O_4 + {}^1/_3\,CO \rightleftharpoons MnO + {}^1/_3\,CO_2 \qquad \Delta H^o_{298} = -16.9\,\text{kJ} \tag{3}$$

These reactions occur in the pre-reduction zone in the furnace. There are also some other reactions occurring in the pre-reduction zone, such as the decomposition of the fluxes, reduction of iron oxide to metallic iron and evaporation of water to vapour. These reactions are endothermic (except reduction of iron oxides), and are given in Equation 4, 5, 6 and 7. The fact that vaporization of water is an endothermic reaction states that the raw materials entering the furnace should contain as little water or moisture as possible, so that it is not used more energy in the process than necessary [5].

$$MgCO_3 \rightleftharpoons MgO + CO_2 \qquad \Delta H^o_{298} = 101.1\,\text{kJ} \tag{4}$$

$$CaCO_3 \rightleftharpoons CaO + CO_2 \qquad \Delta H^o_{298} = 178.3\,\text{kJ} \tag{5}$$

$$^1/_2\,Fe_2O_3 + {}^3/_2\,CO \rightleftharpoons Fe + {}^3/_2\,CO_2 \qquad \Delta H^o_{298} = -12.9\,kJ \tag{6}$$

$$H_2O\,(l) \rightleftharpoons H_2O\,(g) \qquad \Delta H^o_{298} = 44.0\,kJ \tag{7}$$

In the coke bed zone the the liquid metal is produced. In this area the temperature is the highest. The reactions are given in Equation 8 and 9. These reactions are highly endothermic (especially reduction of silica). From the metal forming reactions the CO-gas is formed, which will rise up inside the furnace and then reduce the oxides in the pre-reduction zone [5].

$$MnO + C \rightleftharpoons Mn\,(l) + CO \qquad \Delta H^o_{298} = 252.3\,kJ \tag{8}$$

$$SiO_2 + 2\,C \rightleftharpoons Si\,(l) + 2\,CO \qquad \Delta H^o_{298} = 754.9\,kJ \tag{9}$$

Equations 8 and 9 can be called the metal forming reactions, and these equations is what produces the desired product. Furthermore, it is desirable to produce as much product, in this case SiMn, and to use as little as possible of energy and raw materials. Hence, it is imperative to understand what parameters that influence these reactions. In Chapter 2 a literature study will be performed where some research on parameters affecting the SiMn production is discussed.

2 Literature

When producing SiMn it is important to understand which parameters that will affect the process, and in what way. In the following chapters, the carbon materials will first be discussed before the thermodynamics and kinetics will be presented. Carbon is a complex material with many different properties, it is therefore important to understand how these properties influence the process. It is important to know the kinetics of this process as this process in general does not reach equilibrium. The kinetics can be determined by the distance from equilibrium, hence it is also important to know the thermodynamics of the process.

2.1 Carbon materials

When producing SiMn carbon is needed as the reducing agent. Carbon can be both as a solid and as a gas in the form of carbon monoxide (CO). The main source of carbon material in the SiMn production is coke, but other sources of carbon can also be utilized, such as anthracite and petroleum coke. Charcoal can also be used as the source of carbon, and Brazil has a long tradition of using charcoal in the production of SiMn [5]. Brazil is the largest producer of charcoal in the world (in 2017), but some countries in Africa also produces quite a lot of charcoal [9]. Furthermore, charcoal produced in the country is sometimes more economically viable compared to importing other carbonaceous materials such as coke [10].

As mentioned above, coke is the main source of carbon used in the production of SiMn. Coke has many properties which makes it very suitable for this process, such as the content of volatiles, ash content and moisture. Coke also has high compressive strength, even after heated, which is a desirable property, due to the fact that it forms a coke bed in the bottom of the furnace. Another important property is that the CO_2-reactivity for coke is low according to the Boudouard reaction (given in Equation 10). As seen from the equation, solid carbon reacts with CO_2 gas and forms CO gas. Hence, this reaction will be decisive of the total consumption of carbon. It will also influence the energy use in the process as the reaction between carbon and CO_2 is endothermic. Furthermore, the Boudouard reaction is an unwanted reaction as it consumes carbon and increases the use of energy [5, 11].

$$CO_2\,(g) + C\,(s) \rightleftharpoons 2\,CO\,(g) \tag{10}$$

Coke is made in a process called coking. In this process, coal is heated in the absence of air, in that way the volatiles are expelled. There are two different types of coking; low-temperature coking and high-temperature coking. The low-temperature coking is around 500 °C and the product from this is called char. Char is rich in hydrogen and hydrocarbons and is mostly used in Si/FeSi production. High-temperature coking is around 1000 °C. From this metallurgical coke is produced and this is further used in the SiMn production [12].

As mentioned above, coke is made from coal, which is a fossil source. The use of fossil sources has to be reduced now and in the future, hence other sources of carbon in the production of SiMn could help reduce the emissions. Charcoal is a "green" source of

carbon that could lower the CO_2 emissions from the process.

Coke and charcoal have different properties, and Table 2.1 shows the typical mechanical and physical properties for coke and charcoal for use in the SiMn/FeMn production. From the table, it can be seen that there are some major differences between the two materials. Charcoal has a lower content of fixed carbon and a much higher content of volatile matter, but the amount of ash is lower in charcoal compared to coke. The composition of ash in charcoal is strongly dependent on which type of tree and on the soil where the tree has grown. Coke has a higher compressive strength than charcoal, although, the compressive strength depends on which type of tree and also on fibre direction for charcoal. In general, the properties of charcoal is dependent on what type of tree is used, where geographically the tree has grown and on the soil. Furthermore, coke has lower electrical resistance and higher volume weight [10].

Table 2.1: Typical properties of coke and charcoal for SiMn and FeMn production [10].

	Charcoal	Coke
Fixed carbon (%)	65-85	86-88
Volatile matter (%)	15-35	≤ 1
Ashes (%)	0.4-4	10-12
Ash composition: (%)		
SiO_2	5-25	25-55
Fe_2O_3	1-13	5-45
Al_2O_3	2-12	13-30
P_2O_5	4-12	0.4-0.8
CaO	20-60	3-6
MgO	5-12	1-5
K_2O	7-35	1-4
Compressive strength (kg/cm^2)	10-80	130-160
Volume weight (kg/m^3)	180-350	500-550
Electrical resistance (ohm m)	High	Low
CO_2-Reactivity (AC-method)	3-4	0.1
CO_2-reactivity	Medium-High	Low-medium

Charcoal is made by pyrolysis, which typically occurs in large kilns or retorts. There are many different methods and concepts for making charcoal. From this process, there are by-products, such as pyroligneous liquid and volatile matter. However, different methods will have different yields of these products. There are three types of heating used to initiate the carbonization of the wood and to maintain this high temperature; internal heating, external heating and heating with recirculated gas. Internal heating is when some of the raw material is burnt, with controlled air-flow. External heating is when the retort is heated from the outside, where no oxygen or gas can enter the reactor. Lastly, when heating with recirculated gas, part of the pyroligneous vapours are burnt in a combustion chamber, where the heat is directed into the reactor [13].

If charcoal is going to replace coke as the reducing agent in the production of SiMn, the differences between coke and charcoal and on how the properties of charcoal influ-

ences the process must be investigated. For the production of ferroalloys in general, the most important properties for the reducing agent are high reactivity, high conversion and low level of impurities (especially sulfur and phosphorous). It is also important that the ash content is low, as each additional percentage of ash will increase the volume of the slag by 10-15 kg per ton of alloy, which will increase the energy needed for the process [14].

There have been performed several studies on the carbon materials used in the SiMn production, due to the fact that the carbon materials is a very important parameter. In this report mostly studies with charcoal and comparisons between charcoal and coke will be mentioned.

To investigate the use of charcoal industrially there have been performed experiments in pilot-scale furnaces. This was done by **Monsen et al.** (2004), where SiMn was reduced using charcoal as the reducing agent. In the experiments, SiMn were reduced in five furnaces with three different reducing agents with a difference in CO_2 reactivity. As was mentioned earlier, the CO_2-reactivity is of importance for the carbon material used in the process. As mentioned earlier, the Boudouard reaction is not wanted in this process, as it will increase both the energy and carbon consumption [10, 15]. The CO_2-reactivity found by **Monsen et al.** (2004) is shown in Figure 2.1, where it can be seen that there is a significant difference between the different materials. Coke has a low CO_2-reactivity while charcoal has a higher reactivity. Furthermore, there is also a difference between the different types of charcoal used, i.e. what type of tree it is from. Lastly, if the charcoal is impregnated with potassium, this will increase the CO_2-reactivity significantly [10].

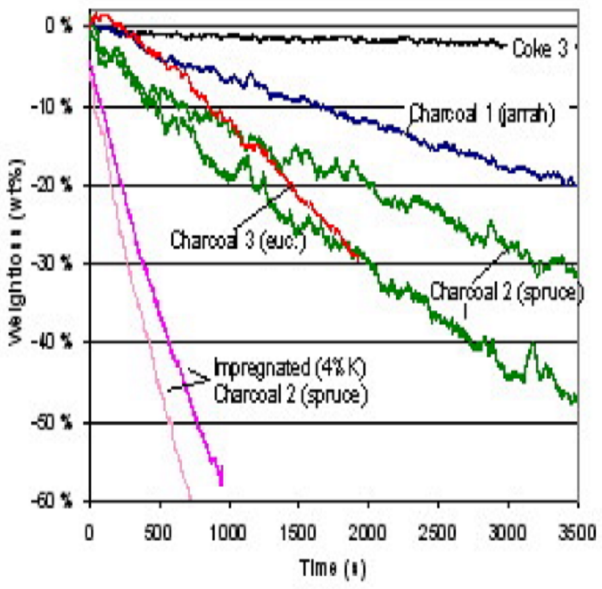

Figure 2.1: CO_2-reactivity of coke, charcoal and K-impregnated charcoal [10].

There have also been performed experiments on measuring the CO_2-reactivity by **Monsen et al.** (2007) [15]. Figure 2.2 shows the CO_2-reactivity for Brazilian charcoal, charcoal from preserved wood and some different metallurgical cokes. From this figure, it can be seen that the CO_2-reactivity for charcoal is significantly higher compared to the cokes.

Charcoal from preserved wood also has a higher CO_2-reactivity compared to Brazilian charcoal [15].

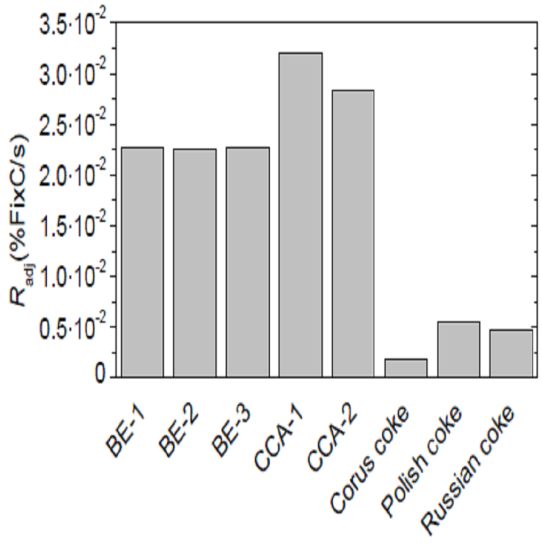

Figure 2.2: CO_2-reactivity at 1060 °C of Brazilian charcoals made from eucalyptus, charcoal made from preserved wood and different metallurgical cokes [15].

There are several important parameters that need to be investigated if charcoal is to be used as the main source of carbon in the production of SiMn. Abrasion strength is such a parameter that is important. **Monsen et al.** (2007) studied the thermal abrasion strength with CO_2 reactivity, the resistance in the coke bed and slag reactivity. The abrasion strength states something about the materials ability to withstand abrasion under the pressure of the charge. In this study, the abrasion test is performed by tumbling partly reacted material for 30 minutes at 40 rpm, and then analysing the size distribution after [15].

Figure 2.3 shows the abrasion strength for Brazilian charcoal, charcoal from preserved wood and different metallurgical cokes. The cohesion index (C.I) is the materials ability to maintain its strength (cohesion) after reaction with the gas from the furnace and the ability to not create fines. In the figure, the cohesion index is the fraction that has a larger size than 4.75 mm before tumbling. The thermal stability index (T.I.3) is measured after tumbling and says something about the materials ability to resist abrasion from the other particles under the pressure of the charge. In the figure, the thermal stability index is given by the fraction larger than 3.33 mm after tumbling. A high number is preferred for both the cohesion index and the thermal stability index. From the figure, it can be seen that charcoal from Brazil has a much lower cohesion index and thermal stability index compared to the other materials. Furthermore, the charcoal from preserved wood has approximately the same values for both the cohesion index and the thermal stability index as the different cokes [15].

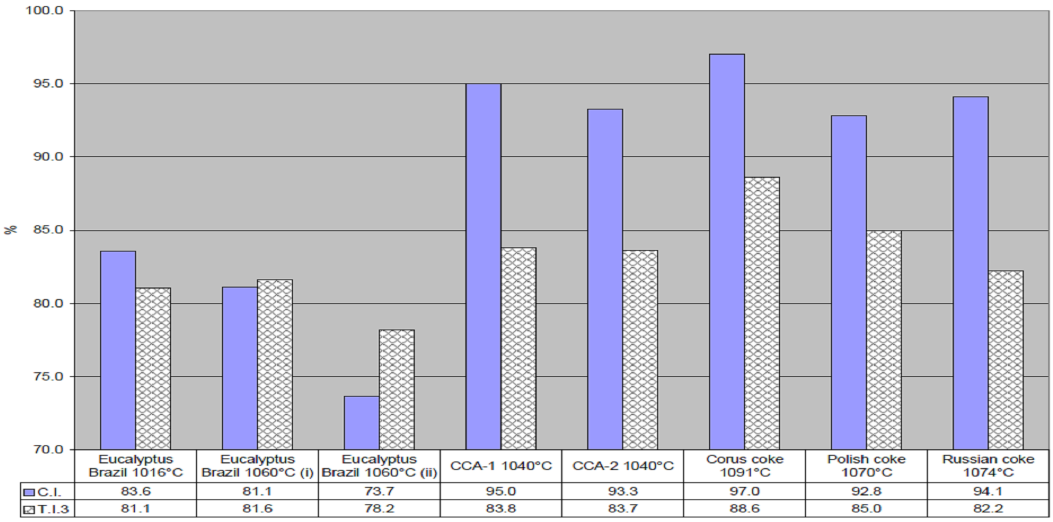

	Eucalyptus Brazil 1016°C	Eucalyptus Brazil 1060°C (i)	Eucalyptus Brazil 1060°C (ii)	CCA-1 1040°C	CCA-2 1040°C	Corus coke 1091°C	Polish coke 1070°C	Russian coke 1074°C
C.I.	83.6	81.1	73.7	95.0	93.3	97.0	92.8	94.1
T.I.3	81.1	81.6	78.2	83.8	83.7	88.6	85.0	82.2

Figure 2.3: Abrasion strength (C.I and T.I.3) for Brazilian charcoal, charcoal from preserved wood and different metallurgical cokes. C.I=Fraction larger than 4.75 mm before tumbling. T.I.3=Fraction larger than 3.33 mm after tumbling [15].

Another important parameter to be investigated is the electrical resistivity of the material, due to the fact that the resistivity in the coke bed is crucial for the whole production of manganese ferroalloys. It was found that charcoal has higher electrical resistivity compared to coke. Figure 2.4 shows the electrical resistivity as a function of temperature, where in general the resistivity decreases with increasing temperature. It can also be seen that the resistivity decreases with increasing particle size. Figure 2.5 shows the electrical resistivity for different carbon materials. From the figure, it can be seen that for temperatures up to 1300 °C the resistivity for charcoal is significantly higher compared to metallurgical coke. However, for temperatures over 1300 °C the resistivity is approximately the same for charcoal and metallurgical coke, or it could also be somewhat higher depending on the particle size [15].

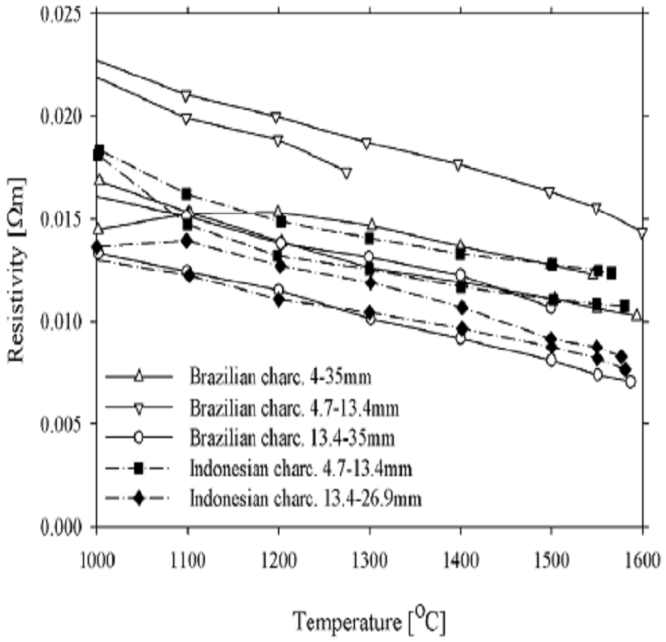

Figure 2.4: Electrical resistivity for charcoal with different particle size as a function of temperature [15].

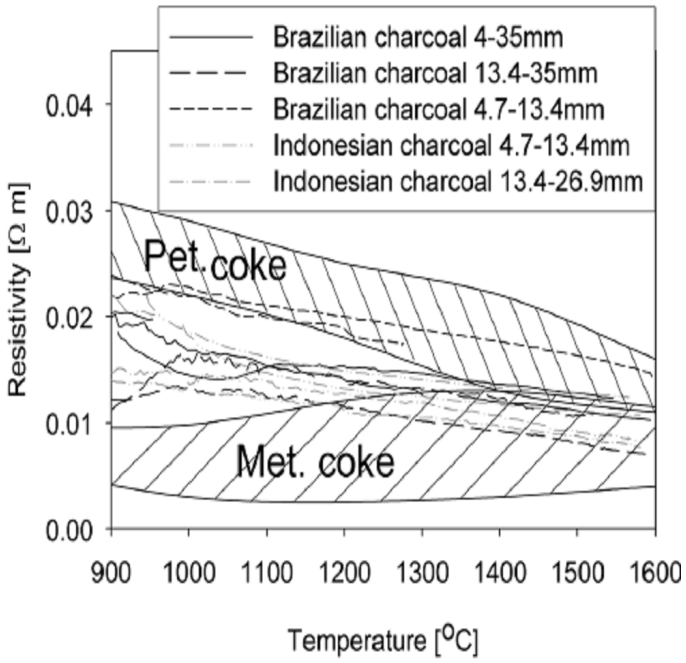

Figure 2.5: Comparison of the electrical resistivity for different carbonaceous materials [15].

The wettability between the carbon material and the slag is also of importance, where if there is a different wettability between two materials this may influence the reactivity. **Jayakumari and Tangstad** (2015) investigated different carbon materials with different size affected the reduction temperature and reduction behaviour of MnO containing slags. It was used an open induction furnace to study the melting and reduction of the

materials. Four different types of coke and anthracite were used in the experiment. It was observed that smaller coke gives a higher flow into the coke bed or the same flow as usual but at lower temperatures. This can be explained by the higher reduction rate of smaller coke. In this experiment, anthracite showed the highest reduction rate. The wettability of the different carbon materials was also investigated, which will be further discussed in Chapter 2.4. The coke which had the highest wettability had an increased reaction rate and flow compared to the other cokes [16].

Above some of the differences between coke and charcoal has been seen. However, there are many different types of charcoal and ways of producing charcoal, as could for example be seen in Figure 2.1 where different types of wood had different CO_2-reactivity. If charcoal is to replace coke as the main source of carbon, one needs to identify a suitable type of charcoal and means of manufacturing this. The properties of the charcoal will depend on what type of tree is used, the geographic location where the tree grows and on the soil. Hence, the knowledge on how the relationship between these parameters and the variables in the production of charcoal needs to be investigated [5, 10, 17].

One of the most important properties for reducing agent when producing ferroalloys, in general, is the content of ash. Each additional percentage of ash will increase the volume of slag with around 10-15 kg per ton of ferroalloy. Furthermore, with an increased amount of slag the energy needed will hence increase [17]. As seen in Table 2.1 the content of ash is lower for charcoal than for coke, which could make it suitable for the production of ferroalloys [10].

Both the chemical and physical properties of wood depend on the structure (e.g. grain deviation and knots) and environment of the three growth (e.g. moisture and temperature). Many of the physical properties of the wood, such as shrinkage, moisture content, density and permeability are affected by the chemical composition. It has also been found that the distribution of various minerals has significant variations between the different parts of the tree, which can be seen in Figure 2.6 where the density and porosity of the different parts are given. From the figure, it can be seen that there is a difference between the bark, needles and the branches, although the difference is not large [17, 18].

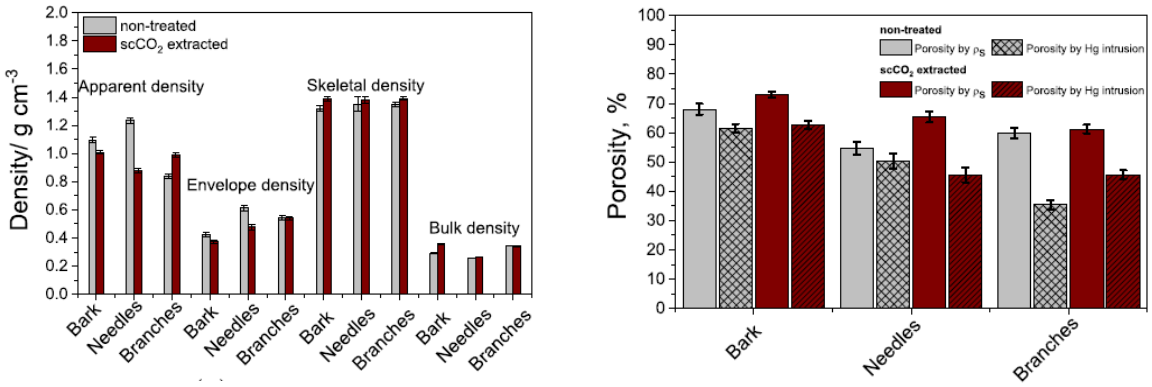

(a) Density *(b) Porosity*

Figure 2.6: Apparent, envelope, skeletal and bulk density and the porosity of the different parts of the tree [17].

Surup et al. (2020) investigated the effect on the wood composition and supercritical CO_2 extraction on charcoal production used on the ferroalloy industry. Using supercritical extraction has been shown to improve various properties of the wood and the charcoal. It was found in this study that with a pretreatment using supercritical CO_2 extraction of the wood will enable removal of many value added compounds. Furthermore, it will not have any significant influence on the physical properties of the wood [18].

Surup et al. (2019) studied the characterization and reactivity of charcoal from high-temperature pyrolysis. Previous studies have found that biocarbon/charcoal has higher reactivity than coke. However, if a reductant with higher reactivity than coke is to be used industrially it may have an impact on the process, such as increase maintenance cost because of a decrease in electrical conductivity. Hence, the reactivity of charcoal is a parameter that must be investigated and understood [14].

Porosity is a parameter that will influence the reactivity of the material. If the porosity increases the reactivity will increase. There is a wide variety of different types of wood and there are many parameters that will affect the physical and chemical properties of wood. The different types of wood can often be divided into hardwood and softwood. Some types of hardwood are birch, oak and eucalyptus, and types of softwood are spruce and pine. In general, charcoal from hardwood is less porous than charcoal from softwood. The porosity and pore size are given in Table 2.2. From the table, it can be seen that spruce has a higher porosity than oak, met. coke and activated charcoal have the lowest porosity. It also is seen that the porosity of spruce increases with increasing temperature in the pyrolysis. This is caused by the removal of volatiles from the pores. In contrast to this, the porosity of oak decreases with increasing temperature. This is probably caused by the high content of alkali metals in the oak. The porosity was decreased to such an extent that the active surface also decreased with increasing temperature [14].

Table 2.2: Porosity and pore size of charcoal from Norway spruce (Pieca abies) and sessile oak (Quercus petraea), metallurgical coke and activated charcoal [14].

Parameter	Spruce			Oak			Met. coke	Activated charcoal
	800 °C	1200 °C	1600 °C	800 °C	1200 °C	1600 °C		
Mercury intrusion porosimetry								
Porosity by Hg intrusion (%)	70	74.5	78.8	61.5	58.2	47.2	39.7	14
Porosity by skeleton density (%)	78.5	81.4	79.5	68.5	60.5	65.5	47.8	33
Inaccessible porosity (%)	8.8	7	0.6	7.1	2.2	18.2	8.1	20
Macropores (%)	93	95	93	60.3	57	57	87	97
Mesopores (%)	6	4	6	16.7	20	20	10	3
Micropores (%)	1	1	1	23	23	23	3	0
Total pore surface area (m^2/g)	11.4	11.8	10.7	57.3	69.8	65.3	5.9	0.2
Average pore diameter (µm)	0.7	0.9	1	0.1	0.1	0.1	0.3	2.3
Median pore diameter (µm)	6.9	7.7	6.9	1.1	0.9	0.9	16.2	21.8
N_2 adsorption								
BET surface area (m^2/g)	196	97.2	3	495	80	80	2.8	0.3
Pore size (nm)	0.6	0.7	1.3	0.6	0.7	0.9	0.9	0.9

The pore size is separated into three categories: micropores (1.8-80 nm), mesopores (80-500 nm) and macropores (0.5-58 µm). Both spruce and oak had a high ratio of macropores, especially spruce. This also corresponds to the total pore area, as the pores of spruce are smaller than oak. From this, it can be concluded with that the pore size distribution and area of pores are mainly determined by the feedstock and less on the heat treatment [14].

One of the main issues regarding charcoal is its mechanical strength, which is a problem in the production of manganese ferroalloys due to the fact the carbon material makes a coke bed in the bottom of the furnace. Hence, there will be much weight on top of the material. One method of improving the mechanical strength of charcoal is through pelletization. However, the properties of the pellet can be influenced by the feedstock, the particle size and the pelletization process itself [17].

Riva et al. (2019) analysed the optimal pressure, temperature and binder quantity in a biocarbon pellet, where it is to be used as a substitute for coke. According to **Riva et al.** there is very little (if any) research regarding the optimization of the pelletizing parameters. There are many parameters that will influence the quality of the pellet.

Hence, optimizing this process is not straight forward. The parameters investigated in this study was: compressive strength, mechanical durability and thermal strength [19].

To make charcoal the wood went through pyrolysis. The products from the pyrolysis were 28 wt% biocarbon, 26 wt% pyrolysis oil and 46 wt% pyrolysis gas. The characterization of the biocarbon and pyrolysis oil is given in Table 2.3. As can be seen from the table, biocarbon has a high content of fixed carbon and low moisture content [19].

Table 2.3: Characterization of biocarbon and pyrolysis oil [19]

Parameter	Biocarbon	Pyrolysis oil
Moisture [%wb]	0.86 ± 0.03	87.2 ± 2.5
Volatiles [%db]	7.55 ± 0.9	96.85 ± 2.0
Ash [%db]	4.22 ± 0.8	0.43 ± 0.2
Fixed C [%db]	88.23 ± 2.1	2.73 ± 0.5
C [%db]	90.2 ± 1.8	56.21 ± 1.3
H [%db]	1.3 ± 0.2	6.30 ± 0.85
N [%db]	0.11 ± 0.01	0.15 ± 0.04
O [%db]	8.39 ± 0.31	25.30 ± 0.25

There has also been performed a statistical analysis. The results from the statistical analysis have a good affinity to experimental data. Furthermore, the results from the analysis gave the following results: mechanical durability of 81,7 %, compressive strength of 0.44 MPa and thermal strength of 1.18 MPa. The pellets that were tested had an oil content of 33.9 %, pelletizing temperature at 60 °C and pressure at 116 MPa. It was found that the pelletizing pressure had little effect on the results although, the pelletizing temperature had a higher impact on the results and the oil content the biggest impact [19].

The yield from the pyrolysis shows that there is produced enough oil to be used as the binder. Furthermore, it was observed that the oil will penetrate the porous structure of the biocarbon easily, drastically decreasing the porosity of the biocarbon. Other binders can also be used such as sawdust, lignin and other materials. The water content will also greatly influence the quality of the final pellet [19].

The proposed methodology for biocarbon pellet production from this study is pyrolysis at 600 °C, densification with pyrolysis oil as a binder and reheating the pellet. This method has several advantages, such as using pyrolysis oil as a binder. The oil provides the needed water content and also increases the oxygenated compounds in the pellet. It has been investigated that oxygen-containing groups have an influence on the compressive strength, because of the formation of hydrogen bonds. Furthermore, the reheating will cause an increase in the amount of fixed carbon, and also a decrease in porosity due to the polymerization of the oil. It is also an advantage to utilize by-products from the process (i.e. using pyrolysis oil) instead of e.g. lignin, sawdust or starch. This will hence reduce the cost of the production [19].

Surup et al. (2020) studied the effect of operating conditions and feedstock composition of charcoal pellets to be used in ferroalloy industries. In this study two different types of

wood were chosen, Norway spruce (*Picea abies*) and sessile oak (*Quercus petraea*). The spruce is a type of softwood, and the oak is a type of hardwood. The characterization of these two types of wood is given in Table 2.4 [17]

Table 2.4: Characterization of Norway spruce and oak [17].

Parameter	Norway spruce	Oak	Activated charcoal [14]	Metallurgical coke [20]
Moisture [%wb]	8.6	7.6	3.8	0.6
Ash [%db] (at 550 °C)	0.8	1.6	8.6	11.8
Volatiles [wt% db]	80.6	82.6	10.3	3
Fixed carbon content [%db]	18.6	15.8	81.1	85.2
Ultimate analysis [%db]				
C	53.2	50.6	82.6	85.6
H	6.1	6.1	1.5	0.3
N	0.1	0.2	0.8	1.8
S	0.06	0.02	0.9	0.6
Cl	0.04	0.02	0.02	0.03
Ash compositional analysis (mg/kg on dry basis)				
Al	40	20	4500	12000
Ca	2300	3600	4900	6400
Fe	200	50	3700	6300
K	800	1500	1900	1700
Mg	250	300	850	1300
Na	<50	<50	1100	1100
P	200	250	400	400
Si	550	550	31000	27000
Ti	50	50	200	550

The pellets were made with tar as a binder and water. There were 30 wt% tar and 10 wt% water. It was also made two different types of composite pellets, one with 46 wt% high purity Mn ore and one with 30 wt% microsilica particles. The experiments showed that the solid yields were 5-55% greater when using original charcoal pellets compared to composite pellet. In general, the findings in this study emphasized the idea that pellets made from biocarbon can be used in the production of ferroalloys [17].

Surup et al. (2019) studied the characterization of the renewable reductants and charcoal-based pellets for the productions of ferroalloys. The impact of heat-treatment temperature and also secondary heat-treatment was investigated. The characterization of the charcoal and metallurgical coke is given in Table 2.4 [20].

The product yields from the pyrolysis are of importance as these by-products are often (or should be) used for other purposes. Figure 2.7 shows the product yield as a function

of treatment temperature for oak and spruce. The two types are similar, but spruce has higher water content and oak has a higher ash content. With increasing temperature, the yield of biochar decreases, but in general, there is not much difference in the yield for both feedstocks [20].

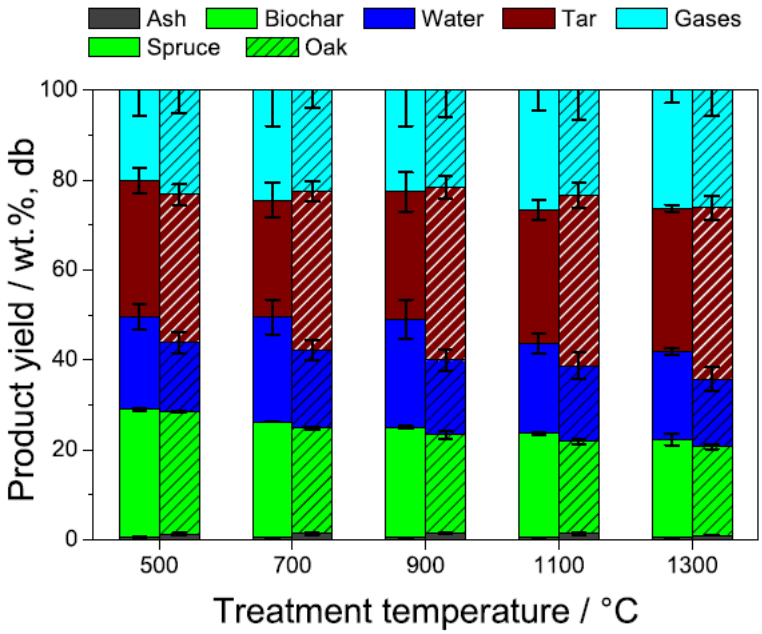

Figure 2.7: Product yields of tar and char of spruce (left) and oak (right) reacted at 500-1300 °C. The yield of tar is separated into organic fractions and water content and the char yield is separated into organic matters and ash [20]

Figure 2.8 shows the yield after a secondary heat treatment. The ash content is somewhat the same for both feedstocks. The amount of volatile matter is much higher for the primary pyrolysis than for the secondary heat treatment. Furthermore, the fixed carbon content is the highest when the secondary heat treatment is done at 700 °C and then decreases with increasing temperature [20].

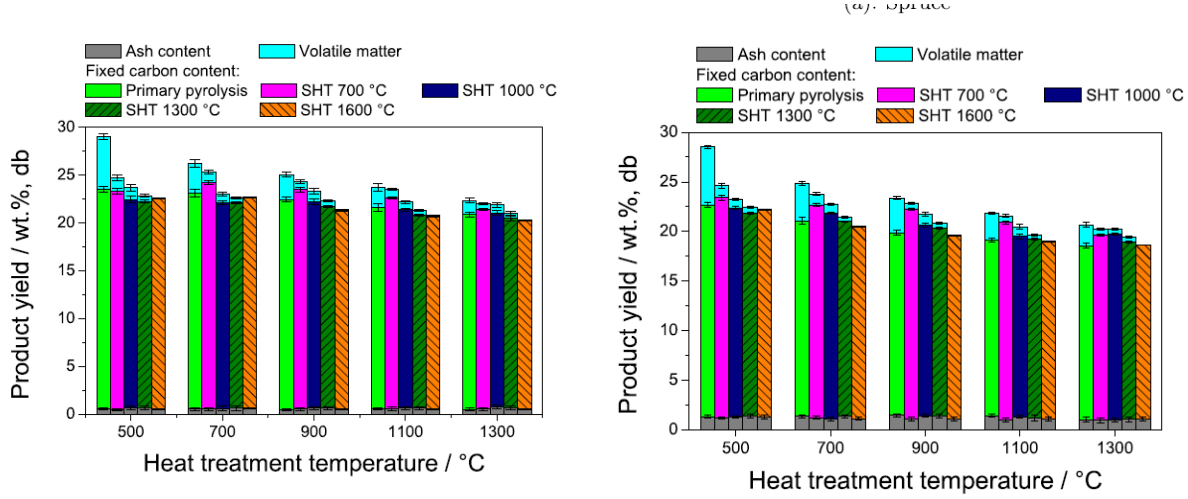

(a) Spruce

(b) Oak

Figure 2.8: Char yields of spruce and oak after secondary heat treatment at 700, 1000, 1300 and 1600 °C. Total yield is separated in ash, fixed carbon and volatile matter [20]

It was found that an increase in heat treatment temperature would improve the hardness of the charcoal pellet during pyrolysis. The heat treatment and the use of tar as a binder would also increase the electrical resistivity of the charcoal pellets. The conclusion of this study states that the yield of char depends mainly on the temperature in the primary heat treatment, and less the origin of the feedstock and the secondary heat treatment. It was also performed a co-pyrolysis of charcoal with recirculated tar and distillation, which increased the char yield [20].

Today, there are no obvious benefits for why SiMn producers in Norway, or Europe for that matter, should replace coke with charcoal. Coke has many good properties such as higher carbon content, high mechanical strength and low CO_2 reactivity. There is also a lack of charcoal producers in Europe, which will entail that it needs to be imported. A good reason to use charcoal is the environmental aspect. As stated in Chapter 1, coke comes from fossil sources, but charcoal is a renewable source. This could mean that if charcoal was used instead of coke, the CO_2 emissions would be lowered.

2.2 Thermodynamics

The production of SiMn is a complex process, and as stated earlier, the kinetics of the process needs to be understood to understand the process. The kinetics is found by the distance from the equilibrium, hence the thermodynamics must also be understood. Manganese alloys have a similarity to iron, as it creates several stable oxides and carbides. The oxides formed from the ores and the other raw materials will end up in the slag phase.

The main components in slag from the SiMn process is MnO, SiO_2, CaO, MgO and Al_2O_3. It is assumed that there are not any iron-oxides in the slag from this process since it will be reduced in the pre-reduction zone, according to Equation 6, and will, therefore, go into the alloy [21]. The binary phase diagram of MnO and SiO_2 is given in Figure 2.9, where the MnO/SiO_2 ratio is given for FeMn (blue) and SiMn (red) slags. As seen in the

figure SiMn slags will begin to be liquid between around 1250-1350 °C, depending on the amount of SiO_2 in the slag [5].

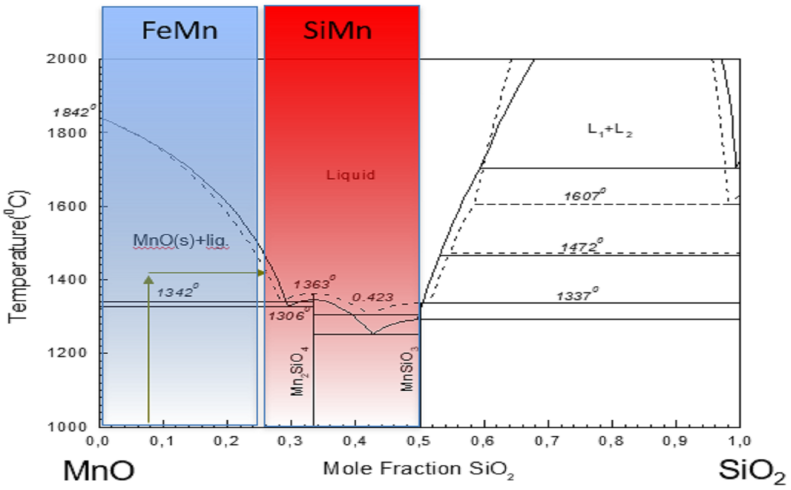

Figure 2.9: MnO and SiO2 phase diagram. The red and blue areas are approximate MnO/SiO_2 ratios for FeMn and SiMn slags [21].

The distribution of Mn and Si in the slag is important since the slag in the SiMn process is considered a waste product. Therefore, minimizing the amount of Mn in the slag as MnO is an important goal in the production process. The relation of Mn and Si at equilibrium in the slag phase can be described by Equations 8 and 9. From this the equilibrium constant can be found, given by Equation 11 and 12 [5, 21].

$$K_{MnO} = \frac{a_{Mn} \cdot p_{CO}}{a_{MnO} \cdot a_C} \tag{11}$$

$$K_{SiO_2} = \frac{a_{Si} \cdot p_{CO}^2}{a_{SiO_2} \cdot a_C^2} \tag{12}$$

Since the reactions occur on the coke bed, the activity of carbon can be assumed to be 1. The partial pressure of CO can also be assumed to be 1 because it is low into the furnace and the temperature is too high for any CO_2 to be present. The reactions for the equilibrium constant can hence be simplified into Equation 13 and 14 [5].

$$a_{Mn} = K_{MnO} \cdot a_{MnO} \tag{13}$$

$$a_{Si} = K_{SiO_2} \cdot a_{SiO_2} \tag{14}$$

If the content of silicon is above 17 wt% the stable phase is SiC and not carbon (graphite). Furthermore, when the content of silicon is above 17 wt% the reduction of silicon is given in Equation 15, which has the equilibrium constant given in Equation 16 [5].

$$SiO_2(l) + SiC(s) \rightleftharpoons 3\,Si(l) + 2\,CO(g) \tag{15}$$

$$K_{II,SiO_2} = \frac{a_{Si}^3 \cdot p_{CO}^2}{a_{SiO_2} \cdot a_{SiC}^2} \tag{16}$$

This means that if the content of silicon is under 17 wt% graphite is stable according to Equation 14, and if it is above 17 wt% Si, silicon carbide is stable according to Equation 17.

$$a_{Si} = \sqrt[3]{K_{II,SiO_2} \cdot a_{SiO_2}} \tag{17}$$

This states that the share of Mn and Si in the slag is dependent on the composition of MnO and SiO_2 which influences the activity. However, the activity of MnO and SiO_2 is also dependent on the composition of the slag, i.e. the amount of MgO, CaO and Al_2O_3. It is also temperature dependent since the equilibrium constant is very temperature dependent [5, 21].

The content of Si at equilibrium has been calculated in a Mn7Fe-Si-C_{sat} alloy, where the activity of SiO_2 in the slag has been assumed to be 1 or 0.2, and the total gas pressure is 1 atmosphere. The total gas pressure is given by p_{CO}, p_{SiO} and p_{Mn}, but at temperatures up to 1650 °C the pressure of SiO and Mn are quite moderate. Hence, the pressure of CO can be assumed to be almost 1 atmosphere. This is shown in Figure 2.10. From this figure, it can be seen that when the slag is saturated with SiO_2 or has an activity of 0.2, the Si content in the metal increases. To achieve a Si concentration of for example 20 wt% in the metal the temperature would need to be around 1640 °C when the activity of SiO_2 is 0.2. When the slag is SiO_2 saturated the temperature is over 100 °C lower. Another parameter that will influence the amount of Si in the alloy is the ratio between manganese and iron. The effect of the Mn/Fe ratio is given in Figure 2.11, where it can be seen that if the Mn/Fe ratio increases the amount of Si in the alloy will increase. The amount of Si in the alloy can also be influenced by the pressure of CO. If the pressure of CO gas is reduced to 0.33 atm the concentration of Si will increase, as shown in Figure 2.12 [5, 22].

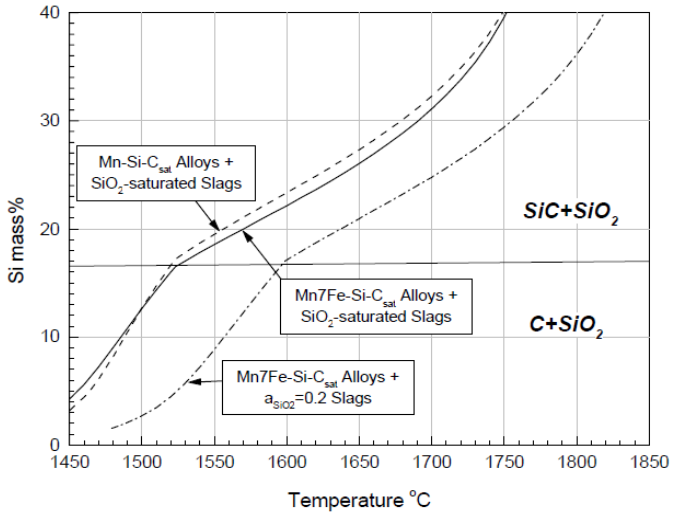

Figure 2.10: Calculated Si content vs. temperature in equilibrium at 1 atmosphere pressure, for two different alloys, Mn-Si-C_{sat} and Mn7Fe-Si-C_{sat} [22].

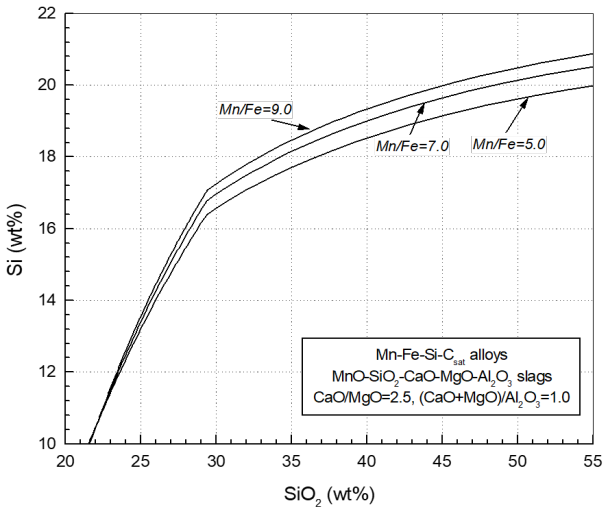

Figure 2.11: Distribution of Si the slag and the alloys depending the ratio between Mn and Fe. Temperature is 1600 °C and the pressure of CO is 1 atmosphere [5].

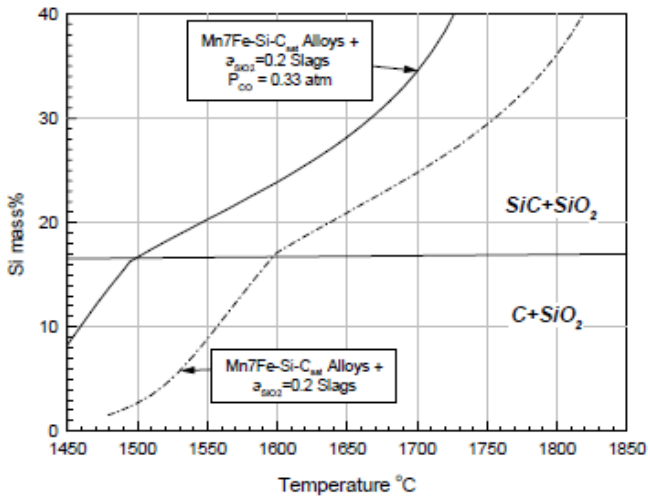

Figure 2.12: The effect of temperature and pressure on the Si content [22].

The Si in the metal and the MnO content in the slag is also very dependent on the slag composition. Figure 2.13 shows that at equilibrium the concentration of MnO in the slag should be below 10 wt% When producing SiMn it is important to have control over the composition of the slag, as this will influence the composition of the alloy. The R-ratio is important in SiMn production as it is very dependent on the concentration of Si in the alloy, as can be seen in Figure 2.14. From the figure, it can be seen that with an increasing R-ratio the amount of SiO_2 in the slag will increase. The R-ratio is given in Equation 18 [7].

$$R = \frac{\%CaO + \%MgO}{\%Al_2O_3} \tag{18}$$

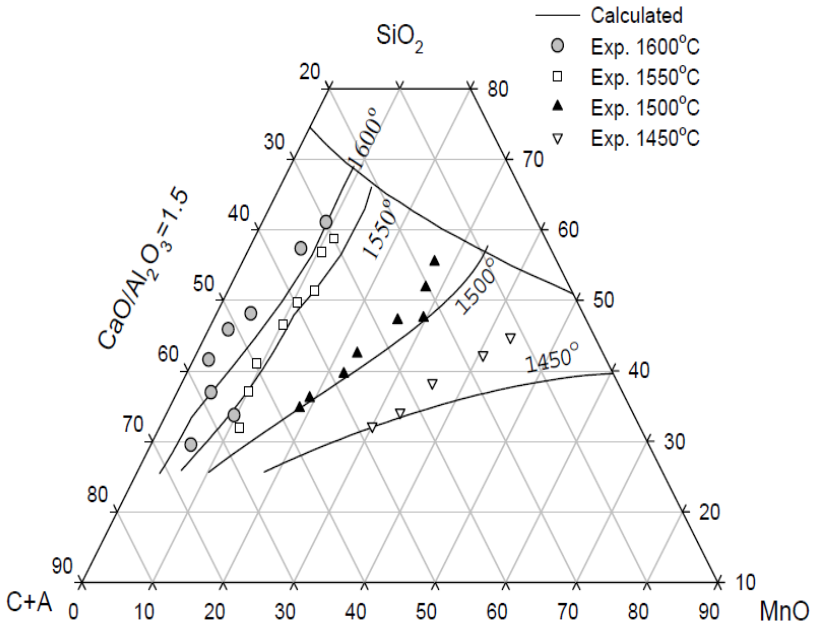

Figure 2.13: Equilibrium composition of SiMn slag at 1450 °C, 1500 °C, 1550 °C and 1600 °C. The ratio between CaO and Al_2O_3 is fixed at 1.5 [22]

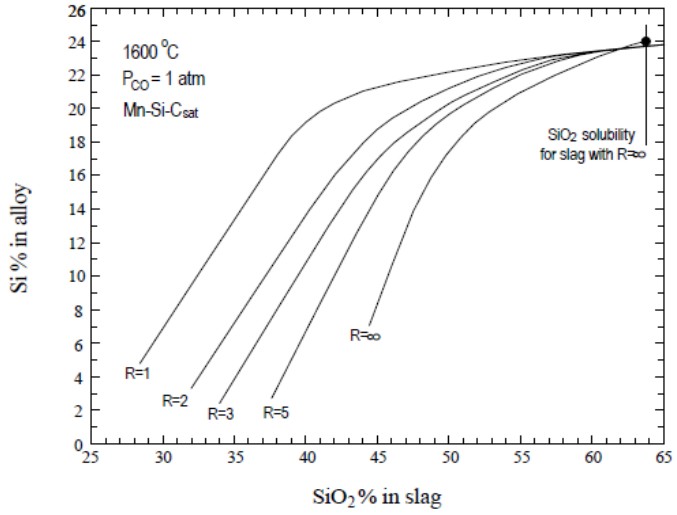

Figure 2.14: Silicon distribution as a function of the R-ratio [7].

When reducing manganese slags the amount of Mn and Fe in the metal phase can vary. **Tangstad** (1996) found that the larger metal particles (>1000 µm) are always found of the surface of the slag phase. The medium sized particles (>100 µm) are in the liquid phase area, and the smallest particles (>10 µm) are found in the solid MnO area. It was found that the Mn/Fe ratio is higher in the biggest particles, as seen in Figure 2.15 [23].

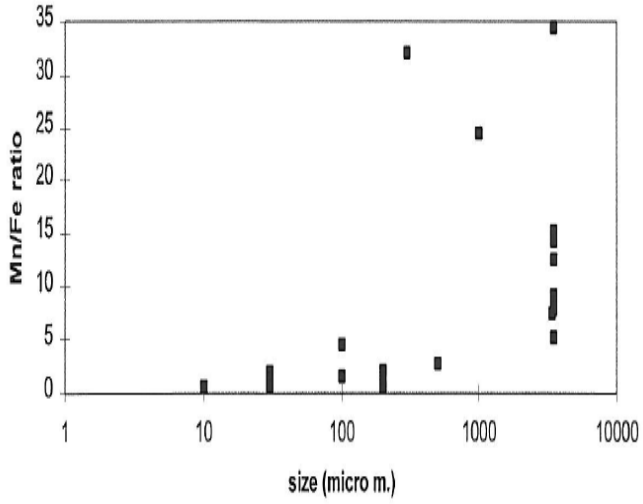

Figure 2.15: Size of the metal particles as a function of the Mn/Fe ratio [23]

Ding and Olsen (2000) investigated Mn and Si distribution in the slag and metal in SiMn production. The understanding of the thermodynamics in this process is essential to understand the composition of the metal and slag. Figure 2.16 shows the equilibrium relations between a MnO-SiO_2-CaO-Al_2O_3-MgO slags and Mn-Fe(10%)-Si-C_{sat} alloy. Furthermore, the state of equilibrium is very dependent on the temperature of the system [24].

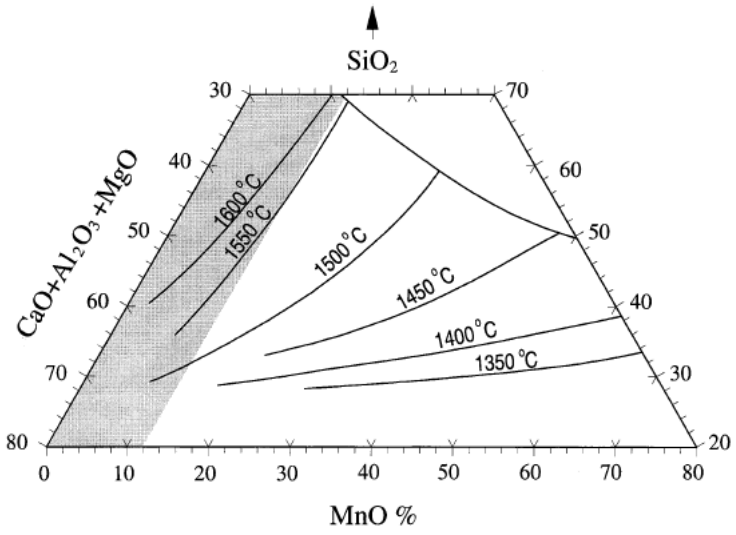

Figure 2.16: Equilibrium composition for SiMn slags at different temperatures for MnO-SiO_2-CaO-Al_2O_3-MgO slags and Mn-Fe(10%)-Si-C_{sat} alloys. CaO/Al_2O_3=1.5 and MgO/Al_2O_3=0.8. The pressure is P_{CO}=1 atm. The shaded area is of interest in this study [24].

The result of a typical slag/metal/gas equilibrium is shown in Figure 2.17. The ratio between CaO/Al_2O_3 is 4. It can be seen that there is a minimum of MnO in the slag when the content of SiO_2 is 44 %. Figure 2.18 shows that the curves at equilibrium changes with the R-ratio. Hence, the R-ratio has a significant effect on the distribution of Mn and Si in the metal and slag [24].

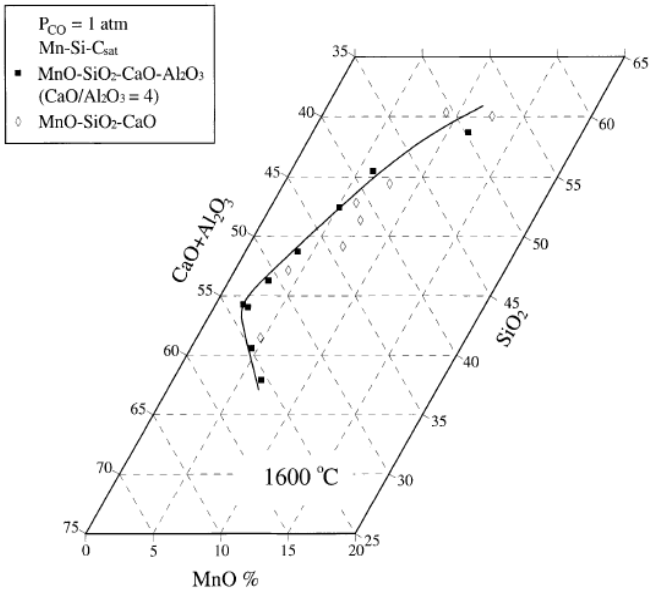

Figure 2.17: Equilibrium compositions of slag MnO-SiO_2-CaO-Al_2O_3. CaO/Al_2O_3=4 at 1600 °C [24]

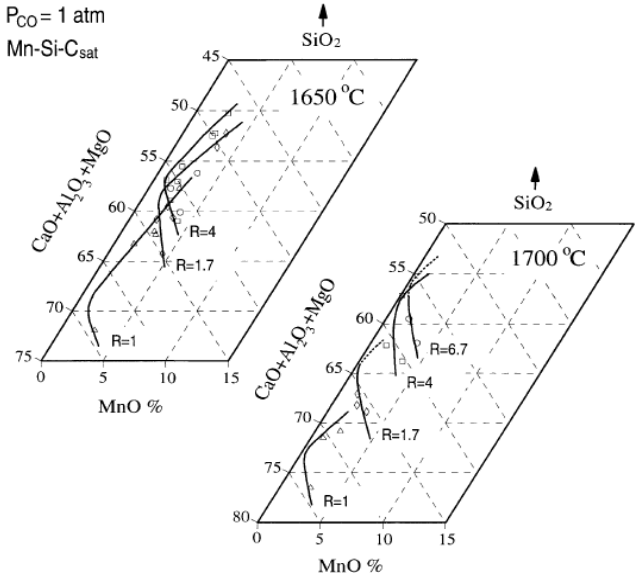

Figure 2.18: Equilibrium compositions for MnO-SiO_2-CaO-Al_2O_3 slags with different R-ratios [24].

Figure 2.19 shows the distribution of Si between a saturated Mn-Si-C alloys and MnO-SiO_2-CaO-Al_2O_3 slags. The figure shows that with increasing temperature the MnO in the slag decreases. It can also be seen that with increasing temperature the amount of Si in the alloy will increase, for example at 40 % SiO_2 in the slag the amount of Si in the alloy will increase from 7 % to 19 % when the temperature increases 100 °C. The distribution of Si is also dependent on other slag compositions and the R-ratio, which could be seen in Figure 2.14 [24].

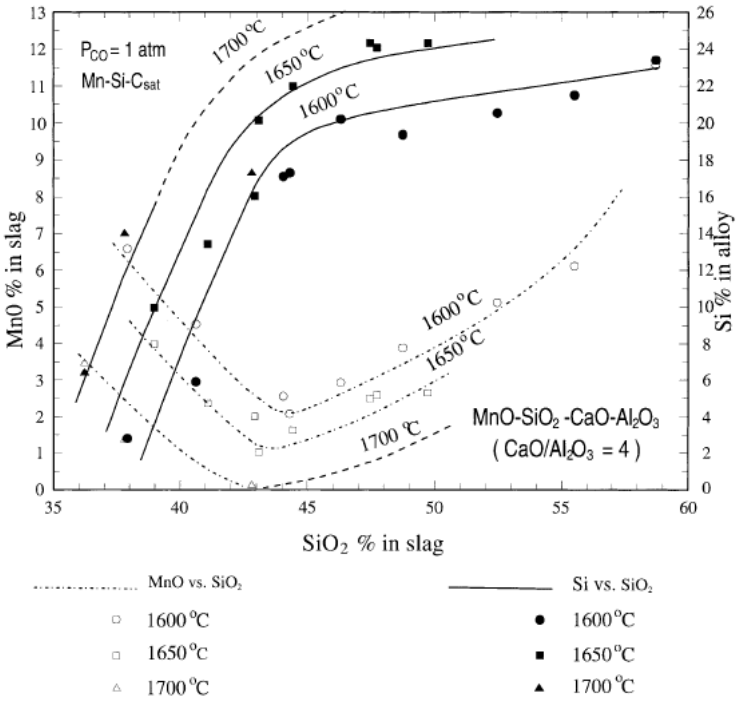

Figure 2.19: Equilibrium compositions for MnO-SiO_2-CaO-Al_2O_3 slags. The ratio between CaO/Al_2O_3 is 4. The temperatures are 1600 °C, 1650 °C and 1700 °C [24].

This study concludes with that the content of MnO in SiMn slag depends first of all on the temperature and then on the SiO_2 content in the slag. Furthermore, the content of MnO in the slag is also dependent on whether the slag is acidic or basic and the addition of Al_2O_3. If Al_2O_3 is added to an acid slag the MnO content will be reduced and if Al_2O_3 is added to basic slag the amount of MnO in the slag will increase. The change between acid and basic slag is when the content of SiO_2 is around 45 %. Furthermore, since a typical slag from the SiMn has a lower SiO_2 content than that, that entails that the effect of Al_2O_3 will decrease the equilibrium content of MnO in the slag. The compositions of Si in the alloy is determined by the temperature, SiO_2 content in slag and the R-ratio. As was seen in Figure 2.19 the effect of temperature is significant.

2.3 Kinetics

In the following chapter, the kinetics regarding the reduction of FeMn and SiMn will be discussed. The thermodynamics only describes the composition at the end, i.e. when it reaches equilibrium, and does not give any information on how fast the reaction(s) occur. When reducing MnO it has been assumed that the chemical reaction limits the reduction rate. Reduction from MnO to liquid metal is given in Equation 8. Since this is an endothermic reaction with a strong influence of temperature, the rate mechanism can be given in Equation 19 [5, 25, 26].

$$r_{MnO} = \frac{-dm_{MnO}}{dt} = k_{MnO} \cdot A \cdot (a_{MnO} - a_{MnO,eq}) = kA\left(a_{MnO} - \frac{a_{Mn}p_{CO}}{K}\right) \qquad (19)$$

The rate constant is given in Equation 20, which is an Arrhenius equation [5, 12].

$$k_{MnO} = k_{0,MnO} \cdot e^{-\frac{E_{MnO}}{RT}} \tag{20}$$

r_{MnO} is the rate of MnO reduction, k_{MnO} is the rate constant of MnO reduction, A is the reduction area, a_{MnO} is the activity of MnO, $a_{MnO,eq}$ is the activity of MnO at equilibrium $k_{0,MnO}$ is the pre-exponential constant of MnO reduction, E_{MnO} is the activation energy of MnO reduction, R is the gas constant and T is the temperature [5, 12].

The driving force for the reduction of MnO can be seen from Equation 19, where the difference from the actual MnO activity and equilibrium activity in the slag. Reduction of MnO is happening in two stages. First, in a two-phase area (MnO(s) + liquid) as can be seen from Figure 2.20. The second stage consists of a homogeneous liquid. The reduction rate is fast in the two-phase area and it will be almost constant until all the solid MnO is consumed, which can be seen in Figure 2.21. The main reduction will take place in the two-phase area. Furthermore, the reduction will decrease rapidly with increasing reduction [5, 27].

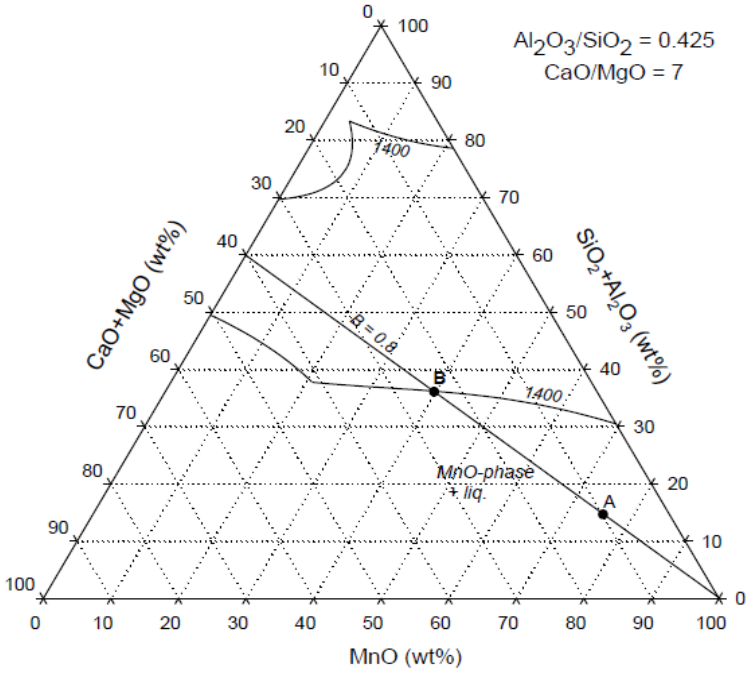

Figure 2.20: The two phase reduction from A to B, and followed by the liquid phase reduction from B [5].

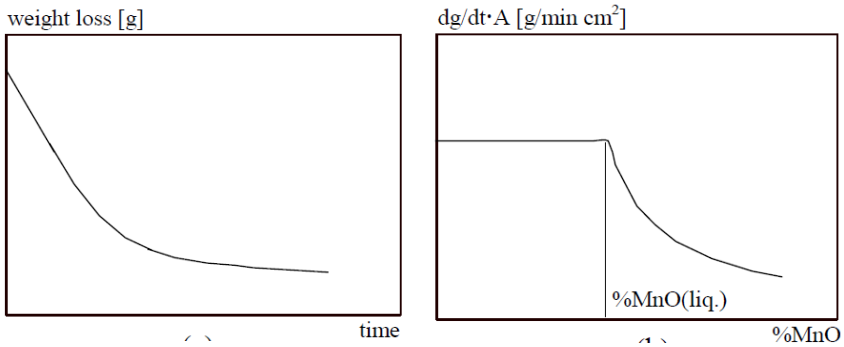

(a) Weight loss over time *(b) Reduction rate vs %MnO*

Figure 2.21: The reduction rate of MnO [5].

2.3.1 Experimental procedures

There are many different methods of measuring or investigating the different parameters that will affect the process. **Safarian and Tangstad** (2010) investigated different methods for establishing a slag-carbon reactivity test. The techniques that were used are thermogravimetery, ASEA induction furnace and sessile drop furnace. The results from thermogravimetery showed that for 1600 °C the reaction rates were equal, but when the materials were calcined at 1200 °C there was a faster weight loss for coke than for charcoal. With this technique, there were some difficulties when preparing crucibles from carbonaceous materials. In the experiments, it was used a MnO saturated slag from the FeMn production, which was investigated in the sessile drop furnace [28].

Table 2.5 shows some of the properties of the carbon materials used in this study. It can be seen that coke has a higher ash content, lower content of volatile matter and is more porous than charcoal. Furthermore, the amount of sulfur is also much higher in the coke than charcoal.

Table 2.5: Properties of coke and charcoal used as the substrates in this study [28]

Property	Polish industrial coke	Eucalyptus charcoal
Fixed C (%)	88.88	81.3
Ash (wt%)	9.5	0.43
Volatile matter (wt%)	1.32	18.3
Total porosity (%)	42.9	27.4
S content (ppm)	5600	20

Figure 2.22 shows the results in volume ($V_s/V_{s,i}$) change for coke and charcoal from the experiments in the sessile drop furnace. The figure indicates that the slag carbon reactivity is higher for the coke substrate than the charcoal [28].

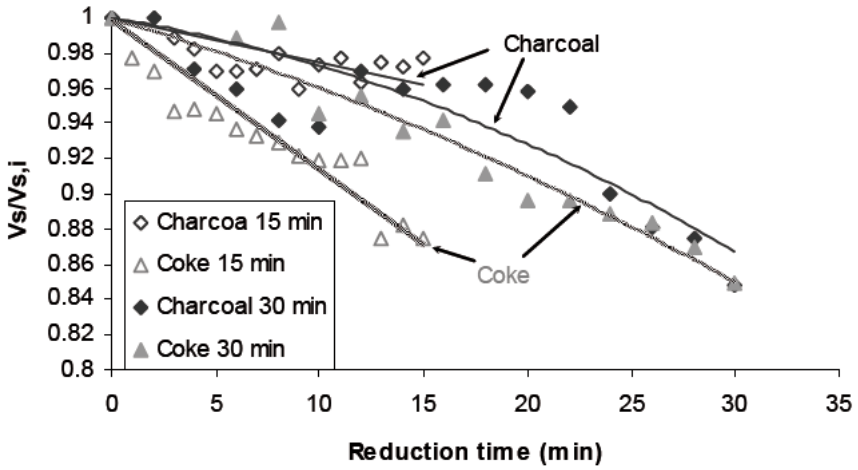

Figure 2.22: Changes in normalized volume of slag droplet by different carbon substrates. The temperature was at 1500 °C and the holding times were 15 and 30 minutes [28].

As mentioned above, **Monsen et al.** (2004) did experiments in a graphite crucible in an induction furnace. The result was quite similar when the reductants are present or not. This indicates that the temperature of the graphite crucible is higher than the carbon charge. Hence, the observed reactions are mainly due to the reaction with the graphite crucible and not the added charge [10, 28].

Lastly, the sessile drop technique was used. The sessile drop is a technique to investigate the wettability between a solid and a liquid sample. This technique has been used in several studies and is mainly preferred before the theromgravimetery test because of the possibility to prepare a more homogeneous substrate. MnO slag from FeMn production is used in this study with different carbonaceous materials [28].

The reactivity between carbon and slag is to be considered an important parameter when choosing the right carbon material. Among the different techniques, the sessile drop is to be considered a fitting technique to examine this [28].

2.3.2 The reduction of FeMn slags

2.3.2.1 Influence of temperature on FeMn slags

There are many different parameters and variables in the production of FeMn and SiMn, and to understand the whole process it is important to understand how each different parameter will affect the process. There have been many studies where different parameters that influence the process have been investigated. One of the most important parameters in this process is the temperature. It has been well established that the reduction is strongly dependent on the temperature, where if the temperature increases it will favour the reduction both kinetically and thermodynamically. Figure 2.23 shows the effect of temperature on the weight loss by **Olsø et al.** (1998), whereas Figure 2.24 shows the temperature dependency on the reduction of MnO from FeMn slags by **Ostrovski et al.** (2002). From these two figures, it can be seen that either the weight loss increases or

the concentration of MnO decrease, both indicating an increase in reduction rate [25, 27].

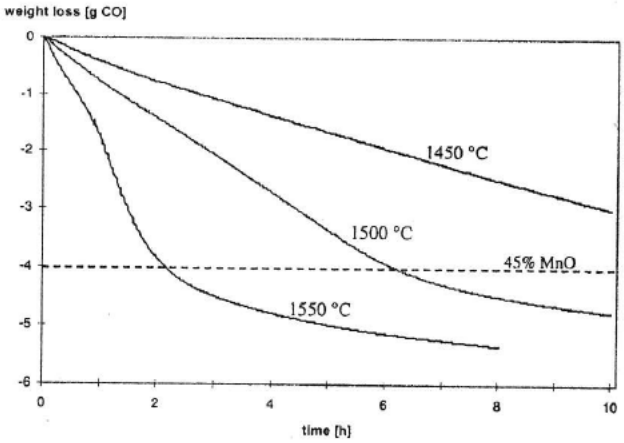

Figure 2.23: The effect of the temperature on the weight loss. The ratio of Al_2O_3 and SiO_2 is 0.25 in the slag used and the basicity is 2/3 [27].

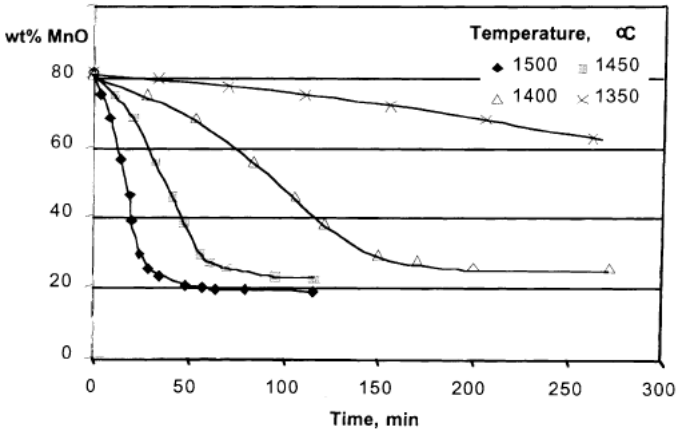

Figure 2.24: Effect of temperature on the reduction rate on MnO [25].

2.3.2.2 Influence of composition of slag

Ostrovski et al. (2002) studied the effects of temperature, ore/slag composition, CO partial pressure and coke size on the MnO reduction from a FeMn slag. It has been previously well established that the reduction rate of Mn ore is strongly affected by temperature and ore composition. The chemical reaction was assumed to be the rate determining step when reducing MnO, and the rate can hence be described in Equation 19. It has been found that when heating manganese ore, there are two phases formed which is a solid MnO phase and a liquid slag phase [25]. This was also found by **Olsø et al.** (1998) [27].

As previously mentioned the driving force of the reduction is the difference between the actual and the equilibrium activity of MnO, as seen in Equation 19. Hence, the activity of MnO is of importance. It was found by **Ostrovksi et al.** (2002) that the activity coefficient of MnO is strongly affected by the basicity of the slag form FeMn production,

shown in Figure 2.25. The basicity would also decrease during the reduction of MnO [25]. The slag basicity is defined by the ratio between basic and acid oxides, given in Equation 21 [5]. **Olsø et al.** (1998) found that when increasing the basicity in the two-phase area would decrease the reduction rate of MnO from FeMn slags, which can be seen in Figure 2.26. From this figure, it can be seen that the weight loss of the slag from FeMn production will decrease when the basicity increases [27].

$$B = \frac{\sum \text{Basic oxides}}{\sum \text{Acid oxides}} = \frac{\text{CaO} + \text{MgO}}{\text{SiO}_2 + \text{Al}_2\text{O}_3} \tag{21}$$

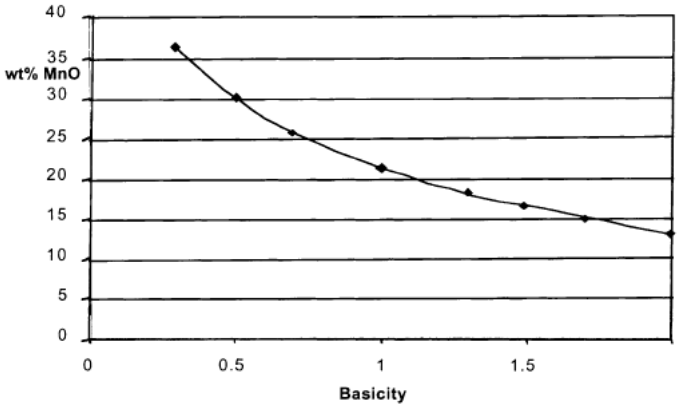

Figure 2.25: Influence from basicity on the equilibrium concentration of MnO at 1450 °C and 1 atm of CO gas [25].

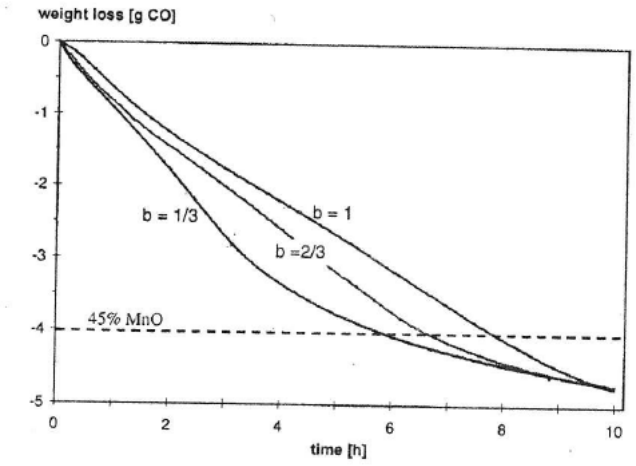

Figure 2.26: Measured weight loss at 1500 °C where the ratio of Al_2O_3 and SiO_2 is 0.50

From Figure 2.27 it can be seen that if the basicity increases the MnO concentration in the slag will decrease, hence increases the extent of MnO reduction [25].

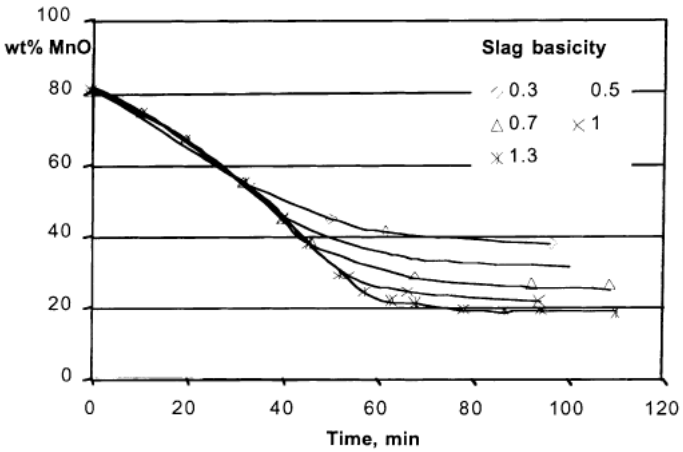

Figure 2.27: Effect from slag basicity in the reduction of MnO in the slag at 1450 °C [25].

2.3.2.3 Influence of iron content in the slag

The FeO in the slag will also influence the reduction of MnO. The correlation between the reduction of FeO and MnO is given by the following equations. The FeO from the slag is first to be reduced by the carbon, which is given in Equation 22. This will lead to the formation of metal droplets at the interface between the slag and carbon. Furthermore, the iron will then be saturated with carbon, according to Equation 23. MnO can be reduced by the carbon in the Fe-C alloy (according to Equation 24) or by CO-gas (according to Equation 25). It can also be reacted with the metallic iron forming Mn-metal and iron oxides, according to Equation 26 [28].

$$(\mathrm{FeO}) + \mathrm{C} \rightleftharpoons \mathrm{Fe} + \mathrm{CO\,(g)} \tag{22}$$

$$\mathrm{C\,(s)} \rightleftharpoons \underline{\mathrm{C}} \tag{23}$$

$$(\mathrm{MnO}) + \underline{\mathrm{C}} \rightleftharpoons \underline{\mathrm{Mn}} + \mathrm{CO\,(g)} \tag{24}$$

$$(\mathrm{MnO}) + \mathrm{CO\,(g)} \rightleftharpoons \underline{\mathrm{Mn}} + \mathrm{CO_2\,(g)} \tag{25}$$

$$(\mathrm{MnO}) + \mathrm{Fe} \rightleftharpoons \underline{\mathrm{Mn}} + (\mathrm{FeO}) \tag{26}$$

Safarian et al. (2009) studied the kinetics and mechanisms of the simultaneous reduction of FeO and MnO from HC FeMn slag. Three different carbon materials were used, pure graphite, single coke produced from single coal and eucalyptus charcoal. A synthetic slag with CaO, MgO, SiO_2, Al_2O_3, MnO and FeO was used. The content of MnO was 38.7 % and 10.4 % of FeO. To examine the different materials, the sessile drop technique was used. Wettability parameters such as contact angle, rate of changes in contact angle, and the contact area between the carbon and slag were not used to discuss the kinetics. This was because of considerable bubble formation in the slag droplet, which made it difficult to measure this. Furthermore, the differences in the chemical composition of the reduced slag state that it does not change much. Therefore, it is not dependent on the distance from the interface. This study states that the reduction of MnO and FeO occur

at the same time. The initial rate of FeO is fast and is followed by a slower reduction of MnO. It also shows that the kinetics is affected by the choice of carbonaceous material [29].

Table 2.6 shows the properties of the carbon materials used in this study. As could also be seen from Table 2.5, coke has a much higher content of sulfur and ash content [29].

Table 2.6: Properties of coke, charcoal and graphite [29]

Property	Coke	Charcoal	Graphite
Fixed C (wt%)	89.39	99.5	99.9
Ash content (wt%)	10.11	0.53	0.04
Surface Area (cm^2/g)	11 100	38 600	32 000
S content (ppm)	4800	20	-

The activity of FeO and MnO changes when the concentration of FeO and MnO changes. Figure 2.28 shows the calculated activities at 1600 °C.

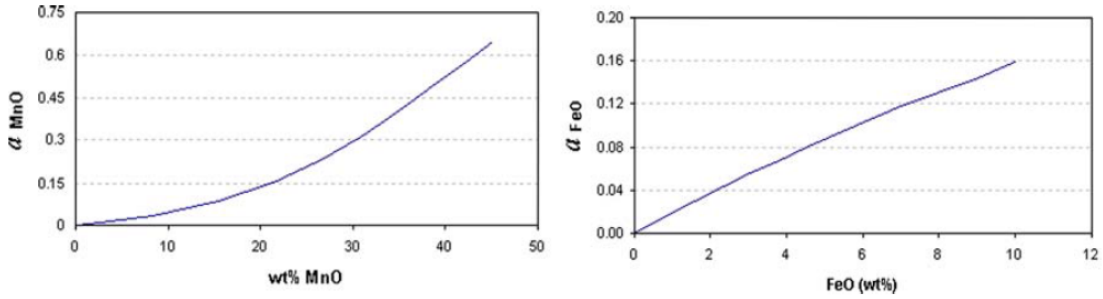

Figure 2.28: Calculated changes of MnO and FeO activity at 1600 °C [29].

Figure 2.29 shows the changes in MnO and FeO concentration in the slag. For reduction of FeO, it is approximately the same when using coke or charcoal, but for the reduction of MnO, there is less MnO in the slag when using coke [29].

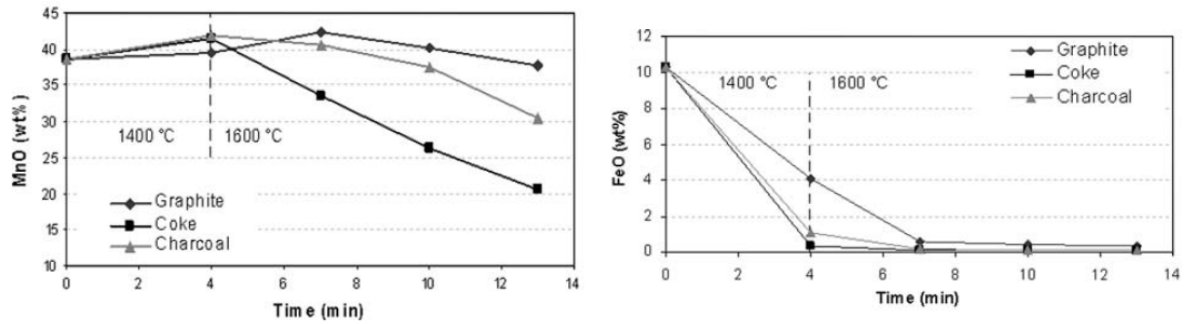

(a) Concentration changes of MnO

(b) Concentration changes of FeO

Figure 2.29: Concentration changes of MnO and FeO in slag with different carbon materials [29].

The reduction rate is dependent on if there is FeO in the slag. Figure 2.30 shows the reduction of MnO from a slag that does not contain any iron oxides. Furthermore, it can

be seen that there is a significant difference in the reduction of MnO if there are iron oxides in the slag or not. From the experiments without iron oxides in the slag, there were not observed any metal phase. Hence, when there is no metal produced charcoal will have the highest reactivity (Figure 2.30) and if there is metal present, coke will have the highest reactivity (Figure 2.29a) [29].

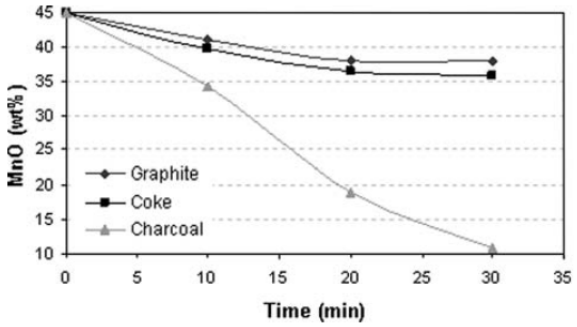

Figure 2.30: Concentration change of MnO from a slag with no iron oxides [29].

Figure 2.31 shows the changes of Fe, Mn, C and Si in the metal phase. When using coke the concentration of Fe and Si is higher compared to charcoal. The concentration of Mn is higher when using charcoal at the longest experiment, and at 4, 7 and 10 minutes the concentration of Mn is higher when using coke. The content of Si is very low, but increases with longer reduction times, especially when using coke [29].

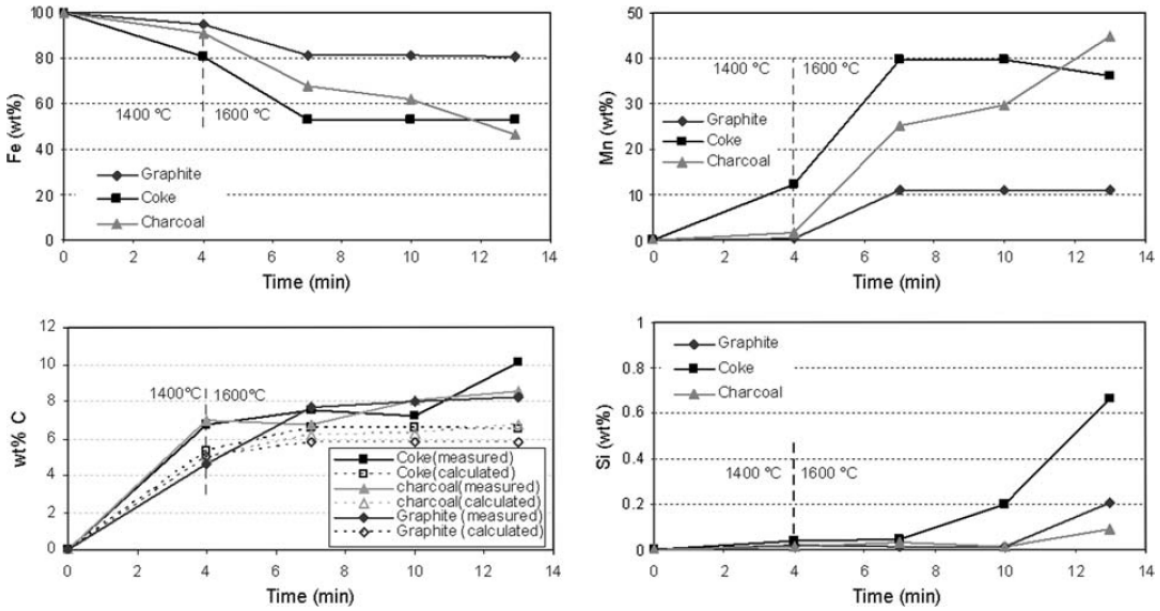

Figure 2.31: The concentrations of Fe, Mn, C and Si in the metal phase with different carbon materials [29].

2.3.2.4 Influence of different atmospheres on the reduction of FeMn slags

For the reduction of FeMn slags, the atmosphere has been found to be of importance. **Ostrovski et al.** (2002) found that the reduction of MnO was dependent on the partial

pressure of CO. It was found that if the CO partial pressure decreases, the activity of MnO will decrease, hence the MnO concentration in the slag will also decrease. This can be seen in Figure 2.32a. However, the experiments performed in Figure 2.32a is done at 1450 °C and the effect of the CO partial pressure has a relatively small effect. Furthermore, in Figure 2.32b the experiments are done at 1350 °C, and it can be seen that the effect of the CO partial pressure is much greater. Hence, the effect of the partial pressure of CO is greater at lower temperatures [25].

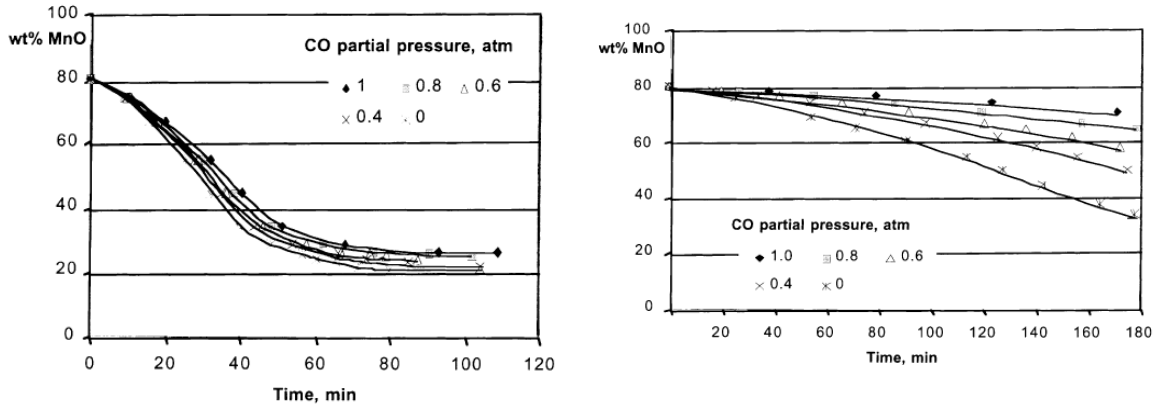

(a) MnO reduction at 1450 °C

(b) MnO reduction at 1350 °C

Figure 2.32: Effect of partial pressure of CO on MnO reduction at 1450 and 1350 °C [25].

There have also been performed experiments with an argon atmosphere. **Tranell et al.** (2007) [30] studied the reaction between slag from FeMn production and coke or charcoal in a sessile drop furnace with a CO or Ar atmosphere. The findings from this study showed that charcoal gave a higher reduction rate compared to coke in general. This study also found that CO gas gave a higher reduction rate than Ar atmosphere in the furnace, also something found by **Safarian and Tangstad** (2010) [28].

Safarian and Tangstad (2010) stated that the gas phase composition was observed to affect the kinetics of the system. It was also proposed a mechanism where the kinetics of reduction of MnO is controlled by the chemical reaction and the transfer of CO gas into the ambient gas. Furthermore, it was observed that in a sessile drop furnace that an Ar atmosphere had a lower reduction rate compared to CO, for all types of carbon materials. Even though an industrial furnace contains CO gas, this study recommends that experiments carried out in a sessile drop technique use an inert gas phase [28].

Figure 2.33 and 2.34 shows the reduction rate in different atmospheres. From these figures it is a clear difference of the two different atmospheres, where the reduction rate of MnO is higher when using a CO atmosphere compared to argon.

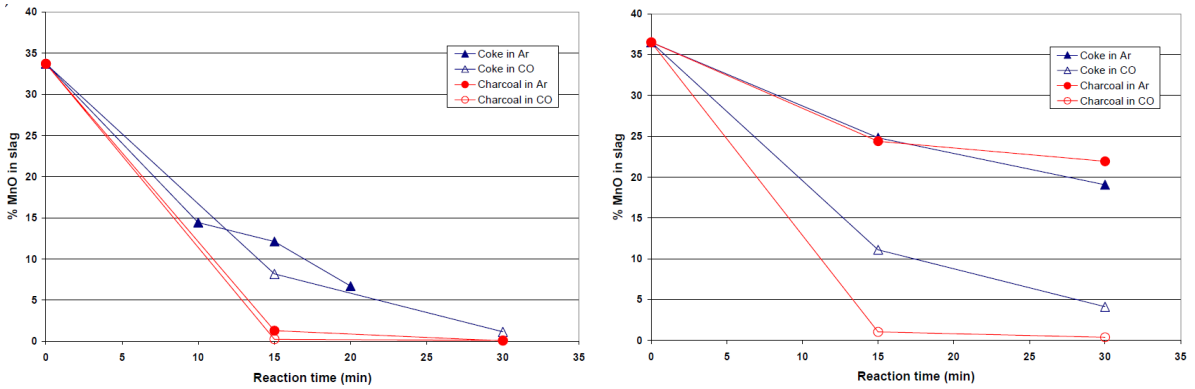

(a) With metal *(b) With no metal*

Figure 2.33: Concentration of MnO in slag as a function of time [30].

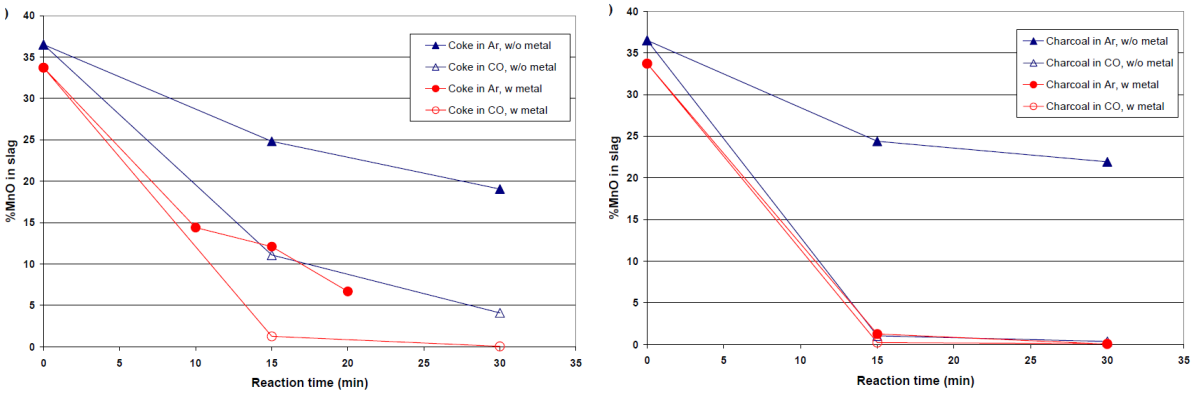

(a) Using coke as substrate *(b) Using charcoal as substrate*

Figure 2.34: Concentration of MnO in slag as a function of time [30].

Safarian et al. (2008) also investigated the kinetics of MnO reduction from FeMn slag with different carbon materials and reaction atmosphere. The study was carried out in a sessile drop furnace. This study states that CO gas gives a higher reduction rate compared to Ar atmosphere, which was also found by **Tranell et al.** (2007) [30, 31]. The argon atmosphere gave a higher extent of the reaction which correlates to the equilibrium activity. When using CO gas, the activity of MnO and the temperature are important parameters which will influence the MnO reduction. This can be seen in Figure 2.35 where the concentration of MnO is given as a function of time. From the figure, it can be seen that it is a difference if using a CO atmosphere or an argon atmosphere, especially when using single coke. Furthermore, when using charcoal, the reduction rate is higher when using argon gas. This study also found that charcoal has a higher reduction rate compared to coke. Industrial cokes also have a higher reduction rate than coke made from single coals [32].

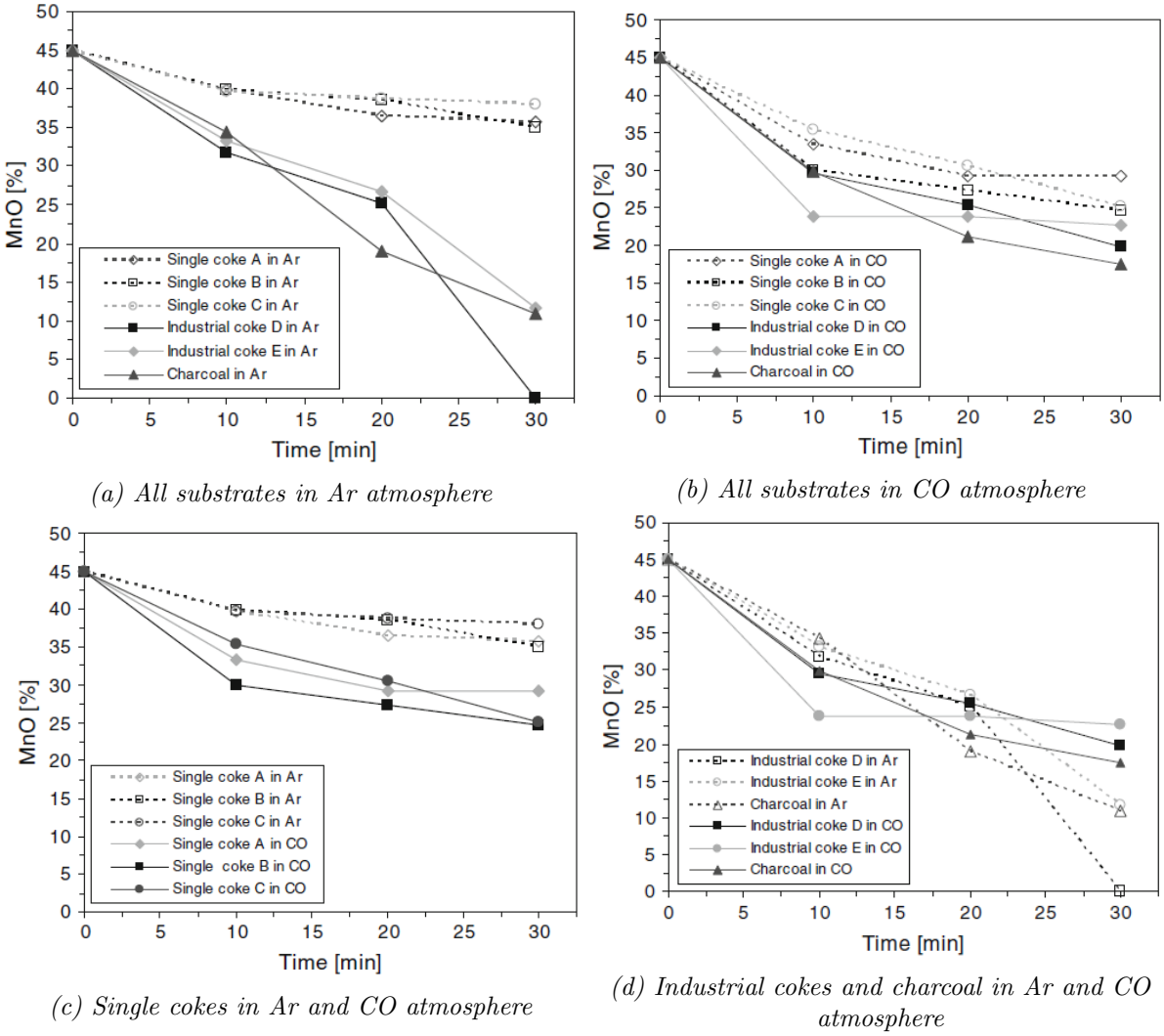

(a) All substrates in Ar atmosphere

(b) All substrates in CO atmosphere

(c) Single cokes in Ar and CO atmosphere

(d) Industrial cokes and charcoal in Ar and CO atmosphere

Figure 2.35: MnO concentration in reacted slag with a carbonaceous material [32].

From the figure above it can be seen that the industrial cokes have a higher reduction rate than the single cokes. However, the reduction rate difference between the cokes is less in CO atmosphere than in Ar, which may indicate that the kinetics of the reduction is less dependent on the substrate compared to Ar atmosphere. Figure 2.36 shows that the reduction rate is higher in Ar atmosphere than in CO atmosphere. This figure also shows that the difference between coke and charcoal is bigger in CO atmosphere than on Ar. The experiments performed in Figure 2.35 is with a synthetic slag and the experiment in Figure 2.36 is with an industrial slag. These two slags are very similar but the industrial slags contain 0.3 % of sulfur, as most industrial slags do. From the two figures, it can be seen that the industrial slag has a reduction rate than the synthetic slag [32].

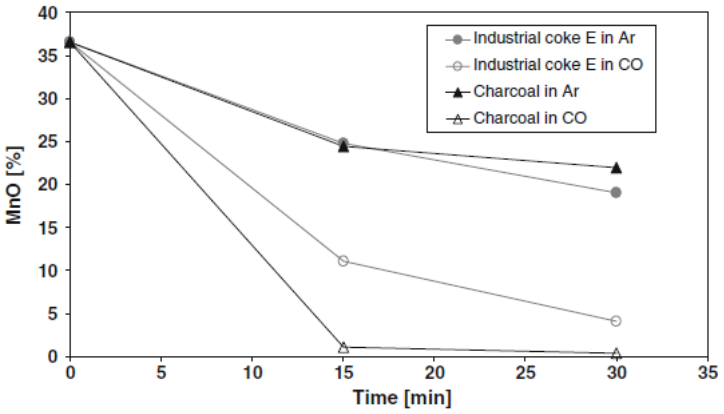

Figure 2.36: MnO concentration in different atmospheres [32].

2.3.3 The reduction of SiMn slags

There are many similarities between FeMn and SiMn production, although there is a higher temperature needed to produce SiMn due to the reduction of SiO_2. Hence, in addition to understand the reduction of MnO, one must also understand the reduction of SiO_2. In general, the same parameters that will influence the FeMn production will also influence the production of SiMn, such as temperature, the basicity of the slag, atmosphere, etc.

There have been several studies on the reduction rate of MnO and SiO_2, where slags from the SiMn is investigated. **Kim and Tangstad** (2018) studied the reaction rates of MnO and SiO_2 in SiMn slags using different raw materials, and estimated the kinetic parameters [33]. As mentioned earlier, **Ostrovski et al.** (2002) found that the reduction rate of MnO in FeMn slags can be described by Equation 19 [25]. If one assumes SiO_2 also is controlled by chemical reaction a similar rate model for SiO_2 can be described by Equation 27. These models for the reduction rate states that the driving force contributes to the reduction rates. The driving force is the difference between the activity at the current state of time and equilibrium [33].

$$r_{SiO_2} = k_{SiO_2} \cdot A \cdot \left(a_{SiO_2} - \frac{a_{Si} \cdot p_{CO}^2}{K_T} \right) = k_{0,SiO_2} \cdot A \cdot e^{\frac{-E_{SiO_2}}{RT}} \cdot \left(a_{SiO_2} - \frac{a_{Si} \cdot p_{CO}^2}{K_{T,SiO_2}} \right) \quad (27)$$

The experiments in this study was carried out in a TGA furnace with a CO atmosphere. It was found out that the mass change of MnO and SiO_2 below 1500 °C was insignificant which indicate a low reduction rate. When the temperature was above 1500 °C the reduction rate accelerated. The three different types of charge which were used are; As=Assmang + quartz + coke, As/HCS=Assmang + quartz + HC FeMn slag and HCS=quartz + HC FeMn slag + coke.

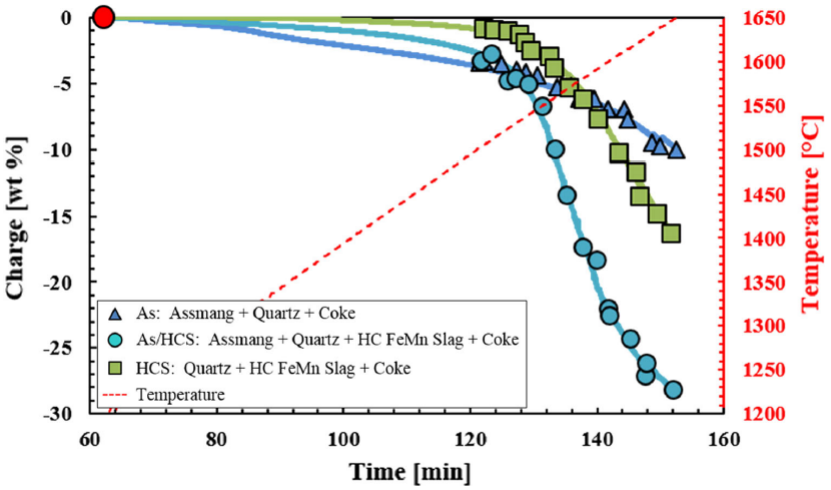

Figure 2.37: Results from TGA furnace. For each type of charge the average mass change was calculated [33]

To calculate the reduction degree of MnO and SiO_2, Equations 28 and 29 were used, and the reduction degree of the three different charges are given in Figure 2.38. From the figures, it can be seen a clear difference in reduction degree between the three different charges, especially for the reduction of MnO. Furthermore, it also shows that both the reduction degree when As/HCS and HCS is used is very dependent on the temperature [33].

$$\text{Reduction Degree MnO} = \frac{\text{Produced Mn [g]}}{\text{Initial MnO [g]}} \cdot \frac{70.97 \frac{\text{g MnO}}{mol}}{54.94 \frac{\text{g Mn}}{mol}} \tag{28}$$

$$\text{Reduction Degree } SiO_2 = \frac{\text{Produced Si [g]}}{\text{Initial } SiO_2 \text{ [g]}} \cdot \frac{60.08 \frac{\text{g } SiO_2}{mol}}{28.09 \frac{\text{g Si}}{mol}} \tag{29}$$

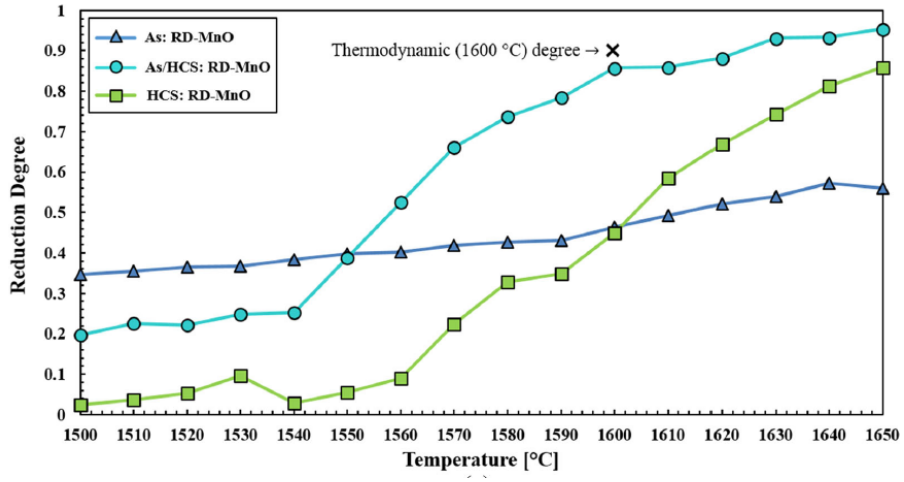

(a) Reduction degree of MnO

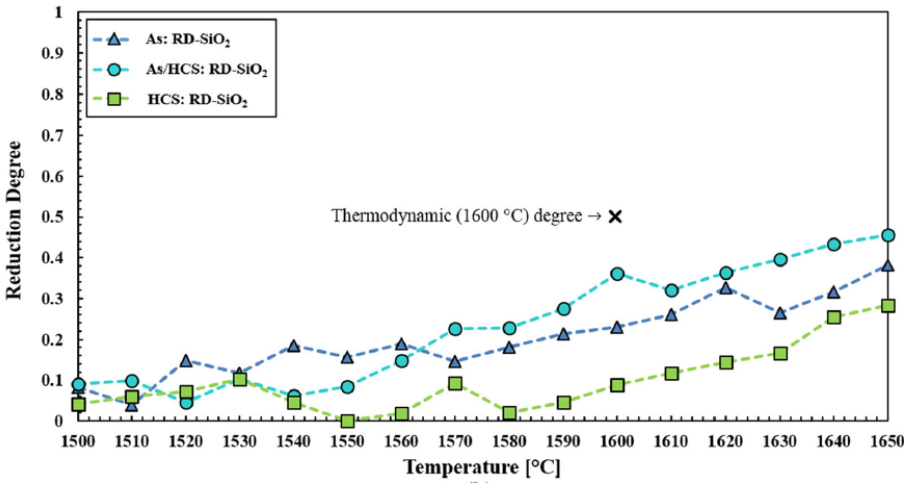

(b) Reduction degree of SiO_2

Figure 2.38: The reduction degrees of MnO (a) and SiO_2 (b) [33].

This study found that the reduction of MnO and SiO_2 starts at around 1500 °C, and the charge with Assmang ore, quartz, HC FeMn slag and coke had the fastest and highest reduction. The rate models described in Equations 19 and 27 were able to describe the reduction of MnO and SiO_2 in SiMn slag, which indicates that the same rate model for FeMn slags is also applicable for SiMn slags. Table 2.7 is a summary of the activation energies and pre-exponential constants for the three different charges. [33].

Table 2.7: Summary of the activation energy and pre-exponential constants [33]. (As: Assmang ore, HCS: High-Carbon FeMn Slag)

Charge	Ea (kJ/mol)	k_0 (g/min cm^2)
MnO reduction		
As	250	$9.66 \cdot 10^3$
As/HCS	920	$1.62 \cdot 10^{24}$
HCS	780	$5.87 \cdot 10^{19}$
SiO_2 reduction		
As	160	$3.04 \cdot 10^0$
As/HCS	870	$5.92 \cdot 10^{21}$
HCS	1130	$6.61 \cdot 10^{28}$

There was also performed an investigation into the kinetics of MnO and SiO_2 in SiMn slags by **Kim, Larssen and Tangstad** (2019). The temperature was between 1500 °C and 1650 °C under a CO atmosphere. The experiments were conducted in a TGA furnace. Under 1500 °C the mass change was insignificant, which indicates low reduction rate. Furthermore, the rate increased when the temperature was above 1500 °C [34]. This was also found by **Kim and Tangstad** (2018) [33]. The study found that the reduction rate was higher when the charge contained HC FeMn slag. It was also found that the viscosity does not have a significant impact on the reduction of MnO. A summary of the estimated activation energies are given in Table 2.8 [34].

Table 2.8: A summary of the estimated activation energy [33, 34]

Charge	MnO reduction (kJ/mol)	SiO_2 reduction (kJ/mol)
As	250	160
As/HCS	920	870
Com	305	450
COM/HCS	500	790
HCS	780	1130

Canaguier and Tangstad (2020) investigated three different SiMn charges, to investigate if different ore mixtures affect the reduction of MnO and SiO_2. The three charges were Assmang (Asm) ore, Comilog (Com) ore and Assmang + high carbon FeMn slag (As/HCS). In addition, approximately the same amount of quartz and coke was added to the charge. There were done experiments with different reduction duration's and different temperatures [35].

Figure 2.39 shows the isothermal reduction mass loss curves. Each line represents one experiment and the end of the experiment is indicated by a marker. The reduction mass loss is found by subtracting the mass loss from the pre-reduction to the mass loss from the isothermal stage. From the figure, it can be seen that there are two stages during this isothermal reduction, and the transition between the two is marked with a fast increase in the mass loss rate. This rapid change is indicated by the dashed line. The rate change shift can be seen clearly for Assmang and Comilog, it is not so clearly seen for Assmang + HCS and has been conjectured. Furthermore, the higher temperature the earlier the rate change shift occurred. However, it appeared to be constant for relative to the mass

loss for a given charge. This entails that the rate change is connected to the chemical and/or physical properties of the slag. It can also be seen that the experiments with equal temperature overlapped remarkably [35].

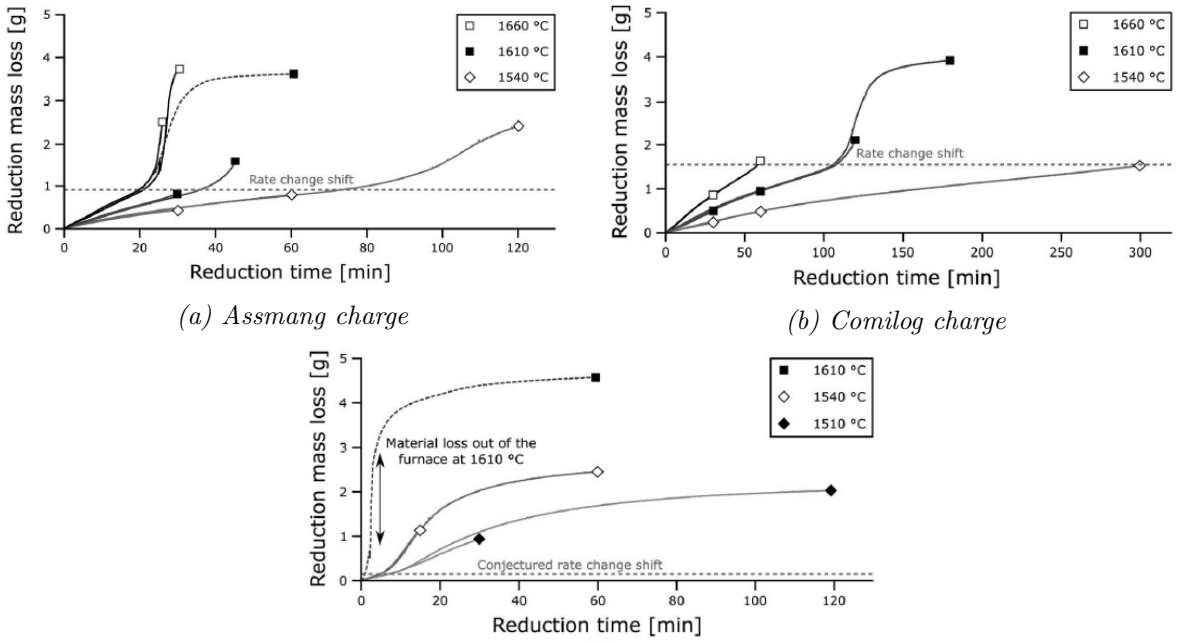

(a) Assmang charge

(b) Comilog charge

(c) Assmang + HCS charge

Figure 2.39: Reduction mass loss curves for the different charges [35].

Figure 2.40 shows the relation between the reduced MnO and SiO_2, which have been calculated from the chemical analysis of the slag. It can be seen that even though there are different charges the reduction paths are somewhat the same. Furthermore, the reduction path has little dependency on temperature, which could indicate that the MnO and SiO_2 reductions are linked. The connection between MnO and SiO_2 have been suggested from previous work [5], although there have been studies which did not find this connection [36]. Furthermore, the dashed line in the figure is the calculated slag-metal equilibrium at 1610 °C. Hence, the reactions did not achieve equilibrium [35].

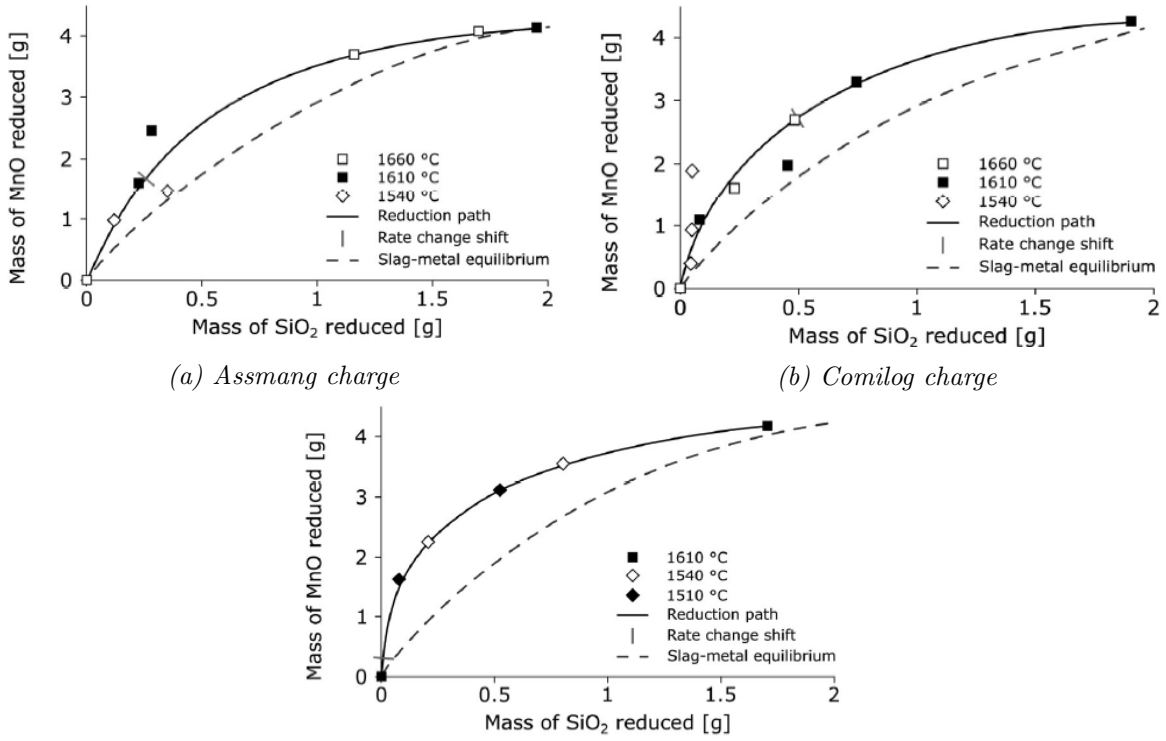

(a) Assmang charge

(b) Comilog charge

(c) Assmang + HCS charge

Figure 2.40: Reduced MnO and SiO_2 for the different charges [35].

Canaguier (2019) investigated the reduction kinetics in the SiMn production. Figure 2.41 shows the relative volume of slag on a graphite substrate. The composition of the slag is given in Table 2.9. The experiment goes to 1610 °C and is held for 60 minutes at this temperature. From the figure it can be seen that the relative volume slowly decreases until around 40 minutes where there most likely was formed a large bubble or there is foaming on the slag droplet before it decreases in volume again. The red line gives the lowest point on the graph at any given point. From this, it can be seen that the relative volume has almost decreased to half the original size. The black line shows that there is formation and release of CO gas, which may cause foaming. The blue line shows the CO gas liberated from the slag droplet during the experiment. It can be seen when the relative volume of the slag droplet increases the amount of CO gas liberated is also increased [37].

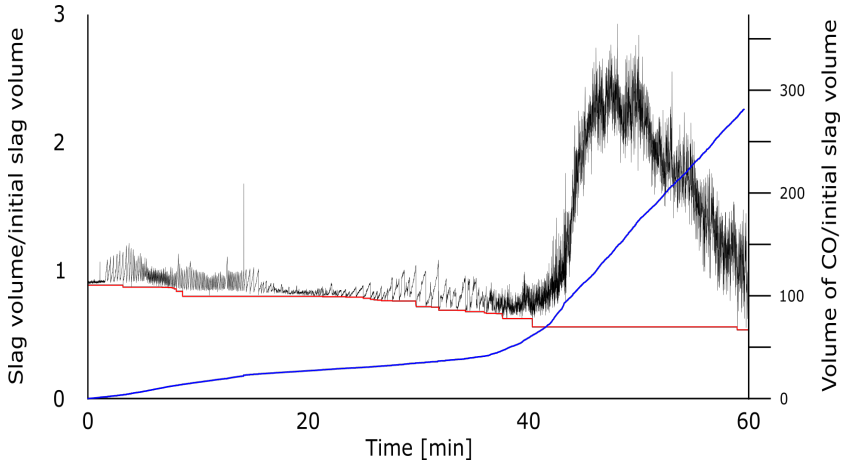

Figure 2.41: Relative volume of slag on a graphite substrate. The red line is the minimum point on the black graph. The blue line represents the volume of CO liberated from the slag droplet [37].

Table 2.9: Composition of slag used in this experiment [37].

	wt%
SiO_2	33.62
MgO	1.49
Al_2O_3	0.75
CaO	6.64
MnO	57.49

2.3.3.1 Reactivity between carbon materials and SiMn slag

The reactivity between the slag and the carbon material is an important parameter to investigate. **Nadir** (2015) investigated the reactivity of different carbon materials and the kinetics of MnO and SiO_2 in SiMn production. In this study, there were done experiments in an induction furnace with an industrial slag and a synthetic slag. In the industrial slag there was S present, but not in the synthetic slag. Figure 2.42 shows the experiments in the induction furnace. For test 1 and 2, it shows a low reduction rate and a higher reduction rate for test 3 and 4. For test 1 and 2, the graphite crucible in the furnace was used as a reductant, and for test 3 and 4 there was added coke. This may entail that there was a lack of reduction in the first two tests where only the crucible was the reductant. Furthermore, test 3 has a higher reduction rate compared to test 4, and there was not added any sulfur to test 4. Hence, the addition of sulfur increases the reduction rate [38].

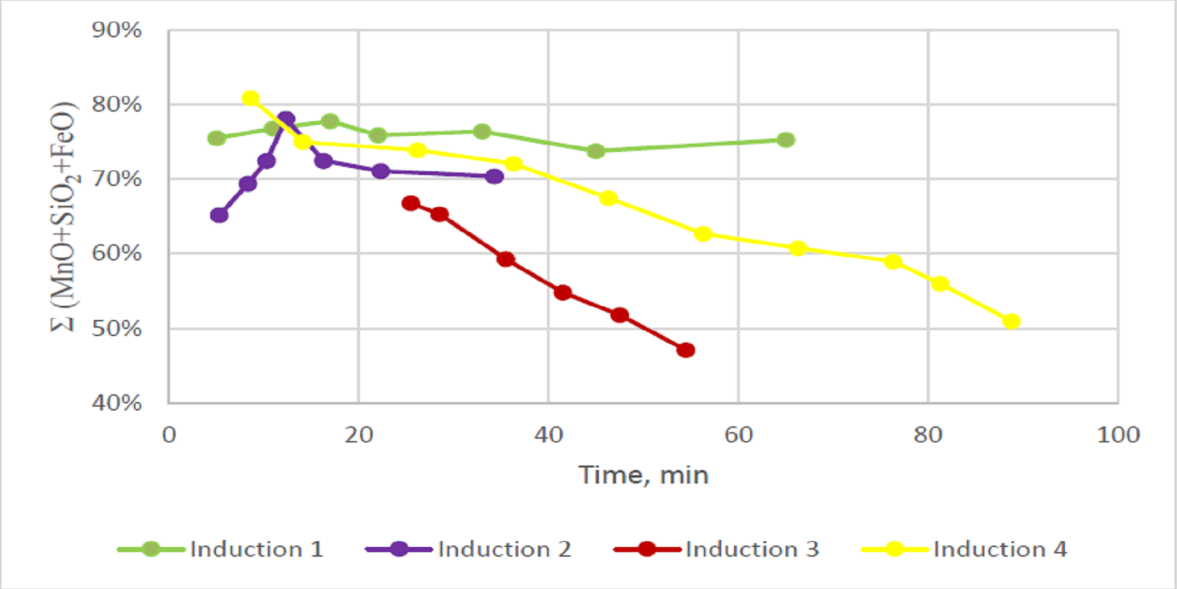

Figure 2.42: Comparison of tests in the induction furnace. The different induction tests are; Induction 1 - Graphite crucible as reductant and synthetic slag added 1 % FeS, Induction 2 - Graphite crucible as reductant and industrial raw materials, Induction 3 - Graphite crucible and coke as reductants and synthetic slag added 1 % FeS and Induction 4 - Graphite crucible and coke as reductant and synthetic slag without adding FeS [38].

There was also done some experiments in a sessile drop furnace where both synthetic and industrial raw materials were used. Figure 2.43 shows the relative volume (V/V_0) of the slag droplet. There were done seven experiments in the sessile drop furnace, where each experiment is shown as a curve on the figure. The legend on the figure states that if the abbreviation starts with "I" it is an industrial slag, and if it starts with "S" it is synthetic slag, the other abbreviations are explained as follows: A=Anthracite, G=Graphite, C2=Coke and CB=Carbon black. At first, there is a high reduction rate, and this is due to the reduction of iron oxides. After the iron oxide is reduced the slope of the curve decreases. The experiments from the sessile drop furnace conclude with that the reactivity of different carbonaceous materials is minimal [38].

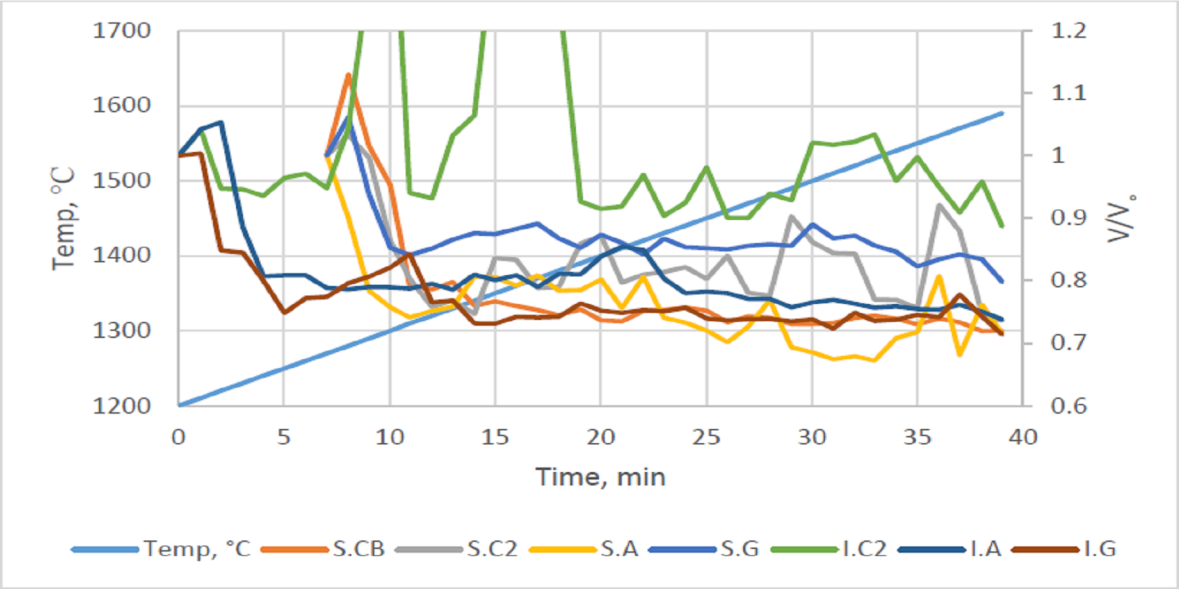

Figure 2.43: Comparison of tests in the sessile drop furnace. Explanation of graph: S=Synthetic slag, I=Industrial slag, A=Anthracite, G=Graphite, C2=Coke and CB=Carbon black [38].

Values calculated for the different experiments are given in Table 2.10. From the table, it can be seen that the k_0-values differ a lot in value in the two experiments. The high k_0-value for the sessile drop experiments are due to the low contact area [38].

Table 2.10: Calculated values for k_0 for all induction (Ind.) and sessile drop (Ses.) experiments [38]. (Syn.=Synthetical slag, Ind=Industrial slag)

Exp.	Reducing agent / Sub-strate	Raw materi-als	Ak_0 (MnO) [g/min]	Ak_0 (MnO + SiO_2 + FeO) [g/min]	A (cm^2)	k_0 (MnO) $[\frac{g}{min \cdot cm^2}]$	k_0 (MnO + SiO_2 + FeO) $[\frac{g}{min \cdot cm^2}]$
Ind.1	Graphite	Syn.	$0.51 \cdot 10^7$	$0.51 \cdot 10^7$	826	$6.2 \cdot 10^3$	$6.2 \cdot 10^3$
Ind.2	Graphite	Ind.	$0.07 \cdot 10^7$	$0.07 \cdot 10^7$	826	$0.85 \cdot 10^3$	$0.85 \cdot 10^3$
Ind.3	Graphite + coke	Syn.	$16.1 \cdot 10^7$	$3.7 \cdot 10^7$	1666	$96.6 \cdot 10^3$	$22.2 \cdot 10^3$
Ind.4	Graphite + coke	Ind.	$7.38 \cdot 10^7$	$3.62 \cdot 10^7$	1383	$53.3 \cdot 10^3$	$26.1 \cdot 10^3$
Ses.1	Carbon black	Syn.	$0.36 \cdot 10^7$	$0.63 \cdot 10^7$	0.78	$0.46 \cdot 10^7$	$0.80 \cdot 10^7$
Ses.2	Coke	Syn.	$1.28 \cdot 10^7$	$0.69 \cdot 10^7$	0.78	$1.64 \cdot 10^7$	$0.88 \cdot 10^7$
Ses.3	Anthracite	Syn.	$4.26 \cdot 10^7$	$2.39 \cdot 10^7$	0.78	$5.46 \cdot 10^7$	$3.06 \cdot 10^7$
Ses.4	Graphite	Syn.	$1.32 \cdot 10^7$	$1.05 \cdot 10^7$	0.78	$1.69 \cdot 10^7$	$1.34 \cdot 10^7$
Ses.5	Coke	Ind.	$2.05 \cdot 10^7$	$1.95 \cdot 10^7$	0.78	$2.62 \cdot 10^7$	$2.50 \cdot 10^7$
Ses.6	Anthracite	Ind.	$2.37 \cdot 10^7$	$2.03 \cdot 10^7$	0.78	$3.03 \cdot 10^7$	$2.6 \cdot 10^7$
Ses.7	Graphite	Ind.	$1.60 \cdot 10^7$	$1.85 \cdot 10^7$	0.78	$2.05 \cdot 10^7$	$2.37 \cdot 10^7$

Haugli (2019) investigated the reactivity of SiMn slags with different carbon materials. In this experiment, there were done experiments in a sessile drop furnace with two dif-

ferent synthetic slags with different contents of MnO and SiO_2, and both slags contained 0.43 wt% sulfur. These two slags were tested against industrial coke and charcoal made from hardwood [39].

Figure 2.44 shows the relative volume for the experiments with coke. The crosses are for slag 1, and the lines are slag 2. Slag 2 has a higher content of MnO and SiO_2 than slag 1. Furthermore, the figure shows that there is little difference between the two different slags. It can also be seen at the two tests for 30 minutes the lowest point is at around 0.3 [39].

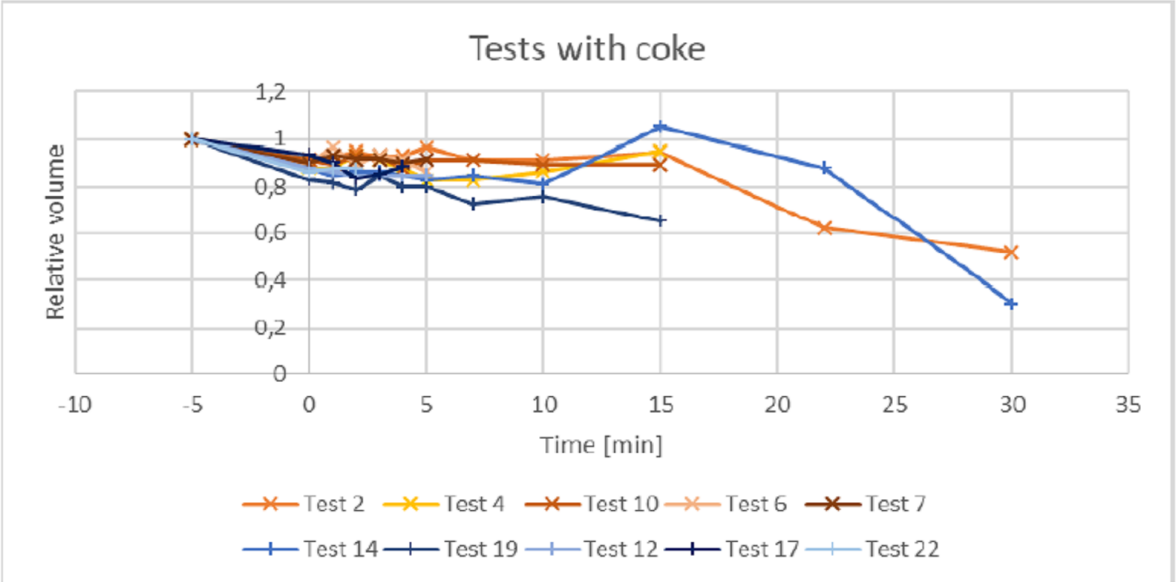

Figure 2.44: Comparison of the tests with coke. The crosses are for slag 1, and the lines are slag 2 [39].

Figure 2.45 shows the relative volume for the experiments with charcoal. There can also be seen from this figure that there is little difference between slag 1 and slag 2. The experiments with charcoal had a much lower relative volume compared to coke. Hence, the reduction of MnO and SiO_2 was larger when charcoal was used compared to coke. This could however also be due to the fact that slag descended into the charcoal more than the coke, and hence the volume seems smaller [39].

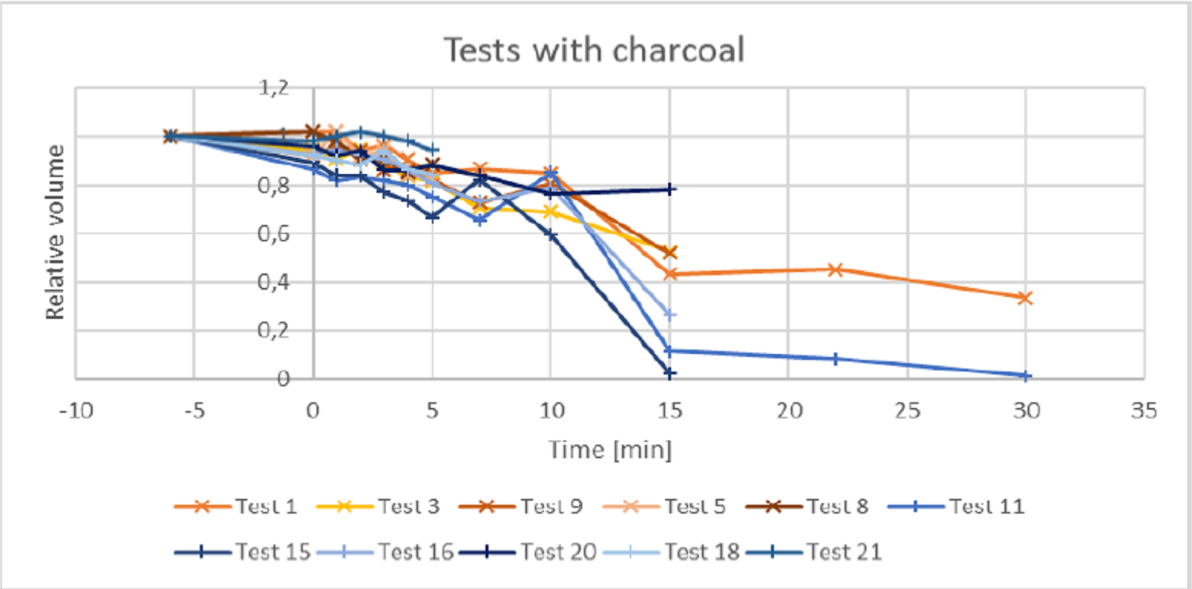

Figure 2.45: Comparison of tests with charcoal. The crosses are for slag 1, and the lines are slag 2 [39].

From the chemical analysis of the slag and metal there could be seen that the MnO content was lower for the tests when charcoal was used compared to coke. The content of Si in the metal was also higher when charcoal was used. Hence, the reduction rate was higher when charcoal was used. Furthermore, it could also be seen that there was a higher degree of reduction with slag 2 compared to slag 1. This was concluded to be due to the higher content of MnO in slag 2 [39].

Hosum (2019) investigated the interaction between coke and charcoal and reduced slag from SiMn production. In this experiment, there were done six experiments in a sessile drop furnace, where the differences between coke and charcoal were investigated [40].

To investigate the behaviour of the slag, the relative volume was measured, which can be seen in Figure 2.46 and 2.47. From these figures it can be seen that there is no significant difference between coke and charcoal as the slag, in general, has a very low volume change, other than the experiment with charcoal for 30 min where the slag droplet increased much more compared to the other in size. However, it can be seen to some extent that when using charcoal the general trend of the volume increases, while when coke is used as the substrate there is a general decrease in volume [40]. As mentioned the volume of the slag is generally much lower in this study, compared to the experiments by **Canaguier**, **Nadir** and **Haugli** [35, 38, 39]. However, in the study by **Hosum** it was used already reduced slag which has a lower content of MnO, hence there will be less reduction and therefore lesser volume change [40].

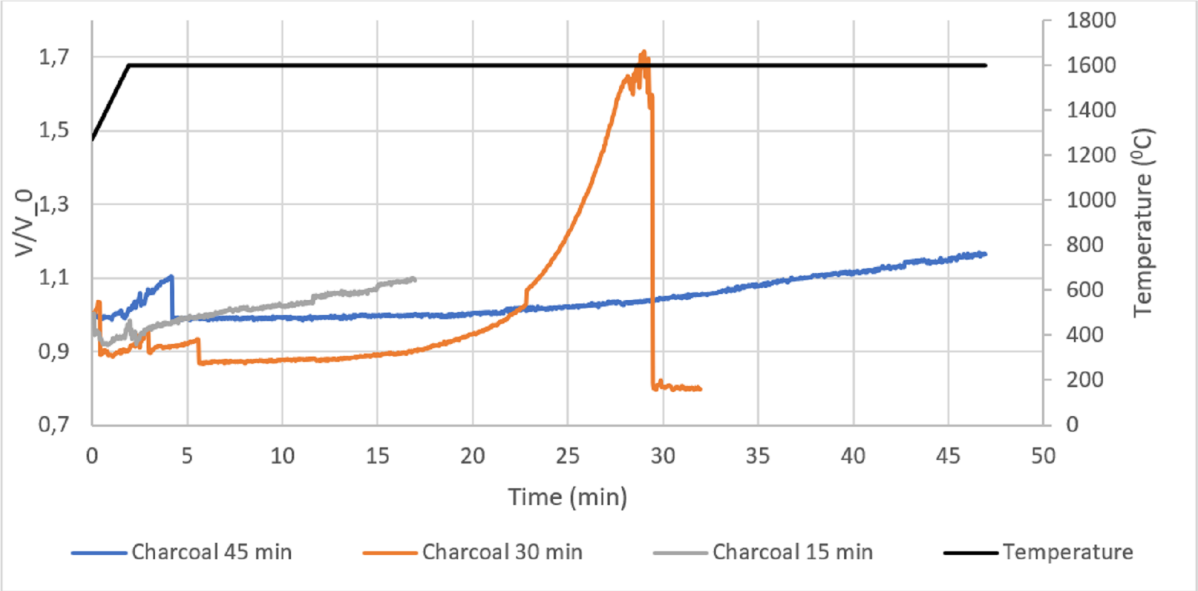

Figure 2.46: Relative volume for experiments with charcoal as the substrate, where the samples were held in a sessile drop furnace for 15, 30 and 45 minutes at 1600 °C [40].

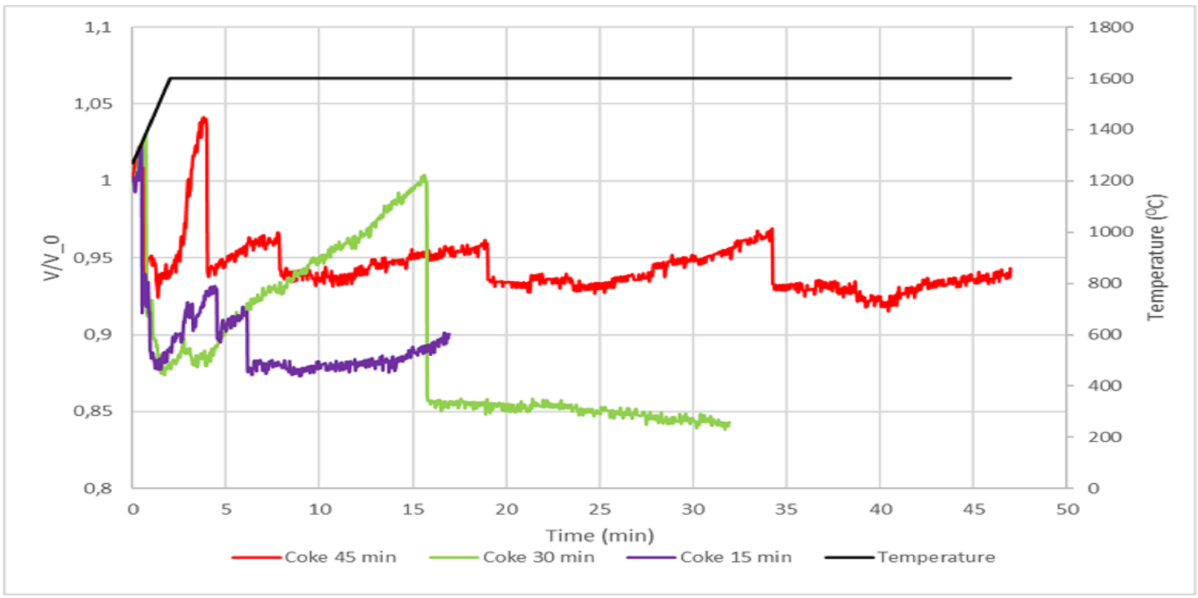

Figure 2.47: Relative volume for experiments with coke as the substrate, where the samples were held in a sessile drop furnace for 15, 30 and 45 minutes at 1600 °C [40].

From the relative volume it could not be seen any significant difference between coke and charcoal. Figure 2.48 shows the concentration of MnO found by analysis in EPMA. From the figure, it can be seen that at both 15 and 45 minutes the concentration of MnO in the slag is approximately the same when coke or charcoal was used as the substrate. For the experiment with charcoal at 30 minutes, it has a lower content of MnO than coke. The experiment with charcoal held for 30 minutes can be seen in Figure 2.46 that has a significant increase in volume, where a high amount of gas is generated, hence more reduction of MnO.

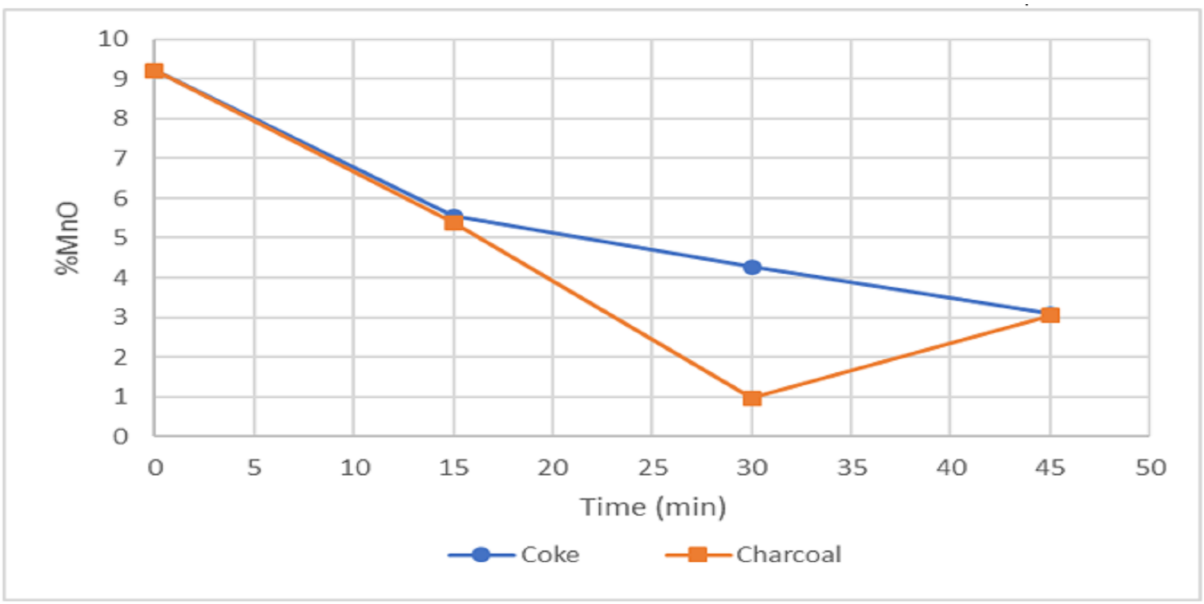

Figure 2.48: Concentration of MnO in the slag for all experiments, where the samples were held in a sessile drop furnace for 15, 30 and 45 minutes at 1600 °C [40].

2.3.4 Viscosity

Viscosity is a parameter which has an impact on the flow patterns in the furnace and also possibly the kinetics of the reaction between slag and carbon. Basicity is a parameter which can be closely related to the viscosity of the slag. Basicity is defined as the ratio between basic and acid oxides, given in Equation 21. The definition of basic and acid oxides is if they are network breaking or network forming oxides. The basic oxides are network breaking, and the acid oxides are network forming [26]. For SiMn production, the basic oxides are CaO and MgO and the acid oxide is Al_2O_3. This basicity is often referred to as the R-ratio, given in Equation 18. The R-ratio will influence the amount of Si in the alloy, which was discussed in Chapter 2.2 [5].

It is important to understand the viscosity of the slag, as it affects the production of the ferroalloys. Firstly, the tapping of the furnace will be more difficult and problematic with a high viscosity. Secondly, if the slag is viscous it may entrap metal droplets which will lead to a lower metal yield in the process. The viscous slag may also entrap gas which can lead to bubbling or foaming. Lastly, a parameter which is of great importance is the flow patterns inside the furnace, especially when modelling the furnace operation [5].

From experiments, it has been found that the viscosity is temperature dependent, and can be represented as an Arrhenius equation, given in Equation 30.

$$\mu = \mu_0 \cdot exp\left(\frac{G^*}{RT}\right) \tag{30}$$

where μ_0 is the pre-exponential factor, G^* is the activation energy, T is the temperature and R is the gas constant. However, this expression varies with different theoretical expression, which applies especially to the pre-exponential factor [41].

As mentioned above, the viscosity is temperature dependent. Figure 2.49 shows the viscosity (poise) as a function of temperature for several different slag systems. From the figure, it can be seen that if adding FeO and CaO the viscosity will decrease.

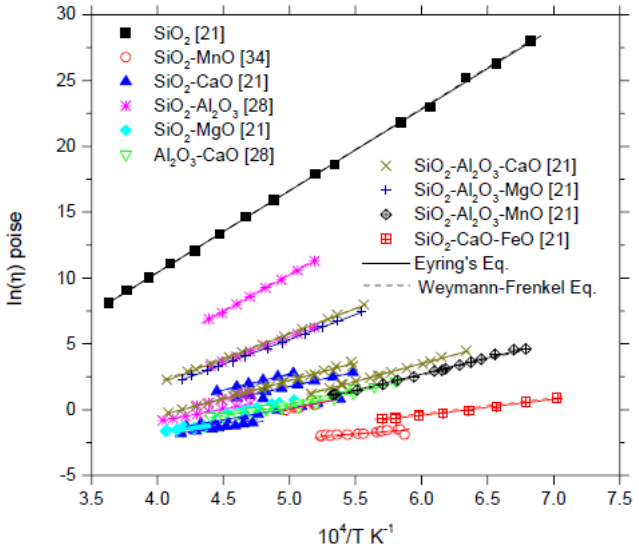

Figure 2.49: Temperature dependency of the viscosity in different silicon melts [41].

Figure 2.50 shows calculated iso-viscosity contours at 1500 °C. From the figure it can be seen that if there is an increase in SiO_2, it will lead to a rise in the viscosity [41].

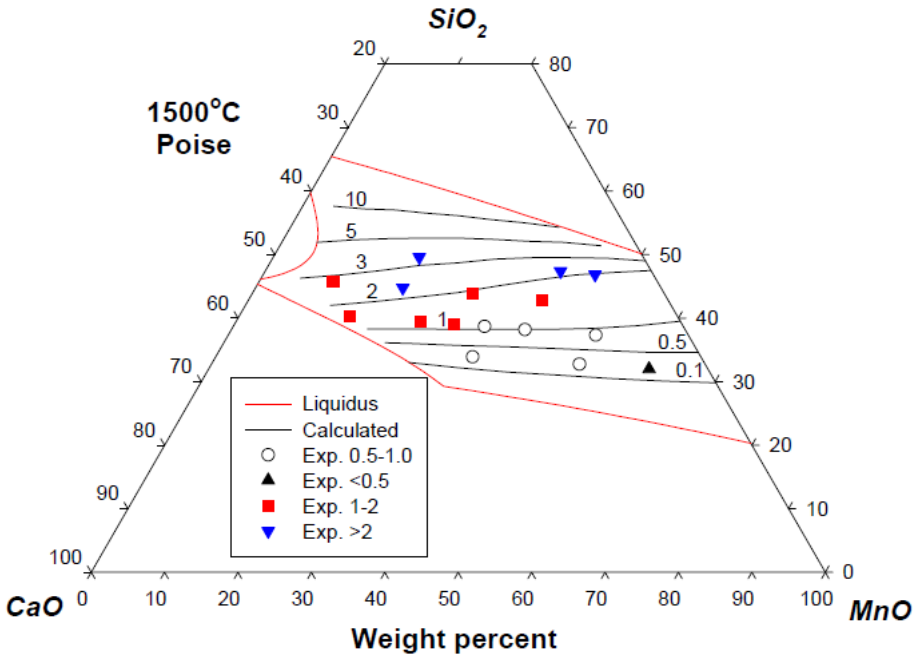

Figure 2.50: Comparisons between the calculated iso-viscosity curves with the measured points for the MnO-CaO-SiO_2 system at 1500 °C [41].

Kim and Tangstad (2018) found that the viscosity does not explain the lower degree of

reduction when using Assmang ore as the raw material compared to the use of HC FeMn slag. This can also be seen from Figure 2.51 [33].

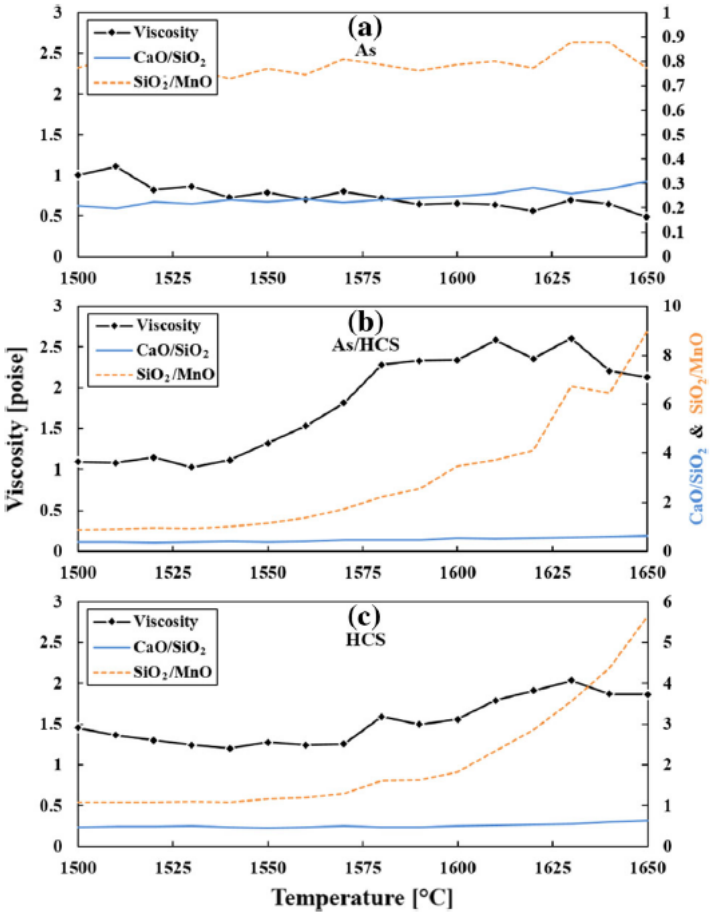

Figure 2.51: The viscosity of As (a), As/HCS (b) and HCS (c) compared with the ratio between CaO/SiO_2 and SiO_2/MnO [33].

2.3.5 Slag foaming

Slag foaming is a phenomenon where gas bubbles are entrapped in the slag which will lead to foaming on the surface of the slag. As mentioned above, if the slag is very viscous it will entrap more gas bubbles which can lead to more foaming. Foaming is mainly caused by two factors; (1) the rate of gas evolution from the reaction(s) and (2) the stability of the foam in the melt. The stability of the foam depends on the stability of the gas bubble, which depends strongly on the bubble lamellae or the bubble wall [42].

There has been little investigation into the slag foaming phenomena in SiMn production, or the ferroalloy industry in general. However, it has been studied to some extent in the iron industry. It has been found that aggressive foaming appears if the slag contains components such as SiO_2, P_2O_5 and CaF_2. These components will mainly stabilize the bubble wall [42].

As mentioned earlier, the viscosity will affect the foaming but other parameters can also impact the amount of foaming. This can be explained from the Morton number, which

is a non-dimensionless number that describes the motion of bubbles in a liquid, given in Equation 31 [43].

$$Mo = \frac{g\mu^4}{\rho\sigma^3} \tag{31}$$

where g is the gravitational acceleration, μ is the viscosity if the liquid, ρ is the density of the liquid and σ is the surface tension of the liquid. This indicates the three properties that will influence the behaviour of the gas bubble and if foaming occurs [43].

In some studies, a foaming index is defined as the thickness of the foam layer divided by the gas velocity [44]. **Ito and Fruehan** (1989) investigated several parameters that affect foaming in a CaO-SiO_2-FeO slag. It was first observed that the addition of 1 wt% P_2O_5 would decrease the size of the bubble because the addition of P_2O_5 decreases the surface tension of the slag. The effect of basicity on foaming was also investigated. It was found that the foaming index and the foam life decreases with increasing basicity. From this study, it was found that the surface does not have a large effect on the foamability of the slag. Since both P and S are components that will lower the surface tension but the addition of P_2O_5 will increase the foam index and the addition of S will decrease the foam index. The addition of CaF_2 will decrease the foam index by lowering the viscosity of the slag [45]. There have also been observed that a foam layer developed when the gas bubbles were less than around 2 mm in diameter [43].

Safarian et al. (2009) found that in the sessile drop furnace the slag droplet moved around. This is caused by the formation of CO gas, which created a bubble on top of the slag or foaming. After some time the bubble bursts making the slag droplet move around. This phenomena is shown in Figure 2.52. The formation of bubbles can indicate that the reduction of oxides in the slag occurs [29]. It is in general interesting to investigate how the slag droplet interacts with the carbon material and how the droplet behaves in the furnace. If the droplet moves around this may influence the contact area between and the slag and the carbon, which also can influence the reactivity.

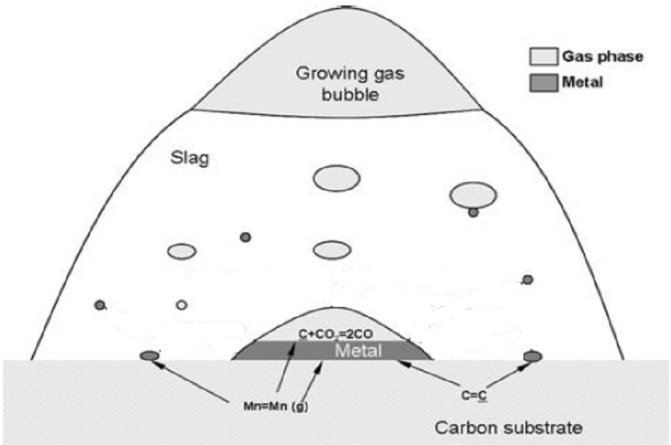

Figure 2.52: Bubble formation on slag droplet. The possible involved reactions are also shown [29].

The findings from **Safarian et al.** (2009), was also found by **Hosum** (2019), where a

bubble on the top of the slag droplet could be seen in the furnace [40]. This can be seen in Figure 2.53 where a gas bubble can clearly be seen on the top of the liquid slag.

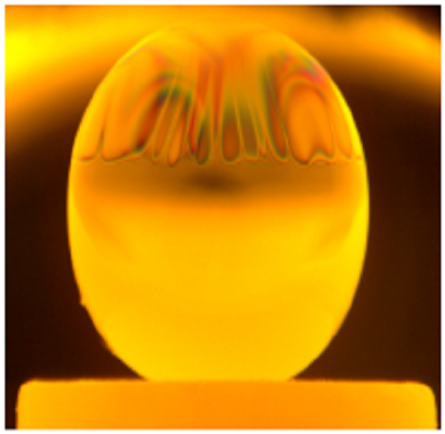

Figure 2.53: Picture taken inside the sessile drop furnace, showing a gas bubble inside the liquid slag [40].

2.3.6 Effect of sulfur on reduction rate

From previous studies, it has been seen that sulfur may affect the reduction of the slag from SiMn (or FeMn) process. As mentioned earlier, sulfur is known to be a surface-active element and will hence decrease the surface tension of the slags [21, 46]. **Skjervheim and Olsen** stated that the reduction rate was considerably increased when adding 0.2 % S to an Mn-C alloy. Furthermore, there will also most likely always be some sulfur present in industrial slags, and this could be the reason why industrial slags achieve a higher reduction rate in several studies [38, 47].

As mentioned earlier, **Kim and Tangstad** (2018) investigated three different charges, where all three have a different amount of initial sulfur. Where As has a sulfur content of 0.16 wt%, As/HCS has 0.29 wt% and HCS 0.39 wt%. Sulfur has been known to act as a strong surface-active element for metals. The initial amount of sulfur in this study seems to explain the difference in reduction rates. Hence, Assmang ore, which had the lowest S content, had also the lowest reduction rate. This implies that the content of S in the charge will have a significant effect on the kinetics of the process. Figure 2.54 compares the rate constants with different amounts of initial sulfur. HCS had a higher amount of initial S but a lower reduction rate, which implies that there could be an optimal amount of initial sulfur in the charge. However, it must be noted that it is not clear whether it was only the S content that gave different reduction rates. Since HCS lacks iron, and other studies have found that initial iron content also will affect the kinetics [33].

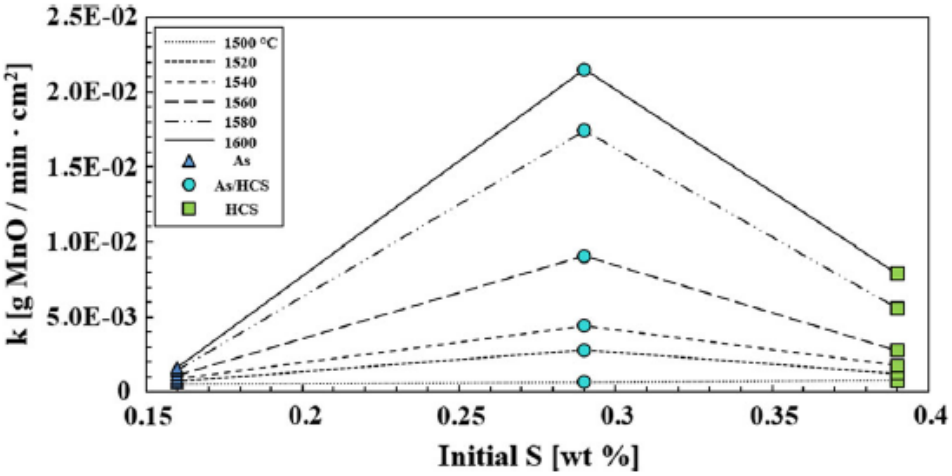

Figure 2.54: Initial sulfur amount compared with the rate constants at different temperatures [33]

Li and Tangstad (2019) investigated the influence of sulfur on the reduction of SiMn slags. In this study, there are 4 different synthetic slags investigated, where Slag 1 is without S, and slag 2, 3 and 4 have an S content of 0.20, 0.44 and 1.0 wt%, respectively. The carbonaceous materials used as the reducing agent is carbon black, and the ash content in the carbon black is 0.02 wt% where 0.006 wt% of this is sulfur. Figure 2.55 shows the results from experiments in a TG furnace. It can be seen that slag 3 (RM-3) has the highest weight loss of all the different slag. This can imply that there is an optimal sulfur content regarding reduction rate of SiMn slag [46]. This was also proposed by **Kim and Tangstad** [21] and can be seen in Figure 2.54.

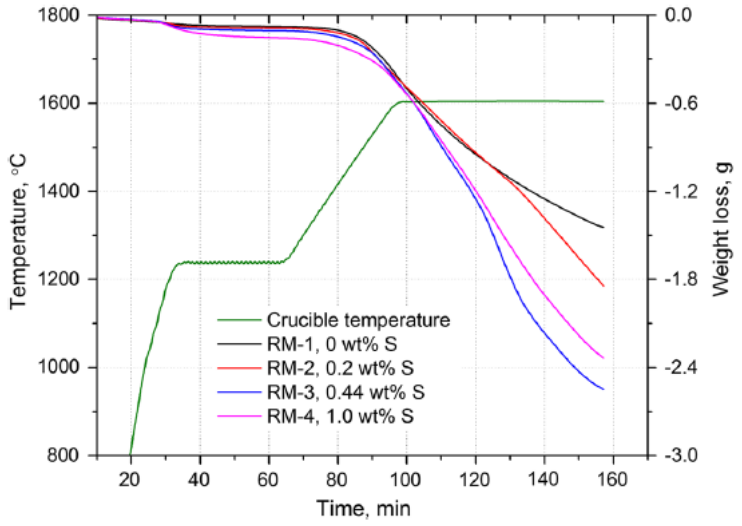

Figure 2.55: Weight loss curves for experiments with slags containing different amounts of sulfur [46].

Figure 2.56 shows the wetting angle of the different slags on the carbon black substrates. For slag 1 there is no significant change in the wetting angle when the temperature

increases. For the 3 slags containing sulfur, the wetting angle decreases with increasing temperature. Furthermore, slag 4 has the lowest wetting angle, but the differences between slag 2, 3 and 4 are not very large.

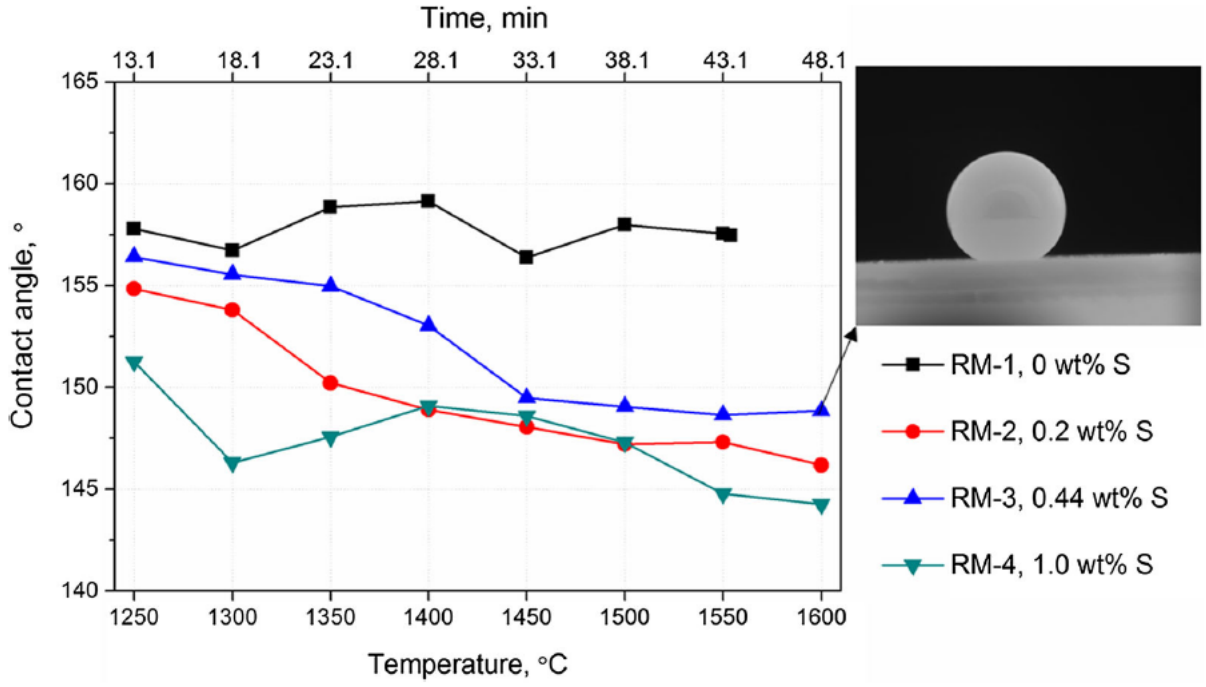

Figure 2.56: Wetting angle for the slags containing different amounts of sulfur as a function of temperature and time [46].

The contact area between the slag and the substrate can be calculated from Equation 32

$$S = \pi \cdot r^2 \cdot sin^2(180 - \theta) \tag{32}$$

where S is the contact area, r is the radius of the slag droplet and θ is the wetting angle. The contact area between the slag and substrate can be seen in Figure 2.57. It can be seen a clear difference between the slags containing sulfur and slag 1. The contact area does not change significantly for slag 1 when the temperature increases, but for all the slags containing sulfur the contact area increases with increasing temperature [46].

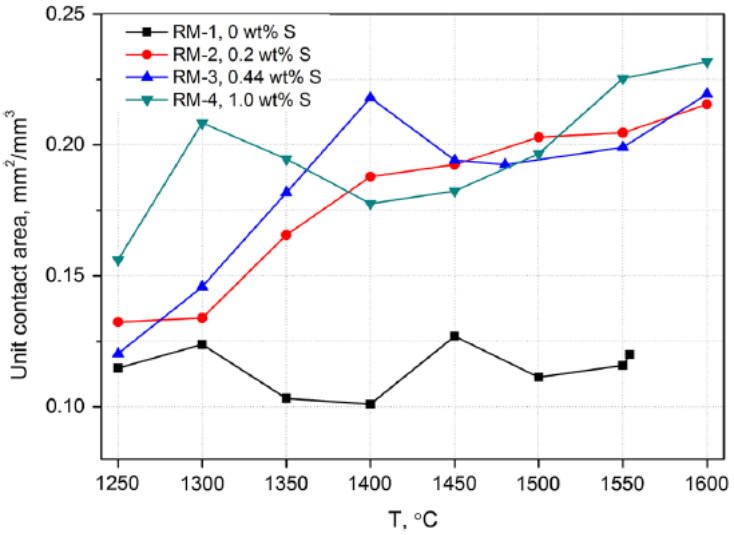

Figure 2.57: Contact area for the slags containing different amounts of sulfur as a function of temperature [46].

2.4 Wettability

Measuring the contact angle is an effective method to investigate the surface interactions between solid, liquid and gas. The contact angle between a gas-liquid-solid interface is the tangent the liquid surface has with the solid surface at the point of contact, as shown in Figure 2.58 [48].

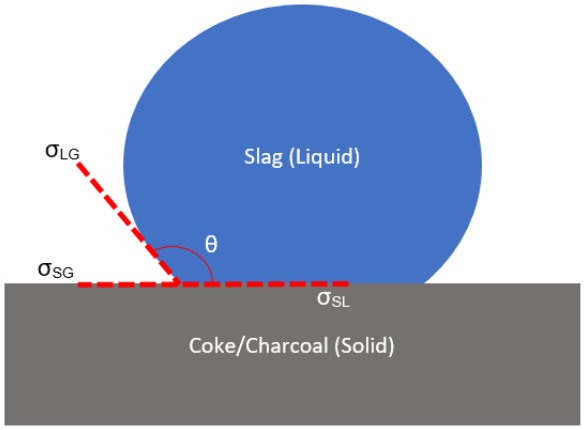

Figure 2.58: Contact angle between the slag (liquid) and coke/charcoal (solid) (after [26]).

To calculate the contact angle the Young-Duprè equation is used, given in Equation 33 [26].

$$\sigma_{SG} - \sigma_{SL} - \sigma_{LG} \cdot \cos\theta = 0 \tag{33}$$

where σ is the interfacial tension between the surfaces and θ is the contact angle between the liquid and solid. This equation was derived on the basis that the surface was so-called ideal. Hence, it is flat, nonreactive, inert, homogeneous and nonporous. However, any real surface does not fulfil these assumptions. Due to the fact that no real surface is ideal,

there are many physical properties of the substrate that will influence the contact angle. The roughness of the surface is a property that will play a vital role in the measurement of the contact angle [49].

Sun et al. (2010) investigated the wetting and reduction of MnO containing slags from FeMn production in an Argon atmosphere. It was used a graphite furnace in the experiments to study the in-situ observations of the wettability of slag. The rate of reduction can be approximated from Figure 2.59 where the concentration of MnO and SiO_2 in the slag as a function of time. In this case, the reduction rate for MnO was undetectable at 1450 °C, but when the temperature was increased to 1550 °C the rate significantly increased. Coke had a higher reduction rate compared to a graphite substrate. A correlation between increasing MnO content in the slag and increasing reduction rate was also found [50].

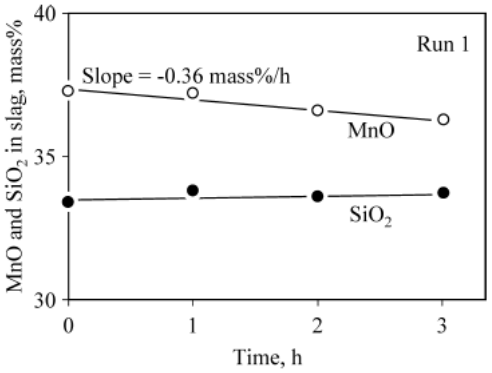

Figure 2.59: MnO and SiO_2 content in slag with graphite as the substrate [50].

The wettability between slags and carbonaceous materials is generally poor. In this study, the contact angle was lower with industrial slags and coke compared with synthetic slags and graphite, although not by much. It was found that the reduction rate increases with decreasing contact angle (i.e. better wettability). The contact angle for three of the runs is given in Figure 2.60. Table 2.11 shows the wetting angle and the reduction rates for the MnO reduction. Slags A, B and C are synthetic slags and D, E and F are industrial slags. The MnO content is highest for A and D and decreases for the next two types of slag. It can be seen that the runs with slag A and D have the highest reduction rate. Furthermore, coke has in general a higher reduction rate than graphite [50].

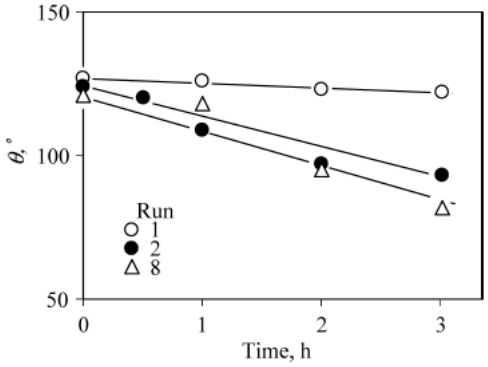

Figure 2.60: Contact angle between slag and carbonaceous material. Run 1 is with graphite, run 2 is with coke and run 8 is with graphite but with a different slag than in run 1 [50].

Table 2.11: Wetting angles between different types of slag and carbon materials, the reduction rate (Rate) and apparent reduction rate (k) for the MnO reduction [50].
**: RSG = Rough surface graphite*
***: Experimental temperature is 1450 °C for run 14 and 1550 °C for the other runs*

Run	Slag	Carbon	Wetting angle	Rate (wt%/h)	k (mass%/h)
1	A	Graphite	126.5	0.36	3.67
2	A	Coke	116.5	3.60	36.7
3	A	Coke	120.5	5.10	52.0
4	A	Coke	114.5	5.28	54.0
5	D	Coke	110	9.72	56.5
6	D	Coke	109.5	8.10	47.1
7	D	Coke	97	10.20	59.3
8	D	Graphite	119.5	4.38	25.4
9	B	Graphite	129	0.18	8.16
10	C	Graphite	134	0.012	0.83
11	E	Graphite	110.5	2.16	16.4
12	F	Graphite	112	0.66	43.7
13	A	RSG*	129	0.42	4.40
14**	A	Graphite	129	0	0

As mentioned in Chapter 2.1, **Jayakumari and Tangstad** (2015) investigated the wettability of various carbon materials. Figure 2.61 shows the wetting angle (contact angle) on different carbon materials as a function of temperature. From the figure, it can be seen that coke3 has the highest wetting, i.e. lowest wetting angle. Table 2.12 shows the density and void fractions for the different carbon materials is given. Furthermore, it can be seen that coke3 has the lowest density and highest void fraction, which may explain the difference in wettability.

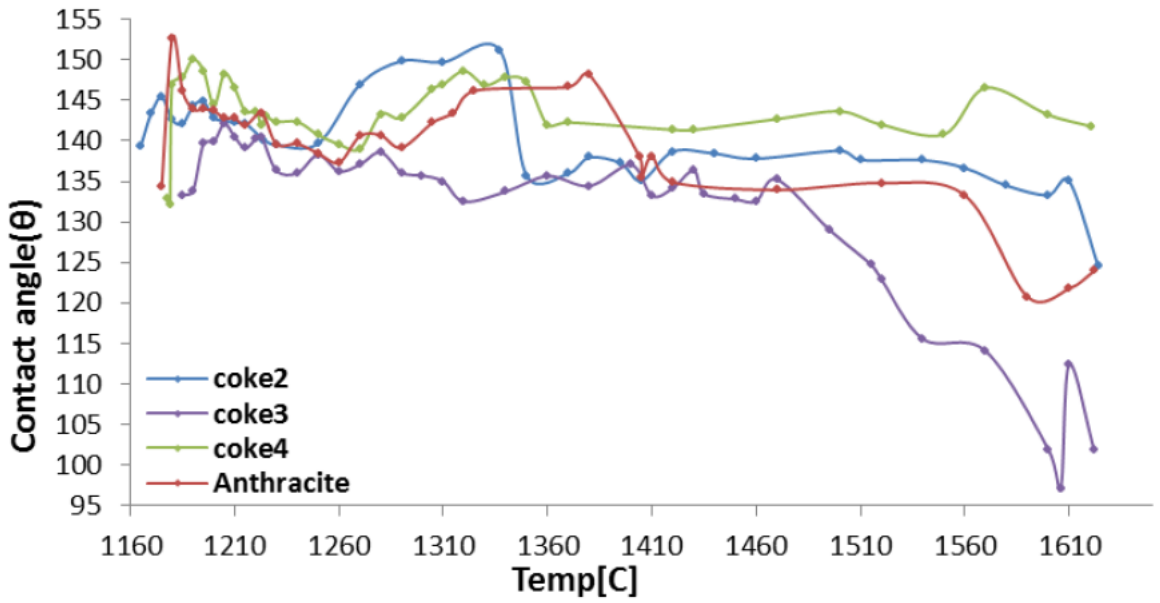

Figure 2.61: Wetting angle as a function of temperature during the reduction of MnO containing slags [16].

Table 2.12: Calculated void fractions of the carbon materials used in this study [16]

Carbon materials	Bulk density [kg/dl^3]	Particle density [g/cm^3]	Void fraction (α)
Coke2	0.749	1.82	0.59
Coke3	0.630	1.78	0.65
Coke4	0.745	1.78	0.58
Anthracite	1.007	1.91	0.42

where the void fraction is calculated by Equation 34.

$$\alpha = 1 - \frac{\delta_{bulk}}{\delta_{particle}} \tag{34}$$

In general, the wetting angle between a slag from the SiMn production and a carbonaceous material will start in the range of 120-140°. However, depending on the composition of slag and carbon material, too what extent will the wetting angle increase or decrease. From the experiments performed by **Hosum** (2019) [40] the wetting angle decreased to some extent, as seen in Figures 2.62 and 2.63. However, from the experiments performed by **Nadir** (2015) [38] and **Haugli** (2019) [39] the wetting angle decreases significant over time, depending on carbon material, as seen in Figures 2.64 and 2.65.

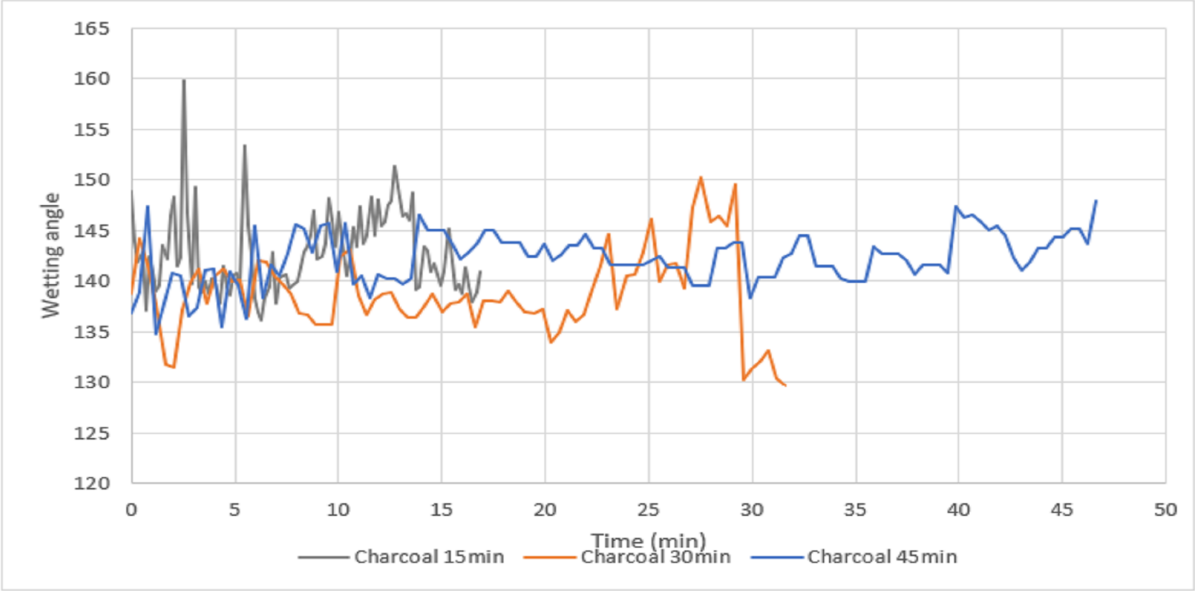

Figure 2.62: Wetting angle for experiments with charcoal as the substrate, where the samples were held in a sessile drop furnace for 15, 30 and 45 minutes at 1600 °C [40]

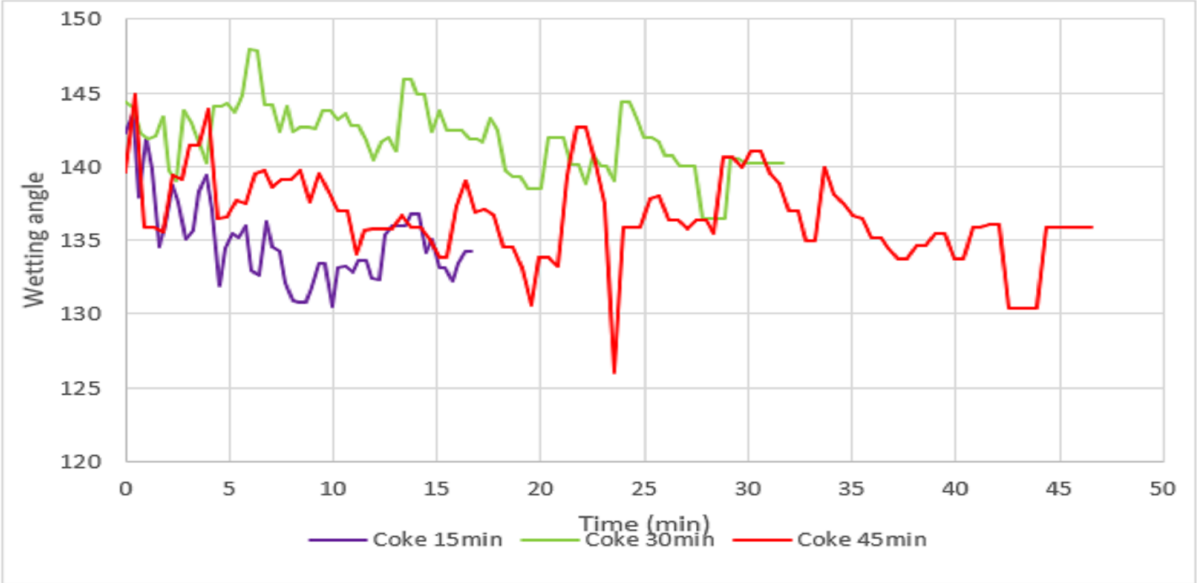

Figure 2.63: Wetting angle for experiments with coke as the substrate, where the samples were held in a sessile drop furnace for 15, 30 and 45 minutes at 1600 °C [40]

From Figure 2.64 it can be seen that the experiments with anthracite has better wettability compared to the other carbon materials investigated in this study.

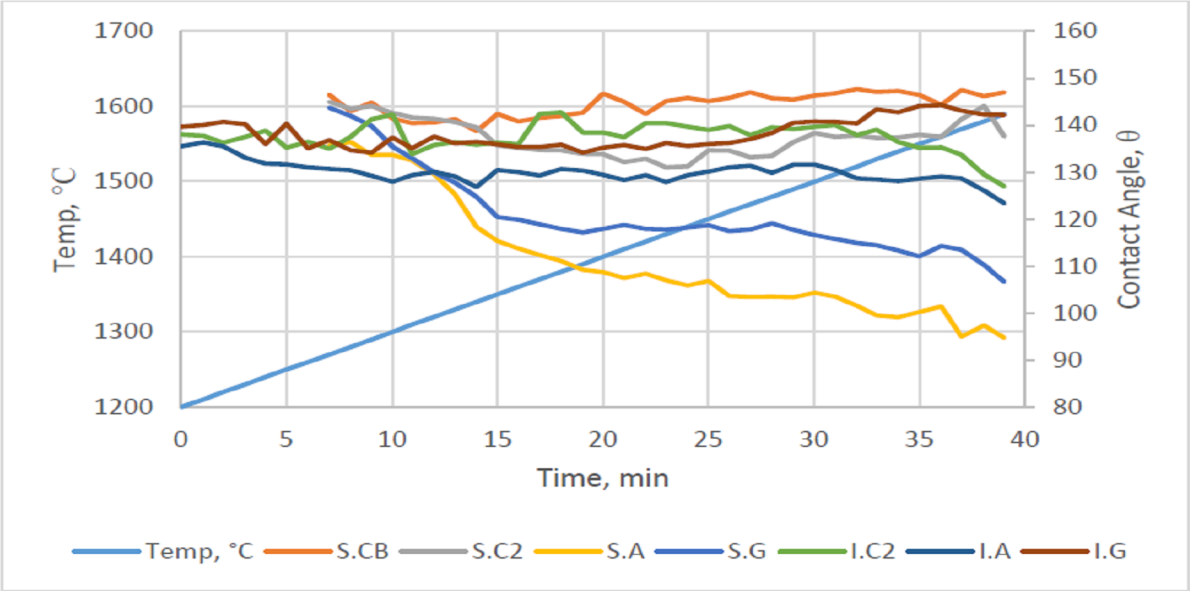

Figure 2.64: Wetting angle of tests in the sessile drop furnace performed by ***Nadir****. Explanation of graph: S=Synthetic slag, I=Industrial slag, A=Anthracite, G=Graphite, C2=Coke and CB=Carbon black [38].*

From Figure 2.65 it can be seen that the experiments with charcoal has a better wettability compared to coke.

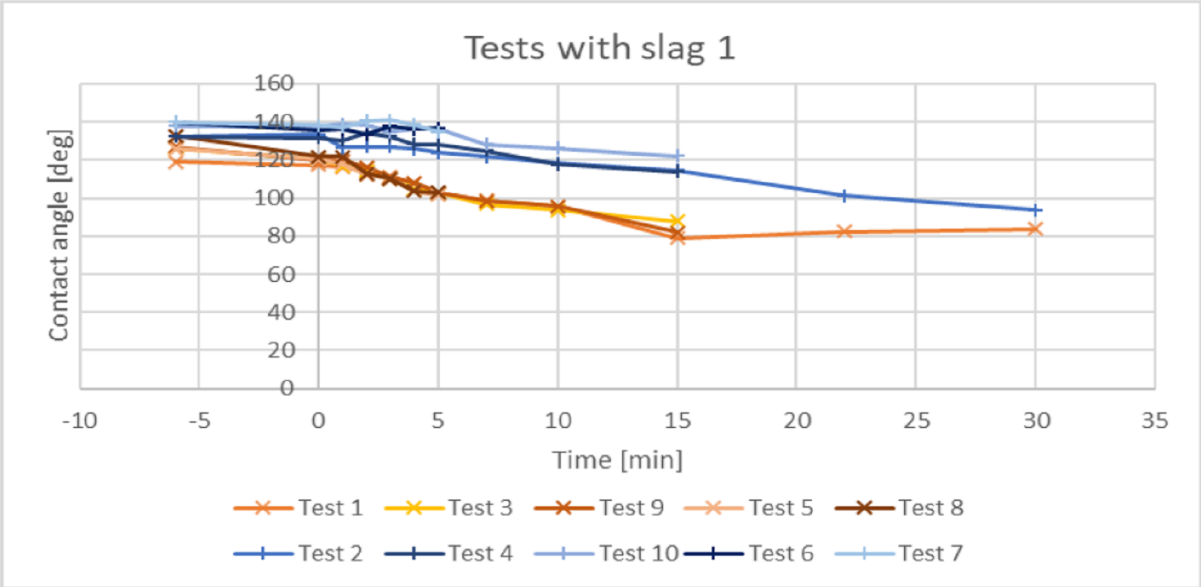

Figure 2.65: Wetting angle of tests in sessile drop furnace performed by ***Haugli****, where the orange lines are with charcoal and the blue lines are with coke [39].*

2.5 Surface roughness

The term roughness means that parts of the surface is not flat, and will, therefore, form peaks or valleys. The surface roughness of the pellets can be analysed to investigate the pellets itself, and also to see if there are any differences between the pellets. Surface

roughness or surface topography is an imperfection on the surface. However, almost every known surface has some kind of surface topography, either at macrolevel or nanolevel. There are many different methods or techniques to characterize the roughness of a surface, where height characteristics are most used. Height characteristics are most described by roughness average (R_a), root mean square roughness (R_q) and maximum peak-to-valley height (R_z). R_a is the most used parameter when measuring surface roughness. However, since R_a is an average any outlier such as a peak or valley will only have a small effect on this parameter, where R_q will be more influenced by these. R_a and R_q can be calculated from Equations 35 and 36, where L is the sample length and z is the height of the profile along the x-axis. R_z is calculated by finding the average between the five highest peaks and the five lowest valleys on the sample, as seen in Equation 37 and visualized in Figure 2.66 [51].

$$R_a = \frac{1}{L}\int_0^L |z|dx \tag{35}$$

$$R_q = \sqrt{\frac{1}{L}\int_0^L z^2 dx} \tag{36}$$

$$R_z = \frac{p_1 + ... + p_5 + v_1 + ...v_5}{5} \tag{37}$$

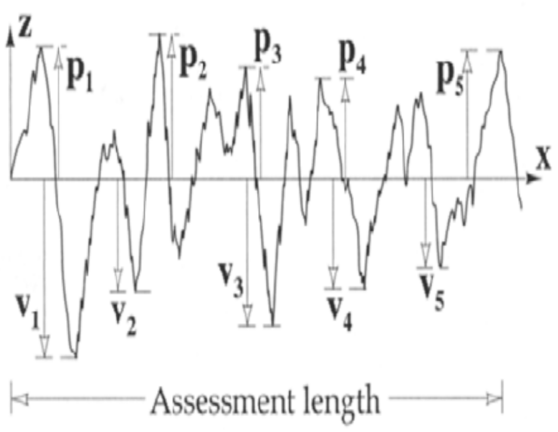

Figure 2.66: Calculating R_z by measuring the 5 highest peaks and 5 lowest valleys, and finding the average from Equation 37

From the study performed by **Hosum** (2019), there was found differences when the same substrate was used, which can be seen in Figure 2.46 and 2.47, hence it may be the surface of the pellets that are the difference [40]. **Kanai et al.** (2007) investigated the wetting and the reaction between a Si droplet and SiO_2 substrate. It was carried out experiments with grooves or dimples on the substrate, shown in Figure 2.67 [52].

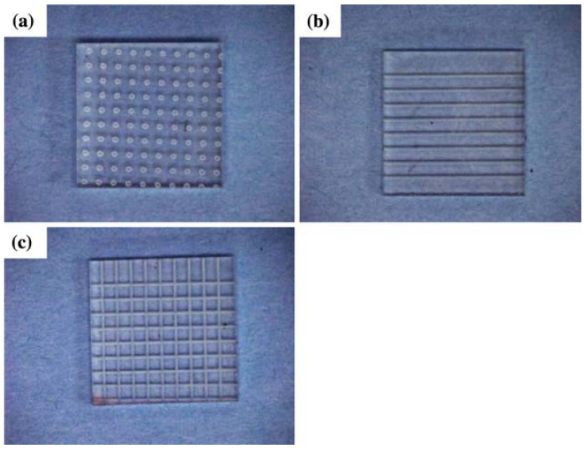

Figure 2.67: Top view of the substrates [52].

It was observed more movement (vibrations) on the droplet when the flat surface was used. The movement of the droplet is due to the formation of SiO gas, according the Equation 38 [52].

$$Si + SiO_2 \rightleftharpoons 2\,SiO \tag{38}$$

The formation of gas inside the droplet forms a gas bubble which will expand. After some time the gas bubble will burst making the droplet move. When using the dimples or mesh pattern the bubble did not move around. The produced SiO gas will leak through the dimples or grooves, as shown in Figure 2.68. Since the gas leaks out before a bubble is formed the droplet will hence not move around. If the gas was to leak out underneath the droplet, there would not be as much bubbling or foaming as if all the gas went through the slag. [52].

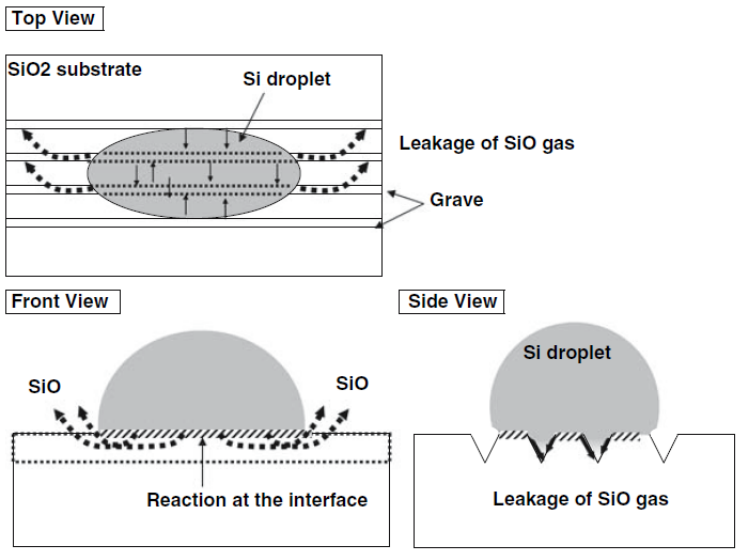

Figure 2.68: Schematic explanation of the gas flow under the droplet [52]

3 Experimental work

In this report, the reduction rate of two different slags was investigated with different carbon materials. The procedure of the experimental work is described in this chapter. First, making of the samples of both the slags and the carbon materials. Then the procedure on the sessile drop furnace, and lastly analysis in an optical microscope, SEM and EPMA. Furthermore, the pellets itself was investigated, where the density and porosity were measured and also the surface roughness of the pellets was analysed. The coke and charcoal materials were also analysed. An overall view of the experimental work is given in Figure 3.1.

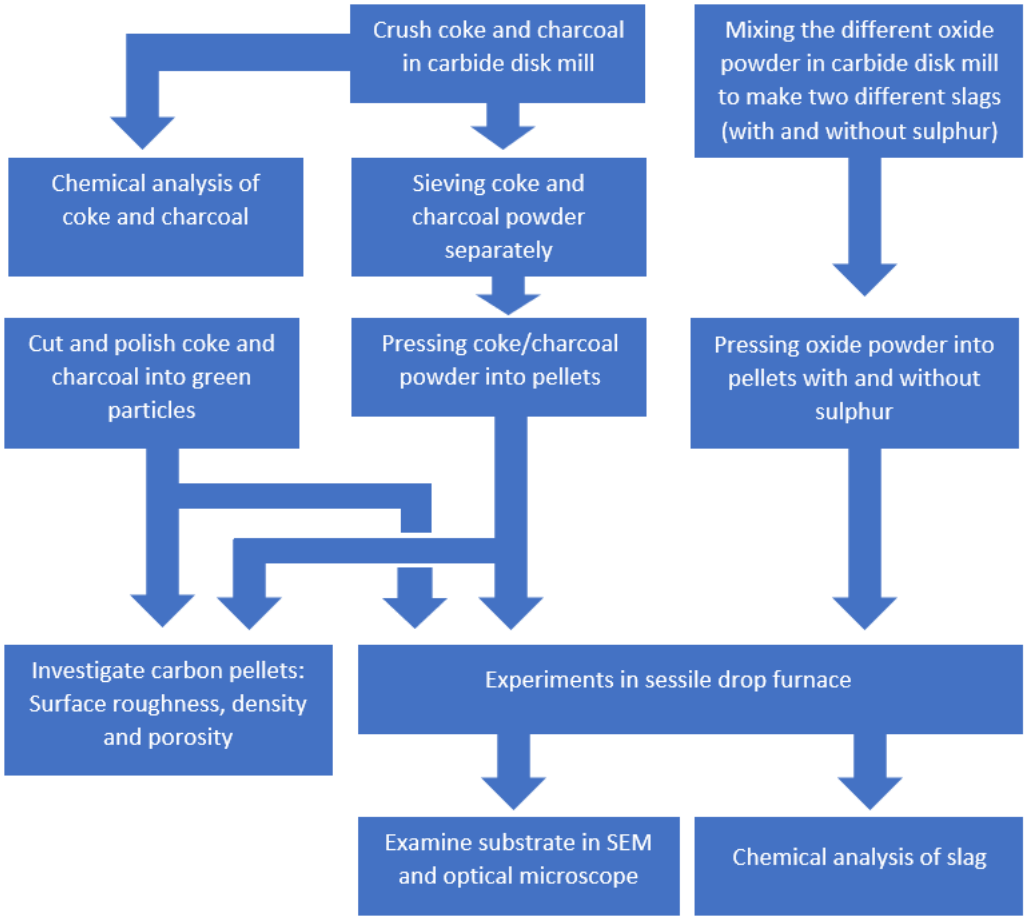

Figure 3.1: Overview of the experimental work

3.1 Pellets

The carbon materials and the slag was separately pressed into pellets. The reasons for this was, firstly to make the materials fit inside the furnace as the furnace can not fit large samples. Second, the carbon materials were pressed into pellets to remove much of the porosity so that the reactivity between the slag and carbon will increase, and also make the surface flat so the slag droplet would not roll off during the experiment. Lastly, to make the physical properties of the coke and charcoal as similar as possible, as it is the reactivity of the carbon materials that are investigated in this study. Moreover, the physical properties of the carbon material will influence the reactivity, however, the

physical properties of the carbon materials will not be investigated to an extent in this study.

3.1.1 Slag pellets

The different oxides were mixed in a carbide disk mill to ensure complete mixing. After mixing the powder was pressed into a pellet using a uni-axial press. A drop of water was added to the powder to bind the powder together. The diameter of the pellets is 5 mm, and the load on the press was 1 kN ($\approx$ 100 kg). After pressing, the pellets were placed in a heating cabinet at 100 °C for approximately 24 hours.

In this report, two different types of slag are analyzed, one with sulfur and one without. This is done to investigate the influence of sulfur on the reduction of the slag. These two different slags are named slag1 and slag2, where slag1 contains sulfur. The composition of slag1 and slag2 are given in Table 3.1. The compositions are somewhat the same for both slags, except for the addition of FeS in slag1. Hence, there was added more Fe_2O_3 to slag2 to achieve approximately the same amount of Fe in both slags. In the table, it can be seen that it is added 0,9 wt% FeS, which corresponds to 0,31 wt% S in the slag. Tables 3.2 and 3.3 shows the properties of the slag pellets.

Table 3.1: Composition of slag1 and slag2

Compound	Slag1 [wt%]	Slag2 [wt%]
SiO_2	29.70	30.39
MgO	2.88	2.97
Al_2O_3	7.16	6.88
CaO	11.15	10.93
MnO	42.92	43.02
Fe_2O_3	5.28	6.14
FeS	0.90	-

Table 3.2: Properties of slag1 pellets

	Mass pressed [g]	Wet weight [g]	Dry weight [g]	Dry height [mm]	Density $[\frac{kg}{m^3}]$
1	0.14	0.13	0.13	3.31	505
2	0.11	0.11	0.10	2.59	513
3	0.14	0.14	0.14	3.53	489
4	0.15	0.15	0.15	3.67	505
5	0.13	0.13	0.12	3.02	514
6	0.13	0.12	0.12	3.01	515
7	0.10	0.11	0.10	2.61	493
8	0.10	0.10	0.09	2.55	500
9	0.14	0.14	0.14	3.50	496
10	0.10	0.11	0.09	2.46	476
11	0.13	0.13	0.13	3.29	501
12	0.10	0.10	0.09	2.40	502
13	0.11	0.12	0.11	2.65	511
14	0.10	0.10	0.10	2.50	485
15	0.11	0.11	0.10	2.64	500
16	0.14	0.14	0.14	3.57	494
17	0.12	0.12	0.11	2.80	508

Table 3.3: Properties of slag2 pellets

	Mass pressed [g]	Wet weight [g]	Dry weight [g]	Dry height [mm]	Density $[\frac{kg}{m^3}]$
1	0.14	0.15	0.13	3.40	514
2	0.13	0.13	0.12	2.99	516
3	0.11	0.11	0.10	2.59	508
4	0.09	0.10	0.08	2.18	494
5	0.13	0.13	0.12	3.12	495
6	0.13	0.13	0.12	2.99	520
7	0.14	0.14	0.12	2.90	524
8	0.13	0.13	0.13	3.12	516
9	0.14	0.14	0.13	3.31	514
10	0.12	0.13	0.12	3.03	511
11	0.12	0.12	0.12	2.90	517
12	0.11	0.12	0.12	2.70	503
13	0.15	0.15	0.15	3.67	505
14	0.12	0.11	0.11	2.74	504

3.1.2 Charcoal and coke pellets

The coke and charcoal were first crushed separately in a carbide disk mill before it was sieved. The powder size used in the pellets was between 100 and 250 µm. After sieving, the coke/charcoal powder was mixed with binder and water before being pressed into

separate pellets. For the coke pellets, the amount of binder was 3 wt% and the amount of water was 30 wt%. For the charcoal pellets, the amount of binder was 3 wt% and the amount of water was 39 wt%. The binder used in this study is carboxymethyl cellulose (CMC). The water content needed for the pellets was found through trial and error in the study by **Hosum** (2019) [40].

It was used graphite cups for all the pellets used in the furnace experiments, except when graphite and the green particles were used. This was done to make the pellets more robust and to add more mass to the pellets. From previous experiments it was a problem that the coke pellets (without a graphite-cup) was extremely fragile after the experiment and thus could not be handled any further as they would disintegrate [40, 53]. Furthermore, it is added more weight to pellet so that the movement inside the furnace of the coke/charcoal pellet will be minimised.

The properties of the pellets are given in Tables 3.4 and 3.5. The wet weight (i.e. weight before drying) is also given where the weight of the graphite-cup is removed. From the tables the density of the pellets can be seen, where the coke pellets have a higher density than charcoal. The average density for the coke pellets is 1149 kg/m^3, and for charcoal the average density is 691 kg/m^3. From the tables the load when pressing the pellets is given. From this, there can not be seen any significant difference in the density on whether what load is used. Five random graphite cups were selected so that the average properties could be calculated. The properties of the graphite cups are given in Table 3.6.

Table 3.4: Properties of the coke pellets

	Mass pressed [g]	Wet weight [g] (Wet weight without graphite cup [g])	Dry weight [g]	Dry height [mm]	Density $[\frac{kg}{m^3}]$	Load on the press [kg]
1	0.37	0.66 (0.34)	0.59	5.28	1148	1000
2	0.37	0.65 (0.32)	0.58	5.24	1098	1000
3	0.36	0.67 (0.35)	0.59	5.26	1136	1000
4	0.41	0.71 (0.38)	0.62	5.71	1119	1000
5	0.38	0.68 (0.35)	0.59	5.33	1131	1000
6	0.34	0.64 (0.31)	0.56	4.96	1132	1000
7	0.35	0.66 (0.33)	0.58	5.09	1190	1000
8	0.36	0.66 (0.33)	0.58	5.24	1094	1000
9	0.35	0.63 (0.31)	0.55	5.04	1075	500
10	0.41	0.67 (0.35)	0.61	5.23	1253	2000
11	0.35	0.67 (0.35)	0.59	5.06	1259	1000

Table 3.5: Properties of the charcoal pellets

	Mass pressed [g]	Wet weight [g] (Wet weight without graphite cup [g])	Dry weight [g]	Dry height [mm]	Density $[\frac{kg}{m^3}]$	Load on the press [kg]
1	0.30	0.62 (0.29)	0.51	5.82	662	1000
2	0.37	0.68 (0.36)	0.55	6.33	702	1000
3	0.31	0.63 (0.31)	0.52	5.88	690	1000
4	0.29	0.63 (0.30)	0.52	5.89	703	1000
5	0.39	0.69 (0.37)	0.55	6.54	688	1000
6	0.38	0.70 (0.37)	0.56	6.62	684	1000
7	0.35	0.66 (0.33)	0.53	6.19	680	1000
8	0.35	0.66 (0.33)	0.54	6.17	703	1000
9	0.35	0.68 (0.36)	0.56	6.59	688	500
10	0.38	0.66 (0.33)	0.52	5.94	678	2000
11	0.34	0.67 (0.34)	0.54	6.24	697	500
12	0.37	0.67 (0.35)	0.55	6.26	719	2000
13	0.32	0.65 (0.33)	0.53	5.94	709	1000
14	0.32	0.63 (0.31)	0.52	5.87	716	500
15	0.32	0.65 (0.32)	0.52	6.28	639	500

Table 3.6: Properties of graphite cups

	Weight [g]	Outer diameter [mm]	Inner diameter [mm]	Outer height [mm]	Inner height [mm]
1	0.33	9.96	7.99	3.06	0.98
2	0.33	10.00	8.03	3.01	1.2
3	0.33	9.98	8.05	3.07	1.1
4	0.33	10.00	8.00	3.02	1.0
5	0.33	9.98	8.05	3.01	0.99
Average	0.33	9.984	8.024	3.03	1.05

As discussed in Chapter 2.4 it is important that the surface of the pellets is as flat and even as possible. From Tables 3.5 and 3.4 it can be seen that there is a somewhat large difference between the mass pressed and the wet weight, which is the weight of the pellet after it has been pressed. Some of this weight loss is water being pressed out, although there can be seen a difference between the loss of mass between some of the pellets. Hence, there is a loss of mass other than water. If the difference between these is large, there is probably more mass stuck to the press, which can lead to a more uneven surface. **Hosum** (2019) found that there was a difference in the behaviour of the slag when using the same substrate, which can be explained by differences in the pellets [40]. Figure 3.2 shows two photographs of a pellet on the press after pressing. The surface in the middle indicated by the arrow is in direct contact with the top of the pellet. From Figure 3.2a it can be seen that there is some material stuck to the press, hence the surface of this pellet will

be uneven. Figure 3.2b shows little mass from the pellet stuck to the press, which makes this pellet more suitable for the experiments compared to the pellet in Figure 3.2a as it is flatter. However, even if there is little material stuck to the press there are still some that do, hence the pellet is not completely flat.

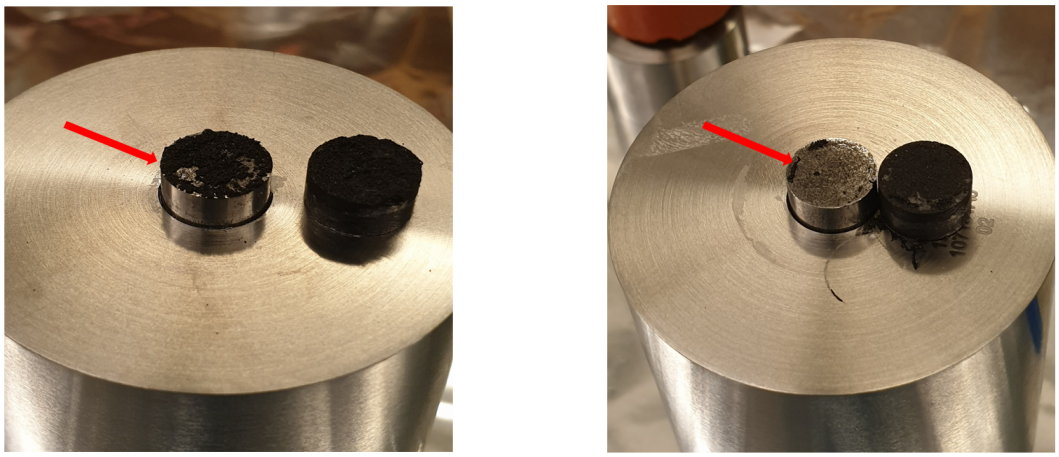

(a) Mass from the pellet stuck to the press *(b) Little mass from the pellet stuck to the press*

Figure 3.2: Photographs of the pellet and the press after pressing showing that there can be much or little mass stuck to the press

As was mentioned above, there was performed experiments where the pellets were pressed with different loads on the uni-axial press. This was performed to investigate if there are any differences in the reduction of the slag when using a different load. The different loads used on the press in this study is 500 kg, 1000 kg and 2000 kg. Figure 3.3 shows the density of the pellets as a function of the load used when pressing. From this figure it can be seen that when the load is increased the density of the pellets increase, up to a certain point at least [54]. The blue triangles and the blue stars are the density of the materials used in this study. As mentioned earlier, there can be seen no significant difference between the density of the pellets in this study. However, the coke pressed with 2000 kg has a higher density than the other two points in this figure, there was also pellets pressed with 1000 kg with approximately the same density (see Table 3.4). Furthermore, there was made much more pellets with 1000 kg compared to 500 kg and 2000 kg, which means that for example coke pressed with 2000 kg could be an outlier.

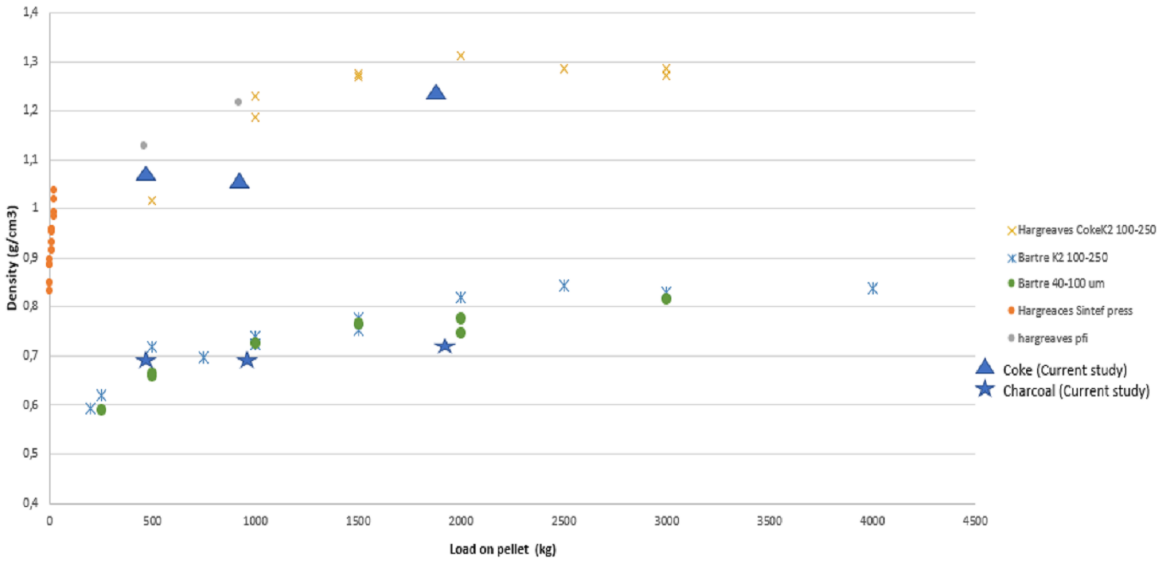

Figure 3.3: Density (kg/m^3) as a function of load (kg) for different carbon materials. Hargreaves is a coke, which is the orange dots, yellow crosses and grey dots, and charcoal are the blue crosses and green dots [54]

As mentioned earlier, one of the reasons for pelletizing the materials was to achieve more similar physical properties there is still some difference regarding density between coke and charcoal.

There was also studied the effect of green coke and charcoal. For these experiments, a piece of coke and charcoal was cut and polished by hand to a size that would fit inside the furnace. It is also important that the surface is even so the liquid slag droplet does not roll off during the experiment. There was made one particle of green coke and two with charcoal. The two charcoal particles were made so one of them had the top of the fibres on the surface, and the other was made such that the surface was along the tree fibres. The weight of the coke pellet before the experiment was 0.26 g, and for the charcoal it was 0.16 g and 0.13 g for test 26 and 27, respectively. Both the coke and charcoal have been analysed, where a chemical analysis was performed by SINTEF Norlab, and a porosity and density analysis performed by Irene Bragstad from SINTEF. The results from these analysis are given in Chapters 4.1.1 and 4.1.2. The charcoal used in this study is from eucalyptus which is supplied from the industry and the coke used is a Hargreaves coke.

There was also done experiments where graphite was used as the substrate. The experiments with graphite are to further investigate the difference between whether the slag contains sulfur or not. The mass of the graphite pellets is 0.43 g for both the pellets. Unlike the coke and charcoal, the graphite has not been analysed. However, from other studies it has been found that graphite in general has a very high fixed carbon content (>99 wt%) and very low ash content; 0.3 wt% [55], <0.1 wt% [31] and 0.04 wt% [29].

3.2 Sessile drop furnace

The experiments were carried out in a sessile drop furnace. The furnace is circular with an outer shell of steel with graphite element inside as insulation. The coke/charcoal pellets and the slag pellets are placed on the sample holder and then pushed inside the furnace, and then closing the furnace. Before the experiments start, the gas/air inside the furnace is removed, making a vacuum. Argon gas is then pumped in the furnace so that the pressure is atmospheric. When the sample is pushed inside the furnace the Argon gas (and air) is then removed, which again creates a vacuum. Then CO gas is pumped into the furnace, which is the atmosphere the experiments were conducted in. When the pressure of the CO gas was atmospheric the flow rate of the gas was changed to 0.1 L/min, which was during the entire experiment. The temperature in the furnace is controlled by a thermocouple placed inside the furnace and a Keller PZ40 pyrometer.

The experiments on the sessile drop furnace were mainly performed by the author of this thesis, although, due to the situation regarding Covid-19, six of the experiments were performed by Ingrid Hansen from SINTEF.

In Figure 3.4 a schematic overview of a sessile drop furnace is given, and from the figure it can be seen that there is a camera which takes pictures of the experiment. The camera used to take the pictures is a Basler acA1280-60gc. From these pictures, the general behaviour of the reduction of the slag can be investigated. Furthermore, several parameters can be measured from these pictures such as the expansion of the slag, the wetting angle and the contact area between the slag and the substrate. Figure 3.5 shows some of these pictures. Figure 3.5a is at the start of the experiment where the slag pellet is seen on top of the substrate. Figures 3.5b and 3.5c shows the slag starts to soften and melt, and Figure 3.5d shows a completely melted slag. From Figure 3.5d and the pictures similar to this the wetting angle and the volume measurements are performed. During this experiment there were taken 5 frames per second from 1300 °C to 1600 °C and during the holding time.

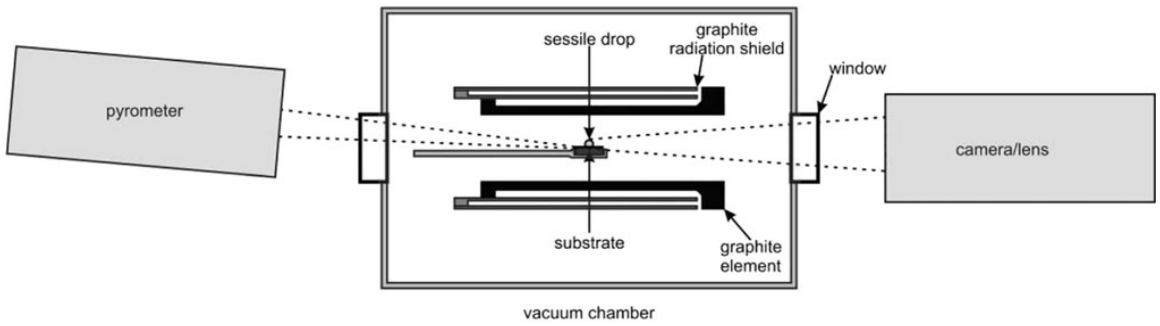

Figure 3.4: Schematic overview of the sessile drop furnace [56].

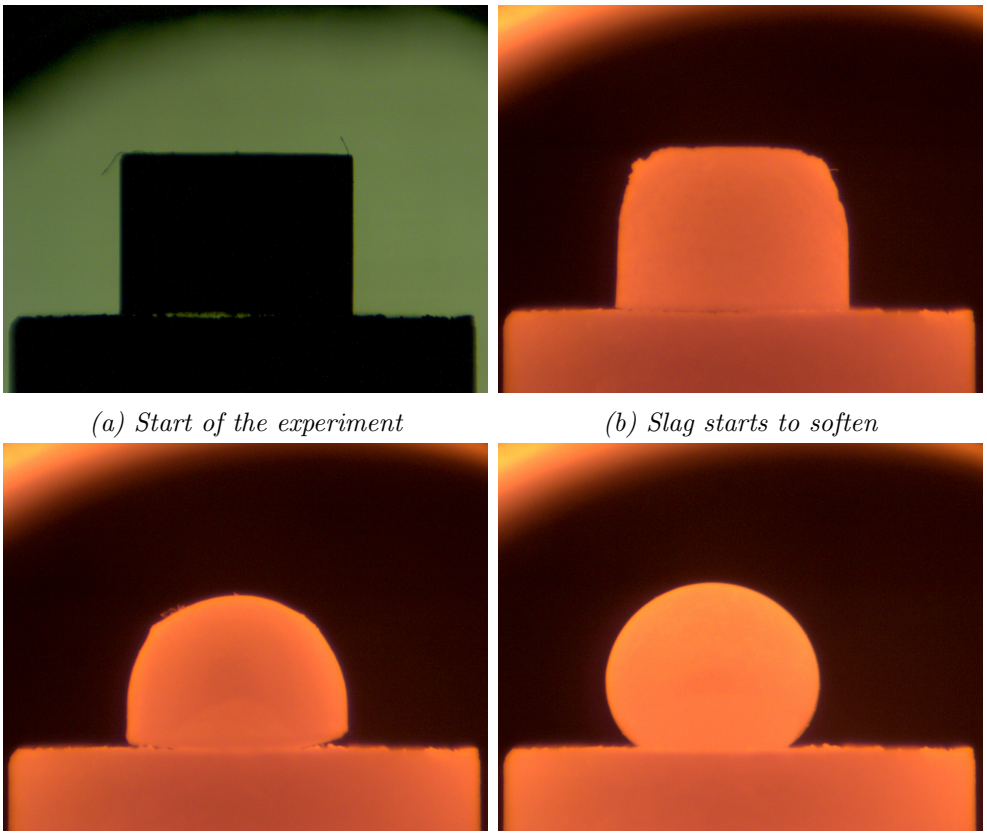

(a) Start of the experiment *(b) Slag starts to soften*

(c) Slag is almost melted *(d) Slag is completely melted*

Figure 3.5: Pictures from the sessile drop furnace

As mentioned above, the pictures taken off the experiment is analysed. To perform this analysis, a software called ImageJ has been used. The toolbar from this software is given in Figure 3.6, and from this it can be seen that there are several different tools to analyse the pictures. Furthermore, to analyse the pictures (or video), it is made binary colours (i.e. black and white), which is shown in Figure 3.7a. To measure the expansion of the slag droplet, a line is drawn to separate the slag from the substrate, using the line tool (5th from the left in Figure 3.6), and then the "wand" tool (7th from the left on Figure 3.6) is used to trace around the slag droplet, which can be seen in Figure 3.7b. This is then done on each frame in the video which will give the expansion-plot or the relative volume. Furthermore, the line tool can also be used to measure length, for example to measure the contact area between the slag and the substrate or the length of the substrate. For measuring the wetting angle, the "angle tool" is used (6th from the left on Figure 3.6), which is the yellow line in Figure 3.7c.

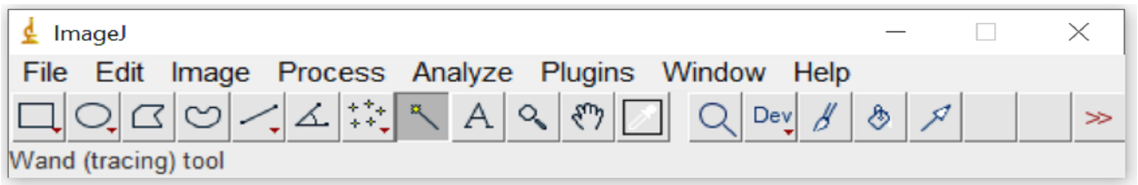

Figure 3.6: Screenshot of the toolbar in ImageJ

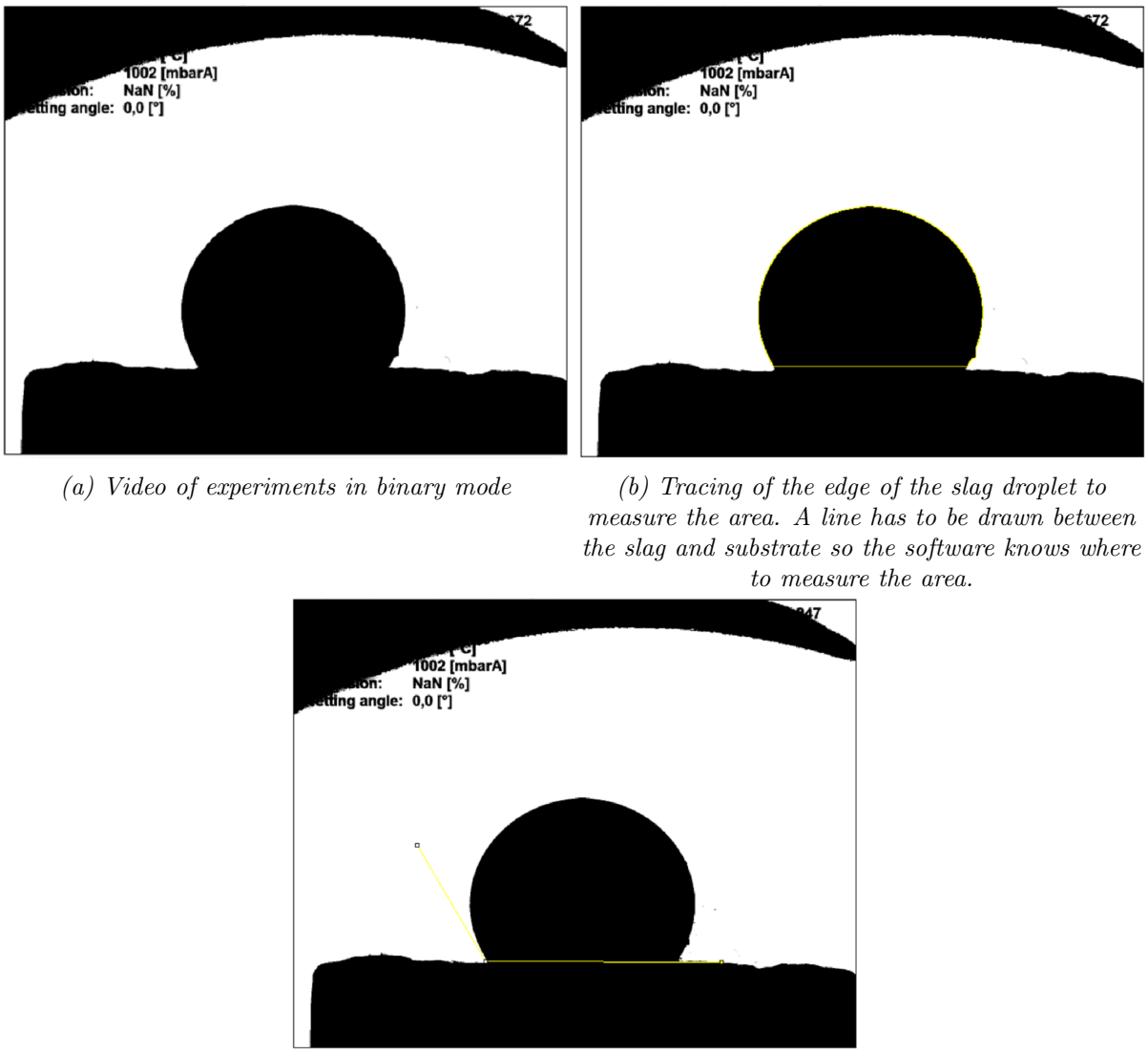

(a) Video of experiments in binary mode

(b) Tracing of the edge of the slag droplet to measure the area. A line has to be drawn between the slag and substrate so the software knows where to measure the area.

(c) Measure the wetting angle between the slag and substrate

Figure 3.7: Screenshots from ImageJ: Measurements of area and wetting angle of the videos from the experiments

Because it is photographs that are analysed they are two-dimensional. Hence, it is the area that is measured and not the volume. The relative volume was then calculated from Equation 39. The reference area was chosen when the temperature was 1300 °C.

$$\left(\frac{A}{A_0}\right)^{2/3} = \frac{V}{V_0} \tag{39}$$

This also applies for calculating the contact area between the slag and the substrate. It is assumed that the area between the slag and substrate is a perfect circle and that the length measured is the diameter in this circle, and then the area is calculated.

ImageJ gives good results, but it is very time-consuming to analyse every frame from the video of the experiment. As a consequence of this, when measuring the wetting angle and the contact area between the slag and substrate, not every frame was analysed. When

measuring the wetting angle very 100th frame was measured, and every 1000th frame for the contact area. For the experiments which were held at 15, 30 and 60 minutes have approximately 5800, 9000 and 14000 frames respectively. One problem with this method of analysing the videos, other than being time-consuming, is that it is a fairly manual method. When measuring the area of the slag droplet it is possible that the line drawn between the slag and substrate is not always on the same place, which will influence the measurement. Furthermore, when measuring the wetting angle, the line in Figure 3.7c is dragged by hand from the substrate into the edge of the slag droplet, which will create some uncertainty on the measurements.

The holding temperature was set to 1600 °C in this study, and the samples were held at 15, 30 and 60 minutes at this temperature. The heating schedule is given in Figure 3.8. It takes 6 min and 30 seconds to heat up to 1270 °C, where it is held for 1 minute. After this, it takes 2 minutes to heat up to 1600 °C. Due to some problems with the thermocouple in the furnace, some of the experiments were performed at 1550 °C and one experiment at 1700 °C. The heating rate was the same for all the experiments, regardless of the holding temperature.

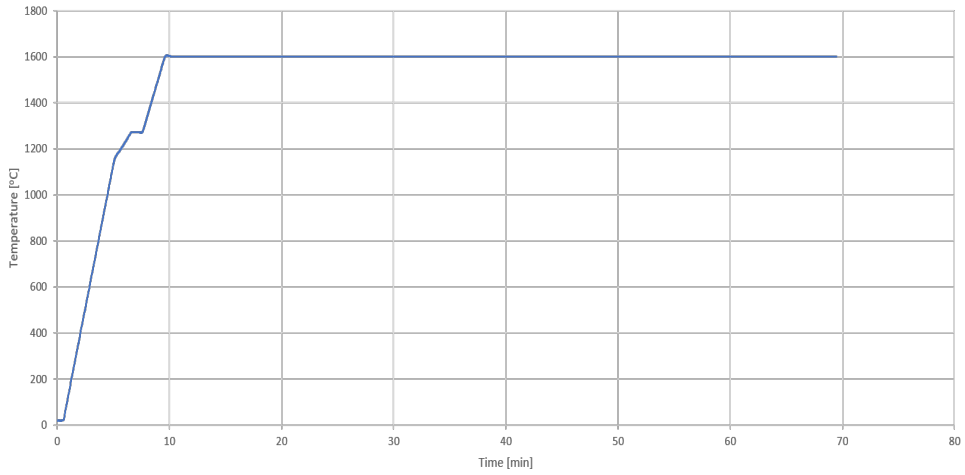

Figure 3.8: Time schedule used in the experiments in sessile drop furnace, where the holding temperature is 1600 °C.

There has been performed 31 experiments in this study. An overview of these are given in Table 3.7. First, to compare coke and charcoal it was performed 4 experiments with both coke and charcoal, with the holding times of 0 min, 15 min, 30 min and 60 min. These experiments were performed with both slag1 (with sulfur) and slag2 (without sulfur), so that the total number of experiments is 16 to compare coke and charcoal. Other parameters have also been investigated in this report, such as different load on the press. The coke/charcoal pellets on the first 16 experiments had a load of 1000 kg. It was performed experiments where a load of 500 kg and 2000 kg was used on the coke/charcoal pellets. There was also performed experiments on "green" particles of coke and charcoal. The "green" particles are not crushed to a powder but cut and polished into a size that fits inside the furnace, and also even surfaces so that the liquid slag droplet does not roll of inside the furnace during the experiment. Furthermore, it was done two experiments

with green charcoal, one along the fibre direction, and one on top of the fibre direction. Lastly, there was done two experiments, one with slag1 and one with slag2 where graphite was used as the substrate to further investigate the difference between slag1 and slag2. Some of the experiments have different holding temperatures, and because temperature is a crucial parameter for this process the results with different temperatures can not be directly compared.

Table 3.7: Overview of experiments in sessile drop furnace. Slag1 contains sulfur, and slag2 does not. Pressure is the pressure used when pressing the pellets in the uni-axial press. Holding time is the time the materials were at the given holding temperature in the furnace.

Test	Carbon material	Slag	Pressure (kg)	Holding time (min)	Holding temperature (°C)
1	Coke	1	1000	15	1600
2	Coke	1	1000	30	1600
3	Coke	1	1000	60	1600
4	Coke	1	1000	0	1600
5	Coke	2	1000	15	1600
6	Coke	2	1000	30	1600
7	Coke	2	1000	60	1600
8	Coke	2	1000	0	1600
9	Charcoal	1	1000	15	1600
10	Charcoal	1	1000	30	1600
11	Charcoal	1	1000	60	1600
12	Charcoal	1	1000	0	1600
13	Charcoal	2	1000	15	1600
14	Charcoal	2	1000	30	1600
15	Charcoal	2	1000	60	1600
16	Charcoal	2	1000	0	1600
17	Coke	2	500	30	1600
18	Coke	2	2000	30	1600
19	Charcoal	1	500	30	1600
20	Charcoal	1	2000	30	1600
21	Charcoal	2	500	30	1600
22	Charcoal	2	2000	30	1600
23	Coke	1	1000	30	1550
24	Coke	1	Green	30	1550
25	Charcoal	1	1000	30	1550
26	Charcoal	1	Green - top	30	1550
27	Charcoal	1	Green - along	30	1550
28	Graphite	1	-	30	1550
29	Graphite	2	-	30	1550
30	Charcoal	1	500	30	1700
31	Charcoal	2	500	30	1550

3.3 Surface roughness

As discussed in Chapter 2.4 the surface of the pellet is important. The surface of the pellet should ideally be flat but as shown in Figure 3.2 the pellet are not completely flat and they could also be different. Therefore, an analysis of the surface roughness has been performed. A 3D optical microscope measures the surface roughness. The microscope used in this study was Alicona Infinite Focus G4, and the analysis was performed by Cristian Torres Rodriguez from NTNU. This microscope uses variations in the focus to measure the roughness of the surface. 10 samples were analysed where 5 was charcoal, 4 was coke and one graphite, which can be seen in Table 3.8.

Table 3.8: Samples sent to surface roughness analysis

Material	Type of pellet
Charcoal	500 kg
Charcoal	1000 kg
Charcoal	2000 kg
Charcoal	Green - Along the fibres
Charcoal	Green - On top of the fibres
Coke	500 kg
Coke	1000 kg
Coke	20000 kg
Coke	Green
Graphite	-

3.4 Porosity and density analysis

In this experiment, 8 samples were sent to porosity and density analysis, 4 of both coke and charcoal. There was sent 1 green particle and 3 pellets with a load of 500, 1000 and 2000 kg, respectively. The analysis was performed by Irene Bragstad from SINTEF.

Absolute/apparent density is obtained when the volume measured excludes the pores as the void spaces between particles in the bulk sample. Helium or other gases are used to measure the volume. the absolute density determined by helium pycnometry is often referred to as "helium density".

Envelope density (also called bulk density) is determined for porous materials when pore spaces within material particles are included in the volume measurement. To measure this a free-flowing dry powder (e.g. sand) is used. The material to be tested is surrounded by this medium that does not penetrate pores but conforms to irregular surfaces to form a tight-fitting envelope. envelope density values are less than absolute density when the material is porous, they are equal for non-porous materials.

3.5 Analysis of the samples

After the experiments in the sessile drop furnace the samples were analysed.

3.5.1 Chemical analysis of coke and charcoal

Samples of coke and charcoal sent to SINTEF Norlab (Previously known as MOLAB), to get a chemical analysis of the carbon material, such as the content of fixed carbon, amount of volatiles and ash composition.

3.5.2 Chemical analysis of the slag

Electron probe micro analyser (EPMA) is a type of electron microscope, which is used to provide chemical information of a specimen. It has many similarities as an SEM, but the chemical analysis from the EPMA is mostly better than SEM. An electron microprobe works under the principle that a solid specimen is bombarded by an electron beam, and this ray of electrons has sufficient energy to generate x-rays from the material [57, 58].

The EPMA has a dedicated operator at NTNU, so after the samples were prepared they were given to the operator of the microscope to perform the analysis. The operator which performed the analysis for this study was Morten Peder Raanes. It was done 3 point analysis on each slag droplet. The 3 points were randomly selected on the prepared surface. On the samples that contained a metal phase 3 points on this surface was analyzed to get the composition of the metal.

All the slag samples were analysed in the EPMA. Before the analysis, the samples were cast in epoxy and then grinded and polished. Some of the samples were cast with the substrate. In many of the experiments the slag droplet did not stick to the substrate afterwards and could therefore not be cast together. Another reason for not to cast the substrate and slag together was that some of the substrates were fragile after the experiment and would disintegrate. Before the samples are to be analysed in the EPMA they have to be wrapped with aluminium foil and coated with carbon to make the samples conductive.

Scanning electron microscope (SEM) is a type of microscope that used accelerated electrons to investigate a sample. When the electron hits the sample it will generate secondary electrons, backscatter electrons and x-rays. The secondary electrons can be used to take pictures of the surface and to investigate the topography. The x-rays can be analysed by using an electron dispersive spectrometer (EDS), which can identify the elements in the sample [59, 60]. In this study, secondary electrons were used for taking pictures and EDS analysis of the samples.

4 Results

In this report the differences between coke and charcoal have been investigated in addition to the influence of sulfur on the reduction of slag in the SiMn production. There has been performed experiments in a sessile drop furnace to investigate this. After the experiments in the sessile drop furnace the samples were analysed in EPMA, SEM and OM. The pictures taken in the furnace during the experiments were also analysed to find the relative volume of the slag, the wetting angle and contact area between the slag and the substrate throughout the experiments in the furnace.

In the following chapter the results from this study will be presented. First, some analyses of the coke and charcoal and the pellets. Second, the chemical analysis from the EPMA. Lastly the analysis of the pictures from the experiments in the sessile drop furnace, where relative volume of the slag, wetting angle between the slag and substrate and the contact area between the slag substrate is measured.

4.1 Properties of coke and charcoal substrates

Coke and charcoal have been investigated in this study. There have been performed a chemical analysis of the coke and charcoal in addition to a density and porosity analysis of the materials. Lastly, a surface roughness analysis has been performed to investigate the surface of the pellets.

4.1.1 Chemical analysis of coke and charcoal

Table 4.1 shows the results from the analysis of the coke and charcoal performed by SINTEF Norlab. From the table, it can be seen that the content of fixed carbon is approximately the same for both coke and charcoal. The amount of volatile matter is much higher for charcoal than for coke, but coke has a higher content of ashes. From the ash composition, it can be seen that coke has a higher content of sulfur and SiO_2 compared to coke, but coke has a higher amount of alkali and alkaline earth metals, such as calcium, magnesium and potassium.

Table 4.1: Analysis of charcoal and coke from SINTEF Norlab

Parameter	Charcoal [%]	Coke [%]
H_2O	2.24	0.24
Fixed Carbon	85.27	85.74
Volatile matter	14.53	2.07
Ashes	0.80	12.19
Ash composition		
SiO_2	22.00	53.2
Fe_2O_3	0.20	6.7
Al_2O_3	0.30	22.7
P_2O_5	11.32	0.69
CaO	30.95	7.8
MgO	10.70	5.1
K_2O	19.72	1.55
S	0.01	0.61
TiO_2	0.01	1.28
MnO	4.36	0.09
Na_2O	0.11	0.78

4.1.2 Porosity and density analysis

Table 4.2 shows the results from the porosity and density analysis of coke and charcoal. From the table it can be seen that there is very little difference between the coke/charcoal with the different pressures used when making the pellets. For both coke and charcoal the porosity is higher for the green particle compared to the pellets, and especially for charcoal which has a significant decrease in porosity. Hence, the density will then be larger for the pellets compared to the green particles. It can also be noted that the apparent density of the material is not expected to change with pressure, and hence the variances in these numbers may show the variance in the raw material as well as in the measuring method.

Table 4.2: Results from porosity and density analysis. Numbers in brackets behind the samples is the load on the press when making the pellets.

Sample	Porosity [%]	Envelope density [g/cm^3]	Apparant density [g/cm^3]
Charcoal (Green)	79.4	0.31	1.52
Charcoal (500kg)	49.1	0.73	1.43
Charcoal (1000kg)	48.7	0.73	1.43
Charcoal (2000kg)	52.1	0.68	1.43
Coke (Green)	42.5	1.02	1.77
Coke (500kg)	36.0	1.20	1.87
Coke (1000kg)	34.3	1.23	1.87
Coke (2000kg)	35.5	1.24	1.92

4.1.3 Surface roughness analysis

In this study, a 3D optical microscope was used to analyse the surface roughness of the pellets. From the analysis three parameters were found, which is R_a (Average roughness), R_q (root mean square roughness) and R_z (maximum peak-to-valley height). These parameters are given in Table 4.3. In this analysis, there was done three measurements on each of the pellets, except graphite where only one measurement was done. These measurements were done in the top part, middle and bottom part of the chosen area. The results given in the table is the average of these three measurements, where the standard deviation is also given which states in some cases there was a significant difference between the three measurements. The full analysis can be seen in Appendix A1. From the table, it can be seen that the roughness decreases with the load, for both charcoal and coke. Furthermore, the coke pellets have a higher average surface roughness compared to charcoal. This could also be seen when making the pellets, as the coke got more stuck to the press than charcoal. The green coke has a much higher surface roughness compared to all the other, where the green charcoal pellets had a very low surface roughness, especially the one that was made on top of the tree fibres.

Table 4.3: Results from surface roughness analysis. The average of the three analysis and the standard deviation is given, where the full analysis is given in Appendix A1. No standard deviation given for graphite as it was only performed one analysis.

Material	Type of pellet	R_a [µm]	R_q [µm]	R_z [µm]
Charcoal	500 kg	5.34 ± 0.44	7.92 ± 0.35	50.83 ± 1.97
Charcoal	1000 kg	4.94 ± 0.56	6.93 ± 0.82	45.00 ± 5.25
Charcoal	2000 kg	3.33 ± 0.24	5.05 ± 0.81	31.11 ± 4.71
Charcoal	Green - Along the fibres	16.11 ± 2.85	22.31 ± 4.02	91.33 ± 22.08
Charcoal	Green - On top of the fibres	4.63 ± 1.04	7.26 ± 2.99	62.48 ± 39.40
Coke	500 kg	18.20 ± 5.74	24.01 ± 7.35	107.97 ± 16.33
Coke	1000 kg	10.91 ± 1.44	15.64 ± 1.47	84.78 ± 3.45
Coke	20000 kg	9.67 ± 0.95	13.64 ± 1.48	75.69 ± 5.75
Coke	Green	89.76 ± 13.12	124.14 ± 20.76	414.04 ± 62.15
Graphite	-	3.69	4.54	20.82

Figures 4.1 to 4.10 shows the surface roughness analysis for the pellets given in the table above. From each figure a colour range of the surface from the chosen area in the middle of the pellet can be seen, and also a graph showing the roughness of the surface. Note that there are different colour ranges and ranges of the graphs for some of the pellets, and also different ranges on the y-axis on the graphs. The area measured is 10 mm long (i.e. full length of the pellet) and approximately 550 µm wide. From these figures, it can be seen that on the pellet there are peaks and valleys, which explains the differences when measuring the surface roughness on different places in the chosen area. As mentioned above, there was performed three analysis of each pellet, except graphite, and the full

analysis can be found in Appendix A1.

Figure 4.1 shows the surface roughness of pelletized charcoal made with a load of 500 kg. From the analysis, it can be seen that there are some valleys, and also a crack can be seen. In this case, R_a is 5.01 µm, R_q is 7.52 µm and R_z is 48.70 µm. The average of all three measurements can be seen in Table 4.3.

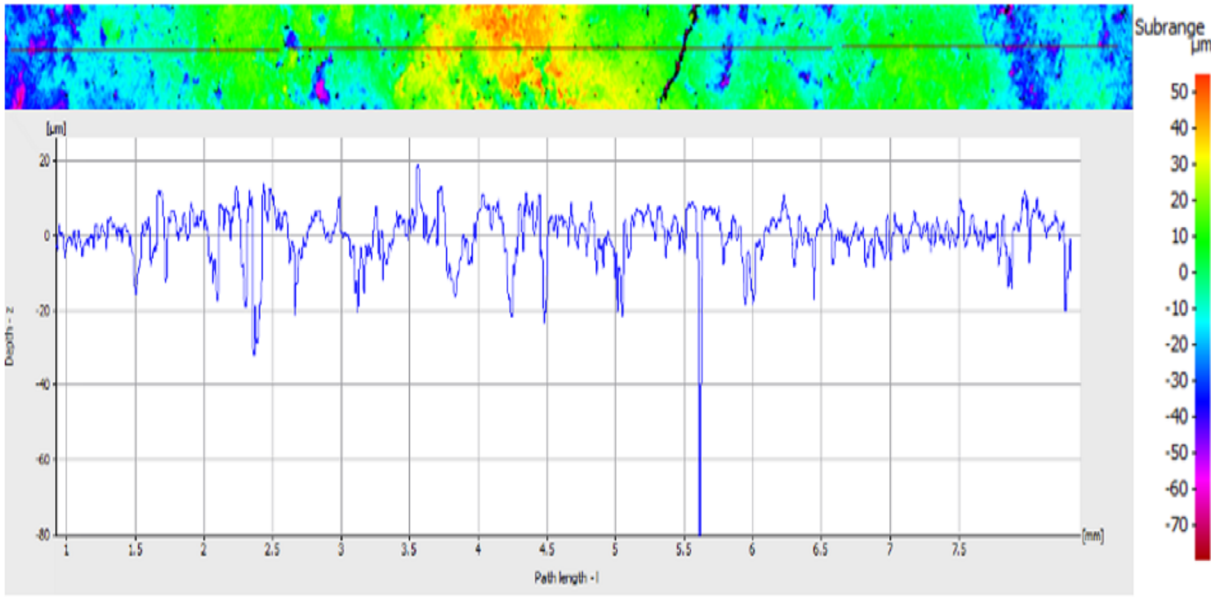

Figure 4.1: Analysis of the surface roughness for pelletized charcoal, made with a load of 500 kg on the press. Above the graph is a picture of the selected area of the pellet, showing the roughness of the surface. The line through the picture of the area shows where the analysis have been done.

Figure 4.2 shows the surface roughness of pelletized charcoal made with a load of 1000 kg. From the analysis, it can be seen that there are some valleys and peaks and is very similar to Figure 4.1. In this case, R_a is 4.62 µm, R_q is 6.43 µm and R_z is 40.14 µm. The average of all three measurements can be seen in Table 4.3.

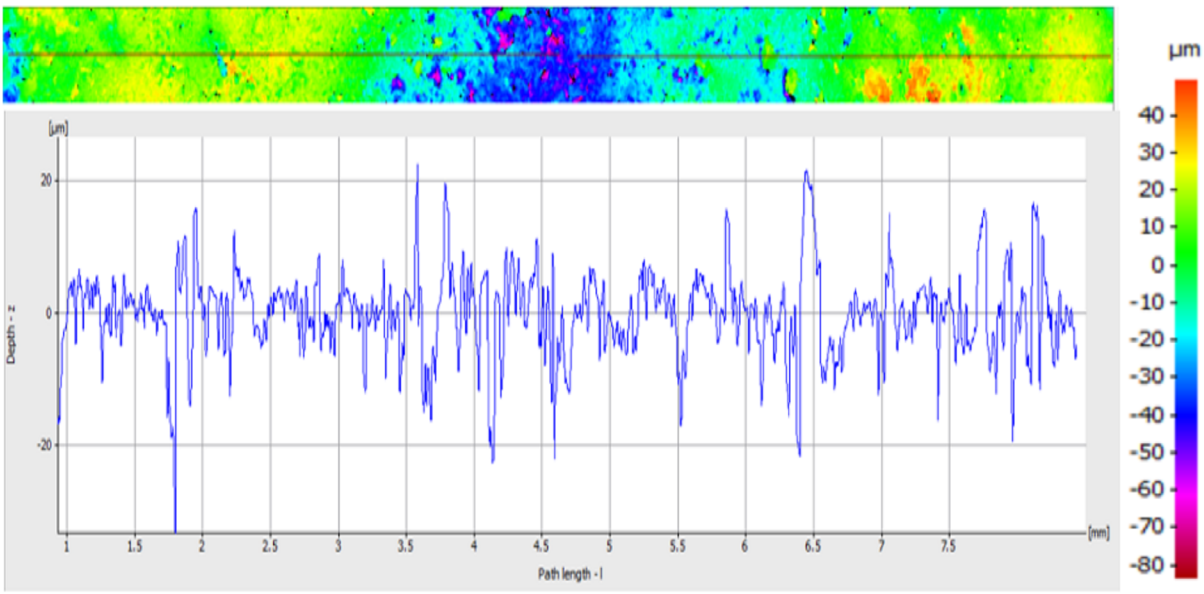

Figure 4.2: Analysis of the surface roughness for pelletized charcoal, made with a load of 1000 kg on the press. Above the graph is a picture of the selected area of the pellet, showing the roughness of the surface. The line through the picture of the area shows where the analysis have been done.

Figure 4.3 shows the surface roughness of pelletized charcoal made with a load of 2000 kg. From the analysis, it can be seen that there are some valleys and peaks at the ends of the pellet, but in the middle, the roughness is fairly low. In this case, R_a is 3.65 µm, R_q is 6.19 µm and R_z is 37.71 µm. The average of all three measurements can be seen in Table 4.3, where it could be seen that the surface roughness decrease with increasing load used when making the pellets.

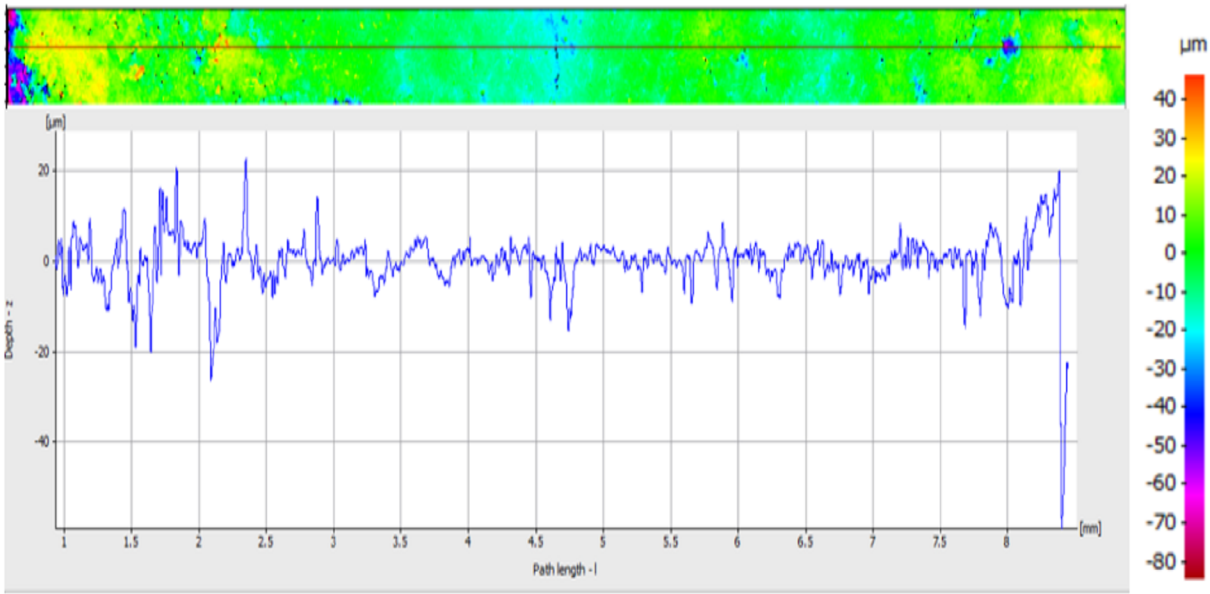

Figure 4.3: Analysis of the surface roughness for pelletized charcoal, made with a load of 2000 kg on the press. Above the graph is a picture of the selected area of the pellet, showing the roughness of the surface. The line through the picture of the area shows where the analysis have been done.

Figure 4.4 shows the surface roughness of green charcoal where the surface goes along the fibres. From the analysis, the fibres can be seen to some extent, as these are valleys. In this case, R_a is 14.46 µm, R_q is 19.42 µm and R_z is 74.28 µm. The average of all three measurements can be seen in Table 4.3. From the figure, it can be seen to the right the fibres in the charcoal.

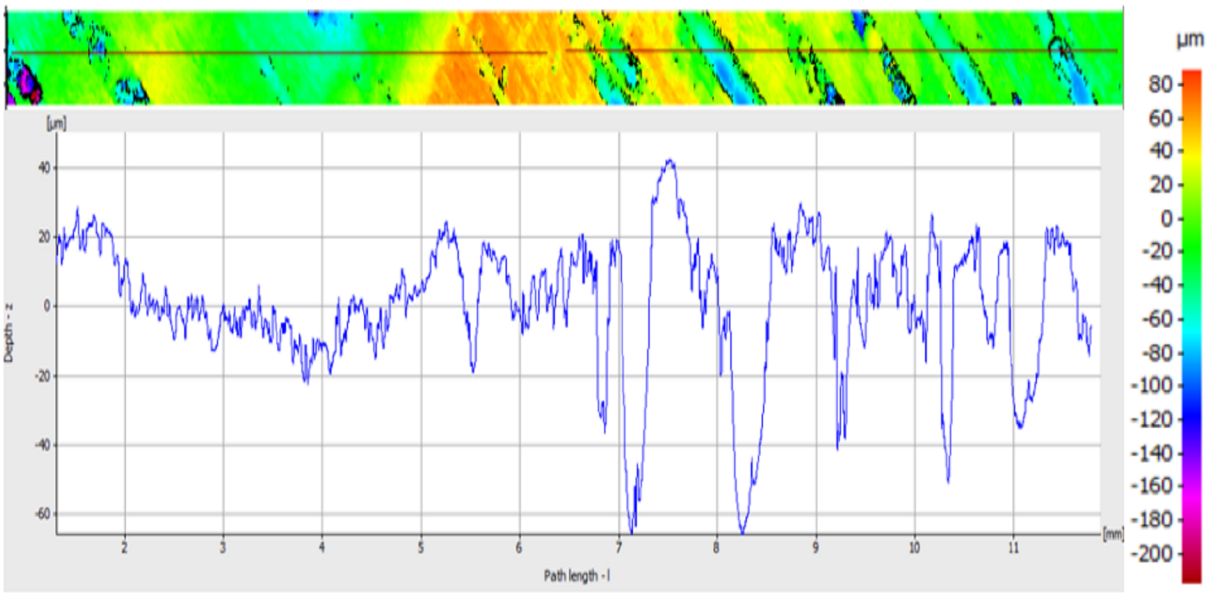

Figure 4.4: Analysis of the surface roughness for green charcoal where the surface is along the fibres. Above the graph is a picture of the selected area of the pellet, showing the roughness of the surface. The line through the picture of the area shows where the analysis have been done.

Figure 4.5 shows the surface roughness of green charcoal where the surface goes on top of the fibres. On the left-hand side of the pellet, some high peaks and low valleys can be seen. However, the rest of the pellet has a fairly low roughness. In this case, R_a is 5.93 µm, R_q is 11.37 µm and R_z is 117.52 µm. The average of all three measurements can be seen in Table 4.3. From this measurement the difference between the three parameters R_a, R_q and R_z is seen because R_z is much higher than the other two. Both R_a is R_q averages and will therefore not be as influenced by a few very high peaks and low valleys when the rest of the pellet has a low roughness.

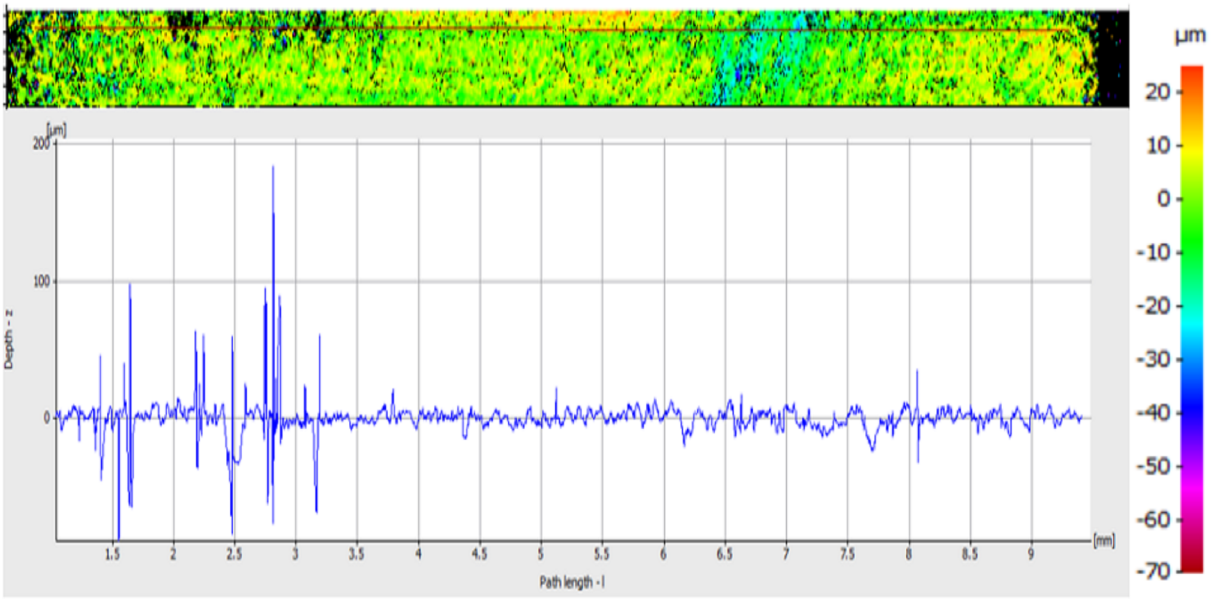

Figure 4.5: Analysis of the surface roughness for green charcoal where the surface is on top of the fibres. Above the graph is a picture of the selected area of the pellet, showing the roughness of the surface. The line through the picture of the area shows where the analysis have been done.

Figure 4.6 shows the surface roughness of pelletized coke made with a load of 500 kg. From the analysis, it can be seen that there are some very low valleys and a few peaks. In general, it has a higher roughness than charcoal pellets. In this case, R_a is 13.34 µm, R_q is 17.98 µm and R_z is 95.49 µm. The average of all three measurements can be seen in Table 4.3.

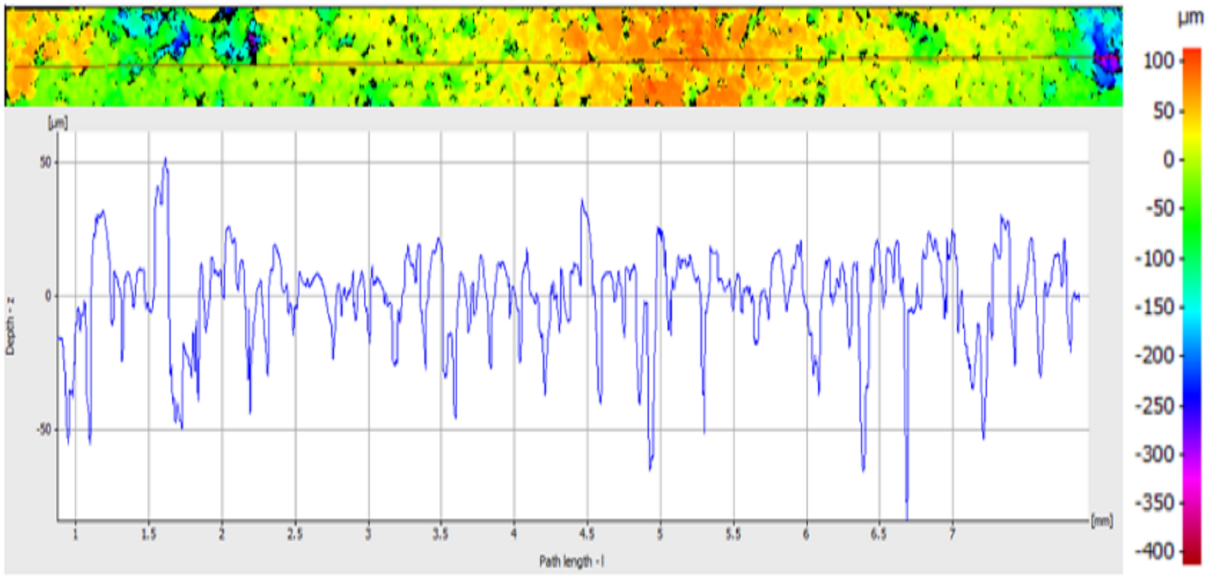

Figure 4.6: Analysis of the surface roughness for pelletized coke, made with a load of 500 kg on the press. Above the graph is a picture of the selected area of the pellet, showing the roughness of the surface. The line through the picture of the area shows where the analysis have been done.

Figure 4.7 shows the surface roughness of pelletized coke made with a load of 1000 kg.

From the analysis, it can be seen that there are some very low valleys and a few peaks. In this case, R_a is 10.15 µm, R_q is 15.40 µm and R_z is 88.19 µm. The average of all three measurements can be seen in Table 4.3.

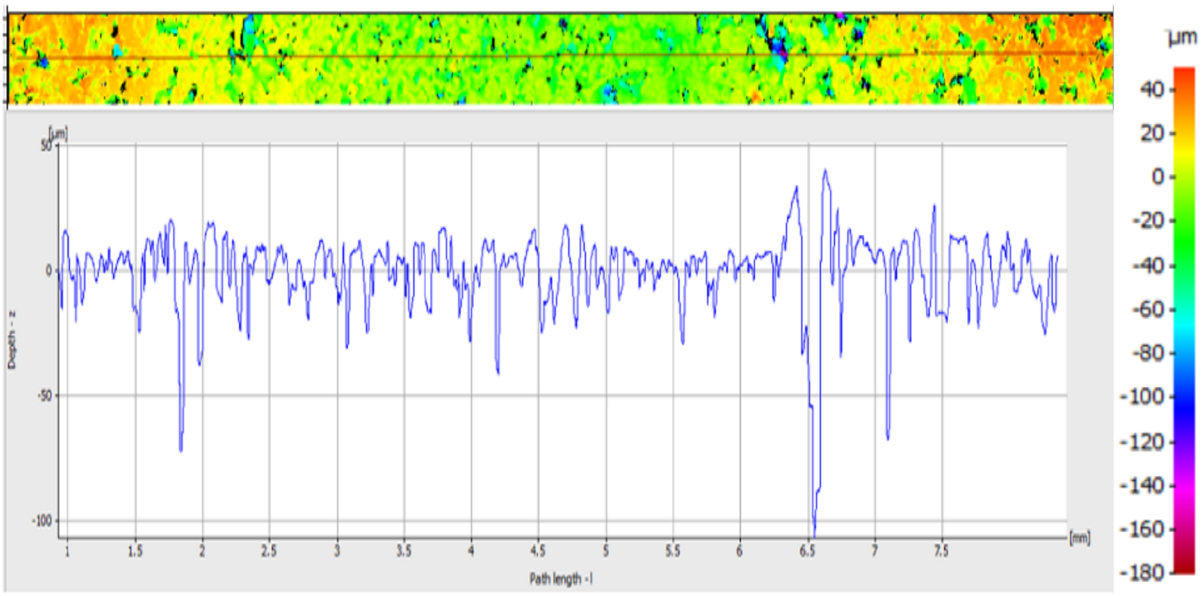

Figure 4.7: Analysis of the surface roughness for pelletized coke, made with a load of 1000 kg on the press. Above the graph is a picture of the selected area of the pellet, showing the roughness of the surface. The line through the picture of the area shows where the analysis have been done.

Figure 4.8 shows the surface roughness of pelletized coke made with a load of 2000 kg. From the analysis, it can be seen that the edges of the pellet have a higher roughness than the middle. In this case, R_a is 10.75 µm, R_q is 14.91 µm and R_z is 74.97 µm. The average of all three measurements can be seen in Table 4.3. The fact that the roughness decreased when increasing the load on the press could also be seen on the pelletized coke.

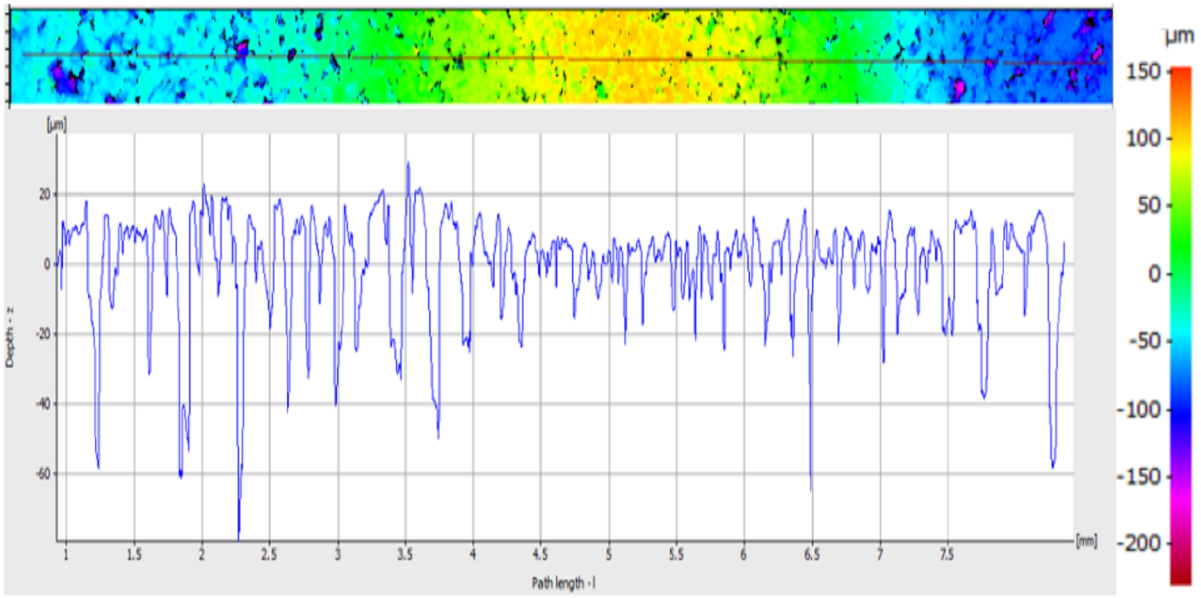

Figure 4.8: Analysis of the surface roughness for pelletized coke, made with a load of 2000 kg on the press. Above the graph is a picture of the selected area of the pellet, showing the roughness of the surface. The line through the picture of the area shows where the analysis have been done.

Figure 4.9 shows the surface roughness of the green coke. From the analysis, the pores are clearly shown. There are some very low valley and high peaks. In this case, R_a is 93.55 µm, R_q is 134.65 µm and R_z is 457.02 µm. The average of all three measurements can be seen in Table 4.3, where it also could be seen that green coke is by far the sample with the highest surface roughness.

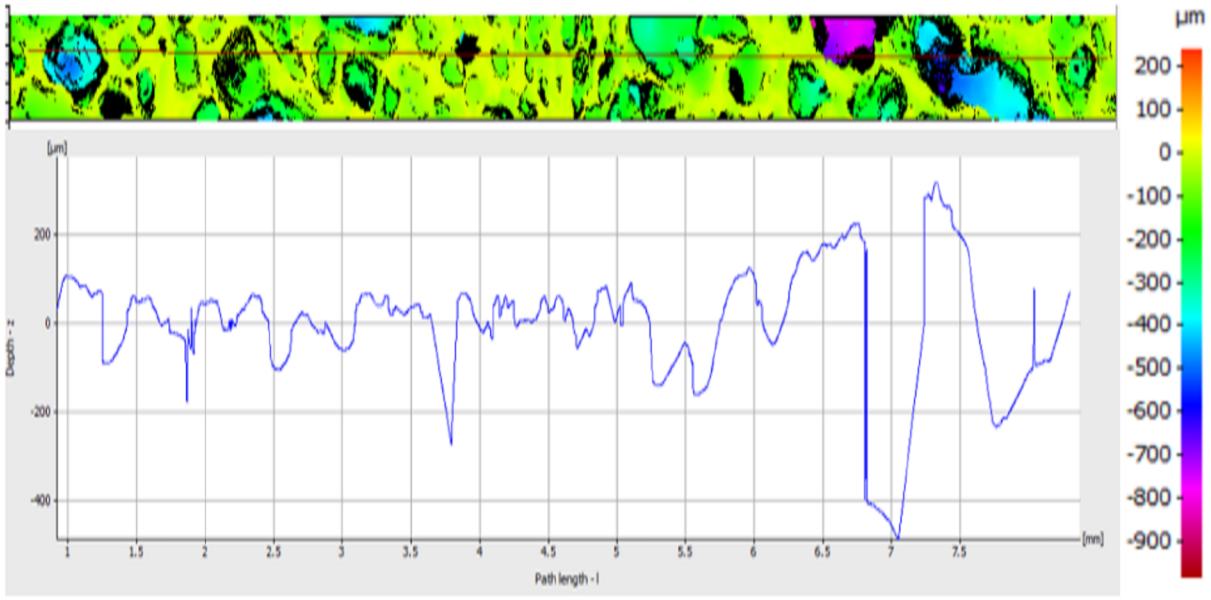

Figure 4.9: Analysis of the surface roughness for green coke. Above the graph is a picture of the selected area of the pellet, showing the roughness of the surface. The line through the picture of the area shows where the analysis have been done.

Figure 4.10 shows the surface roughness of a graphite pellet. From the analysis, it can be

seen that the surface roughness is evenly distributed along the surface, where the peaks and valley have approximately the same height and depth. In this case, R_a is 3.69 µm, R_q is 4.54 µm and R_z is 20.82 µm.

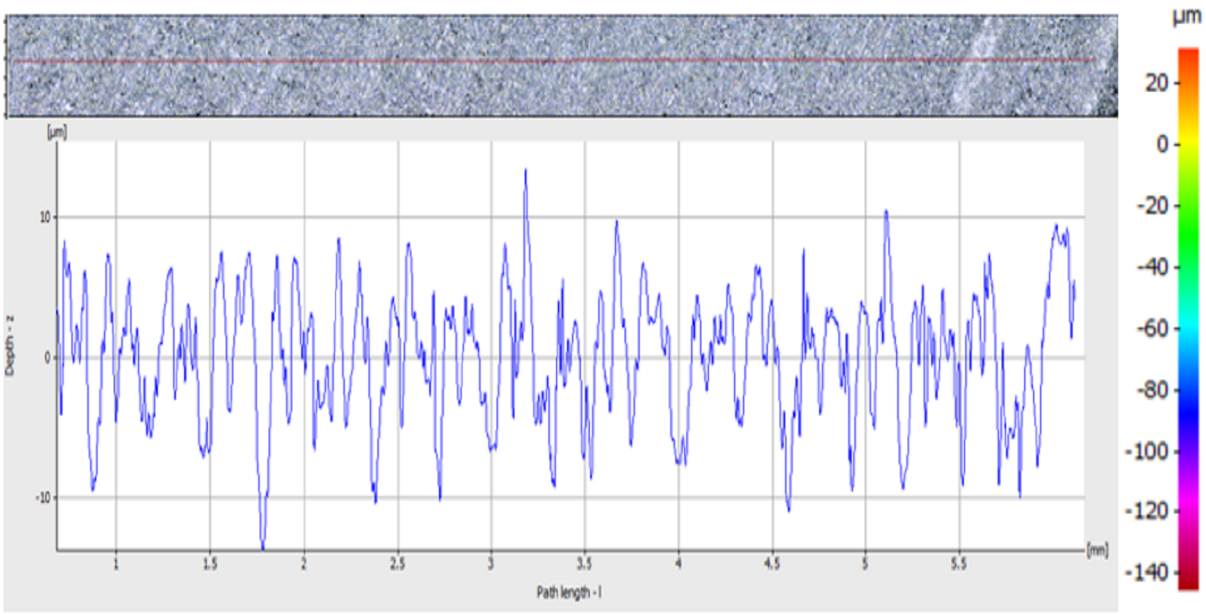

Figure 4.10: Analysis of the surface roughness for the graphite pellet. Above the graph is a picture of the selected area of the pellet, showing the roughness of the surface. The line through the picture of the area shows where the analysis have been done.

4.2 Chemical analysis

The samples were analysed in an EPMA after the experiments in the sessile drop furnace. This was done to find the chemical composition of the reduced slag, where the extent of the reduction is found. Table 4.4 shows the average of the three-point analysis from the EPMA, wherein Appendix A2 the full analysis can be seen. The amount of reduced MnO and SiO_2 have been calculated where the value given is the percentage of the amount of MnO and SiO_2 reduced from the 0 min holding time. From the table, it can be seen that the amount of MnO in the slag decreases with increasing holding time.

For the experiments with coke, there is little difference after 60 minutes, however, when using slag without sulfur it takes a bit longer before the reduction occurs. Hence, the amount of MnO is higher in the experiments at 15 and 30 minutes for slag without sulfur (i.e. less reduction). When charcoal is used as the substrate there can be seen a clear difference in the reduction of both MnO and SiO_2 if the slag contains sulfur or not. When using a slag without sulfur in combination with charcoal, there is a little reduction of the oxides compared to when the slag contains sulfur. It can also be seen when using charcoal and slag with sulfur there is reduced 90.07 % of the MnO and 28.07 % of the SiO_2 after only 15 minutes, indicating that the reduction occurs fairly early. It can also be seen that for some of the values for reduced SiO_2 there are some negative values. This is because there is very little reduced SiO_2. In addition, when calculating the amount reduced MnO and SiO_2 the value is strongly dependent on the reference used, where the reference is the experiment at 0 min with the same parameters. When calculating the amount of MnO

and SiO_2 reduced it was assumed that the rest of the oxides (CaO, MgO and Al_2O_3) is unreducible, hence the same amount of these oxides is in the slag at the end as it was in the beginning. There can also be seen some difference in the R-ratio for the slag after 0 minutes compared to the experiments at 15, 30 and 60 minutes.

Table 4.4: Analysis of slag from EPMA, where the amount of reduced MnO and SiO_2 is calculated.

Test	Holding time [min]	Carbon	Slag	SiO_2 [%]	MnO [%]	CaO + MgO + Al_2O_3 [%]	Reduced MnO [%]	Reduced SiO_2 [%]	R-ratio
1	15	Coke	1	44.61	22.35	34.13	60.64	-1.34	1.57
2	30	Coke	1	46.90	8.04	46.55	89.62	21.88	1.55
3	60	Coke	1	45.16	2.42	52.00	97.21	32.68	1.43
4	0	Coke	1	32.47	41.89	25.18	-	-	1.36
5	15	Coke	2	39.60	32.63	26.76	31.89	-9.30	1.59
6	30	Coke	2	46.64	22.95	31.84	59.74	-8.19	1.70
7	60	Coke	2	48.17	3.34	51.16	96.35	30.48	1.61
8	0	Coke	2	32.32	42.74	23.87	-	-	1.38
9	15	Charcoal	1	44.01	8.33	47.78	90.07	28.07	1.56
10	30	Charcoal	1	44.61	5.32	52.01	94.18	33.02	1.56
11	60	Charcoal	1	44.28	2.30	55.44	97.64	37.62	1.54
12	0	Charcoal	1	31.39	43.06	24.51	-	-	1.46
13	15	Charcoal	2	36.04	37.51	26.54	30.35	4.40	1.60
14	30	Charcoal	2	38.71	33.94	28.14	40.58	3.18	1.66
15	60	Charcoal	2	39.64	31.23	29.20	47.30	4.44	1.64
16	0	Charcoal	2	31.40	44.85	22.10	-	-	1.32
17	30	Coke	2	44.25	3.85	53.68	95.92	39.12	1.55
18	30	Coke	2	48.07	10.72	41.69	85.35	14.84	1.63
19	30	Charcoal	1	40.16	1.36	61.21	98.73	48.76	1.49
20	30	Charcoal	1	38.61	1.41	60.86	98.68	50.46	1.42
21	30	Charcoal	2	40.88	29.99	29.96	50.67	3.95	1.65
22	30	Charcoal	2	46.57	17.38	37.25	77.01	12.00	1.65
23	30	Coke	1	49.75	11.00	39.93	86.40	11.09	1.55
24	30	Coke	1	43.35	25.22	30.66	59.37	-0.91	1.49
25	30	Charcoal	1	44.63	4.41	52.69	95.86	39.56	1.59
26	30	Charcoal	1	45.87	11.53	41.55	86.30	21.22	1.50
27	30	Charcoal	1	46.20	8.46	41.21	89.86	20.00	1.33
28	30	Graphite	1	43.60	17.04	38.21	77.98	18.59	1.53
29	30	Graphite	2	35.44	38.68	24.73	24.44	2.02	1.57
30	30	Charcoal	1	28.76	0.13	65.04	99.90	68.45	1.08
31	30	Charcoal	2	37.54	34.17	27.50	40.00	6.69	1.66

When calculating the reduced amount of MnO and SiO_2 the experiment at 0 min holding time was used to the corresponding experiments. However, for test 23-31 it was used the

starting composition of the slag, as there is no experiment at 0 min corresponding to these experiments, with the exact same parameters.

Figure 4.11 shows the concentration changes of MnO for test 1 to 16, i.e. the tests where coke and charcoal are used as substrate and slag with and without sulfur have been used. From the figure it can be seen that there are significant differences between the four different experiments. When using charcoal and slag with sulfur the reduction rate will be faster than the other experiments. Furthermore, when coke is used as the substrate the reduction is faster when using slag with sulfur compared to slag without sulfur in the beginning, but at 60 minutes the concentration is almost the same for three of the experiments. As mentioned above, there is a clear difference when charcoal and slag without sulfur is used. From the table above it can be seen that after 60 minutes only 47.3 % of the MnO is reduced and only 4.4 % of the SiO_2.

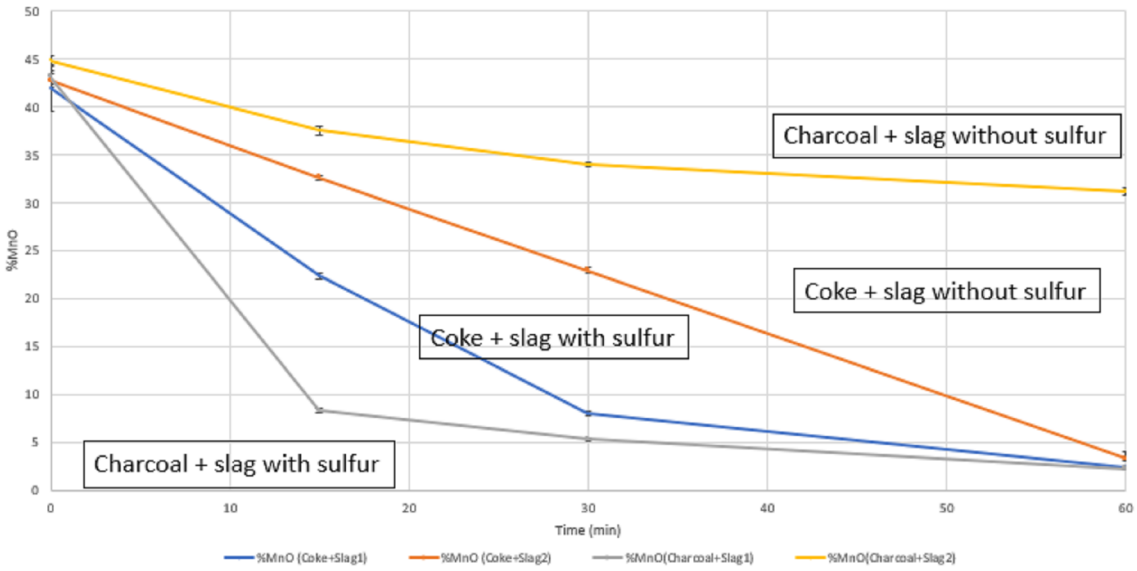

Figure 4.11: Weight fraction of MnO in the slag for test 1-16, where both coke and charcoal is used as substrates and slag with and without sulfur is used. These experiments were held at 1600 °C for 0, 15, 30 and 60 minutes.

In general, the reduction of MnO is faster when slag with sulfur is used compared to slag without sulfur, i.e. higher reduction rate when the slag contains sulfur. Furthermore, from the analysis it can be seen that there is a bigger difference in the reduction rate when charcoal is used as the substrate compared to coke if the slag contains sulfur or not. One reason for this difference between coke and charcoal is that coke has a much higher content of sulfur than charcoal, as seen in Table 4.1 on page 79. As a consequence of this, there will always be some sulfur in the process when using coke even if there is no sulfur in the slag. On the other hand, when charcoal is used with slag without sulfur there is very little sulfur included in the reactions. From this, it can be concluded that sulfur will have an impact on the reduction of MnO and SiO_2, as it will increase.

Figure 4.12 shows the weight fraction of SiO_2 for test 1-16, and Figure 4.13 shows the weight fractions of the sum of the rest of the oxides (CaO, MgO and Al_2O_3).

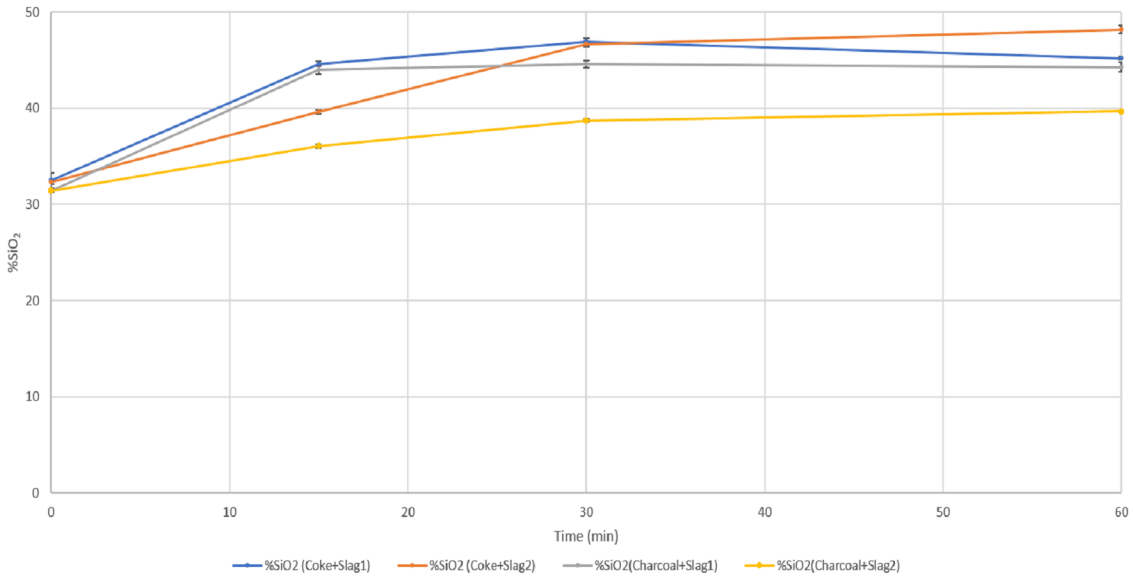

Figure 4.12: Weight fraction of SiO_2 in the slag for test 1-16, where both coke and charcoal is used as substrates and slag with and without sulfur. These experiments were held at 1600 °C for 0, 15, 30 and 60 minutes.

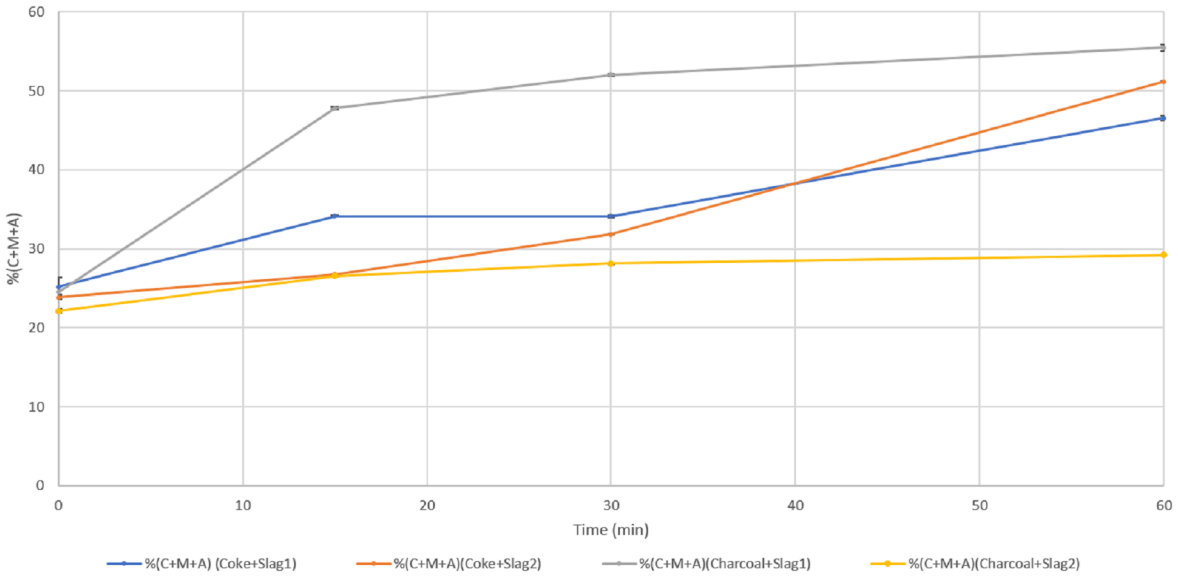

Figure 4.13: Weight fraction of $CaO+MgO+Al_2O_3$ in the slag for test 1-16, where both coke and charcoal is used as substrates and slag with and without sulfur. These experiments were held at 1600 °C for 0, 15, 30 and 60 minutes.

There was also performed experiments where the different pellets were made with different loads on the press (Test 17-22). Figure 4.14 shows the amount of reduced MnO from the slag as a function of the load used when pressing the pellets. From the figure, it can be seen that the load used to make the pellets have no significant impact on the reactivity. When using coke as the substrate there can be seen that there is a slight decrease, although this is not very large. When using charcoal the experiment where the pellet is

made with a load of 1000 kg has the lowest amount of reduced MnO for both the cases. Furthermore, there can be seen that there is a significant difference on the load when charcoal is used with slag without sulfur when the load is 2000 kg, however, this trend was not seen from the other experiments and could, therefore, be seen as an outlier. In general, there can not be seen any correlation if a higher or lower load will increase the amount of reduced MnO from the slag.

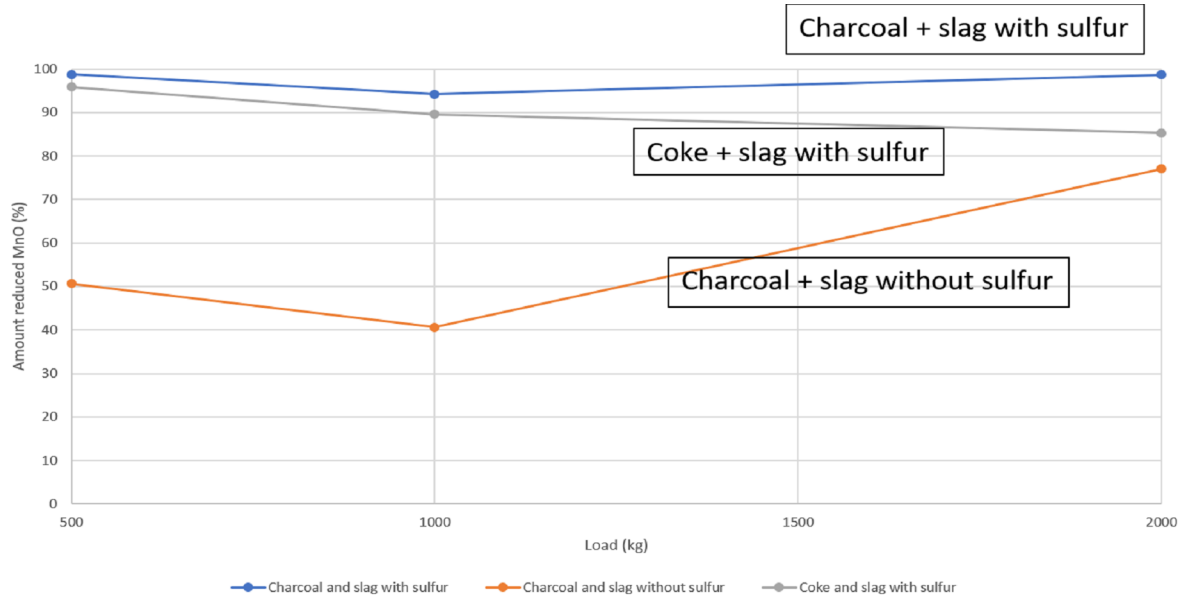

Figure 4.14: Amount reduced of MnO in the slag as a function of the load used to make the pellets. These experiments were held for 30 minutes at 1600 °C.

Figure 4.15 shows the amount of reduced SiO_2 as a function of load. From this figure, it can be seen that there is more difference between the different loads on the reduction of SiO_2 compared to the reduction of MnO. Furthermore, there can not be seen any correlation between if the load increases or decreases and a higher degree of SiO_2 reduction. For the experiment with charcoal and slag with sulfur, the experiment on 1000 kg has the lowest amount reduced, but the experiments with 500 and 2000 kg are approximately the same. When charcoal is used with slag without sulfur there is in general little reduced SiO_2, although there is reduced some from the experiment at 2000 kg. As mentioned earlier, there were some negative values which can also be seen on this figure for the experiment with coke. For the experiment with coke, there is a higher amount SiO_2 reduced for the experiment where the pellet is made with a load of 500 kg. In general, there can be found no correlation between increase or decrease in the load used on the pellets and the reactivity of the carbon material.

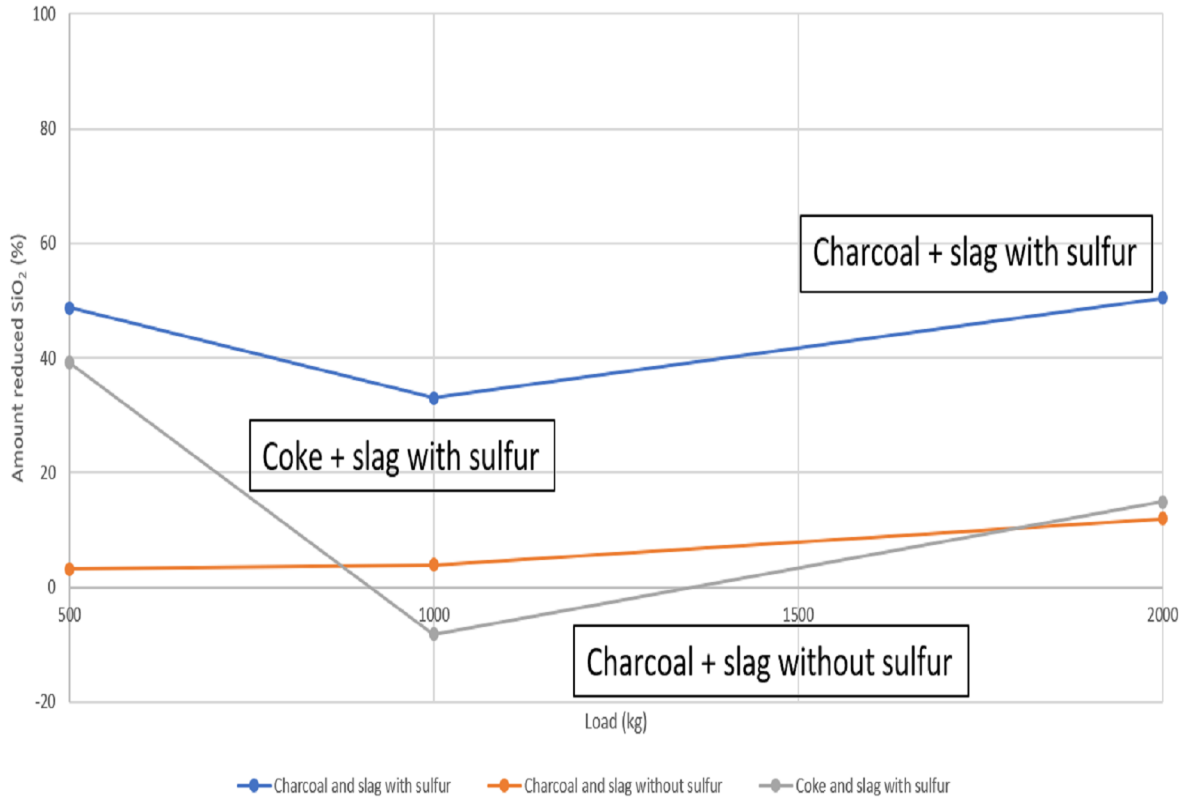

Figure 4.15: Amount reduced of SiO_2 in the slag as a function of the load used to make the pellets. These experiments were held for 30 minutes at 1600 °C.

To investigate the difference between coke and charcoal further there was also performed experiments with green particles (Test 23-27). There was seen some differences in the behaviour of the slag from the relative volume measurements between the pellets and the green particles. Furthermore, for the experiments with coke it can be seen that when using pelletized coke (test 23) there is a higher reduction rate of MnO and SiO_2 compared to green coke (test 24). From the analysis there can be seen that when using green coke there is no (or very little) SiO_2 reduced. For the experiments with charcoal there can not be seen any significant differences between the green particles (test 26 and 27) or the pelletized charcoal (test 25), other than when using pelletized charcoal there is more reduced SiO_2 compared to green charcoal. It is also no real difference between the two types of green particle used, i.e. one along the fibres and one on top of the fibres. Hence, the reduction rate for green charcoal is not dependent on the direction of the fibres.

To further investigate the influence of sulfur on the reduction of the slag, experiments with graphite as the substrate was performed. From Table 4.4 it can be seen clear differences when slag with sulfur (test 28) and slag without sulfur (test 29) was used, where there is a significantly higher reduction rate of both MnO and SiO_2 when using slag with sulfur. Hence, it can be concluded that sulfur will have an impact on the reduction rate of MnO and SiO_2 when graphite is used as the substrate. The difference if there is sulfur in the slag or not could also be seen when using charcoal as the substrate. From the chemical analysis of the coke and charcoal in Table 4.1 on page 79 it can be seen that coke has a much higher content of ash than charcoal and also a higher content of sulfur.

This could explain why the difference between if there is sulfur in the slag or not is bigger for charcoal and graphite. The graphite was not analysed in this study, but other studies have found graphite to have a very low content of ash and also sulfur.

From Figures 4.11, 4.12 and 4.13 there can be seen to some extent there is error bars for the standard deviation. For most of the points on the graph, these can not be seen as the standard deviation is too small. However, at 0 minutes the error bars can be seen. This implies that the slag is not completely homogeneous, when it comes to 1600 °C due to the fact that there are some variations between the three different point analysis. This can be seen in Figure 4.16, which is from test 4 where it can be seen that there are different grey colours on the slag. There is also a metal phase on the left side of the figure. Figure 4.17 shows test 1 which was held at 15 minutes at 1600 °C, where only the slag phase can be seen, and it is more homogeneous than test 4.

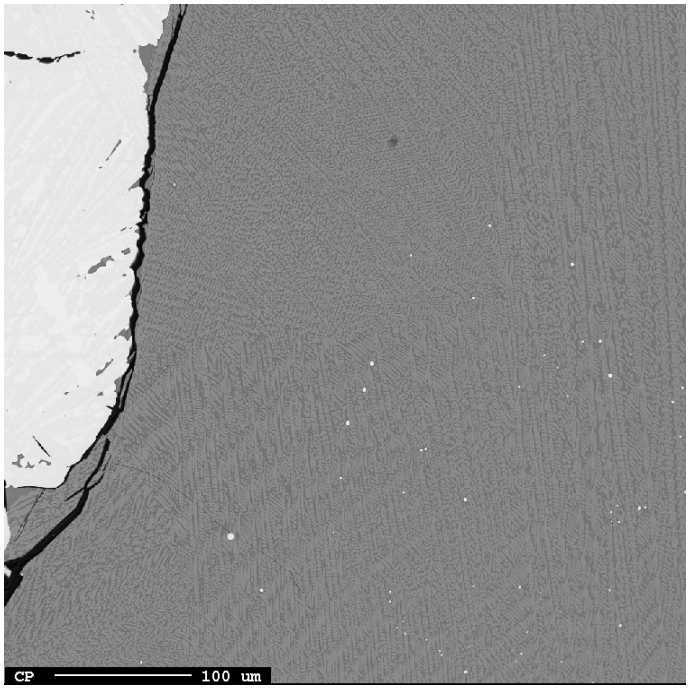

Figure 4.16: Micrograph from EPMA of test 4. Heated to 1600 °C.

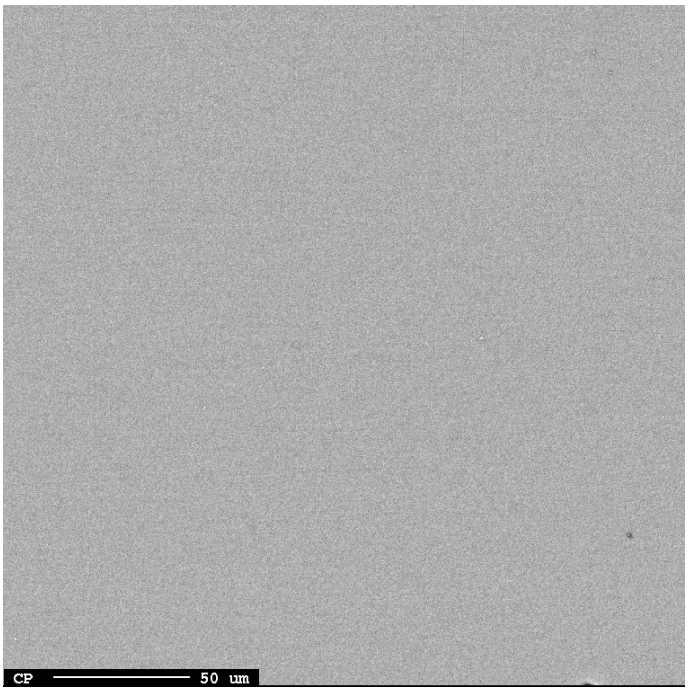

Figure 4.17: Micrograph from EPMA of test 1. Heated to 1600 °C and held for 15 minutes.

From Figures 4.18 and 4.19 there can be seen some white areas on the slag phase. These are metal prills with a precipitated layer of MnS on the outer layer of the metal.

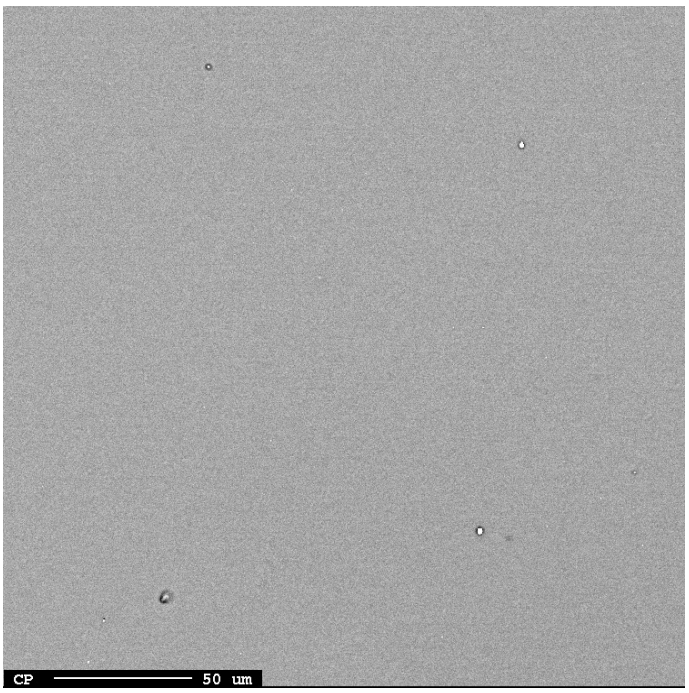

Figure 4.18: Micrograph from EPMA of test 2. Heated to 1600 °C and held for 30 minutes.

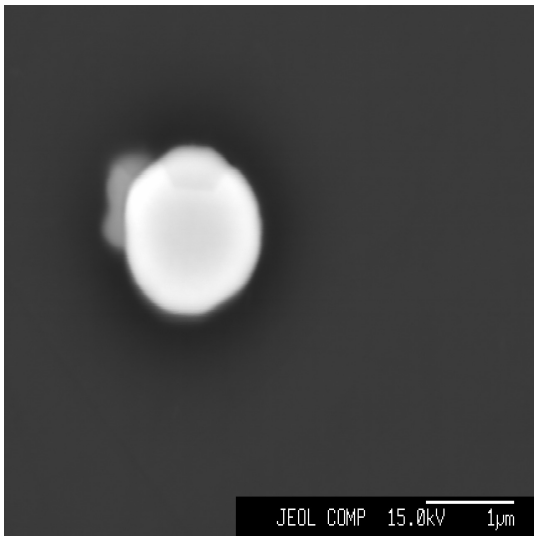

Figure 4.19: Micrograph from EPMA, where a metal prill from the slag phase is seen. Heated to 1600 °C and held for 30 minutes.

There was also produced a metal phase from the experiments. As it was for the slag phase there was performed three point analysis on the metal, and the average of these three analyses is given in Table 4.5 and the full analysis can be seen in Appendix A2. From the table it can be seen there are different compositions of the metal depending on the holding time in the furnace, and also which substrate was used and if the slag contained sulfur or not. Furthermore, there are some of the tests that do not have an analysis of the metal, one reason for this is that it was not produced any metal at that test. However, it may be that the metal phase is either grinded or polished away during sample preparation or that it is "inside the epoxy", i.e. not on the surface of the prepared sample and can therefore not be analysed. It must also be mentioned that there can be different compositions on the metal particles, where small particles inside the slag will have a higher content of iron and larger particles on the surface of the slag will have a higher content of Mn.

Table 4.5: EPMA analysis of the metal produced from the slag.

Test	Carbon	Slag	Holding time [min]	Si [%]	Mn [%]	Fe [%]
1	Coke	1	15	6.15	38.71	57.17
2	Coke	1	30	16.95	87.32	3.70
3	Coke	1	60	17.74	33.95	51.73
4	Coke	1	0	0.04	16.62	81.40
5	Coke	2	15	1.48	35.00	63.18
6	Coke	2	30	5.97	33.22	62.31
7	Coke	2	60	11.19	8.87	80.62
8	Coke	2	0	-	-	-
9	Charcoal	1	15	16.02	91.55	0.72
10	Charcoal	1	30	14.39	46.58	43.98
11	Charcoal	1	60	17.31	42.03	45.54
12	Charcoal	1	0	-	-	-
13	Charcoal	2	15	0.25	28.55	70.47
14	Charcoal	2	30	-	-	-
15	Charcoal	2	60	0.08	6.97	88.48
16	Charcoal	2	0	0.04	20.62	77.66
17	Coke	2	30	16.16	54.03	35.38
18	Coke	2	30	13.55	44.08	47.00
19 Light	Charcoal	1	30	10.43	81.40	7.23
19 Dark	Charcoal	1	30	23.16	72.37	6.51
20	Charcoal	1	30	18.78	77.94	1.85
21	Charcoal	2	30	-	-	-
22	Charcoal	2	30	-	-	-
23	Coke	1	30	-	-	-
24	Coke	1	30	4.15	39.01	58.44
25	Charcoal	1	30	19.48	80.61	1.17
26	Charcoal	1	30	13.66	89.64	4.57
27	Charcoal	1	30	11.76	43.90	48.69
28	Graphite	1	30	10.24	61.63	33.18
29	Graphite	2	30	0.04	10.17	87.26
30	Charcoal	1	30	12.51	50.41	42.21
31	Charcoal	2	30	0.05	12.09	85.16

From the table above it can be seen that there is two analysis for test 19. Figure 4.20 shows a micrograph of this test, and that there is a light and dark phase in the metal, and from the analysis it says that the light phase has a higher content of MnO and less SiO_2 than the dark phase. It could also be seen to some extent that the light phase has a higher content of carbon, but due to the fact that the samples are carbon coated before the analysis the exact amount of carbon in the sample cannot be found by this method. When analysing the metal phase the electron beam has a diameter of 20 μm, and when analysing the slag there is a diameter of 2 μm of the electron beam.

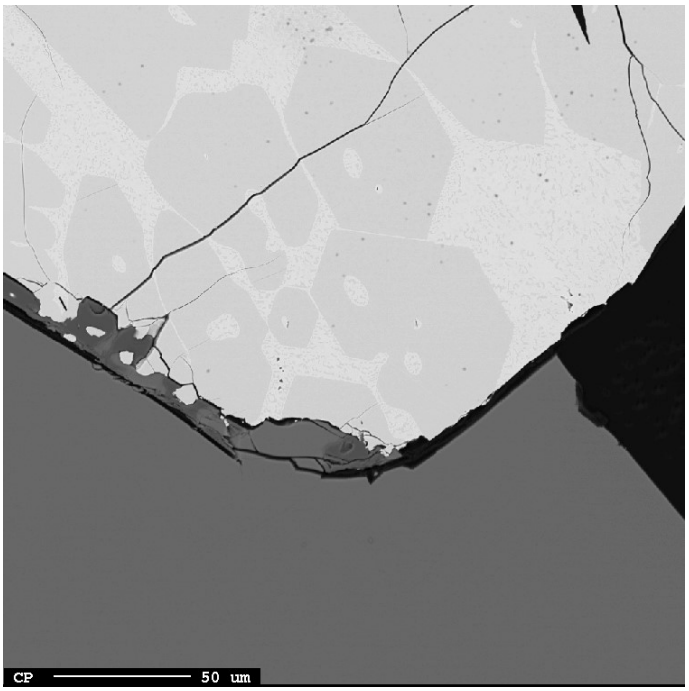

Figure 4.20: Micrograph from EPMA, where the metal phase is seen. Heated to 1600 °C and held for 30 minutes.

4.3 Experiments in sessile drop furnace

It was performed 31 experiments in the furnace which can be seen in Table 4.6. From the table, it can be seen the total mass of the slag and substrate before and after the experiments. The weight of the graphite-cup has been removed, hence the mass in the table is only slag and coke or charcoal, except for the tests with green particles and graphite as substrate as the graphite-cup was not used for these experiments. From the table, it can be seen that loss of mass increases with increasing holding time. Furthermore, there can be seen a significant difference between some of the experiment regarding the loss of mass. For the holding times at 0 and 15 minutes charcoal has a higher mass loss than coke, indicating that reduction may occur earlier when using charcoal as reducing agent, or because of the higher volatile content in charcoal. There is little difference in the mass loss for the experiments with slag1 (with sulfur) and slag2 (without sulfur) when using coke as substrate, although after 60 min when using slag1 there is a slightly higher mass loss. When using charcoal as the substrate there is a clear difference when using slag1 or slag2, where slag1 has a higher mass loss. Furthermore, there can not be seen any clear differences in the loss of mass when the pellets that were made with different loads was used (test 17-22). Lastly, it can be seen that the loss of mass when using graphite is much lower compared to the other experiments, and especially when slag2 are used. This can be explained by that the graphite itself will not lose as much mass in the furnace compared to coke and charcoal, hence the loss of mass is then only from the slag.

Table 4.6: Experiments performed in sessile drop furnace with the total (carbon+slag) mass before and after the experiment. Slag1 is with sulfur and slag2 is without sulfur.

Test	Carbon material	Slag	Holding time [min]	Total mass before [g]	Total mass after [g]	Loss of mass [g]	Loss of mass [%]
1	Coke	1	15	0.40	0.32	0.07	18.47
2	Coke	1	30	0.36	0.27	0.08	23.76
3	Coke	1	60	0.40	0.27	0.13	31.46
4	Coke	1	0	0.44	0.41	0.04	8.08
5	Coke	2	15	0.41	0.35	0.06	13.68
6	Coke	2	30	0.36	0.28	0.08	22.09
7	Coke	2	60	0.36	0.26	0.10	27.28
8	Coke	2	0	0.33	0.31	0.03	7.73
9	Charcoal	1	15	0.31	0.20	0.10	33.44
10	Charcoal	1	30	0.35	0.23	0.12	34.60
11	Charcoal	1	60	0.30	0.19	0.11	36.43
12	Charcoal	1	0	0.29	0.24	0.05	16.19
13	Charcoal	2	15	0.35	0.28	0.07	21.10
14	Charcoal	2	30	0.35	0.26	0.09	25.61
15	Charcoal	2	60	0.33	0.25	0.08	24.17
16	Charcoal	2	0	0.34	0.28	0.06	17.11
17	Coke	2	30	0.36	0.25	0.11	31.23
18	Coke	2	30	0.41	0.31	0.09	23.03
19	Charcoal	1	30	0.37	0.24	0.13	35.61
20	Charcoal	1	30	0.28	0.18	0.10	35.67
21	Charcoal	2	30	0.33	0.25	0.08	24.18
22	Charcoal	2	30	0.33	0.23	0.09	28.82
23	Coke	1	30	0.37	0.30	0.07	17.82
24	Coke	1	30	0.36	0.32	0.04	10.33
25	Charcoal	1	30	0.30	0.20	0.10	33.09
26	Charcoal	1	30	0.25	0.18	0.07	27.87
27	Charcoal	1	30	0.23	0.15	0.08	36.43
28	Graphite	1	30	0.57	0.51	0.06	10.66
29	Graphite	2	30	0.56	0.53	0.02	4.12
30	Charcoal	1	30	0.31	0.18	0.13	41.88
31	Charcoal	2	30	0.32	0.25	0.07	22.25

It must be mentioned that after the experiments in the furnace the substrates are somewhat fragile and there is a possibility that some of the mass was lost before the samples were weighed. This is a bigger problem for coke as the coke is extremely fragile after the experiments. This problem also occurred in the study performed by **Hosum** (2019) [40], however in that study there were not graphite-cups under the coke pellets, which it is in this study.

4.3.1 Experiments with coke

In the following chapters, the results from the experiments with coke as the substrate is presented.

4.3.1.1 Experiments with coke and slag containing sulfur

There was performed three experiments which were held at 15, 30 and 60 minutes, respectively. The reference volume of the slag was chosen to be when the temperature was 1300 °C, and it takes almost two minutes before it is heated to the holding temperature at 1600 °C. Figure 4.21 shows the relative volume of the experiments with coke and slag1 (i.e. the slag with sulfur). From the different graphs it can be seen that there is a similarity in the general shape of the curve. After some time the relative volume starts to increase before the relative volume decreases. The increase in relative volume indicates that there was generation of gas, which will lead to foaming. The bigger the "leap" when the volume increases and then decrease, there is more gas entrapped in the slag, hence more foaming which leads to a higher degree of reduction. At the end of test 3, which were held at 60 minutes, it can be seen that the relative volume is almost a 0.4, indicating there have been reduced oxides from the slag.

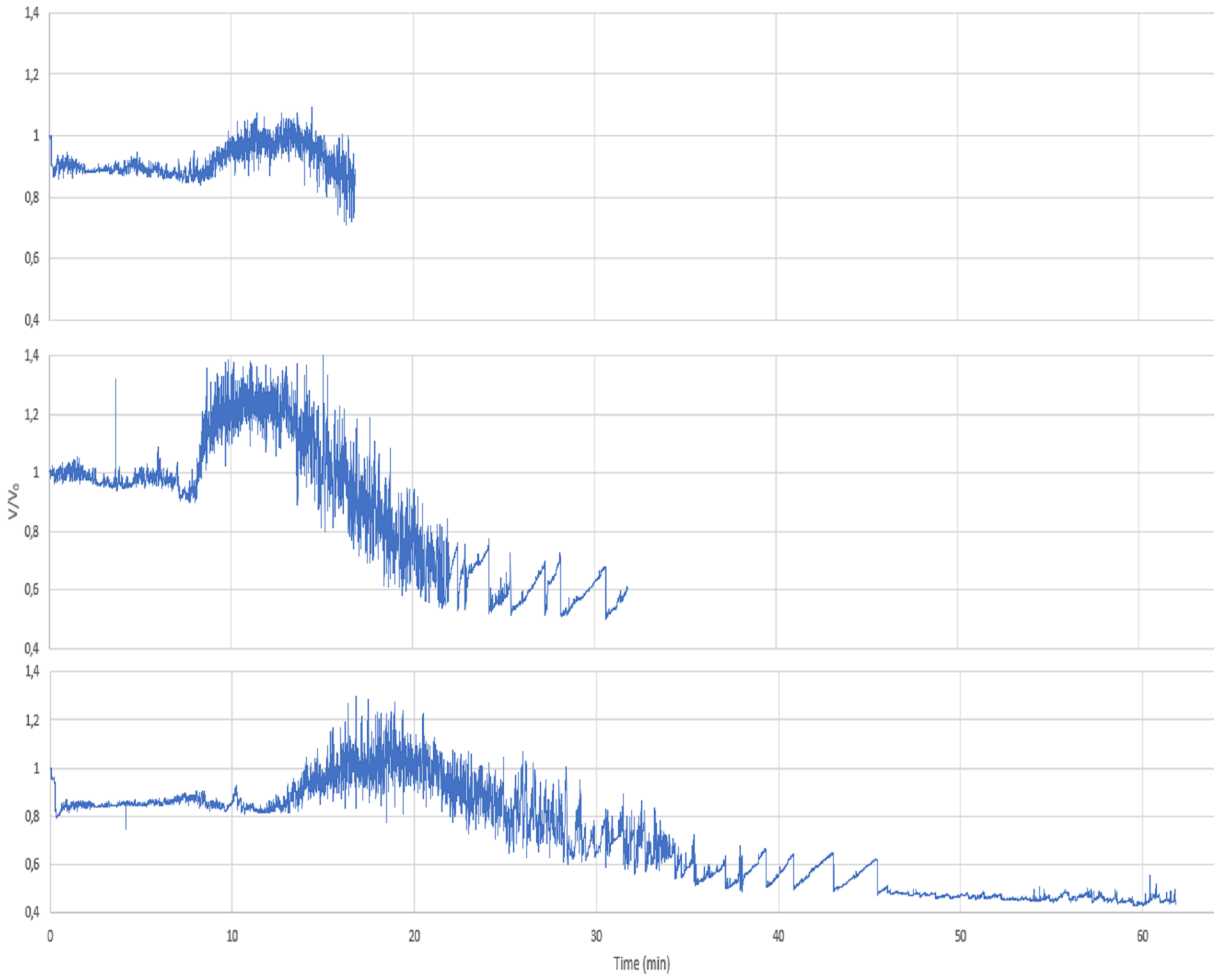

Figure 4.21: Relative volume with coke as substrate and slag with sulfur (slag1), which were held at 15, 30 and 60 minutes at 1600 °C. (Test 1 (top), 2 (middle) and 3 (bottom))

Figure 4.22 shows the wetting angle between the slag and substrate for test 1, 2 and 3. From the figure it can be seen that the plots for the three experiments are somewhat similar. The wetting angle is around 120-130° at the beginning and then decreases over time. The wetting angle decreases faster for test 2. This correlates to Figure 4.21 where test 2 has the highest relative volume at the top of the graph, and that the volume decreases earlier for test 2 than for test 3.

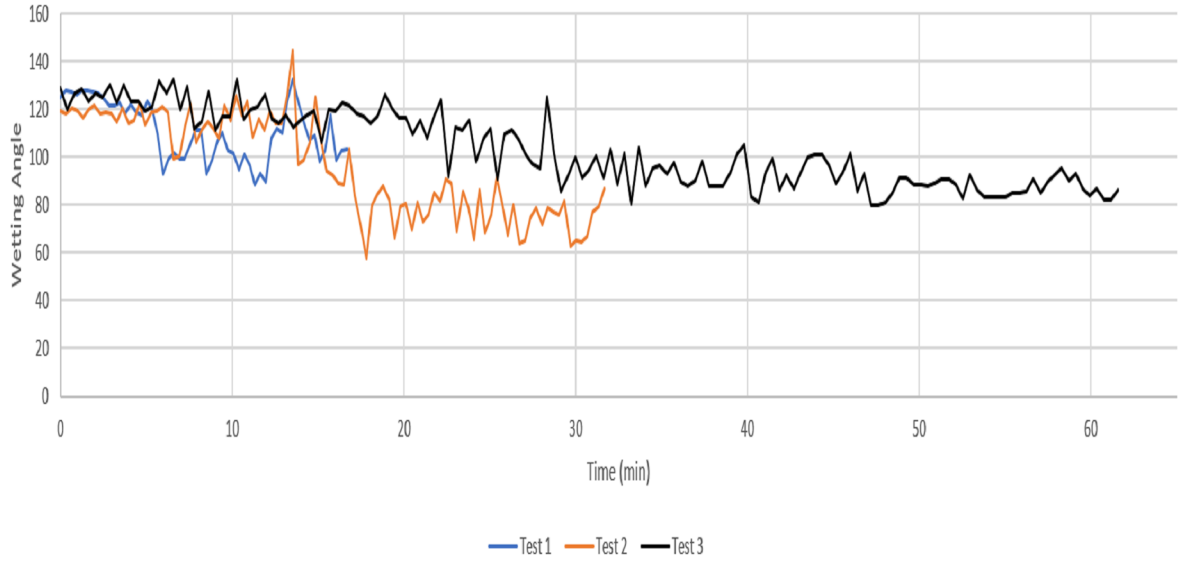

Figure 4.22: Wetting angle with coke as substrate and slag with sulfur, which were held for 15, 30 and 60 minutes at 1600 °C.

Figure 4.23 shows the measured contact area between the substrate and the liquid slag. The contact area is measured by measuring the length of the area where the slag and substrate are in contact with each other. The contact area is assumed to be a perfect circle, and the length measured is the diameter of this circle. The area increases to around 18 mm^2 for all the experiments. For both test 1 and 2, the area increases more quickly compared to test 3. This can also be seen from the relative volume of the experiments, where the relative volume for test 1 and 2 started to increase earlier than for test 3. Furthermore, there can be seen that there is a similarity between the contact area and the relative volume. The relative volume increases after some time and then starts to decrease.

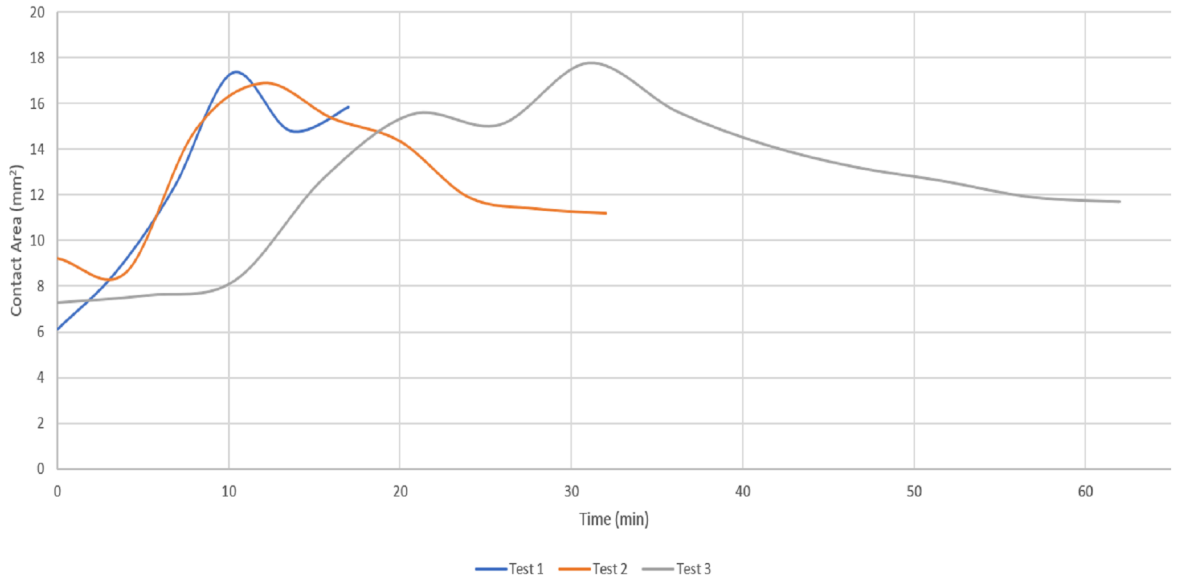

Figure 4.23: Contact area between coke and slag with sulfur, which were held at 15, 30 and 60 minutes at 1600 °C.

4.3.1.2 Experiments with coke and slag without sulfur

Figure 4.24 shows the relative volume of the experiments with coke and slag2 (i.e. slag without sulfur). There was performed three experiments which were held at 15, 30 and 60 minutes, respectively. The reference volume of the slag was chosen to be when the temperature was 1300 °C, and it takes almost two minutes before it is heated to the holding temperature at 1600 °C. From the different graphs it can be seen that there is somewhat of a similarity in the general shape of the curve. From these experiments, it can be seen that it takes more time before the slag starts to foam. This can especially be seen from the experiment at 15 minutes, as there is little change in relative volume. A small change in relative volume can be explained by little gas formation, and hence little reduction of the oxides in the slag. Furthermore, for the experiments held for 30 minutes, it takes about 20 minutes before the slag to start foaming, hence generating more gas.

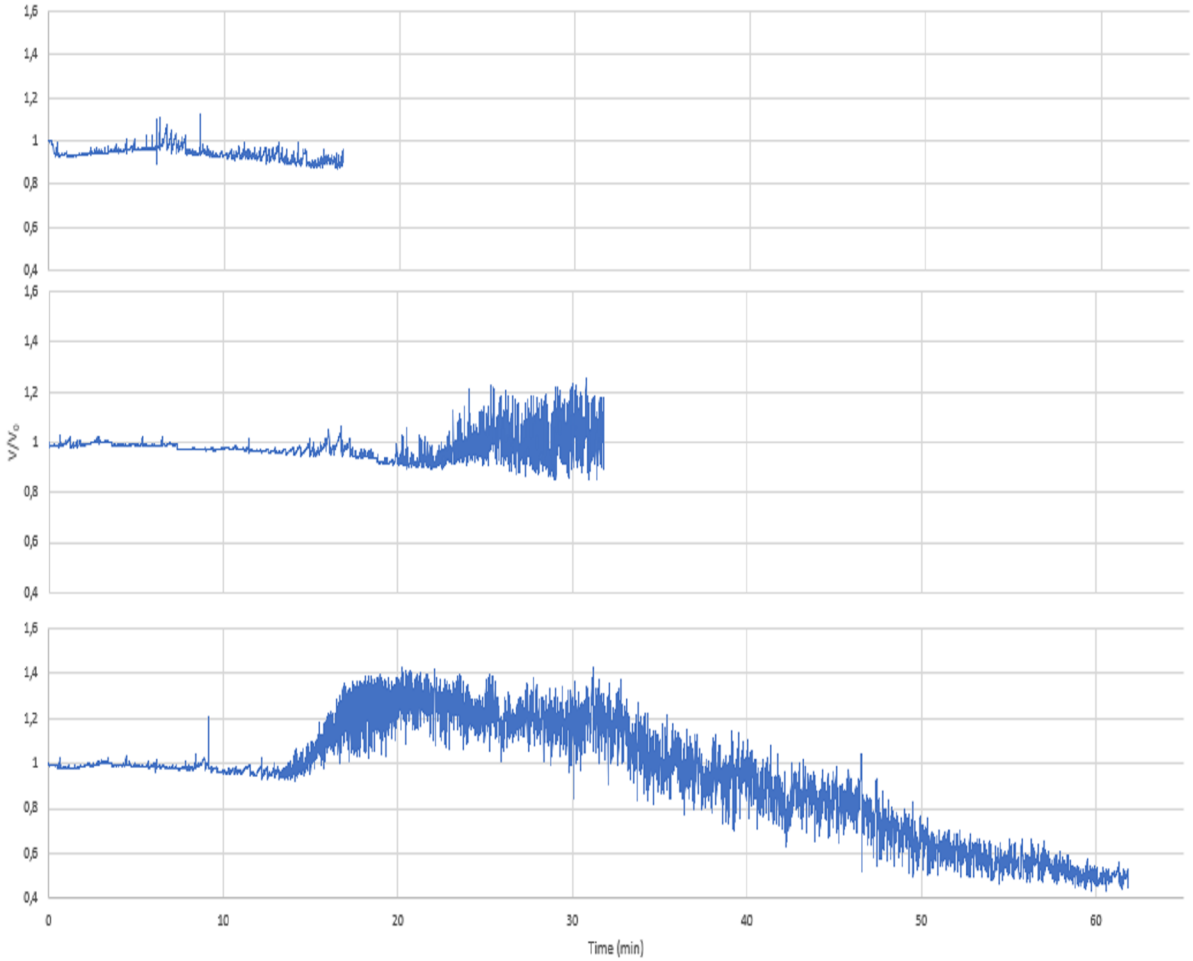

Figure 4.24: Relative volume with coke as substrate and slag without sulfur, which were held at 15, 30 and 60 minutes at 1600 °C. (Test 5 (top), 6 (middle) and 7 (bottom))

Figure 4.25 shows the wetting angle between the slag and substrate for the experiments with coke and slag without sulfur held at 15, 30 and 60 minutes, respectively. From the figure it can be seen that the plots for the three experiments are very similar. The wetting angle is around 120° at the beginning and then decreases over time, and for the experiments held for 60 min went down to 60° at the end.

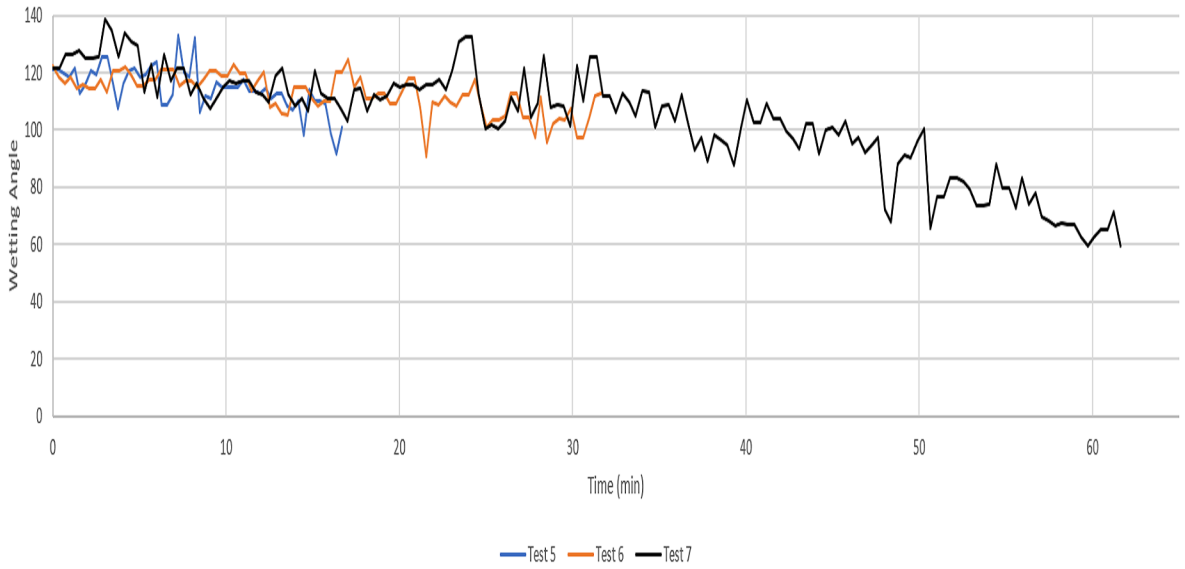

Figure 4.25: Wetting angle with coke as substrate and slag without sulfur (slag2), which were held at 15, 30 and 60 minutes at 1600 °C.

Figure 4.26 shows the measured contact area between the substrate and the liquid slag. The contact area is measured by measuring the length of the area where the slag and substrate are in contact with each other. The contact area is assumed to be a perfect circle, and the length measured is the diameter of this circle. Similar to the last experiment, the contact area starts around 5-8 mm^2 and increases to around 16 mm^2. Furthermore, the similarities between the relative volume and contact area can be seen in this experiment also, especially for the experiment held for 60 min, where the relative volume and area starts to increase and then decreases after some time, correlating to the shape of the curve for relative volume.

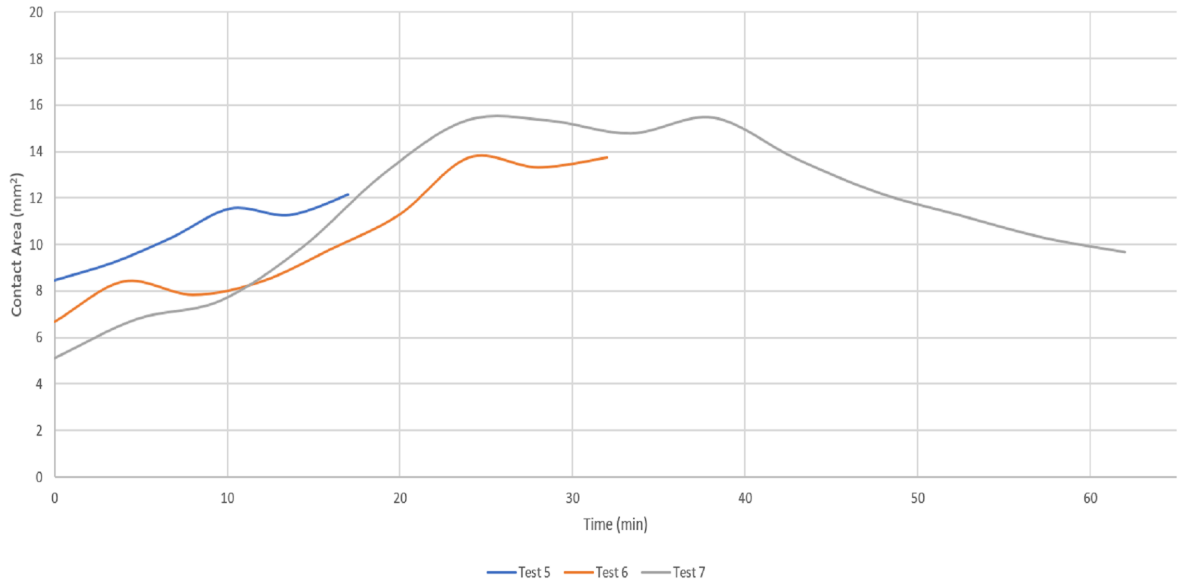

Figure 4.26: Contact area between the coke and substrate and slag, which were held at 15, 30 and 60 minutes at 1600 °C.

4.3.1.3 Experiments with coke pellets made with a different load

Figure 4.27 shows the relative volume of coke and slag without sulfur. In these experiments, the influence of the load on the pellets is investigated. The three different coke-pellets was made with a load of 500 kg (Test 17), 1000 kg (Test 6) and 2000 kg (Test 18). The reference volume of the slag was chosen to be when the temperature was 1300 °C, and it takes almost two minutes before it is heated to the holding temperature at 1600 °C. Test 17 and 18 have a similar shape of the curve, but test 6 with 1000 kg load is somewhat different. However, test 17 and 18 have a more similar shape with test 7 where the pellet is made with a load of 1000 kg, given in Figure 4.24 on page 102. It can also be seen that the experiment with a pellet made with a load of 500 kg (test 17) have the lowest relative volume at the end of the experiment. Which correlates well with the chemical analysis as it was the experiment with 500 kg load on the press that had the highest amount of reduced MnO and SiO_2.

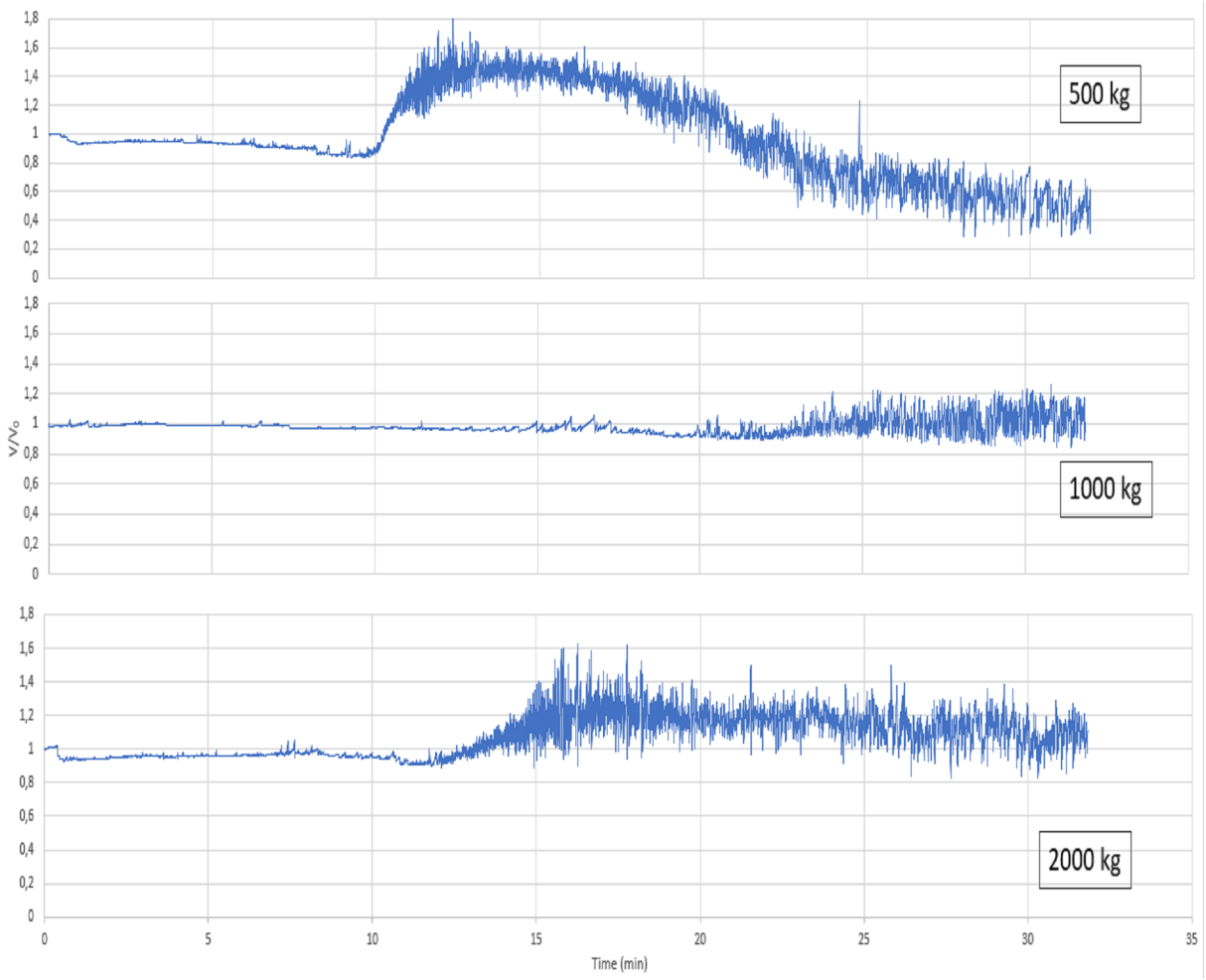

Figure 4.27: Relative volume with coke as substrate and slag without sulfur, which were held for 30 min at 1600 °C, where the pellets is made with a load of 500 kg (test 17 - top), 1000 kg (test 6 - middle) and 2000 kg (test 18 - bottom).

Figure 4.28 shows the wetting angle between the slag and substrate for the experiments from the figure above. The wetting angle starts around 120-130° and decreases over time. The wetting angle is somewhat the same for all the experiments, except the experiment

with a pellet made with 500 kg load (test 17) as that decreases more than the other two experiments. This difference could also be seen from the relative volume as test 17 had the lowest volume at the end of the experiment.

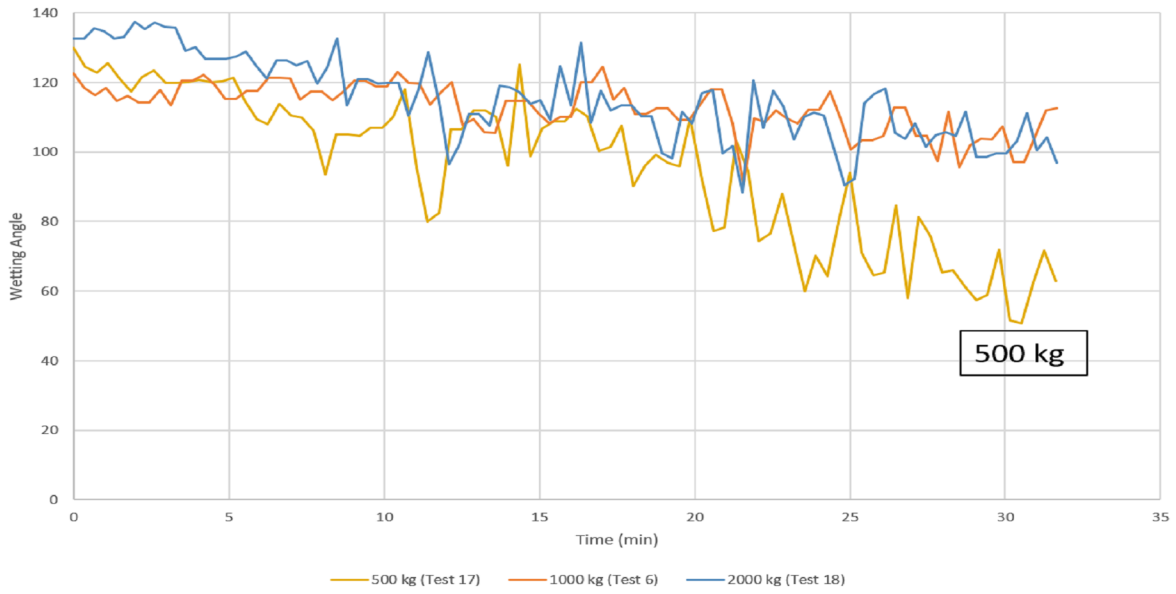

Figure 4.28: Wetting angle with coke as substrate and slag without sulfur for experiments where the pellet is made with a load of 500 kg (test 6), 1000 kg (test 17) and 2000 kg (test 18), which were held for 30 minutes at 1600 °C.

Figure 4.29 shows the measured contact area between the substrate and the liquid slag. The contact area is measured by measuring the length of the area where the slag and substrate are in contact with each other. The contact area is assumed to be a perfect circle, and the length measured is the diameter of this circle. The contact area starts around 6-8 mm^2 and then increases. The experiment with 500 kg (test 17) has the highest contact area in general with a peak of almost 25 mm^2. Furthermore, there can be seen similarities between the relative volume and the contact area. The relative volume for test 17 increases earlier than the two other, in addition to it having the highest peak in relative volume. This similarity can also be seen for the experiment where the pellet is made with 1000 kg (test 6), which have the lowest contact area in addition to little gas formation during the reduction, which can be seen from the relative volume.

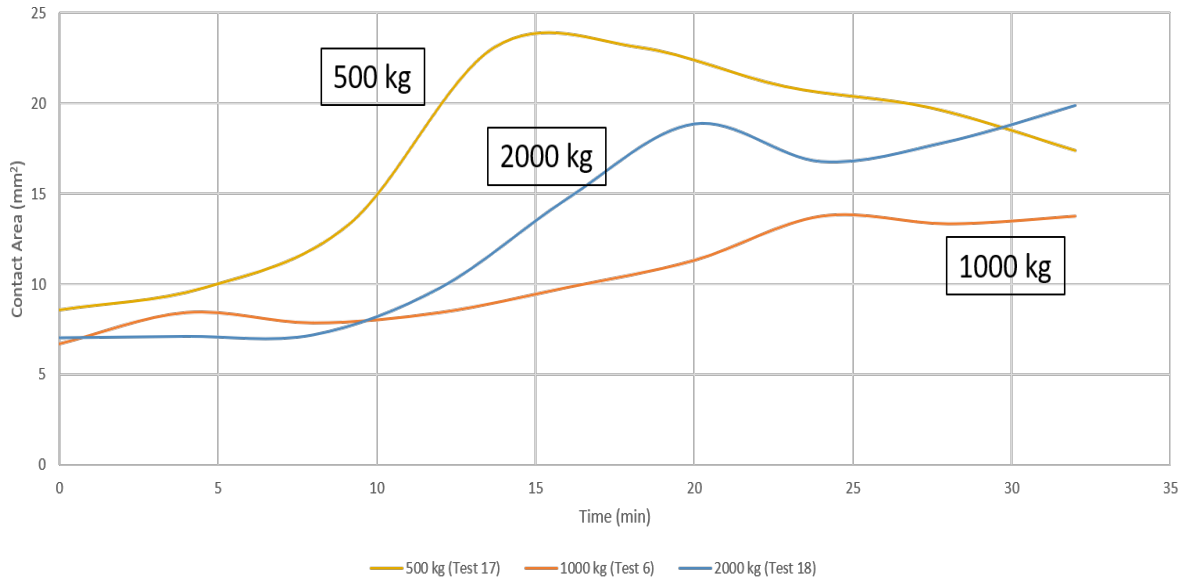

Figure 4.29: Contact area between the coke and slag without sulfur for experiments where the pellet is made with a load of 500 kg (test 6), 1000 kg (test 17) and 2000 kg (test 18), which were held at 30 minutes at 1600 °C.

4.3.1.4 Green coke particle

There was performed experiments with green particles to investigate the difference between the green particle and a pellet where the coke particles are crushed into a powder. Figure 4.30 show the relative volume for the experiments with pelletized coke (test 23) and green coke (test 24). The holding temperature for these experiments were 1550 °C. There can be seen a clear difference between the two experiments. In fact, the green coke has a clear difference between most of the experiments performed with pelletized coke. When using green coke there is foaming from the start as the volume oscillates. Also, the relative volume decreases almost in a straight line. In comparison to the experiments with pelletized coke, the relative volume starts to increase after some time before decreasing, which is the general behaviour for many of the experiments with pelletized coke. Both the experiments were performed with a slag containing sulfur.

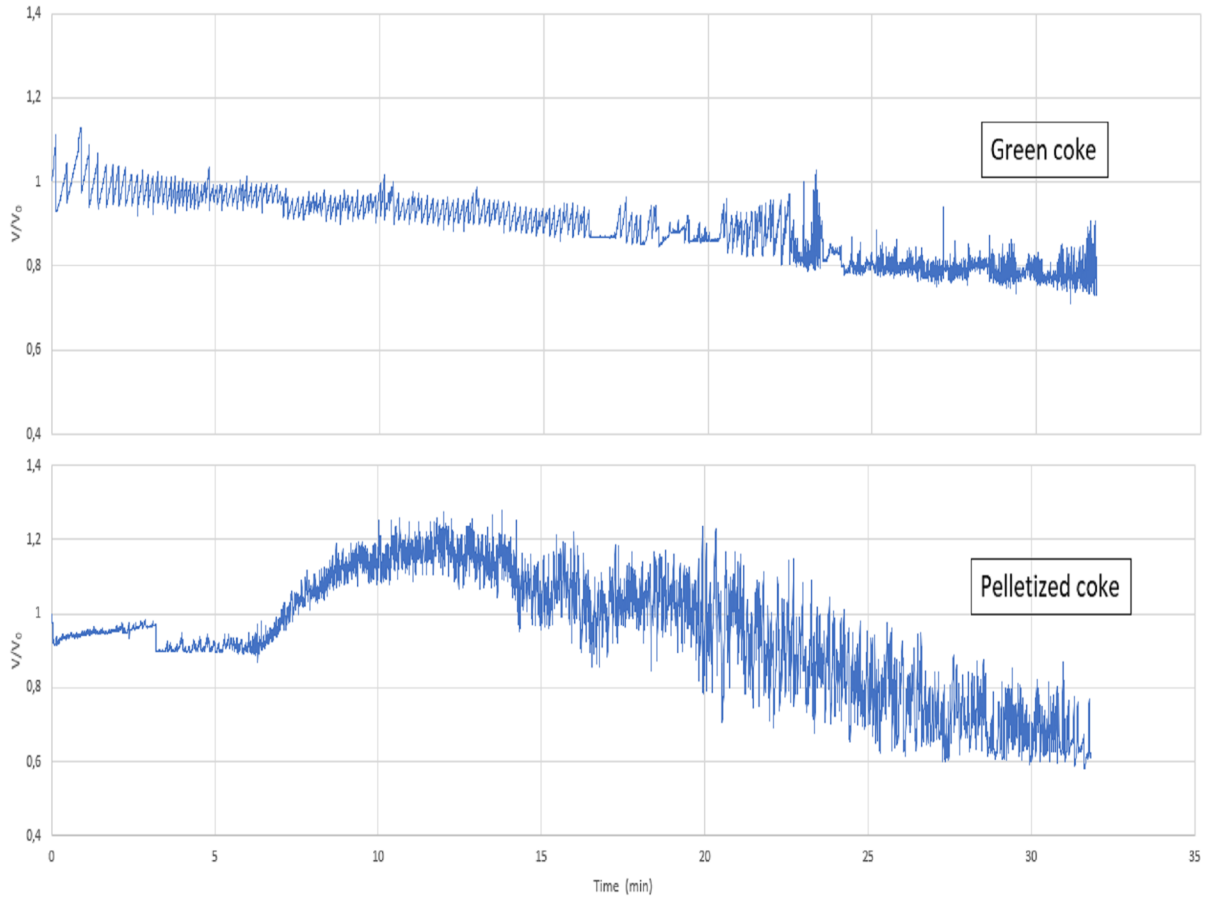

Figure 4.30: Relative volume for experiment with green coke (test 24 - top) compared with an experiment with pelletized coke (test 23 - bottom). Both the experiments have been performed with a slag with sulfur (slag1), and were held at 1550 °C for 30 minutes.

Figure 4.31 shows the wetting angle between the slag and substrate for the experiments with green coke and pelletized coke. The wetting angle starts around 130° and decreases over time. The decrease of the wetting over time is almost linear throughout the experiment. Other than the fact that the experiment with green coke is a few degrees higher, both the experiments have very similar wetting.

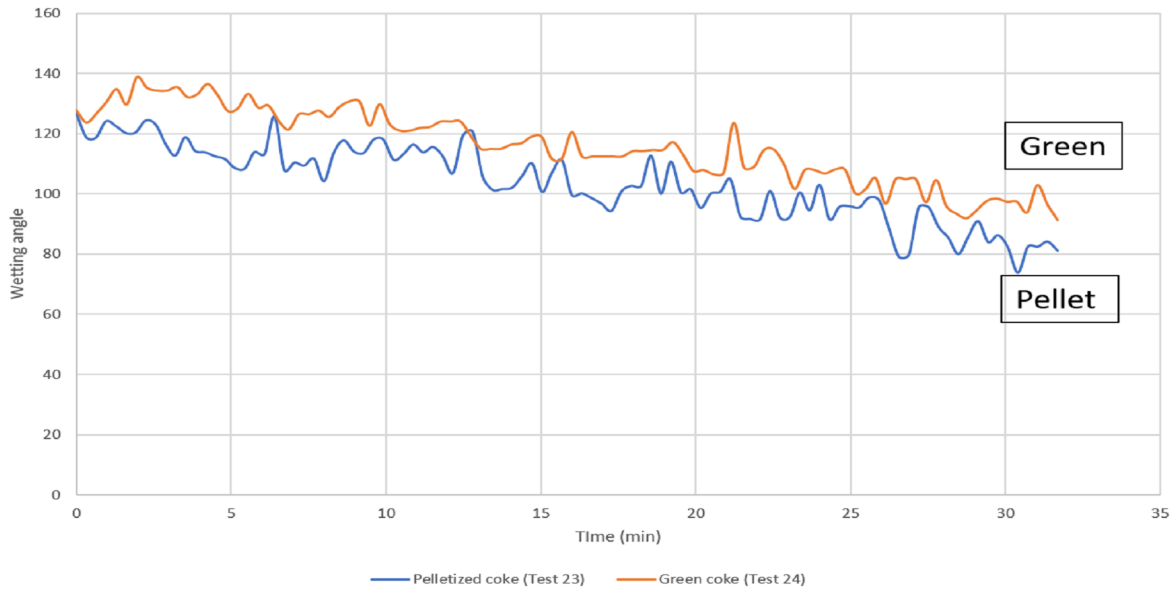

Figure 4.31: Wetting angle for experiment with green coke (test 24) compared with an experiment with pelletized coke (test 23). Both the experiments have been performed with a slag with sulfur (slag1), and were held at 1550 °C for 30 minutes.

Figure 4.32 shows the measured contact area between the substrate and the liquid slag. The contact area is measured by measuring the length of the area where the slag and substrate are in contact with each other. The contact area is assumed to be a perfect circle, and the length measured is the diameter of this circle. The contact area starts around 7-9 mm^2, but for the experiment with green coke, it decreases at the start before it increases again. However, the experiment with pelletized coke increases in area, and the contact area is in general higher for the pelletized coke compared to the green coke.

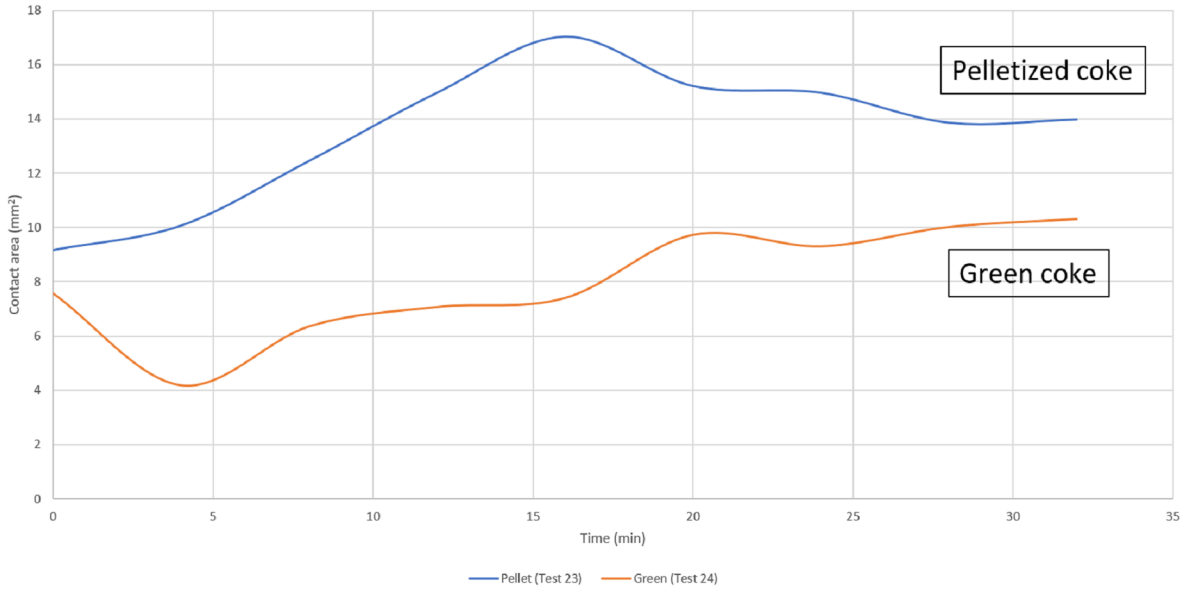

Figure 4.32: Contact area for experiment with green coke (test 24) compared with an experiment with pelletized coke (test 23). Both the experiments have been performed with a slag with sulfur (slag1), and were held at 1550 °C for 30 minutes.

4.3.1.5 Summary of experiments with coke

There have been performed several different experiments where coke has been used as the substrate. The influence of sulfur in the slag has been investigated, different load on the pellets and an experiment with a green particle. In general, from the relative volume measurements, it can be seen that it takes time before something significant happens regarding an increase or decrease in relative volume for most of the experiments. The general behaviour regarding relative volume is that it increases and then after some time starts to decrease. Furthermore, one of the biggest differences between the experiments where the slag contains sulfur or not is that it takes a little more time before there is generation of gas, and the slag starts to foam or generate bubbles when using slag without sulfur. As a consequence of this, the experiment where coke is used with slag without sulfur with a holding time of 15 minutes had no significant gas formation and, hence, a little overall reduction in volume. This difference was also seen from the chemical analysis where it could be seen that after 15 and 30 minutes there was reduced more MnO and SiO_2 when slag with sulfur was used compared to slag without sulfur. However, after 60 minutes the reduced amount of oxides is approximately the same for both slag with and without sulfur. The relative volume for both the experiments at 60 minutes has almost the same relative volume at the end.

Regarding the wetting angle, there is little difference between the experiments, and the addition of sulfur to the slag seems to have little effect on the wettability when coke is used as the substrate. The wetting angle starts at around 120° and decreases after time. Furthermore, the sulfur also has little effect on the contact area between the substrate and slag. The contact area is somewhat smaller for the experiments with slag without sulfur, but not enough to conclude with a significant difference. It was also seen little difference on the loss of mass for these experiments, as seen in Table 4.6 on page 98.

As mentioned earlier the effect of load on the pellets was also investigated. In this case, there was not a significant difference between the experiments, as seen in Figure 4.27 on page 104. The experiment where the pellet is made with 500 kg had the lowest relative volume in the end. However, it could be from the fact that the slag digs into the pellet and it will therefore not be measured on the pictures. From the density and porosity analysis, there was no clear difference in density or porosity between the different pellets. Furthermore, it could also not be seen a significant difference in the wetting angle or the contact area. There is also little difference between the loss of mass from these experiments, as seen in Table 4.6.

Lastly, the experiment with a green particle was performed. The relative volume from this experiment has a different behaviour compared to the other experiments with coke. There is a small degree of foaming or bubble formation, and the relative volume decreases almost linearly over time. From the chemical analysis, it was a higher reduction rate of MnO and SiO_2 when using pelletized coke. There can not be seen a clear difference on the wettability, but on the contact area, the green coke has a lower contact area compared to the pelletized coke. It is a little different on the loss of mass, where the experiment with pelletized coke has a higher loss of mass compared to green coke, as seen in Table 4.6.

4.3.2 Experiments with charcoal

In the following chapters, the results from the experiments with charcoal as the substrate is presented.

4.3.2.1 Experiments with charcoal and slag containing sulfur

Figure 4.33 shows the relative volume of the experiments with charcoal and slag with sulfur. There was performed three experiments which were held at 15, 30 and 60 minutes, respectively. The reference volume of the slag was chosen to be when the temperature was 1300 °C, and it takes almost two minutes before it is heated to the holding temperature at 1600 °C. From the different graphs, it can be seen that there is very similar behaviour of the graphs. There is a high degree of gas generation early, and it can be seen that after around 20 minutes the graphs flattens out, hence there is little generation of gas after this.

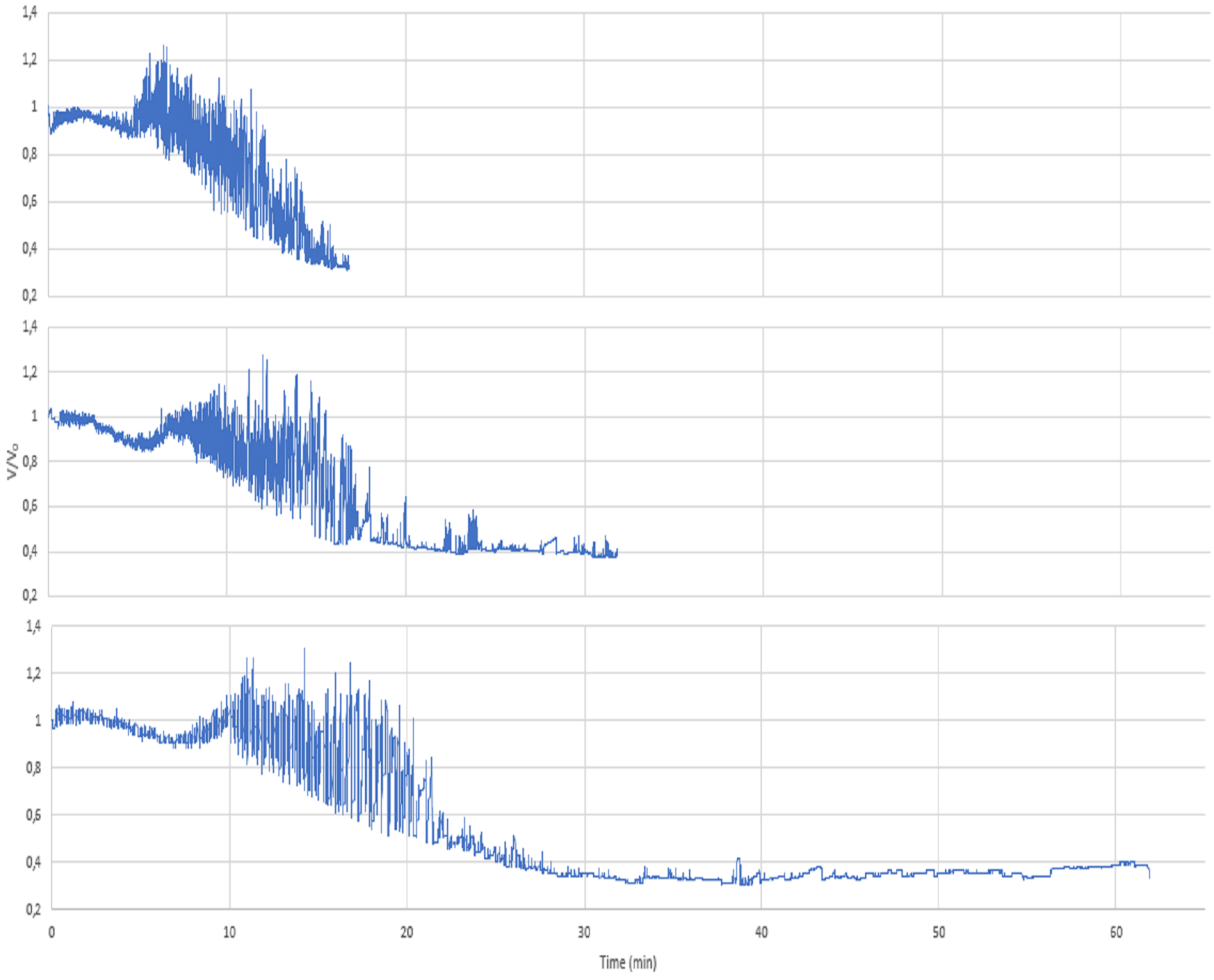

Figure 4.33: Relative volume with charcoal as substrate and slag with sulfur, which were held at 15, 30 and 60 minutes at 1600 °C. (Test 9 (top), 10 (middle) and 11 (bottom))

Figure 4.34 shows the wetting angle between the slag and substrate for test 9, 10 and 11. From the figure, it can be seen that the plots for the three experiments are somewhat similar. The wetting angle is around 120-130° at the beginning and then decreases over

time. From Figure 4.34 it can be seen that the wetting angle decreases until around 20 minutes before the graphs flatten out. This corresponds to the relative volume given in Figure 4.33 where the graph also flattens out after around 20 minutes.

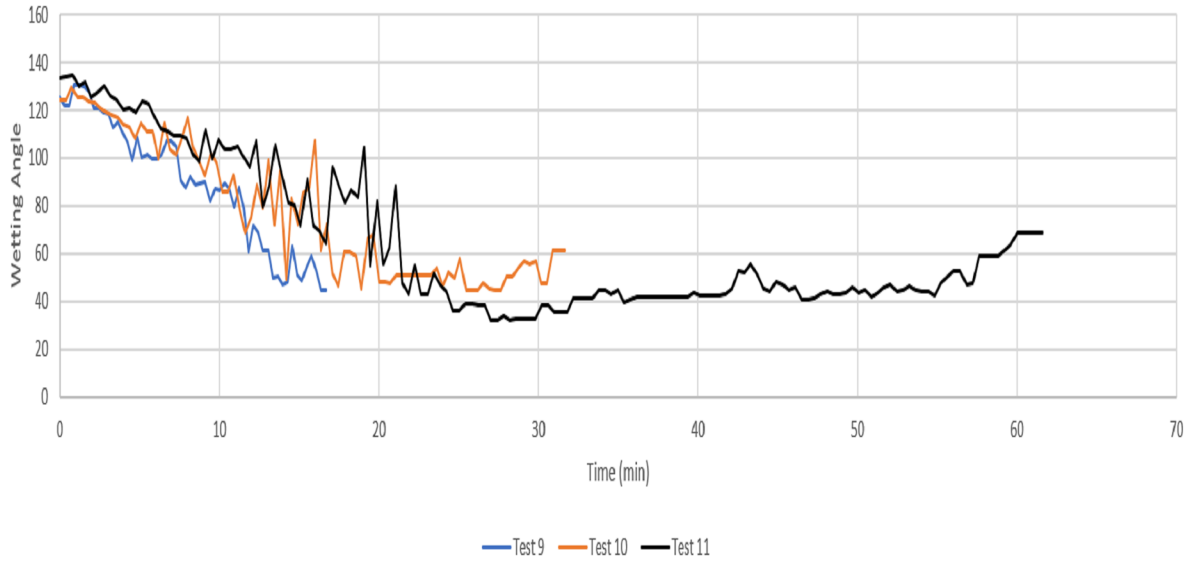

Figure 4.34: Wetting angle with charcoal as substrate and slag with sulfur for test 9, 10 and 11, which were held at 15, 30 and 60 minutes at 1600 °C.

Figure 4.35 shows the contact area between the charcoal substrate and the liquid slag. The different graphs have a similar shape, where it starts at 5-7 mm^2 and then increases rather quickly before it flattens out. Furthermore, there can be seen a similarity between the contact area and the relative volume, where it quickly increases and after around 20 minutes the curves flattens out.

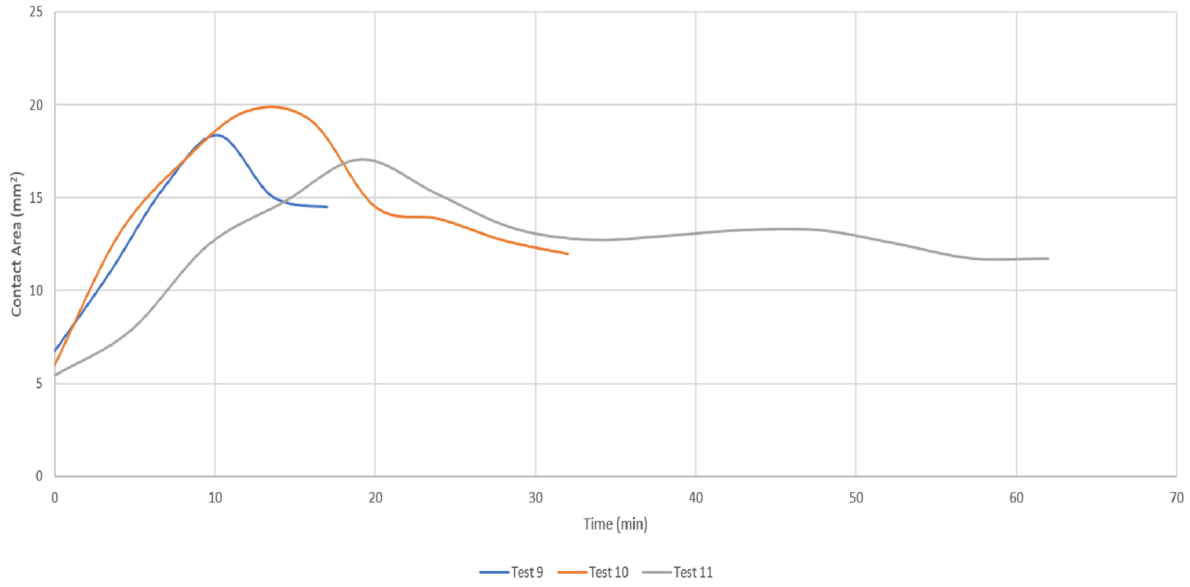

Figure 4.35: Contact area with charcoal as substrate and slag with sulfur for test 9, 10 and 11, which were held at 15, 30 and 60 minutes at 1600 °C

4.3.2.2 Experiments with charcoal and slag without sulfur

Figure 4.36 shows the relative volume of the experiments with charcoal and slag without sulfur. There was performed three experiments which were held at 15, 30 and 60 minutes, respectively. The reference volume of the slag was chosen to be when the temperature was 1300 °C, and it takes almost two minutes before it is heated to the holding temperature at 1600 °C. From the different graphs it can be seen that there is a similarity of the general shape of the curves. From the figure it can be seen that there is in general little activity, compared to the previously shown experiments. For the experiments held for 30 and 60 minutes, there can be seen some increase and decrease in the volume from the peaks around 10-20 minutes. This indicates a small degree gas generation, hence a small degree of reduction compared to the previously shown experiments, which had a larger degree of foaming. The fact that when charcoal is used with slag that does not contain sulfur has a poor reduction rate was also seen from the chemical analysis.

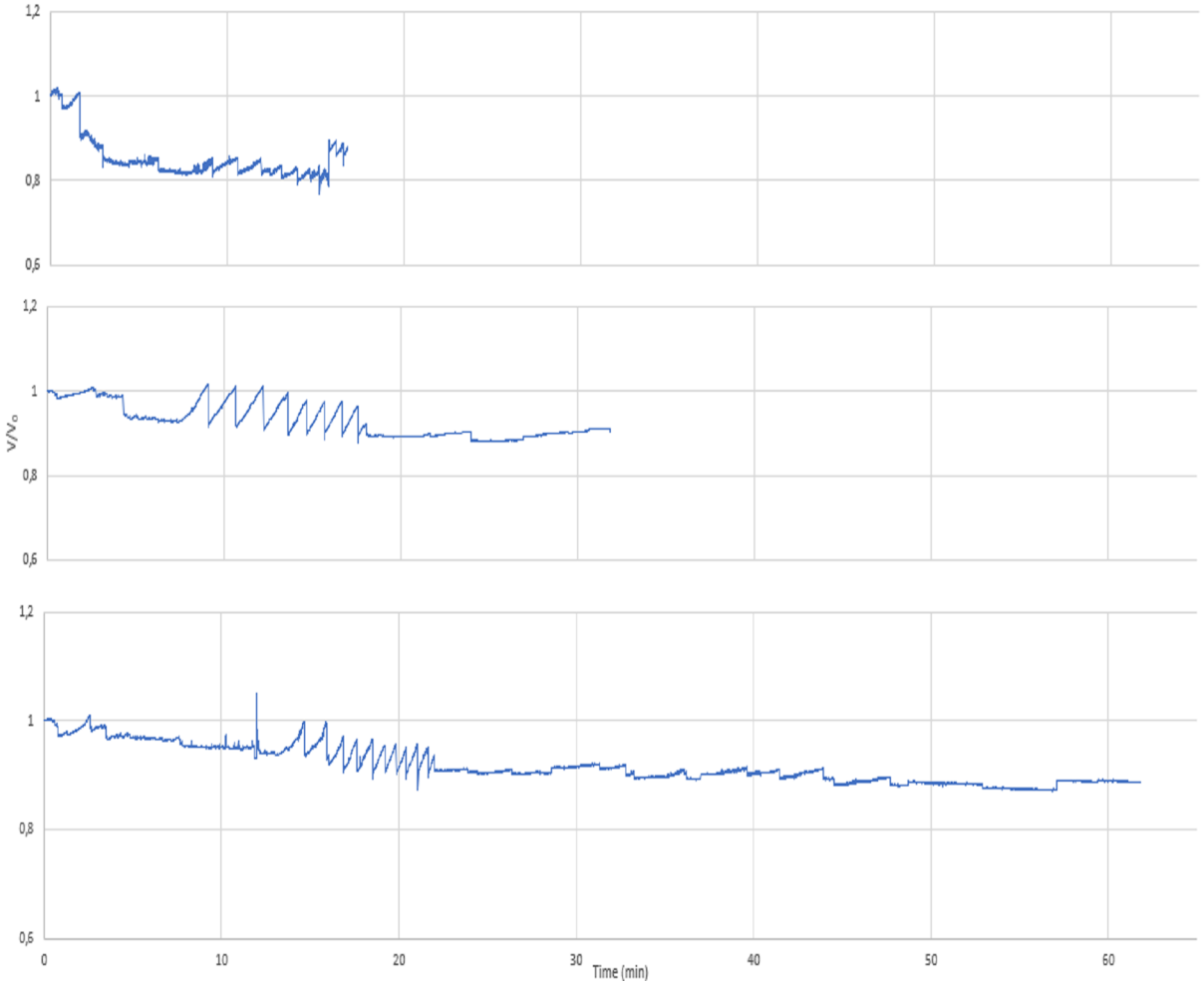

Figure 4.36: Relative volume with charcoal as substrate and slag without sulfur, which were held at 15, 30 and 60 minutes at 1600 °C. (Test 13 (top), 14 (middle) and 15 (bottom))

Figure 4.37 shows the wetting angle between the slag and substrate for test 13, 14 and 15. From the figures it can be seen that the graphs for the three experiments are somewhat similar. The wetting angle is around 110-130° at the beginning. The wetting angle corresponds to the relative volume as the graphs are much flatter than the previous

experiments mentioned, where the wetting angle for test 15 is almost constant throughout the experiment.

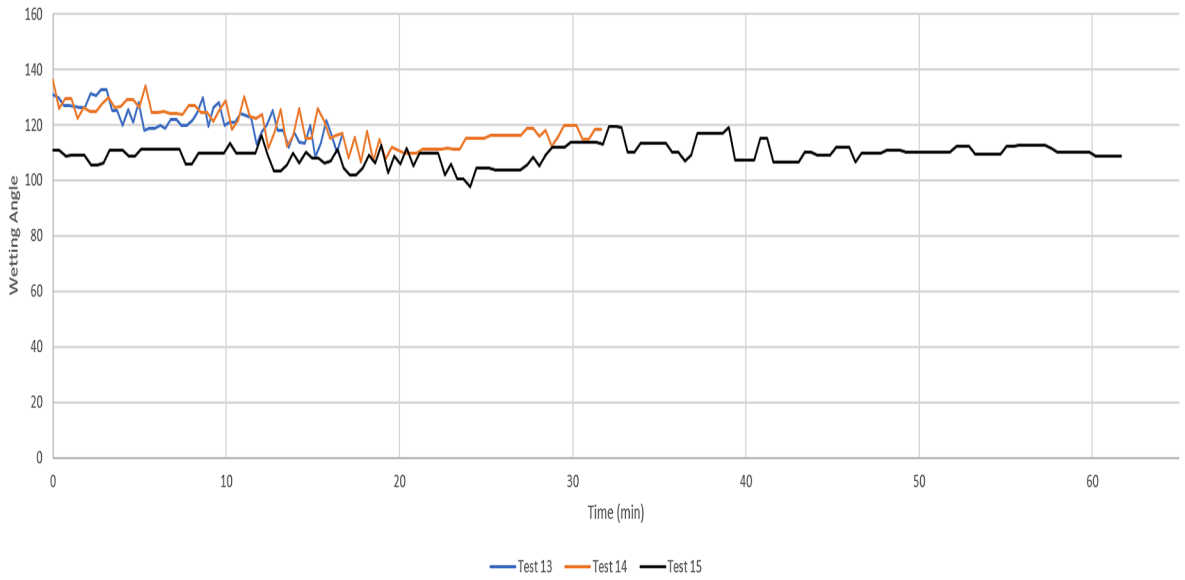

Figure 4.37: Wetting angle with charcoal as substrate and slag without sulfur for test 13, 14 and 15, which were held at 15, 30 and 60 minutes at 1600 °C.

Figure 4.38 shows the contact area between the charcoal as substrate and the slag without sulfur. The contact area is somewhat the same during all the experiments, where it starts around 6-7 mm^2. The experiments which were held for 15 and 30 minutes has a small increase, and the experiment held for 60 minutes has approximately the same contact area during the experiment. This correlates well with both the relative volume and wetting angle, where it can be seen that the reduction of slag without sulfur with charcoal is poor.

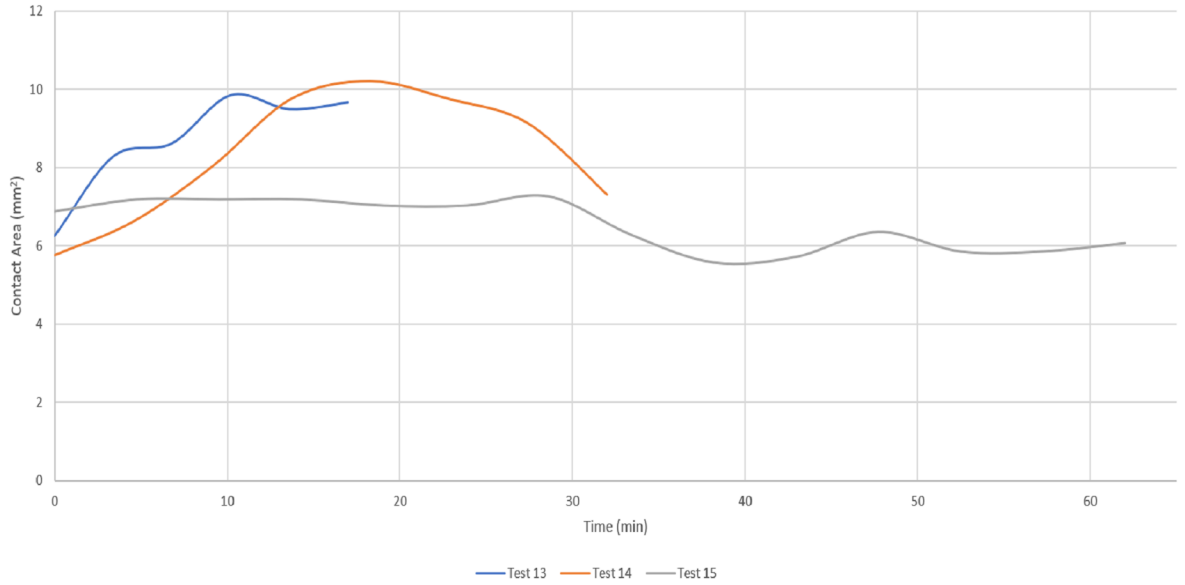

Figure 4.38: Contact area with charcoal as substrate and slag without sulfur for test 13, 14 and 15, which were held at 15, 30 and 60 minutes at 1600 °C.

4.3.2.3 Experiments with charcoal pellets made with different load

There were also done experiments on the pelletized charcoal where different loads were used when making the pellets. The load which was used was with 500 kg, 1000 kg and 2000 kg. There were performed experiments with both slags, with and without sulfur, to investigate this. Figure 4.39 shows the relative volume of the experiments where the slag with sulfur was used. From the figure it can be seen that there are some differences between the different experiments, however, there is no clear correlation if a higher or lower load will increase the reduction rate. There could also not be seen a difference from the experiments with different load from the chemical analysis. Hence, from this it does not seem like the load on the pellet affect the reduction of the slag.

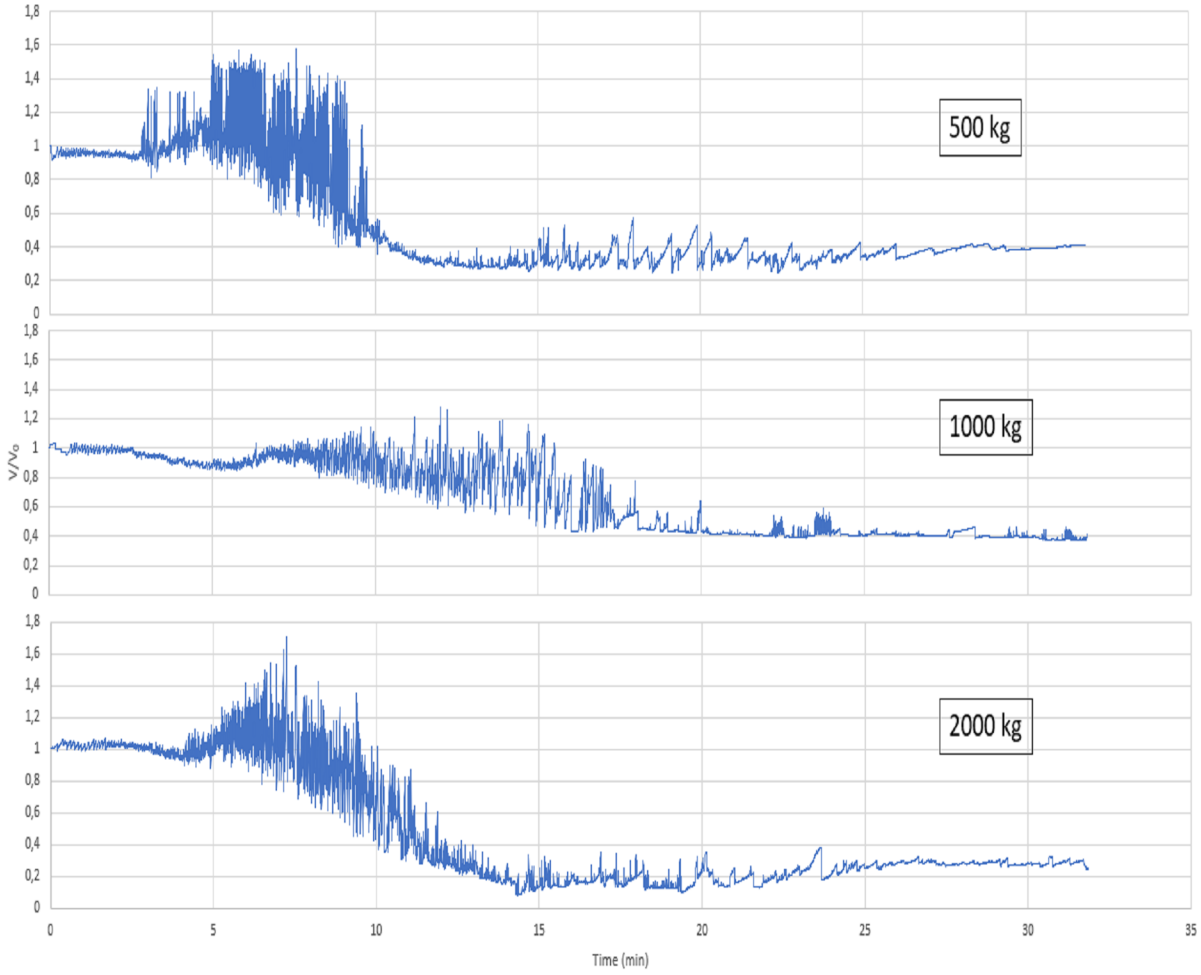

Figure 4.39: Relative volume with charcoal as substrate and slag with sulfur which were held at 1600 °C for 30 min, where the pellets is made with a load of 500 kg (test 19 - top), 1000 kg (test 10 - middle) and 2000 kg (test 20 - bottom).

Figure 4.40 shows the wetting angle for the experiments with charcoal and slag with sulfur where the pellets are made with different loads. The wetting angle starts around 130° and quickly decreases over time. As it was for the relative volume the wetting angle for the experiments where the pellet is made with a load of 500 and 2000 kg has a very similar behaviour. It can also be seen that the angle decreases significantly over time.

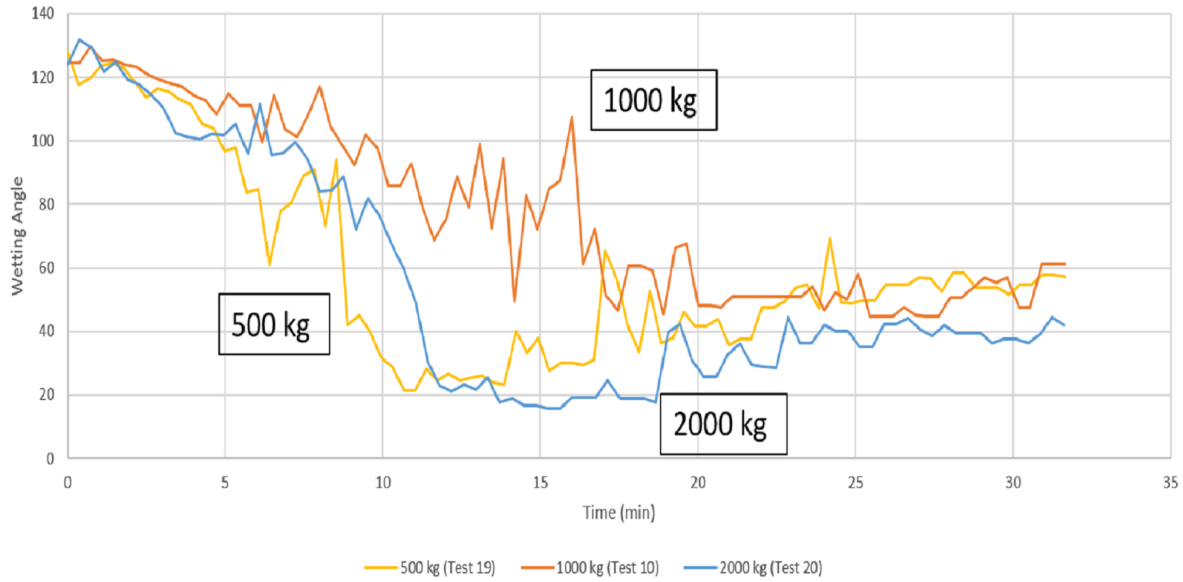

Figure 4.40: Wetting angle with charcoal as substrate and slag with sulfur which were held at 1600 °C for 30 min, where the pellets is made with a load of 500 kg (test 19), 1000 kg (test 10) and 2000 kg (test 20).

Figure 4.41 shows the contact area between the charcoal substrate and the slag. The contact area is measured by measuring the length of the area where the slag and substrate are in contact with each other. The contact area is assumed to be a perfect circle, and the length measured is the diameter of this circle. The contact area starts around 5-7 mm^2, and then quickly increases. From the figure it can be seen that at the experiment with 500 kg has the highest contact area, then 1000 kg and 2000 kg with the lowest contact area. There can also be seen from the relative volume that the experiment with 500 kg has a high degree of foaming early, hence explaining the quick increase in the contact area.

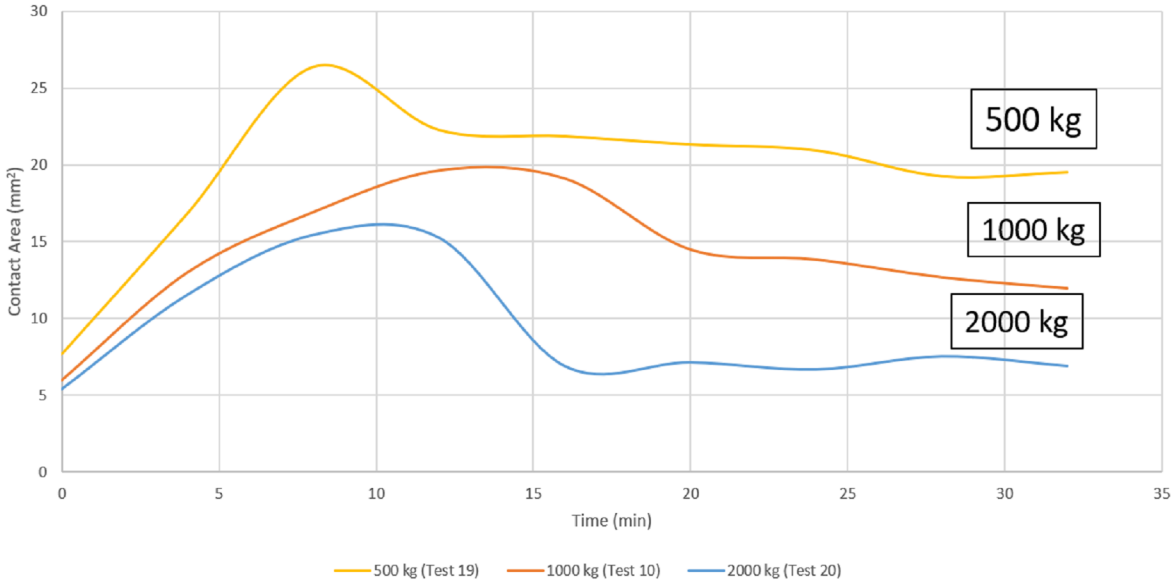

Figure 4.41: Contact area with charcoal as substrate and slag with sulfur which were held at 1600 °C for 30 min, where the pellets is made with a load of 500 kg (test 19), 1000 kg (test 10) and 2000 kg (test 20).

As mentioned above, there were also performed experiments with slag that does not contain sulfur. Figure 4.42 shows the relative volume for the experiments where the pellets were made with a load of 500 kg (Test 21), 1000 kg (Test 14) and 2000 kg (Test 22). From the figure it can be seen that the different experiment is very similar, other than the experiments where the pellet is made with a load of 2000 kg decreases somewhat more over time than the other experiments. From the chemical analysis, it was also seen that the experiment with 2000 kg had a higher reduction of MnO and SiO_2 compared to the other two experiments. Hence, the load used when making the pellets does not seem to affect the reduction of the slag.

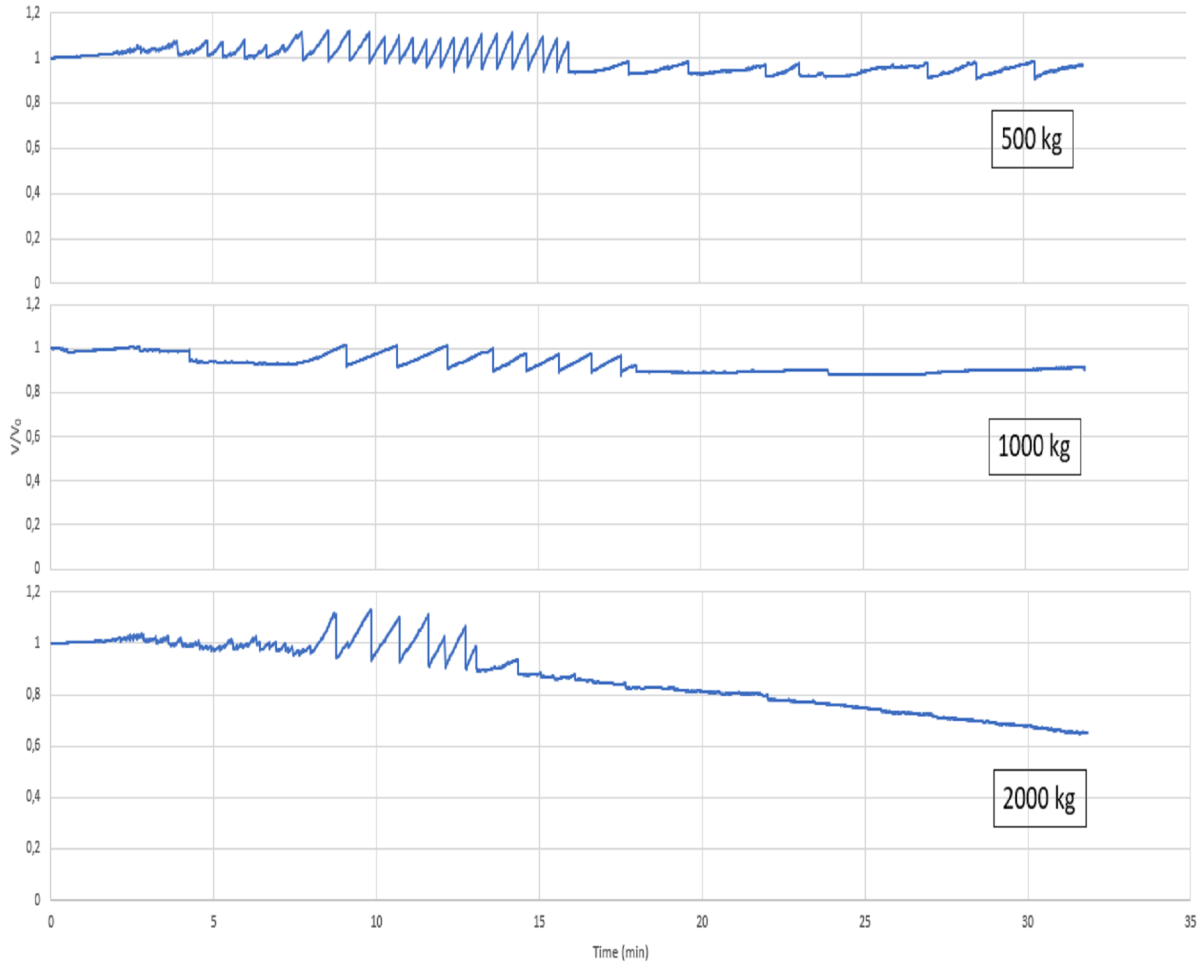

Figure 4.42: Relative volume with charcoal as substrate and slag without sulfur which where held at 1600 °C for 30 min. The pellets is made with a load of 500 kg (test 21 - top), 1000 kg (test 14 - middle) and 2000 kg (test 22 - bottom).

Figure 4.43 shows the wetting angle for the experiments from the figure above. It can be seen that the experiment where the pellet is made with 2000 kg has a slight decrease in wetting angle over time, however, the other two experiments are almost constant. The fact that the wetting angle for the experiments where the pellet is made with 2000 kg decreases correlates with the relative volume, as there was seen a decrease in the volume for this test.

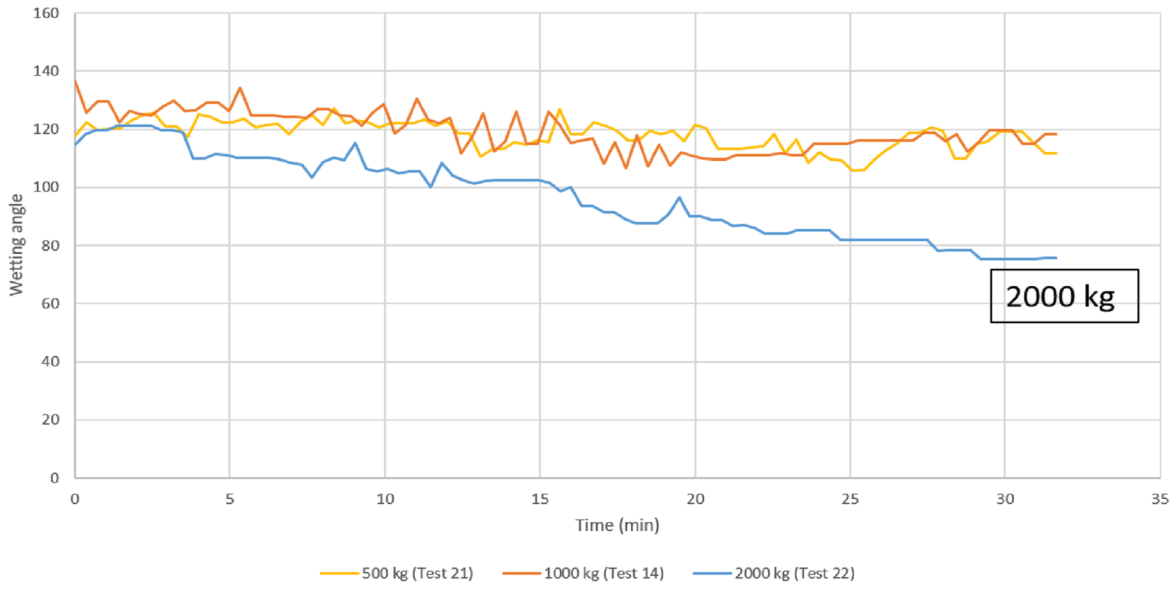

Figure 4.43: Wetting angle with charcoal as substrate and slag without sulfur which was held at 1600 °C for 30 min. The pellets are made with a load of 500 kg (test 21), 1000 kg (test 14) and 2000 kg (test 22).

Figure 4.44 shows the contact area between the charcoal substrate and the slag. It can be seen that there is a slight increase in the experiment where the pellet is made with 2000 kg, and for the other two experiments the contact area is almost constant. This could also be seen from the relative volume and the wetting angle.

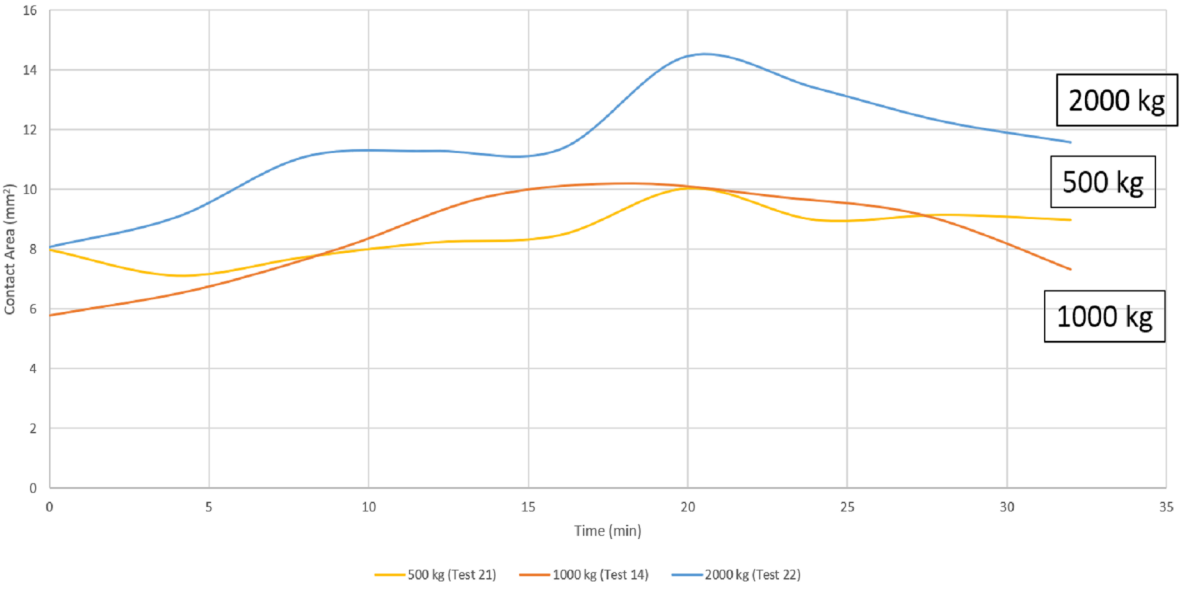

Figure 4.44: Contact area with charcoal as substrate and slag without sulfur which where held at 1600 °C for 30 min. The pellets is made with a load of 500 kg (test 21), 1000 kg (test 14) and 2000 kg (test 22).

4.3.2.4 Experiments with charcoal performed with different temperature

Figure 4.45 shows the relative volume for tests 19 and 30 where pelletized charcoal is used and slag with sulfur. The pellets in these experiments were made with a load of 500 kg on the press. Test 30 has a holding temperature of 1700 °C and test 19 has a holding temperature of 1600 °C. The reference temperature was set to 1300 °C. From the figure, it can be seen that there is no significant difference between these two experiments, other than the fact that test 30 has a somewhat higher peak and somewhat more foaming as the graph oscillates more. It can be seen that the experiment at 1700 °C has a high degree of foaming, hence a high degree of gas generation. This also correlated with the chemical analysis where it can be seen that 99.90 % of the MnO is reduced and 68.45 % of the SiO_2. For the experiment at 1600 °C 98.73 % of the MnO and 48.76 % of the SiO_2 was reduced. Both of the experiments flattens out after 10-15 minutes at a relative volume of approximately 0.3.

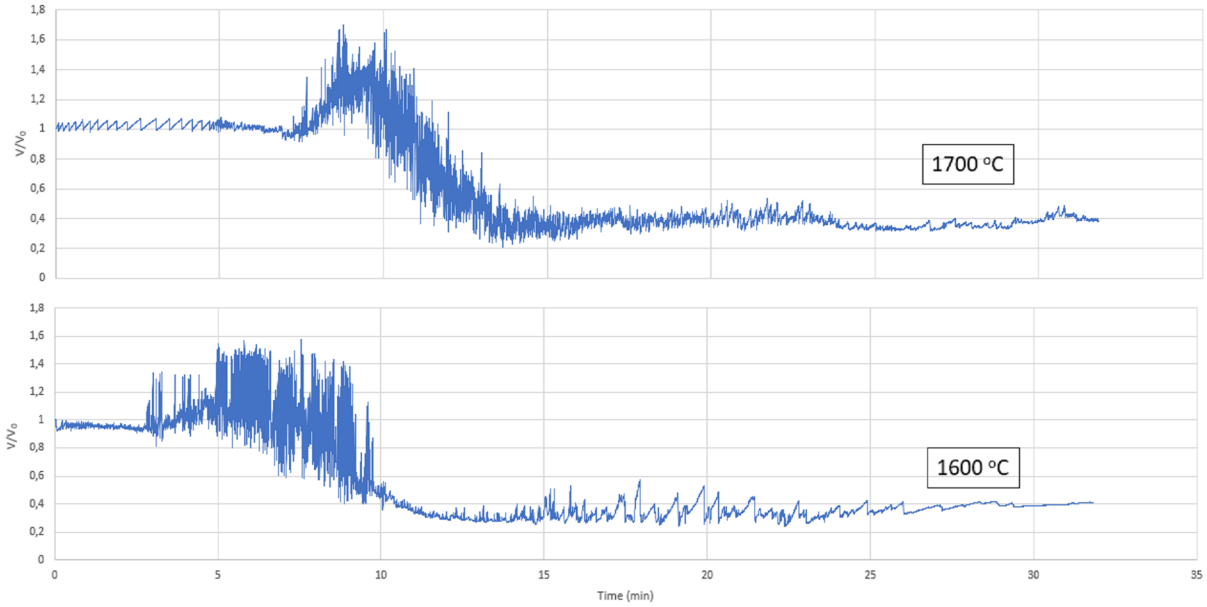

Figure 4.45: Relative volume for experiments with charcoal made with a load of 500 kg on the press and slag with sulfur. The experiments where held at 30 minutes for either 1700 °C (Test 30 - top) or 1600 °C (Test 19 - bottom).

Figure 4.46 shows the wetting angle between the slag and substrate for test 19 and 30. From the figure it can be seen that both of the experiments have very similar behaviour. However, the wetting angle decreases earlier for test 19 than for test 30. This correlates well with the relative volume, in that the volume decreases sooner for test 19. Both start with a wetting angle around 120°.

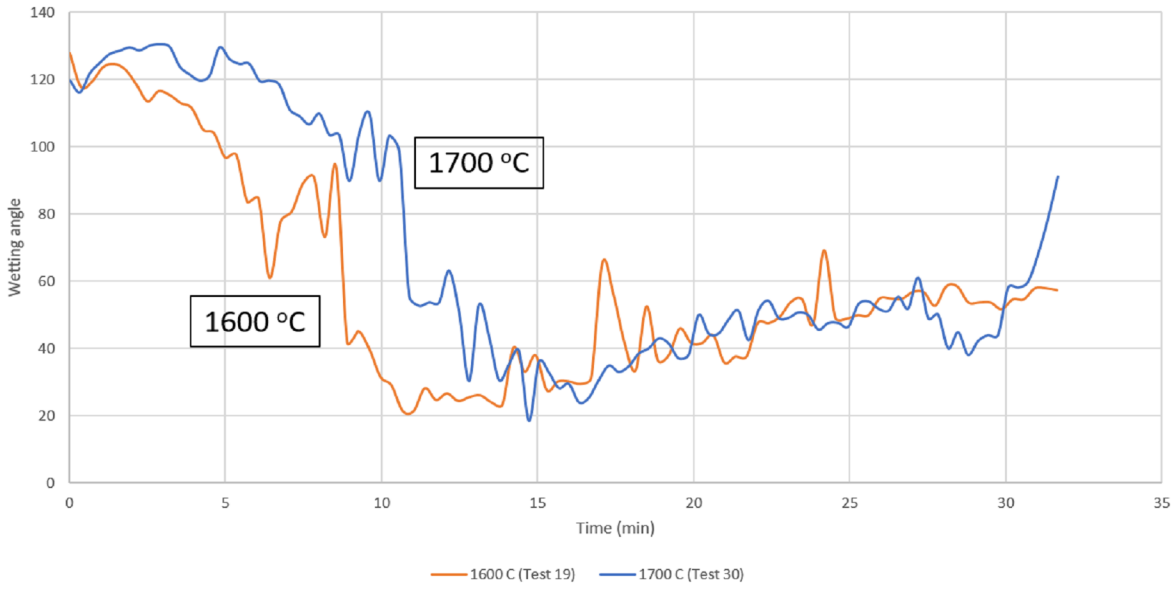

Figure 4.46: Wetting angle for experiments with charcoal made with a load of 500 kg on the press and slag with sulfur. The experiments where held at 30 minutes for either 1700 °C (Test 30) or 1600 °C (Test 19).

Figure 4.47 shows the contact area between the substrate and the slag for test 19 and 30. The contact area is measured by measuring the length of the area where the slag and substrate are in contact with each other. The contact area is assumed to be a perfect circle, and the length measured is the diameter of this circle. The contact area starts around 7-8 mm^2 and then increases over time. It can be seen that test 19 increases earlier than 30, which correlates with the wetting angle, where test 19 had an earlier decrease in wetting angle than test 30. These two experiments have a contact area in general, compared to previously shown experiments, which correlates well with the fact that there is a high degree of MnO and SiO_2 reduction.

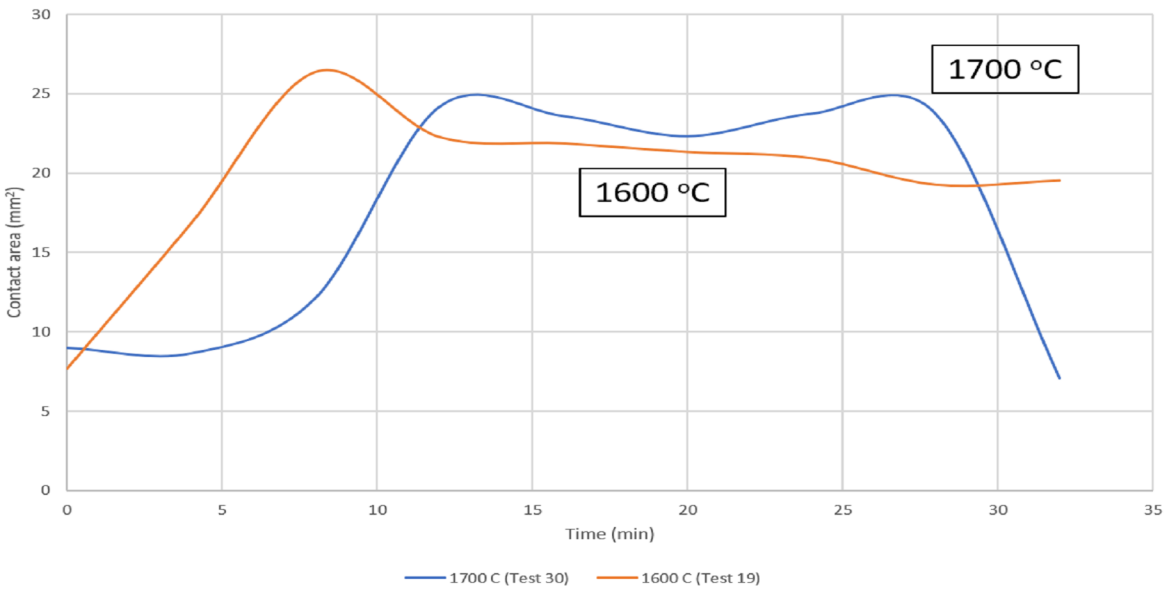

Figure 4.47: Contact area for experiments with charcoal made with a load of 500 kg on the press and slag with sulfur. The experiments where held at 30 minutes for either 1700 °C (Test 30) or 1600 °C (Test 19).

There was also done experiments with slag that does not contain sulfur for different temperatures. Figure 4.48 shows the relative volume for test 21 and 31 where pelletized charcoal is used and slag without sulfur. The pellets in these experiments were made with a load of 500 kg on the press. Test 31 has a holding temperature of 1550 °C and test 21 has a holding temperature of 1600 °C. The reference temperature was set to 1300 °C. From the figure it can be seen that there is very little difference between the two experiments. The behaviour is also very similar to other experiments with charcoal and slag without sulfur, where there is very little gas generation. Hence, there is little reduction.

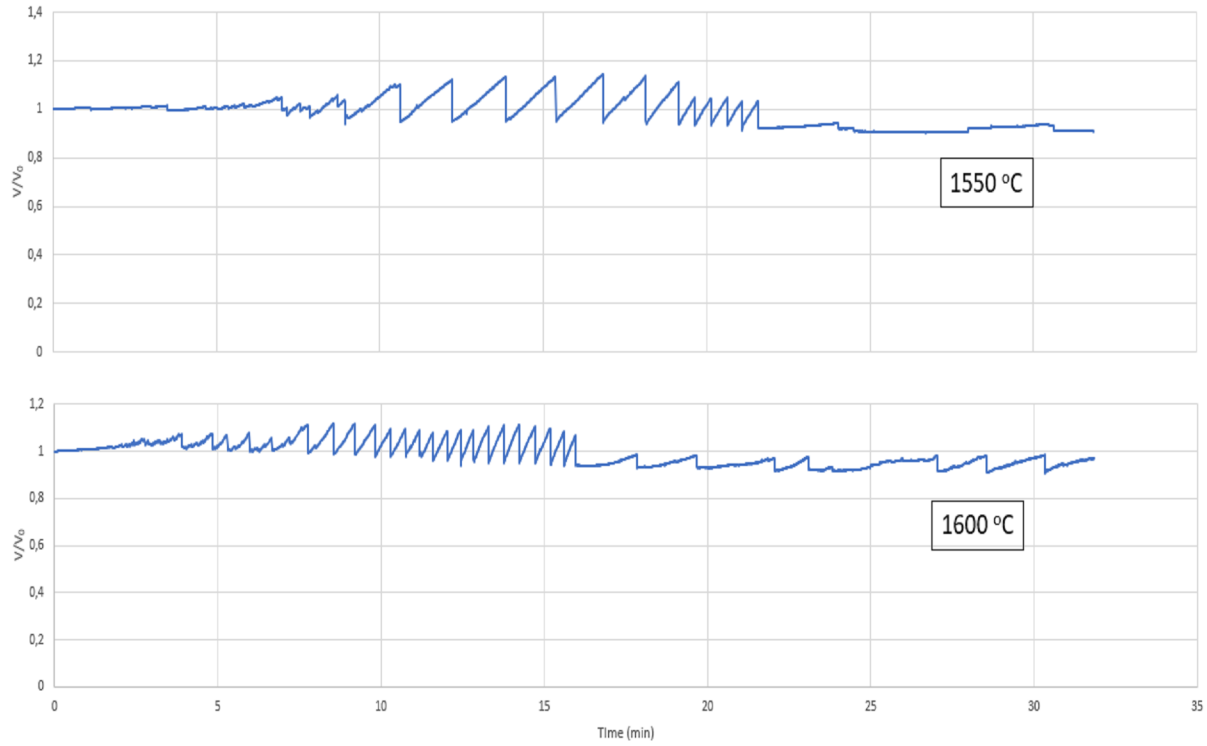

Figure 4.48: Relative volume for experiments with charcoal made with a load of 500 kg on the press and slag without sulfur. The experiments where held at 30 minutes for either 1550 °C (Test 31 - top) or 1600 °C (Test 21 - bottom).

Figure 4.49 shows the wetting angle between the slag and substrate for test 21 and 31. From the figures, it can be seen that for both the experiments the wetting angle starts around 120° and is almost constant throughout the entire experiment, as it also has been for other experiments with charcoal and slag without sulfur.

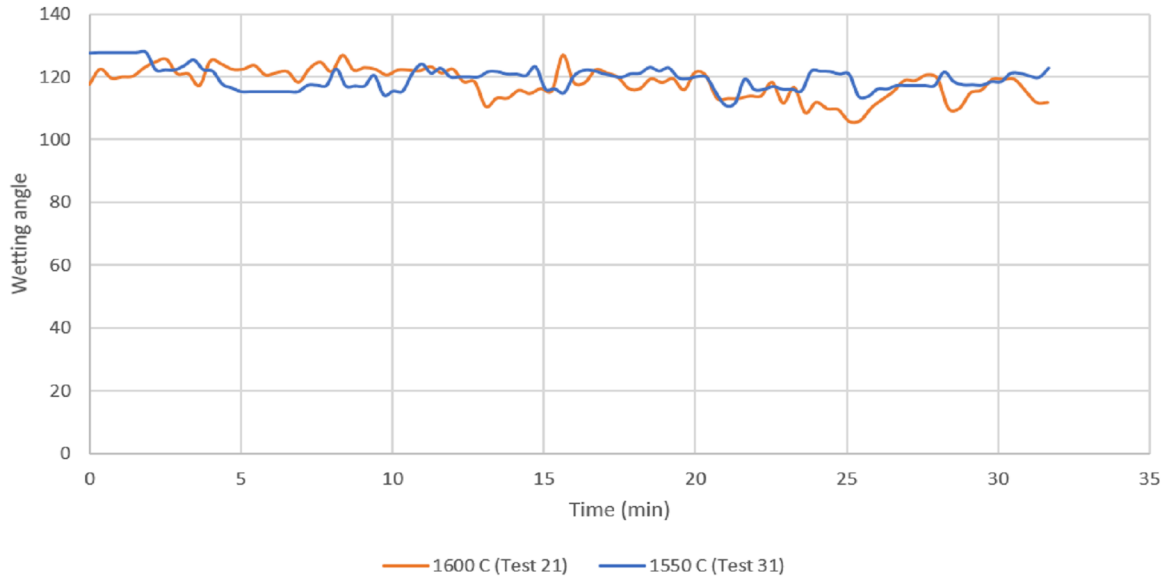

Figure 4.49: Wetting angle for experiments with charcoal made with a load of 500 kg on the press and slag without sulfur. The experiments where held at 30 minutes for either 1550 °C (Test 31) or 1600 °C (Test 21).

Figure 4.50 shows the contact area between the substrate and the slag. The contact area is measured by measuring the length of the area where the slag and substrate are in contact with each other. The contact area is assumed to be a perfect circle, and the length measured is the diameter of this circle. The contact area starts around 7-8 mm^2 and only increases some before it flattens out just above 8 mm^2. The contact area is almost the same for both the experiments throughout the experiment.

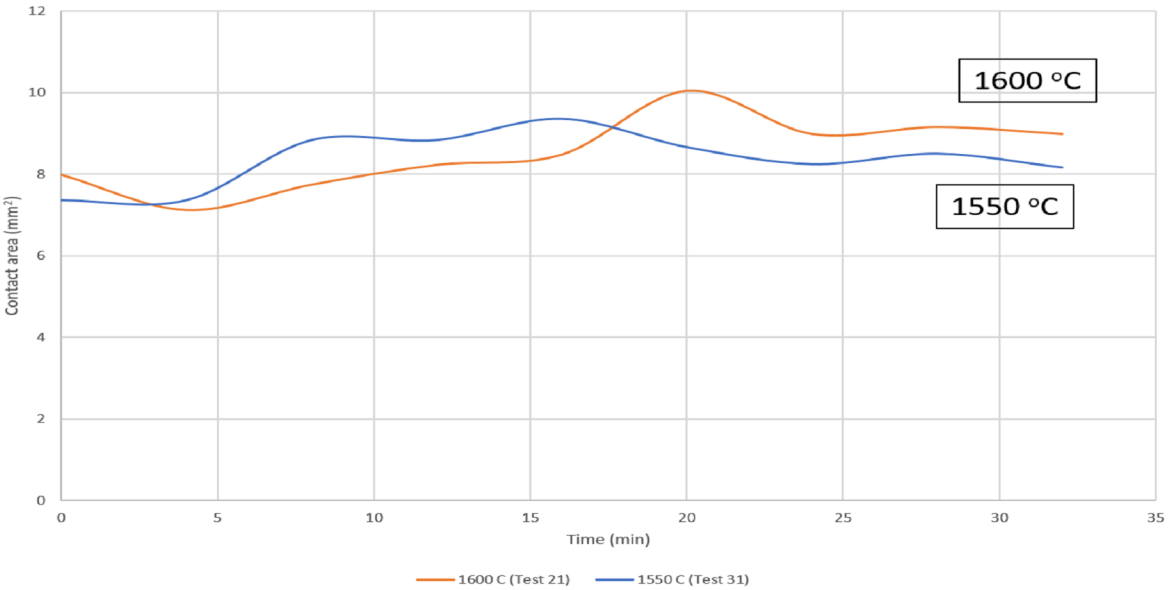

Figure 4.50: Contact area for experiments with charcoal made with a load of 500 kg on the press and slag2. The experiments where held at 30 minutes for either 1550 °C (Test 31) or 1600 °C (Test 21).

4.3.2.5 Green charcoal particle

There was performed experiments with green charcoal particles to investigate the difference between this and pelletized charcoal. Figure 4.51 shows the relative volume for the experiments with pelletized charcoal (test 25) and the green charcoal particles, where one is made so that the surface is on top of the fibres (test 26) and one is made so that the surface is along the fibres (test 27). It was performed two different experiments with green charcoal to investigate if it has any difference of the reactivity of the charcoal regarding the direction of the fibres. As seen from the figure both the experiments with green charcoal is very similar, hence from these two experiments it can not be seen any difference in reactivity regarding the fibre direction. However, the green charcoal has a different behaviour compared to the pelletized charcoal, but the relative volume is approximately the same at the end of the experiment. There can also not be seen any significant difference in the reduction rate on MnO from the chemical analysis, however, when using pelletized charcoal there is a higher amount of reduced SiO_2. It was used slag with sulfur for all three experiments.

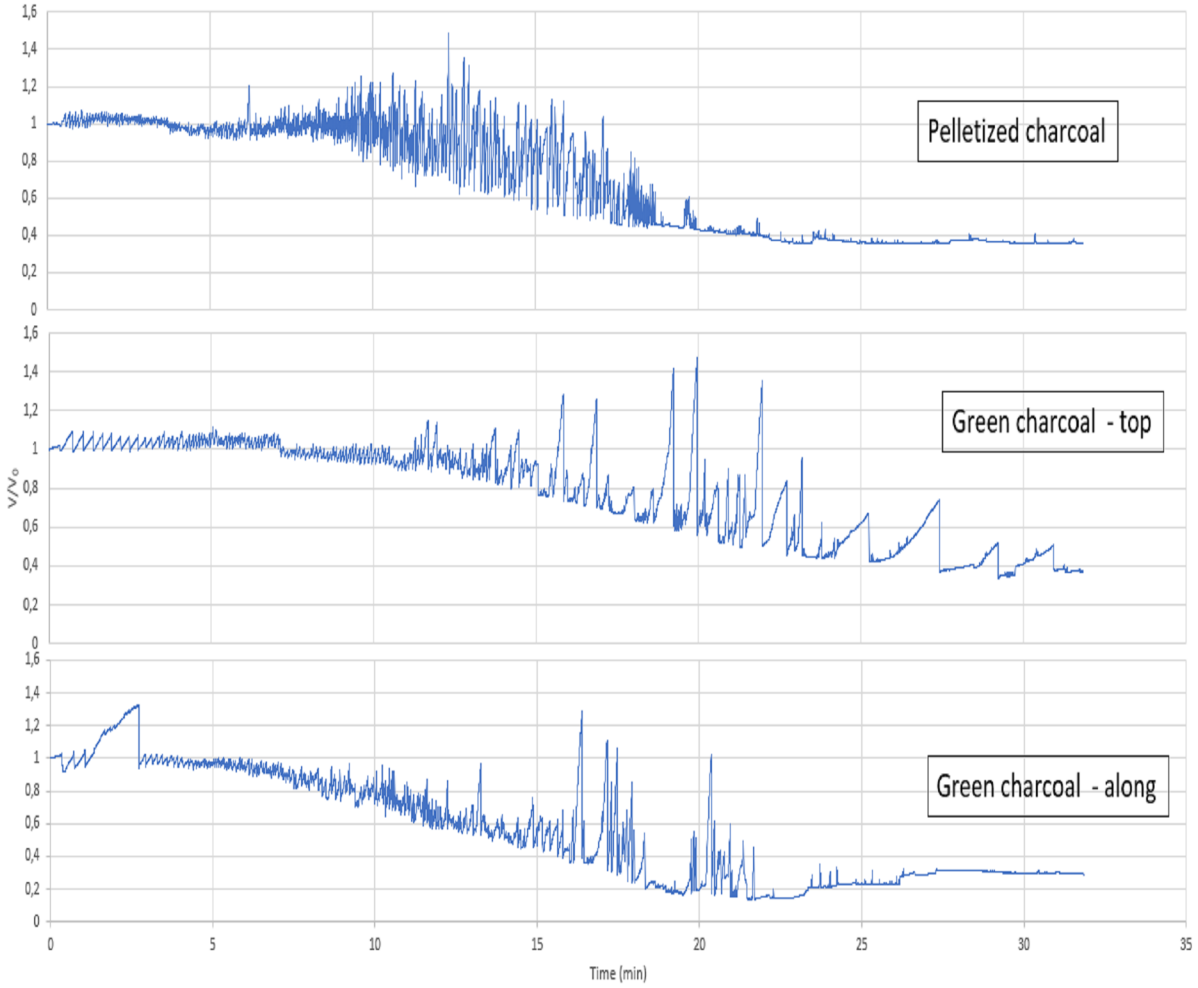

Figure 4.51: Relative volume for experiments with green charcoal and experiment with pelletized charcoal where slag wit sulfur is used. The experiments where held at 30 min at 1550 °C.

Figure 4.52 shows the wetting angle for the experiments with green charcoal and pelletized charcoal. The wetting angle starts at around 130° and then decreases over time.

Furthermore, the wetting angle is somewhat the same for all the experiments and also decreases with approximately the same slope.

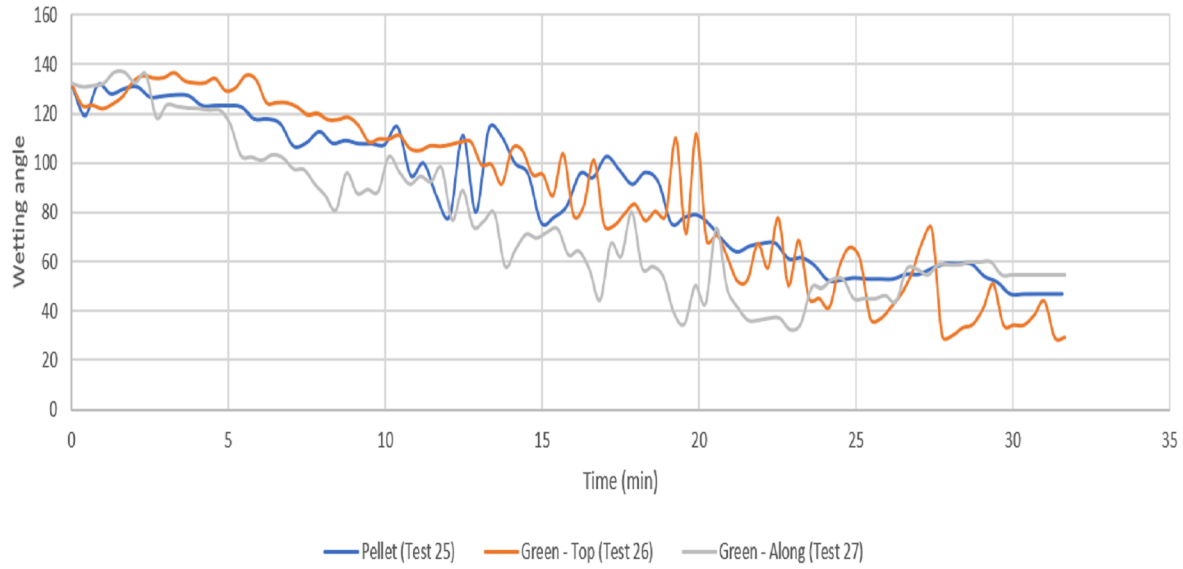

Figure 4.52: Wetting angle with charcoal as a substrate and slag with sulfur for the experiments with green charcoal and pelletized charcoal. The experiments where held at 30 min at 1550 °C.

Figure 4.53 shows the contact area between the substrate and the slag. The contact area is measured by measuring the length of the area where the slag and substrate are in contact with each other. The contact area is assumed to be a perfect circle, and the length measured is the diameter of this circle. The contact area starts around 4-6 mm^2 and then increases. The contact area is somewhat similar for all the experiments, except that for the experiment with green charcoal where the surface is on top of the fibre which decreases after around 20 minutes while the other two flattens out.

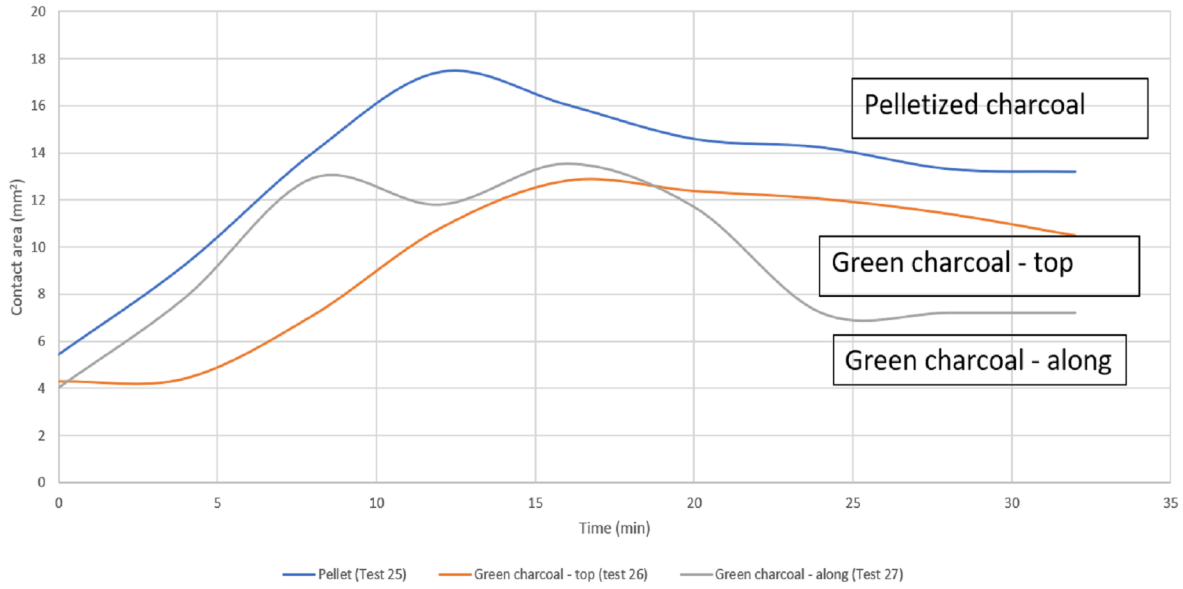

Figure 4.53: Contact area with charcoal as a substrate and slag with sulfur for the experiments with green charcoal and pelletized charcoal. The experiments where held at 30 min at 1550 °C.

4.3.2.6 Summary of experiments with charcoal

There have been performed several different experiments where charcoal has been used as the substrate. The parameters that have been investigated is the influence of sulfur in the slag, different load on the pellets and experiments with green charcoal particles.

For the experiments where slag with sulfur was used there was a high degree of gas generation early, which led to a high degree of foaming, and then the relative volume flattens out after around 20 minutes. Unlike the experiments with coke where there could not be seen a significant difference between if the slag contains sulfur or not, when charcoal was used as a substrate there is a significant difference. From the relative volume measurements for the experiments with charcoal and slag without sulfur, there can be seen a very little generation of gas and hence very little foaming or bubbling. Low gas generation corresponds with a low degree of reduction, which can also be seen from the chemical analysis. Furthermore, when measuring the wetting angle when slag with sulfur was used it started around 120-130° and rather quickly decreased to around 40°. However, the wetting angle when slag without sulfur was used it also started around 120-130° but it was almost constant throughout the experiment. This difference can also be seen in the contact area, where for slag with sulfur it quickly increases to almost 20 mm^2 and for slag without it barely reaches 10 mm^2.

As mentioned earlier, the effect of the load on the pellets was also investigated. As it was for coke there could not be seen any significant difference between the experiments where the different pellets are used. The difference between if the slag contains sulfur or not was also seen in these experiments. From the experiments with different temperature, there could not be seen any significant difference in the relative volume, wetting angle or the contact area.

Lastly, the experiments with green particles were performed. The relative volume for the experiments with green charcoal has a different behaviour compared to the other experiments with charcoal. However, at the end of the experiment the relative volume has approximately the same value. There could also not be seen any significance difference from the chemical analysis on the reduction of MnO, however, when using pelletized charcoal the amount of reduced SiO_2 is higher. From the wetting angle and contact area measurements there was little difference between the two experiments with green charcoal and pelletized charcoal.

4.3.3 Experiments with graphite

There was performed two experiments with graphite as the substrate, where one is with slag that contains sulfur (test 28) and one with slag without sulfur (test 29). Figure 4.54 shows the relative volume of both experiments. The reference volume was chosen to be when the temperature was 1300 °C, and it takes almost two minutes before it is heated to the holding temperature at 1600 °C. It can be seen a clear difference between the two graphs, as the experiment performed with slag with sulfur has a much higher degree of gas generation compared to the experiment with slag without sulfur. Hence, sulfur has a significant impact on the reduction of the slag.

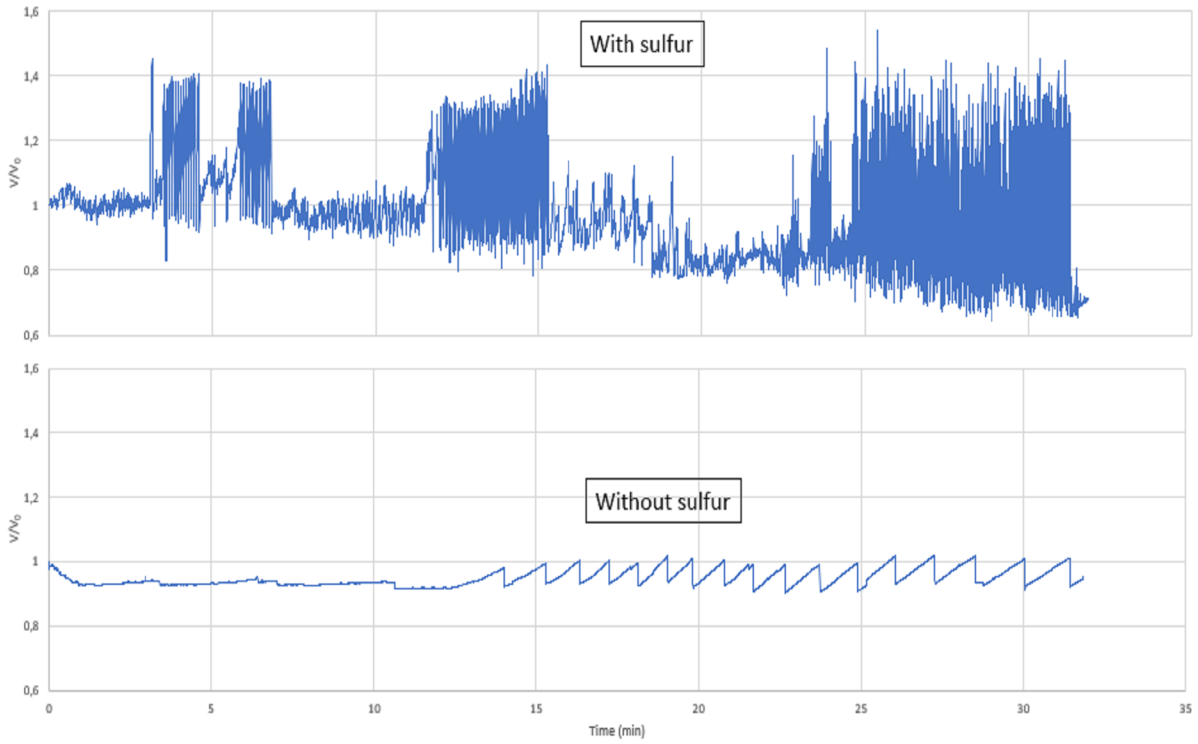

Figure 4.54: Relative volume for experiments with graphite as the substrate where slag with sulfur (test 28 - top) and slag without sulfur (test 29 - bottom) is used. Both the experiments were held at 1600 °C for 30 min.

Figure 4.55 shows the wetting angle for the experiments where graphite was used as the substrate. As it was for the relative volume, there can also be seen a clear difference between the two experiments on the wetting angle. The wetting angle starts just above 100° for the experiment with sulfur, and around 130° for the experiment without sulfur.

Furthermore, for the experiment with sulfur the wetting angle decreases over time, but the wetting angle increases when the slag does not contain sulfur. Hence, when using graphite as the substrate the sulfur will have an impact on the wettability of the slag.

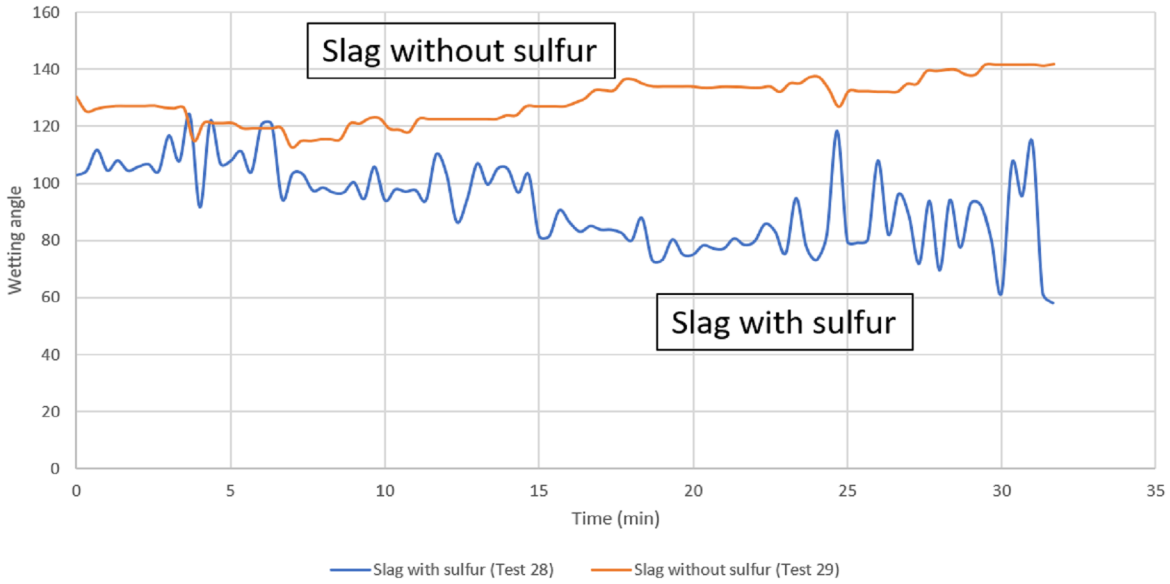

Figure 4.55: Wetting angle for experiments with graphite as the substrate where slag with sulfur (test 28) and slag without sulfur (test 29) is used. Both the experiments were held at 1600 °C for 30 min.

Figure 4.56 shows the contact area between the substrate and the slag. As it was for both relative volume and wetting angle there can be seen a clear difference between the two slags. When using slag with sulfur the contact area starts around 16 mm^2 and increases throughout the entire experiment. For slag without sulfur, the contact area starts around 7 mm^2 and decreases some over time. Hence, the addition of sulfur in the slag will significantly increase the contact area when graphite is used as the substrate.

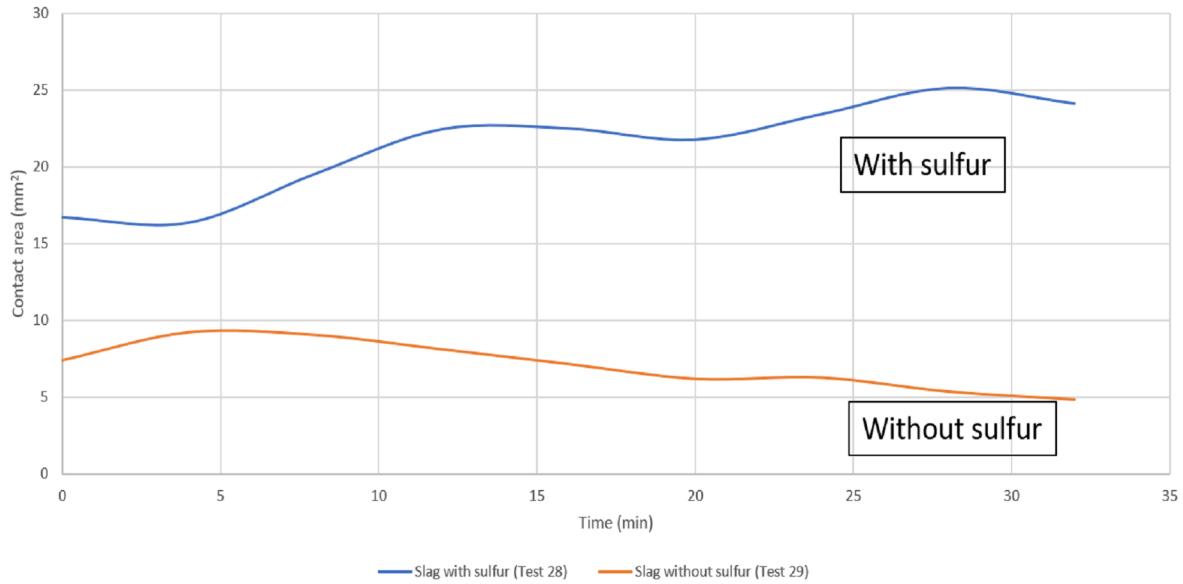

Figure 4.56: Contact area for experiments with graphite as the substrate where slag with sulfur (test 28) and slag without sulfur (test 29) is used. Both the experiments were held at 1600 °C for 30 min.

5 Discussion

In the following chapter, the results will be discussed. First, the chemical analysis will be discussed, then the influence of sulfur in the process before the mechanisms of and behaviour of the slag. The pellets will also be discussed, such as the green particles and the surface roughness. Lastly, the experiments in the furnace and the quality of the results will be discussed.

5.1 Discussion about the chemical analysis

When investigating the reduction of MnO and SiO_2 a chemical analysis of the slag (and metal) is needed to confirm that something has been reduced. The measurements of relative volume, wetting angle and contact area can give some good results regarding if there has occurred any reaction, in this case mostly generation of gas. However, these results are not conclusive and therefore a chemical analysis is needed.

The chemical analysis of the samples from this study was analysed in an EPMA. However, there can be some error when using the EPMA when analysing the sample. This can be seen in the full EPMA analysis given in Appendix A2, where all three of the point analysis is given and there is a difference between them. In addition, the total percentage is not 100.00 %, in fact, it rarely is. Figure 5.1a shows the difference from 100.00 % from the slag analysis. However, the slag was glassy and homogeneous, the difference is not very large. On the other hand, when analysing the metal phase there is a larger variance between the analysis, as seen in Figure 5.1b. The negative values on the figure are the analysis where the total percentage was above 100 %, and the positive values are under 100 %.

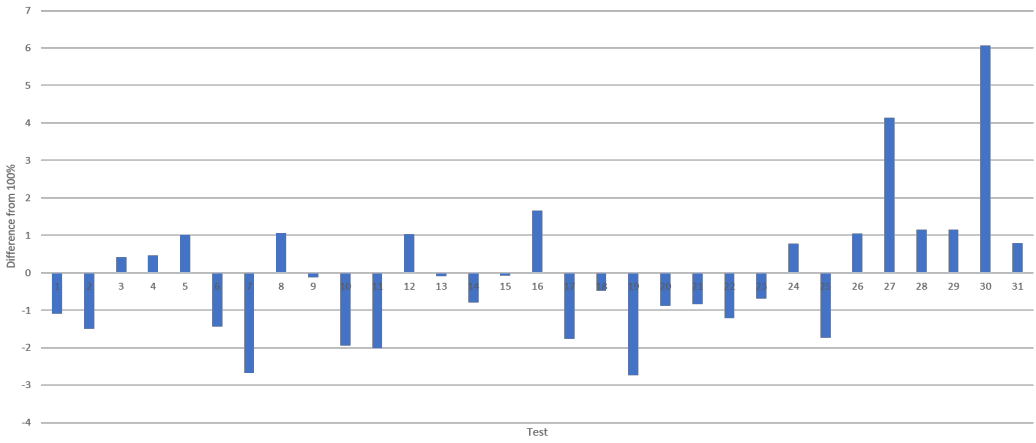

(a) Slag-analysis

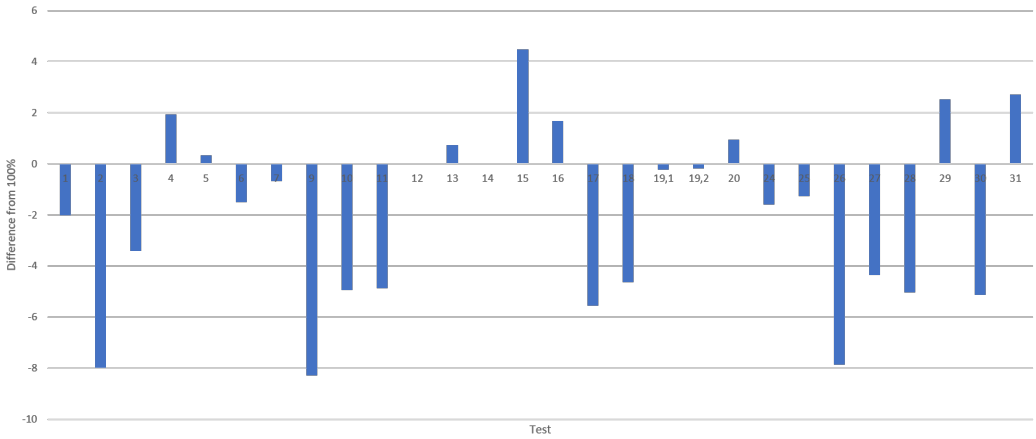

(b) Metal-analysis

Figure 5.1: Difference from 100 % from the EPMA analysis for all the tests, for both slag and metal analysis.

In Table 4.4 on page 88 the chemical analysis of the slag is shown. From the table, it can be seen that there is a clear decrease in the amount of MnO with increasing holding time, as expected. From the chemical analysis, there can be some differences between the different experiments. For the experiments with coke there is little difference at 60 min, however at 15 and 30 minutes the amount of MnO is lower when using slag with sulfur. This indicates that the reduction starts earlier when using slag with sulfur and coke compared to slag without sulfur. Furthermore, for the experiments with charcoal, there can be seen a clear difference in the reduction of both MnO and SiO_2. If the slag contains sulfur (slag1) the reduction rate is much higher than if there is no sulfur in the slag (slag2). It can also be seen that after 15 min when using charcoal and slag with sulfur there is already a large amount of MnO and SiO_2 reduced, indicating that the reduction starts early. This could also be seen from the relative volume measurements, given in Figure 4.33 on page 110, where the gas generation or foaming starts soon after reaching the holding temperature. When the slag without sulfur is used with charcoal there is a very little reduction of both MnO and SiO_2.

From Figure 4.11 on page 89 which shows the weight fractions of MnO in the slag after the experiments with coke or charcoal as substrates and slag with and without sulfur

(Test 1-16) it can be seen that charcoal has a higher reduction rate than coke when slag with sulfur is used. The fact that charcoal has a higher reduction rate than coke is in accordance with [30, 32, 39]. However, from this current study and the studies mentioned ([30, 32, 39]) there is sulfur in the slags and as found in this current study sulfur in the slag will increase the reduction significantly when using charcoal.

Figure 5.2 shows the amount of reduced MnO and SiO_2. When calculating the amount reduced MnO and SiO_2 it was assumed that the other oxides in the slag (CaO, MgO and Al_2O_3) is unreducible, hence, the same amount of these oxides are in the slag after the experiment as it were before the experiment. There can be seen some negative values from the amount reduced of SiO_2. The reason for this is that these calculations are strongly dependent on the reference point used, and the reference used is the experiments at 0 minutes with the same parameters. It can also imply that there is no (or very little) SiO_2 reduced from these experiments. The figure shows the amount MnO reduced on the y-axis and the amount SiO_2 reduced on the x-axis. It can be seen that the reduction of MnO occurs faster than SiO_2, and after around 80 % of the MnO has been reduced the reduction rate of SiO_2 increases. However, there can be seen a clear relationship between the MnO and SiO_2 reduction. This was also found by **Canaguier and Tangstad** (2020), which can be seen in Figure 2.40, where a reduction path is seen [35]. The same shape of the reduction path can be seen in Figure 5.2, where the reduction of SiO_2 occurs after most of the MnO reduction.

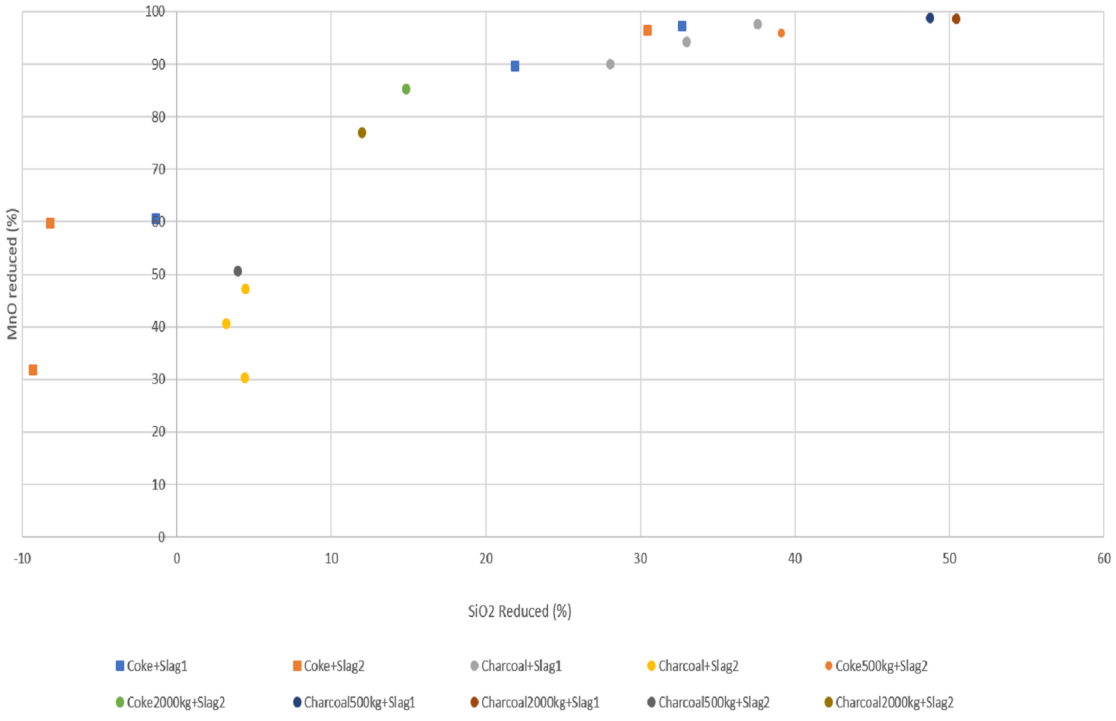

Figure 5.2: Percentage of reduced MnO and SiO_2 from the initial amount of MnO and SiO_2. The values of the reduced MnO and SiO_2 can be seen in Table 4.4 on page 88 for all the experiments.

From the chemical analysis there can be seen that the choice of substrate will have an impact on the reduction. Also, if the slag contains sulfur it will affect the reduction,

and especially if charcoal (or graphite) is used as the substrate. Furthermore, from the chemical analysis, there is no significant effect on which load was used on the press when making the pellets, which can be seen in Figure. 4.14 and 4.15.

Tangstad (1996) found that the Mn/Fe ratio in the metal phase is dependent on the size of the metal particle, as seen in Figure 2.15 on page 23 [23]. This comes from the fact that the reduction of MnO is dependent on the presence of carbon, and the metal particles inside the slag will hence have a high Fe content. The bigger metal particles would be on the surface of the slag, as can be seen in Figure 5.3. The experiment shown in Figure 5.3 is from the experiment were charcoal and slag with sulfur which was held in the furnace at 1600 °C for 60 minutes (test 11). The chemical analysis of the metal particle is 17.3 % Si, 42.0 % Mn and 45.5 % Fe. There was also seen that there would be metal particles inside the slag, as seen in Figure 5.4. The experiment shown in Figure 5.4 is where graphite is the substrate and slag without sulfur is used (test 29), which was held in the furnace at 1600 °C for 30 minutes. The chemical analysis of this metal is 12.1 % Mn and 85.2 % Fe, however, it was seen from the chemical analysis of the slag that there was in general very poor reduction from this experiment.

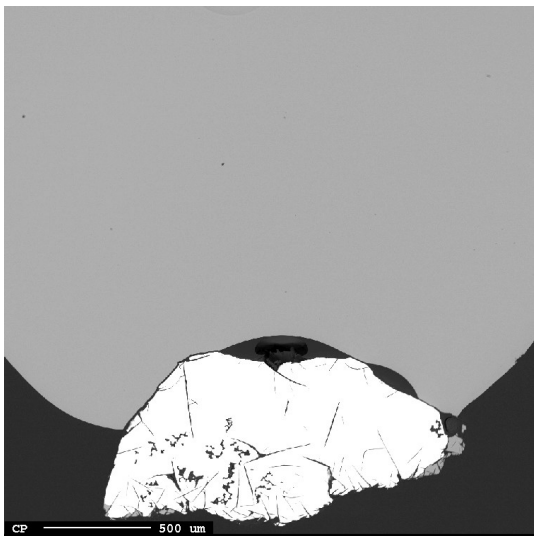

Figure 5.3: Micrograph from EPMA showing a metal particle on the surface of the slag. This micrograph is from the experiment where charcoal and slag with sulfur which was held in the furnace at 1600 °C for 60 minutes (test 11).

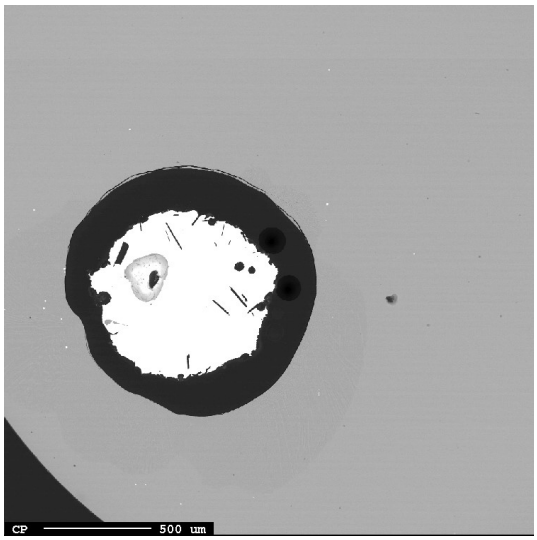

Figure 5.4: Micrograph from EPMA showing a metal particle inside the slag phase. This micrograph is from the experiment where graphite is the substrate and slag without sulfur is used (test 29), which was held in the furnace at 1600 °C for 30 minutes.

Due to the situation regarding Covid-19 there was limited time for the EPMA analyses, and also the author of this study could not be a part of these analyses. As a consequence of this it is not clear where the points on the metal particles were analysed, and the size of the metal particles. Figure 5.5 shows a micrograph from the EPMA showing that there are several metal particles with different sizes. This could explain the fact from the chemical analysis it can be seen that some of the metal particles have a higher amount of Fe than the amount reduced MnO and SiO_2 should indicate. In these cases, the small particles are most likely analysed.

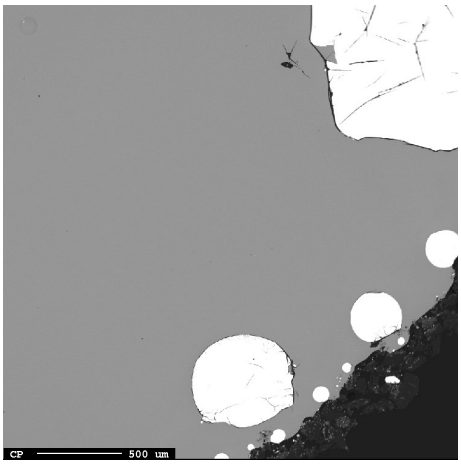

(a) Coke and slag with sulfur held in the furnace for 15 minutes at 1600 °C

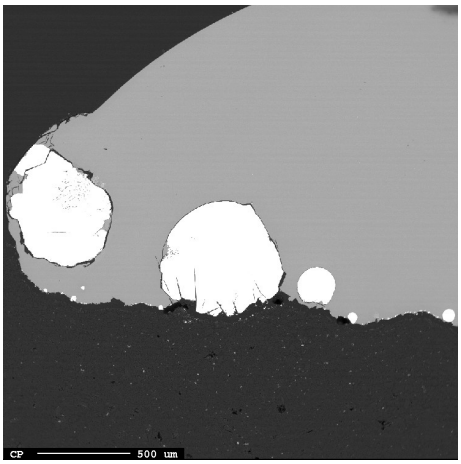

(b) Charcoal and slag with sulfur held in the furnace for 15 minutes at 1600 °C

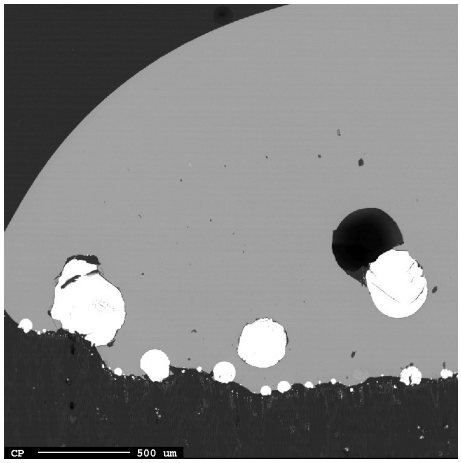

(c) Green charcoal and slag with sulfur held in the furnace for 30 minutes at 1550 °C

Figure 5.5: Micrographs from the EPMA showing different sizes of the metal particles on the sample

5.2 Influence of sulfur in the slag

In this study, there was performed experiments with two different slags, one containing sulfur and one without. Other than the addition of sulfur in one of the slags the two slags are similar. To investigate the effect of sulfur experiments were done on coke, charcoal and graphite.

In Chapter 2.3.6, the effect of sulfur on the reduction rate was discussed. Several studies found that the addition of sulfur will have an effect on the reduction of slag from both FeMn and SiMn production [33, 46, 47]. Figure 5.6 shows some of the experiments from this study where slag1 is used, i.e. the slag with sulfur. The tests shown in the figure are with coke (test 2 - top), charcoal (test 10 - middle) and graphite (test 27 - bottom). There is no significant difference between the experiments with coke and charcoal, other than the fact the degree of oscillation is somewhat larger for charcoal than for coke. However, the general trend of the curve for coke and charcoal is similar to the relative volume starts to increase after some time and then decreases again. When using graphite as the substrate

the behaviour of the slag is different compared to coke and charcoal. It can also be seen that at the end of the experiment the relative volume of the slag is much higher when using graphite, however, this could be from the fact that when using coke and charcoal the slag will dig itself into the pellet, making the slag droplet seem smaller than it actually is. This will be further discussed later. The figure also shows the weight fractions of MnO and SiO_2 from the chemical analysis, where it can be seen that the reduction is similar for all the experiments.

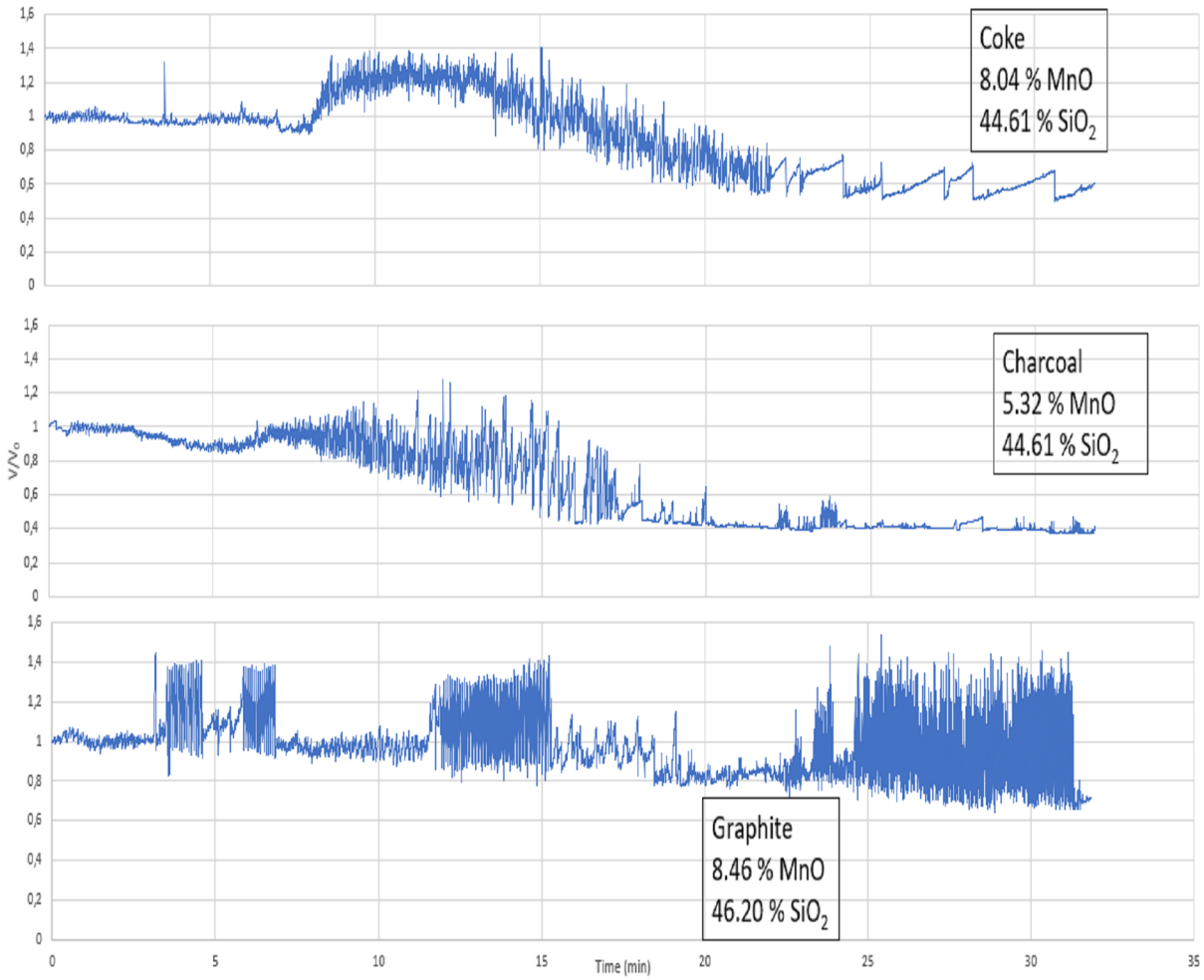

Figure 5.6: Comparison of the relative volume for experiments were slag with sulfur is used. The experiments where held for 30 minutes at 1600 °C. The weight fraction of MnO and SiO_2 can also be seen in the figure. Test 2 (Coke - top), test 10 (Charcoal - middle) and test 27 (Graphite - bottom).

Figure 5.7 shows some of the experiments where slag without sulfur is used. The tests shown in the figure is test 6 (coke - top), test 14 (charcoal - middle) and test 28 (graphite - bottom). When using coke, there can be seen some gas generation after some time. However, when using charcoal and graphite there is very little gas generation or foaming. A few small increases and decreases in the relative volume can be seen although, the generation of gas is not high. The weight fraction of MnO and SiO_2 can also be seen in the figure, where it can be seen that it is reduced significantly more MnO when using coke.

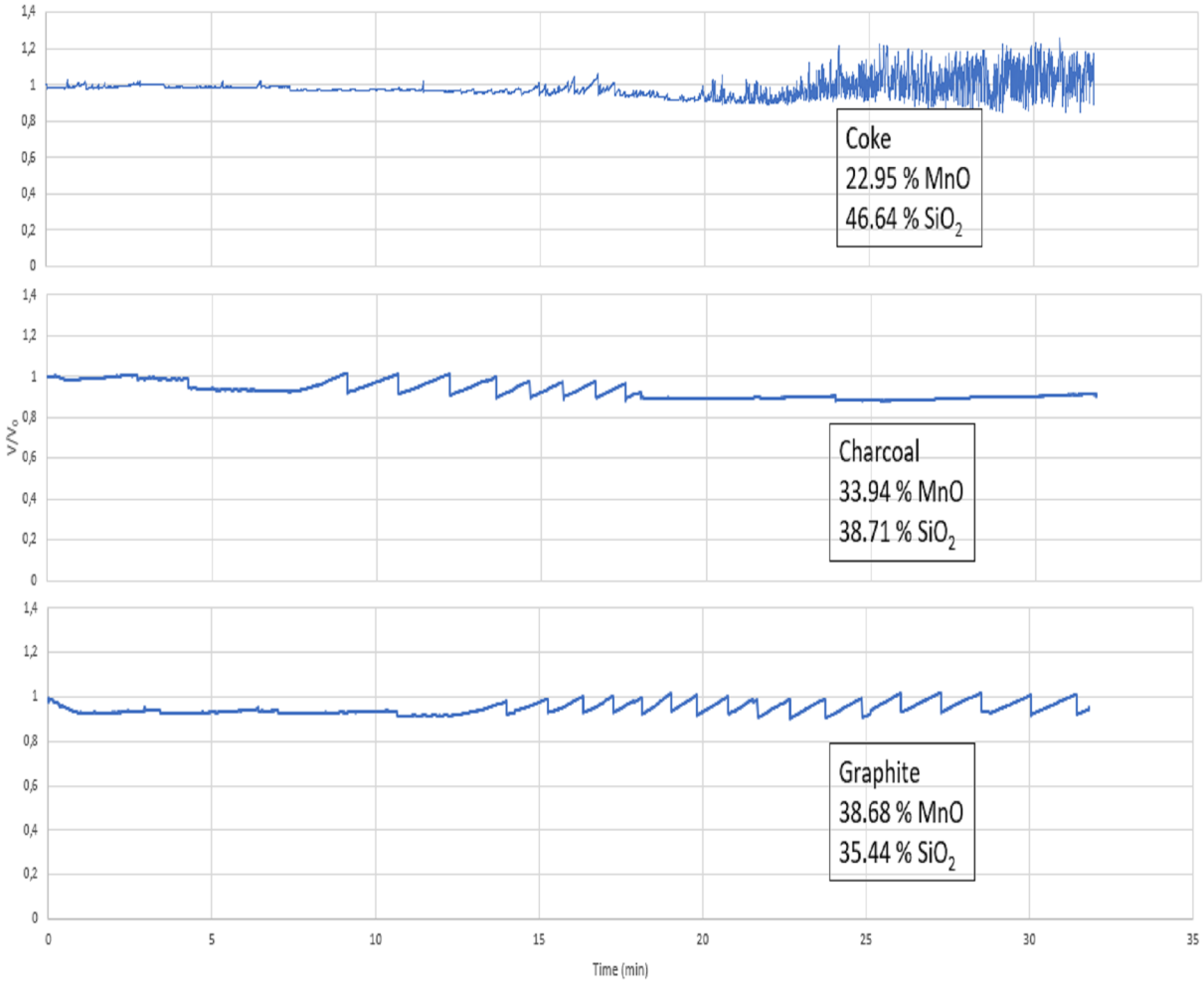

Figure 5.7: Comparison of the relative volume for experiments were slag2 is used. The experiments where held at 30 min at 1600 °C. The weight fraction of MnO and SiO_2 can also be seen in the figure. Test 6 (Coke - top), test 14 (Charcoal - middle) and test 28 (Graphite - bottom).

From the two figures above, there can be seen a clear difference if the slag contains sulfur or not. Especially for charcoal and for graphite. For the coke, the only significant difference whether the slag was added sulfur or not, was that the foaming or gas generation starts at a later time when using slag without sulfur. Other than that, the behaviour of the two slags is similar when using coke. On the other hand, for charcoal and graphite, the difference is significant.

The difference when using slag with sulfur or not can also be seen from the chemical analysis. From Table 4.4 on page 88, there is a clear difference on the composition of the slag if there is sulfur or not in the slag when charcoal or graphite is used as the substrate. For the experiments with charcoal and slag without sulfur, the amount of reduced MnO is 30.35 %, 40.58 % and 47.30 % for test 13, 14 and 15 held at 15, 30 and 60 min respectively, and the amount of reduced MnO for graphite and slag without sulfur is 24.44 % for test 29 held at 30 min. From this, it can be seen that there is a very little degree or reduction of MnO when using slag without sulfur, compared to the experiments where the slag was added sulfur.

The explanation on why the influence of sulfur is greater on charcoal and graphite and not on coke may be that the coke already contains some amount of sulfur. From the chemical analysis performed on coke and charcoal, it was found that coke has an ash content of 12.19 % and charcoal has an ash content of 0.80 %. Furthermore, for coke, the sulfur content stands for 0.61 % of the ash content, while only 0.01 % of the ash in charcoal is sulfur. Hence, the amount of sulfur in charcoal is almost negligible. That entails that even if there is no added sulfur in the slag when using coke as the substrate there will always be some sulfur in the process from the coke itself, and the effect of the sulfur in the slag will hence not be that significant. The fact that coke generally a much higher content of ash than charcoal was also found by **Monsen et al.** (2004) and **Surup et al.** (2019), which can be seen in Tables 2.1, and 2.4 [10, 14, 28].

In this study, there was only investigated one slag with sulfur. However, as proposed by both **Kim and Tangstad** (2018) [33] and **Li and Tangstad** (2019) [46] there could be an optimal amount of sulfur in the slag. **Kim and Tangstad** (2018) found that the rate constant was higher with 0.29 wt% than 0.4 wt% initial S, whereas **Li and Tangstad** (2019) found that 0.44 wt% S gave more weight loss from the slag than the slags containing both 0.2 and 1.0 wt% S, as can be seen in Figures 2.54 and 2.55 on page 54. Both of the studies also found that the experiments with the slags containing sulfur had a higher reduction rate compared to the slag without S [33, 46]. There have also been performed studies which showed that industrial slags generally has a higher reduction rate compared to synthetic slags. Which is because there will always be some sulfur in industrial slags [32, 47]. Hence, adding sulfur in the slag will increase the reduction rate.

5.3 Mechanisms and behaviour of the slag droplet inside the furnace

In this study, there was performed experiments in a sessile drop furnace, and one of the main advantages of this furnace is that there is a camera taking continuous pictures of the process. From these pictures, it can be seen how the slag interacts with the substrate and the general behaviour of the liquid slag inside the furnace as the process is running. In comparison to other types of furnaces and how it is done in the industry where one just knows what goes into the furnace and what comes out. In that, the reactions inside the furnace are found through calculations, modelling, excavations and experience. Hence, to see the slag react with the carbon is very interesting and very useful if the process is to be fully understood.

5.3.1 Measurements of relative volume

As discussed in Chapter 3.1, the pictures taken inside the furnace was analysed by a software called ImageJ. From this software, the relative volume (or expansion) of the slag droplet was measured throughout the experiment. The relative volume of the different experiments is then compared to see if there are any similarities or not, either with all the same parameters or e.g. comparing the use of coke or charcoal.

For most of the experiments in this study performed with the same parameters, i.e. same substrate, slag and temperature, the relative volume was fairly the same for these.

Furthermore, some of them could have a higher peak or stopped at a somewhat lower volume, however, the general shape of the curve was the same. For the experiments with coke, the behaviour of both the slags was very similar other than the fact when using slag without sulfur the generation of gas would start somewhat later. This can especially be seen from the experiment with coke and slag without sulfur (test 5) which were held for 15 minutes and very little gas generation (or foaming) occurred. For the tests with charcoal, there can be seen a very clear difference if the slag contains sulfur or not was used. When the slag with sulfur was used the slag started to foam fairly early, and the curve flattened out after around 20-25 minutes. However, when using slag without sulfur there was no indication of foaming and very little happening during the experiment. Hence, from these different results, one can assume that using slag with sulfur gives a higher reduction rate compared to slag without since there are more gas generation and foaming.

From the measurements of relative volume, there can not be seen any significant difference if the pellets were made with a load of 500, 1000 or 2000 kg. Furthermore, from the porosity and density analysis, it was found that both the density and porosity is approximately the same regardless of what load was used when pressing. Hence, the load used on the pellet does not influence the reactivity of the material within this load range. There was also done experiments with green particles. It can be seen some differences in the behaviour of the slag whether it was used green particles or pellets. When using coke the pellet had a relative volume of 0.6 at the end while the green coke was just below 0.8. It could also be seen from the chemical analysis that there were reduced more MnO and SiO_2 when using pelletized coke, compared to green coke. For the experiments with charcoal, there was a different behaviour of the slag inside the furnace, but in the end, the relative volume was approximately the same for all three experiments. The amount of reduced MnO is approximately the same for the experiments with green charcoal, however, there is slightly more reduced SiO_2 when pelletized charcoal was used compared to green charcoal.

As can be seen from the graphs showing relative volume, there are clear cases of oscillation, i.e. the volume quickly increases, decrease and then increases again and so forth. This occurs since there is a generation of gas in the droplet and the gas is entrapped in the liquid slag forming bubbles. The bigger the difference in the volume the bigger the bubble is in the slag before it bursts, i.e. more gas trapped in the slag. When many smaller bubbles are formed this is termed foaming. Figure 5.8 shows an example of a bubble bursting inside the furnace. The photos in the figure are taken consecutively showing this is occurring at a rapid speed as the camera takes 5 frames per second (fps). After the bubble bursts, the gas begins to build up inside the liquid slag, and increases in size again, before it bursts again and so forth. Figure 5.9 shows a clear case of foaming where there can be seen that the slag droplet has a distorted shape and several bubbles have been formed.

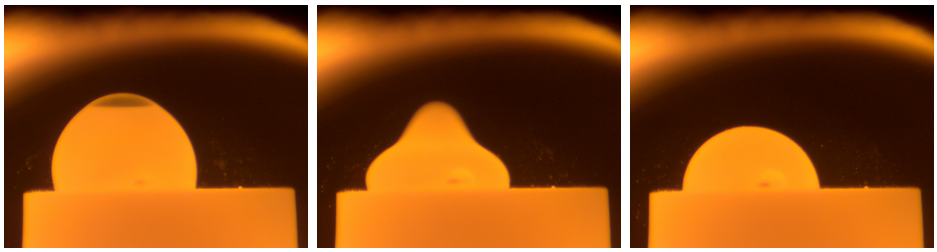

Figure 5.8: Pictures taken inside the sessile drop furnace showing a gas bubble bursting.

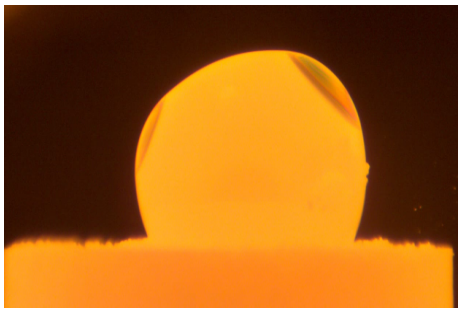

Figure 5.9: Picture taken inside the furnace showing foaming of the liquid slag.

As mentioned earlier, it was the pictures taken inside the furnace that was analysed and measured. However, one main issue with this is when the liquid slag starts to dig down into the pellet. Hence, the whole pellet can not be seen and the volume measured is not the full volume. This can be seen from Figure 5.10, where the slag has dug into the pelletized charcoal. The red line in the top left corner is the top of the pellet. Using the scale in the bottom right corner it can be seen that the bottom of the valley created by the slag is around 1 mm from the top of the pellet-surface. Hence, a significant amount of the slag is below the surface of the pellet, and can therefore not be seen from the camera. This entails that the measured area/volume will be smaller than what it actually is.

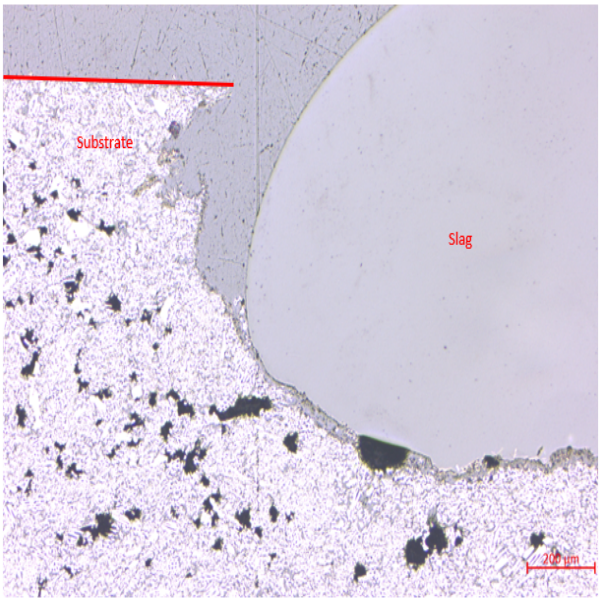

Figure 5.10: Micrograph from an optic microscope showing that the slag has dug into the pellet. The red line is the top of the pellet. In this case the pellet is made from charcoal held for 30 minutes in the furnace at 1600 °C.

Figure 5.11 shows a micrograph of a slag and coke substrate. The sample, in this case, had been held in the furnace for 15 minutes, although there can be seen that the slag digs into the pellet. The red line to the right on the figure is the top of the pellet. Figure 5.12 shows a micrograph when graphite is used as the substrate. From this figure, it can be seen that the slag does not dig into the pellet as much compared to coke and charcoal. As a consequence of this, the relative volume for coke and charcoal should not be directly compared to graphite, because the measured volume will be smaller when coke and charcoal are used compared to graphite. This can be be seen in Figure 5.6, where the experiments with coke and charcoal seem to have a much smaller relative volume than graphite but not as big a difference in the reduction of MnO and SiO_2. However, even though the measured volume is smaller than what it actually is, the behaviour of the slag is still seen and if there is generation of gas or foaming will still be seen on the graphs.

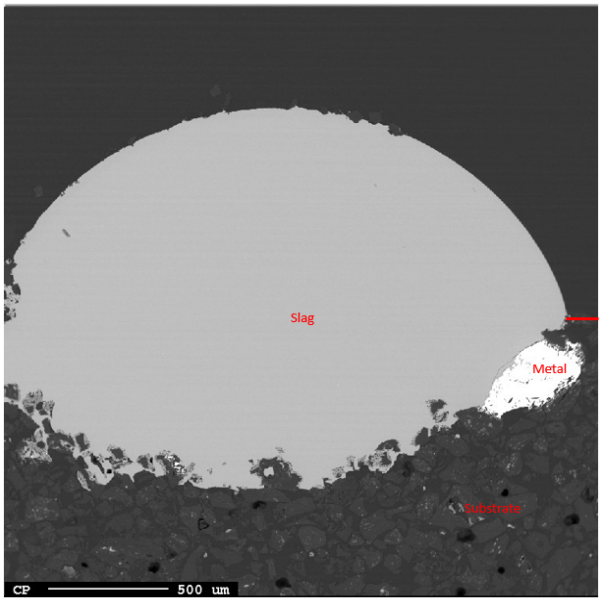

Figure 5.11: Micrograph from the EPMA showing that the slag has dug into the pellet. The red line is the top of the pellet. In this case the pellet is made from coke held for 15 minutes in the furnace at 1600 °C.

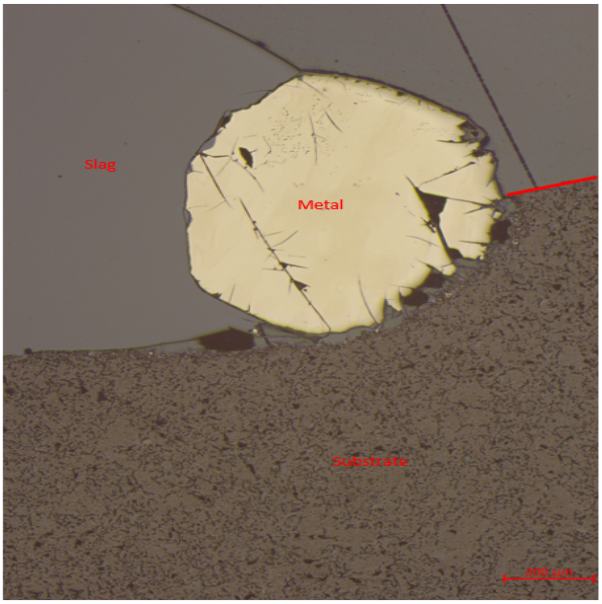

Figure 5.12: Micrograph from an optic microscope showing that the slag has dug into the graphite pellet. The red line is the top of the pellet. The sample was held for 30 minutes in the furnace at 1600 °C.

Even though it can be seen from these figures that the slag digs into the pellet it can not be found any trends or significant difference on coke and charcoal regarding if the slag digs more into one or the other. This is because not all of the samples were cast with both the slag and the substrate.

5.3.2 Wettability

The wettability between the slag and the carbon is an important parameter. If there is poor wettability between a liquid and a solid material there will be less area for the reactions to occur on, hence low reduction. The wetting angle at the beginning, halfway through and at the end of the experiment is given in Table 5.1. These three values are given to summarise the wetting angle for all the experiments. However, since the wetting angle oscillates to an extent throughout the experiment, one must study the graphs of the wetting angle given in Chapter 4.3 to get a full understanding of the wetting angle. Furthermore, the wetting angle for the experiments with 0 minutes holding is not measured.

From Table 5.1 it can be seen that almost all the experiments starts around 120-130°, and the angle will then decrease over time for most of them. This is in accordance with the findings in [39, 50]. There can not be seen any significant difference when using coke as substrate whether the slag contains sulfur or not. However, there can to some extent be seen that the decrease in wetting angle for slag with sulfur starts somewhat earlier than for slag without sulfur when coke is used as the substrate. This difference between the slags with and without sulfur can also be seen from the chemical analysis and relative volume. Furthermore, when charcoal is used as the substrate there can be seen a clear difference whether the slag contains sulfur or not. When slag with sulfur is used there is a significant decrease in the wetting angle over time, while if using slag without sulfur the wetting angle is almost constant throughout the experiment.

Table 5.1: Summary of the wetting angles for all the experiments. "Start" is the wetting angle at the reference temperature, "half" is halfway through the holding time and and "end" is at the end of the holding time.

Test	Carbon	Slag	Pressure [kg]	Holding time [min]	Temp. [°C]	Wetting angle (Start)	Wetting angle (Half)	Wetting angle (end)
1	Coke	1	1000	15	1600	125	98	103
2	Coke	1	1000	30	1600	119	89	87
3	Coke	1	1000	60	1600	128	91	86
4	Coke	1	1000	0	1600	-	-	-
5	Coke	2	1000	15	1600	121	111	101
6	Coke	2	1000	30	1600	122	110	113
7	Coke	2	1000	60	1600	121	110	60
8	Coke	2	1000	0	1600	-	-	-
9	Charcoal	1	1000	15	1600	125	90	45
10	Charcoal	1	1000	30	1600	125	87	61
11	Charcoal	1	1000	60	1600	133	41	68
12	Charcoal	1	1000	0	1600	-	-	-
13	Charcoal	2	1000	15	1600	131	129	116
14	Charcoal	2	1000	30	1600	136	115	118
15	Charcoal	2	1000	60	1600	111	114	109
16	Charcoal	2	1000	0	1600	-	-	-
17	Coke	2	500	30	1600	130	109	63
18	Coke	2	2000	30	1600	132	117	96
19	Charcoal	1	500	30	1600	128	30	57
20	Charcoal	1	2000	30	1600	124	15	42
21	Charcoal	2	500	30	1600	118	127	112
22	Charcoal	2	2000	30	1600	115	99	76
23	Coke	1	1000	30	1550	127	111	81
24	Coke	1	Green	30	1550	128	112	91
25	Charcoal	1	1000	30	1550	131	83	47
26	Charcoal	1	Green - top	30	1550	132	104	29
27	Charcoal	1	Green - along	30	1550	132	62	54
28	Graphite	1	-	30	1550	103	90	58
29	Graphite	2	-	30	1550	130	127	141
30	Charcoal	1	500	30	1700	120	30	91
31	Charcoal	2	500	30	1550	127	115	122

The difference in wettability between coke and charcoal can be seen clearly in Figure 5.13. From the figure, it can be seen that the wetting angle for coke is approximately the same when using slag with or without sulfur. However, when charcoal and graphite is used there can be seen a significant difference whether there is sulfur in the slag or not, where the sulfur will increase the wettability (i.e. decrease the wetting angle). From the fact that charcoal and graphite is more dependent if there is sulfur in the slag or not was also

found in the chemical analysis and the relative volume of the slag. As have been mentioned before, coke has a higher ash content than charcoal, hence a higher sulfur content. This entails that when coke is used as the substrate there will always be sulfur in the reactions to some extent, whereas if charcoal or graphite is used there will be no (or very little) sulfur in the reactions if there is no sulfur in the slag. Hence, when charcoal and graphite is used as the substrate, the influence of sulfur will be more significant compared to when coke is used.

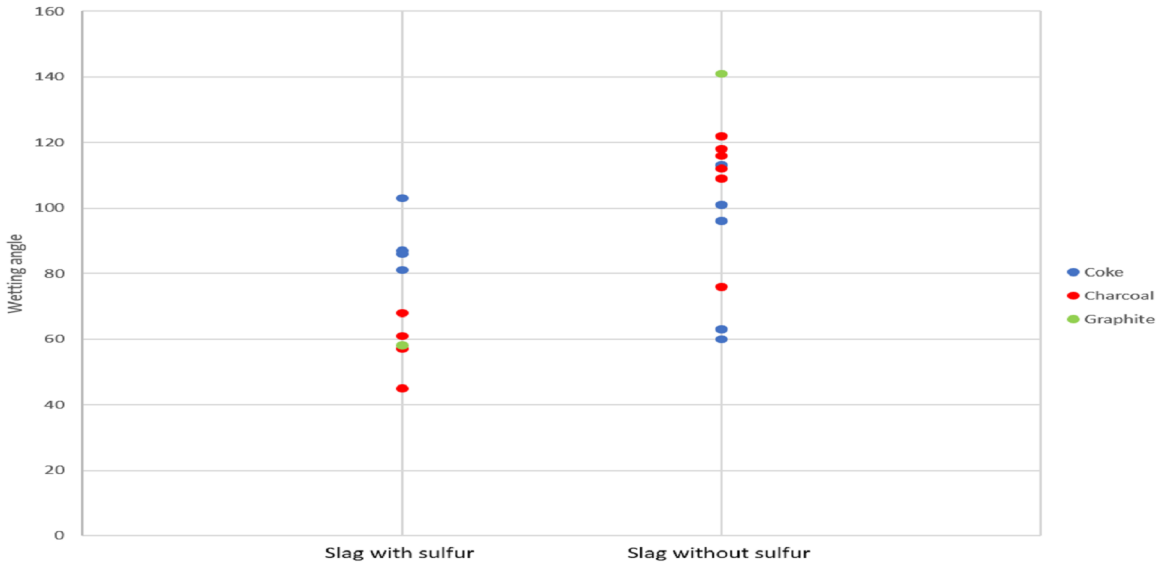

Figure 5.13: Comparison of the wetting angle at the end of the experiments for slag with sulfur and without.

For the experiments where a different load was used when pressing the pellets there can be seen no significant difference on the wetting angle. This can be seen in Figure 4.14 on page 91, where there is no clear indication whether a higher or lower load will increase the reactivity of the carbon material. From the density and porosity analysis, there was also not seen any differences between the pellets made with different loads on the press. The wetting angle can also be seen when green particles were used. There can not in this case be seen a significant difference from the pellets and the green particles on the wettability.

From this study, it can be seen that sulfur will influence the wetting angle on charcoal and graphite, but not coke. This may be explained by the fact that coke already contains some initial sulfur due to its high ash content, whereas charcoal and graphite has a very low sulfur content and ash content. The fact that sulfur influences the wettability was also found by **Li and Tangstad** (2019) where the substrate was carbon black and the wetting angle would decrease when adding sulfur to the slag [46]. Furthermore, it is a small difference between the wettability for coke and charcoal. When slag with sulfur is used with charcoal, the wetting angle at the end of the experiment is lower, in addition to that it decreases earlier. However, charcoal is much more dependent on if the slag contains sulfur or not. **Haugli** (2019) also found that charcoal, in general, had a somewhat better wettability compared to coke [39]. However, **Hosum** (2019) did not find any significant difference in the wettability between coke and charcoal [40].

As mentioned earlier, the software ImageJ was used to measure the wetting angle from the pictures taken inside the furnace. However, for some of the experiments this was problematic. First of all, due to the fact that for the experiments that had a large degree of foaming the slag droplet was not a sphere but could have a distorted shape from the bubbles on the surface. From this, there were different angles on the two different sides of the slag droplet seen on the pictures. Figure 5.14a is a picture taken inside the furnace, where it can be seen that there is a different angle on the two sides between the slag and substrate. Another issue that occurred when measuring the wetting angle was the formation of a metal droplet on the edge of the slag droplet, as can be seen in Figure 5.14b. This metal droplet would do so that the wetting angle would become different on the two sides, and in some cases, this metal droplet could move around. In addition to the wetting angle, the metal droplet can also influence the relative volume and contact area. As mentioned, the metal droplet could move around, hence if the metal is "behind" or directly in front the slag the area of the metal droplet will not be measured. However, if it is on one of the sides, the droplet may contribute to an increase in the area shown, as seen in Figure 5.14b. This can also influence the measurements of the contact area, where if the metal droplet is on the sides, the length between the slag/metal and the substrate will be longer compared to without the metal droplet. From the study performed by **Safarian et al.** (2009), there was also found that foaming (or bubbling) would complicate the measurements of the wetting angle [29]. Another issue when measuring the wetting angle is as mentioned earlier, the slag will dig into the pellet which could influence the wetting angle. For example, in Figure 5.10 it shows that the slag has dug into the pellet. When measuring the wetting angle from the pictures taken in the furnace the area where the slag touches the pellet is not seen as this would be "inside" the pellet. The measured wetting angle is not necessarily the correct one, as it is not measured where the slag and pellet actually meet, but at the point where it seems like they meet from the pictures.

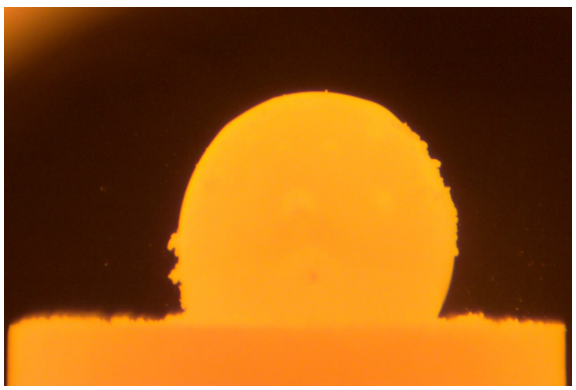

(a) From this figure it can be seen that there are two different angles between the slag and the substrate on the two sides of the slag

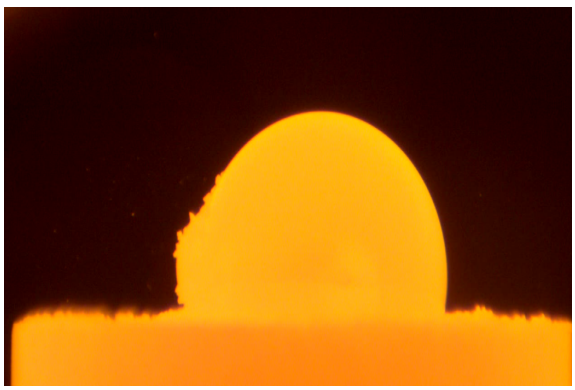

(b) From this figure it can be seen that there is a metal droplet forming on one side of the slag droplet

Figure 5.14: Pictures taken inside the sessile drop furnace

5.3.3 Contact area

The contact area between the slag and the substrate was also measured using ImageJ, as discussed in Chapter 3.1. Furthermore, the contact area between the slag and substrate

was assumed to be a perfect circle, where the distance where the slag touched the substrate was the diameter of this circle. However, the fact that the contact area is a circle may not always be correct. As mentioned earlier, the slag would dig into the pellet which would make the surface very uneven, and the slag could also touch the "walls" of the "slag-valley". This can be seen in Figure 5.10, where the slag touches the walls. Hence, the contact area will increase which can influence the reactivity. There is also another problem with measuring the contact area when the slag digs into the pellet, and that is the length measured will be smaller or larger depending on the initial shape of the slag droplet and how deep the "slag-valley" is.

In Figure 5.15 the contact area for test 1-16 (except the four experiments with 0 min holding time) is given. From the figure, it can be seen that the contact area starts around 5-8 mm^2 for all the tests. The contact area starts to increase, then decreases some before the curve flattens out. There is no significant difference between the experiment when coke was used (Test 1-7) or if charcoal and slag with sulfur were used (test 9-11), however, when charcoal is used with slag without sulfur the contact area is almost constant the entire holding time in during the experiment. The fact that charcoal and slag without sulfur has a different behaviour than the other experiments was also seen from the chemical analysis, relative volume and the wettability.

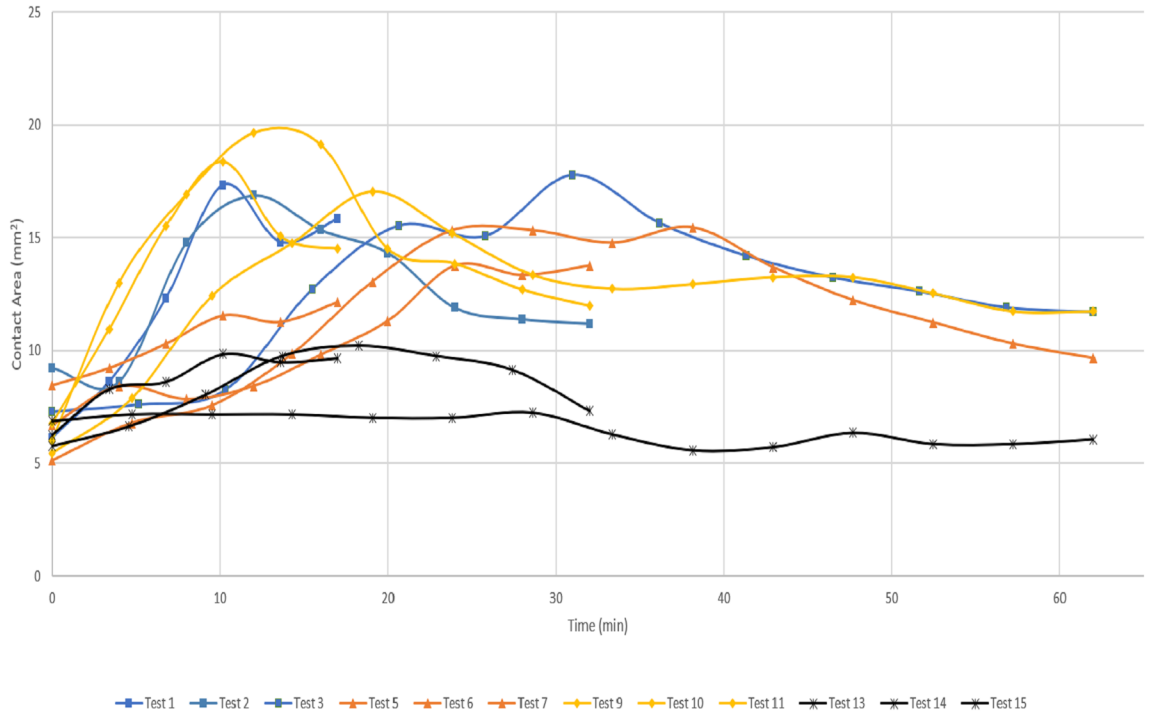

Figure 5.15: Contact area for test 1-16. Test 1-3 (blue lines): Coke and slag with sulfur, Test 5-7 (orange lines): Coke and slag without sulfur, Test 9-11 (yellow lines): Charcoal and slag with sulfur, Test 13-15 (black lines): Charcoal and slag without sulfur

From the results of the measurements of the relative volume, wetting angle and the contact area, it can be seen that these correlate. As mentioned above, the fact that charcoal and slag without sulfur have a low reactivity is seen from all these measurements. Fur-

thermore, from Figure 5.15 it can be seen that charcoal and slag with sulfur (test 9-11) has the earliest increase in contact area, then coke and slag with sulfur and coke and slag without sulfur. This order in reactivity has been seen from the chemical analysis and the relative volume measurements.

On the experiments where the pellets made with different loads, there can not be seen any significant difference on the contact area whether a load of 500, 1000 or 2000 kg was used on the press to make the pellets. Furthermore, the experiments with green charcoal particles had also approximately the same contact area for all the experiments, and for the experiment with green coke, this had a higher contact area compared to the pelletized coke, as seen in Figure 4.32. When using graphite as the substrate a clear difference is seen if the slag contains sulfur or not, which could also be seen from the relative volume and the wetting angle. Already from the beginning, there is a large difference for the test where the slag contains sulfur starts at 16 mm^2, and the slag without sulfur starts at 7 mm^2. As the experiments go on the area when using slag with sulfur increases and slag without sulfur it will decrease, as seen in Figure 4.56 on page 129.

From these measurements, it can be seen that sulfur does have an influence on the contact area when charcoal and graphite is used as the substrate. There can not be seen a very clear difference when coke is used as the substrate. **Li and Tangstad** (2019) also found that sulfur would increase the contact area, wherein that study it was used carbon black as the substrate which has a negligible amount of sulfur [46]. Hence, the sulfur will influence the contact area on materials that do not contain initial sulfur.

5.4 Pellets

The pellets are a crucial part of this study. From the study by **Riva et al.** (2019) it was stated that there is very little research into the utilization and optimization of carbon pellets [19]. Many parameters are influencing the properties of the pellets making the optimization difficult. **Riva et al.** proposed the following methodology for making the pellets; pyrolysis at 600 °C, densification with pyrolysis oil as binder and then reheating the pellet [19]. There has also been performed studies by **Surup et al.** (2019) where tar was used as the binder, and if heat treated the pellets electrical resistivity would increase [14, 20]. In this study, a binder called carboxymethyl cellulose (CMC) was used. This has been used in similar studies as this study [39, 40, 54]. Studies have found that the properties of the pellet are also influenced by binder and water content [14, 19].

As was discussed in Chapter 3.1 there were problems with the pellet sticking to the press (seen in Figure 3.2 on page 69). Since the surface of the pellet is an important parameter, the fact that there is mass from the pellet sticking to the press is unwanted. Firstly, it will make the pellets uneven which could cause problems during the experiment where the liquid slag droplet would roll off the substrate. Second, when comparing different experiments it is important that everything is as similar as possible, and with uneven surfaces, this can influence the reactivity between the slag and substrate. This was found by **Hosum** (2019) where there was seen a difference when using the same substrate [40]. However, for the cases where much of the press was covered with coke or charcoal that pellet would not be used for an experiment in the furnace.

In this study, the effect of the load used on the press was investigated. Where the load on the press was 500, 1000 and 2000 kg. As mentioned earlier, there can not be seen any significant difference in the reactivity on the different pellets made with different loads. This was also found by **Riva et al.** (2019) [19]. From the density and porosity analysis, given in Table 4.2 on page 79, there can be seen no difference between the pellets regardless on the load used. However, from the surface roughness analysis (given in Table 4.3 on page 80) there can be seen that the roughness decreases with increasing load, and especially for coke which has a significant decrease in the roughness.

5.4.1 Experiments with green substrates

In this study, there was performed experiments where the substrates were not pressed into pellets but cut and polished from a green particle from coke or charcoal. This was done to investigate the difference between the green material or if it is pelletized. To make these pellets a larger piece of coke or charcoal was chosen and then cut and polished into a size that would fit into the furnace, and also be even so the liquid slag would not roll off during the experiment. Making the coke particle was straight forward, but somewhat tedious as coke is a very hard material. However, charcoal has a much higher porosity and in general more fragile. There were also some problems with the charcoal as there was pores inside the material and the material is fragile and could break. Figure 5.16 shows an attempt at making this charcoal pellet. From the figure a large pore can be seen in the middle of the particle, hence this could not be used in an experiment. Many of the particles would also break when cutting them. As a consequence of this, a quite dense part of a charcoal piece was found and the particles used in the experiment and for surface roughness analysis was made from this. Figure 5.17 shows the green charcoal pellet made along the fibre direction. From the figure, the fibres can be seen. Furthermore, Figure 5.18 shows the green charcoal pellet made on top of the fibres. From this figure the fibre can not be seen, in addition to that, the particle is very dense. This particle also had a very low surface roughness, given in Table 4.3. Hence, it is not clear that the surface of this particle is actually on top of the fibres.

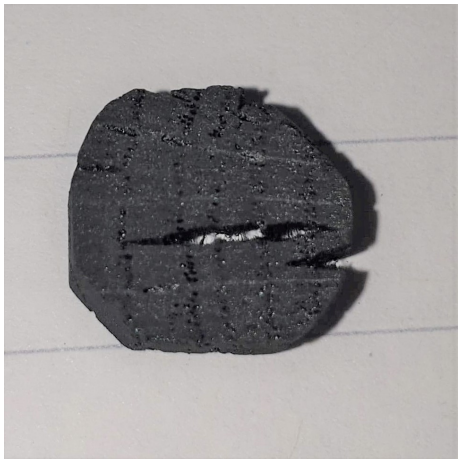

Figure 5.16: Attempt at making a charcoal particle

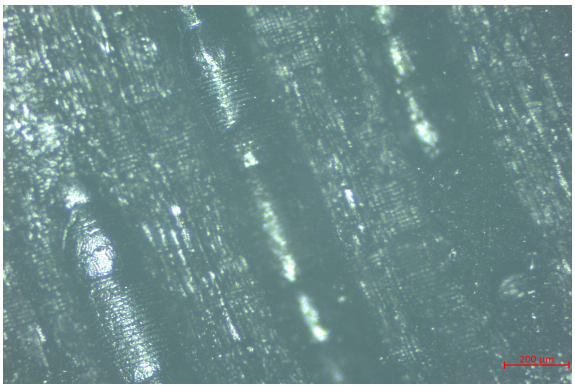

(a) Micrograph taken by optical microscope at 5x zoom

(b) Photograph taken by camera

Figure 5.17: Green charcoal particle along fibres

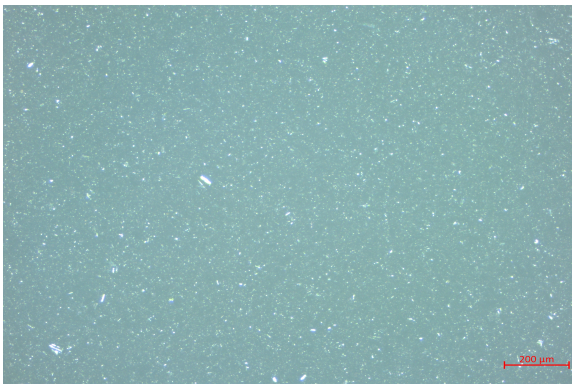

(a) Micrograph taken by optical microscope at 5x zoom

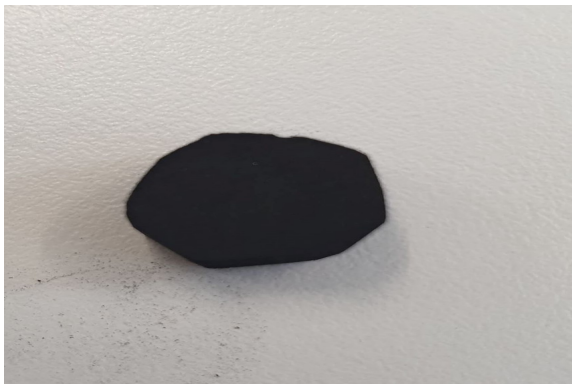

(b) Photograph taken by camera

Figure 5.18: Green charcoal particle on top of fibres

When performing the experiments there was a problem where the green charcoal substrate would move on the sample holder inside the furnace, making the slag also move. However, when using the green coke there was no problem with the coke particle moving. The reason for why the charcoal pellet moved more than the coke, can be because there is a higher content of volatile matter in charcoal compared to coke, where this is expelled. Another reason could be that there is some tension in the charcoal which is released when heating. When performing the experiment with green charcoal where the surface is on top of the fibres (test 26) the first attempt was stopped at 730 °C since the slag pellet had moved to the edge, which can be seen in Figure 5.19. The same particle was used for the second attempt, and would not move around as much, indicating that the volatile matter or tension had been released in the first attempt. For the experiments with green charcoal where the surface is along the fibres (test 27), two attempts were made before it worked. The first attempt was stopped at 1100 °C and the second stopped at 800 °C, for the same reasons as for test 26. From the fact that both the experiment with green charcoal particles was first heated up to a high temperature and then stopped before performing the experiment that was used, indicates that these particles were heat-treated. Hence, if green charcoal is to be used it may be wise to heat-treat the material first to expel the

volatile matter and any tensions in the material and the binder.

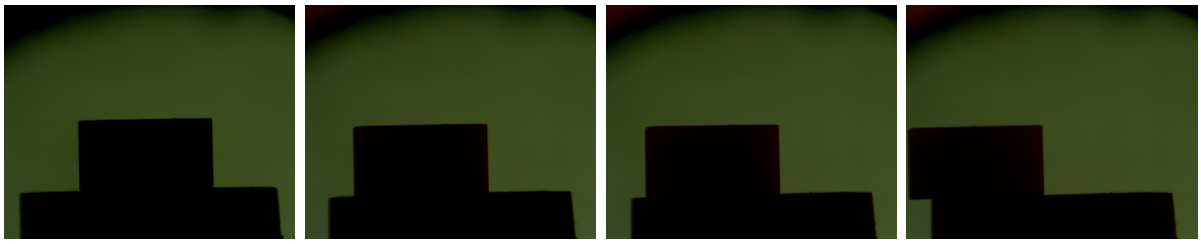

(a) (b) (c) (d)

Figure 5.19: Pictures from inside the sessile drop furnace showing the slag pellet being moved on top of the green charcoal substrate. As a consequence of this, the experiments had to be stopped and started over with the slag pellet in the centre of the substrate.

The particles would shrink as a consequence of the volatile matter and tensions being expelled from the carbonaceous materials. Figure 5.20 shows the sample before and after the experiment in the sessile drop furnace, showing clearly that the particle is smaller after the experiment compared to before. From the pictures taken in the furnace, the length of the substrates was measured at the start of the experiment and at the end. From this, it can be calculated to what extent the pelletized and the green coke and charcoal have shrunk. For the coke pellets, there was close to none shrinkage, all below 0.5% shrinkage, including the green coke. However, for the charcoal pellets, the shrinkage had an average of 6.8 % and was between 6.0-7.4 %. It could not be seen any difference on the pellets made with different loads on the shrinking. From the measurements of the green charcoal particle where the surface is along the fibres (test 27), there was 11.1% reduction in size. There could not be done measurements of the other experiments with green charcoal (test 26) as the particle was "out of frame", hence the whole particle can not be seen in the pictures, and thus not measured. From this, it can be seen that in general charcoal has a significantly higher reduction in size compared to coke and especially green charcoal. Furthermore, charcoal should always be heat-treated before being used in a furnace so that the volatile matter (and perhaps the tension) is released from the material.

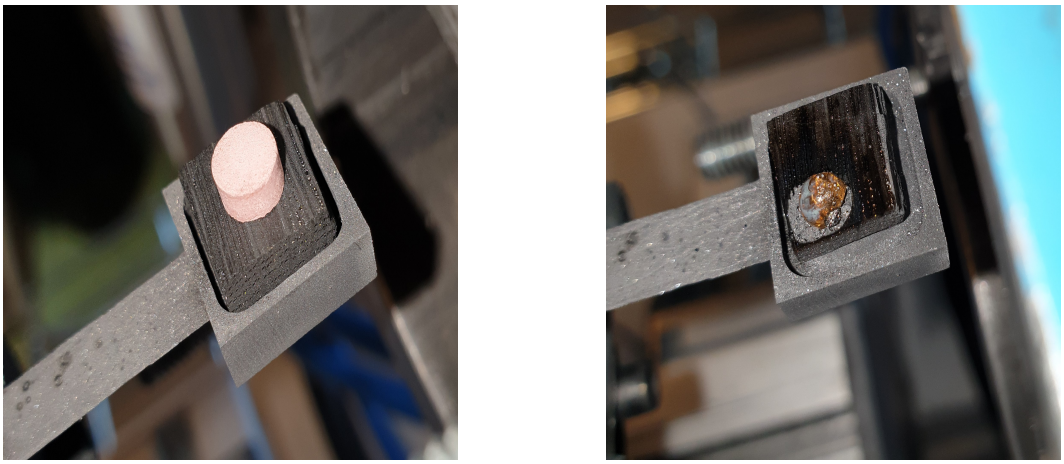

(a) Before experiment *(b) After experiment*

Figure 5.20: Pictures of the green charcoal substrate with the surface along the fibres (test 27) and the slag pellet on the sample holder before and after the experiment in the sessile drop furnace.

As was mentioned earlier, the relative volume has a different behaviour when using green particles compared to pellets, and especially for green coke seen in Figure 4.30 on page 107. From this figure, it can be seen that when using green coke the decrease is almost linear and also that the slag will not increase very much in volume, compared to the experiment with pelletized coke. From the surface roughness analysis, it was seen that the green coke had large pores on the surface. **Kanai et al.** (2007) found that when the surface had grooves or dimples the gas would leak out from under the liquid droplet, hence there will be less gas inside the liquid and the extent of the bubbling or foaming would be less compared to when all or most of the gas goes through the liquid [52]. This can be seen in Figure 2.68 on page 63. Due to the large pores in the green coke, much of the gas will escape from underneath the slag droplet, hence there will be less gas inside the slag droplet. For the charcoal pellets there can be seen in Figure 4.51 on page 124 that in the beginning the behaviour is similar to green coke. However, after around 15 minutes it can be seen for both the experiments with green charcoal that the relative volume increases clearly, hence large bubbles are formed due to gas being trapped inside the liquid slag. The fact that it takes some time before there is bubbling or foaming could be that after some time the slag will dig into the particle and the grooves or dimples on the surface helping the gas escape underneath the slag is not there anymore, making more of the gas go through the slag.

5.4.2 Surface roughness

As mentioned earlier, from the study by **Hosum** (2019) there was found differences when using the same type of substrate on the reduction of the slag, hence the surface can influence the reactivity [40]. In Chapter 3.1 it was discussed that when pressing the pellets there could be mass sticking to the press, making the surface uneven and they would also be different from each other. In this study, the roughness of the surface was then analysed.

From the analysis, there are three parameters given, which is R_a, R_q and R_z. In the field of surface roughness, R_a is the most used parameter. However, this has a big disad-

vantage because R_a is an average and would hence not be affected by a few high peaks or low valleys. The root mean square (R_q) will be more affected by this. This is especially seen on the green charcoal where the surface of the particle is on top of the fibres (Figure 4.5). From this analysis, there was some high peaks and low valleys on one side of the pellet, while most of the pellet was fairly even. Hence, the average value (i.e. R_a) is not affected by these peaks. This is why R_z is also given so that the height of the peaks and depth of the valleys can be seen.

From the results, it was seen that the roughness of the pellets would decrease with an increasing load on the press. This can be seen to some extent on the charcoal pellets, while there is a significant decrease for the coke pellets. In general, the coke pellets have a much higher roughness compared to charcoal. This could be seen when making the pellets, as the coke pellets would stick more to the press compared to charcoal.

The area which was investigated has a height of 550µm and the width of the pellet (10 mm). From the measurements there can be seen that from this area there were differences in the roughness, and it is safe to assume that these differences are on the whole pellet. This can also mean that the area chosen for the analysis could be a "nicer" area compared to the rest of the pellet, or a "rougher" area.

5.5 Experiments in the sessile drop furnace

In this study, all the experiments were performed in a sessile drop furnace. **Safarian and Tangstad** (2010) had investigated four different methods for establishing a slag-carbon reactivity test, and there it was concluded that the sessile drop method was a suitable technique [28]. The sessile drop method has been used for several studies to investigate the behaviour of different slags or charges on different carbon materials from the production of FeMn and SiMn [16, 37, 38, 39, 40]. As have been well established by several studies, the temperature is a very important parameter in the production of SiMn (and FeMn) [25, 27]. Hence, the temperature in the furnace must be the same, and also the heating schedule from room temperature up to the holding temperature. In the sessile drop furnace, there is a thermocouple that controls the temperature. There is a possibility for this thermocouple to show the wrong temperature, as it gets older and more used. To find the error of the thermocouple pure iron is melted, and then the temperature which the thermocouple states is compared to the theoretical melting point of iron which is 1538 °C. When doing the calibration the thermocouple stated that the iron melted at 1520 °C, hence the thermocouple is showing 18 °C lower than what it actually is. In that case, the holding temperature in this study was then 1618 °C and 1568 °C.

As have been mentioned before, one of the main advantages of the sessile drop furnace is the fact that one can see the actual process, and a camera taking pictures of it. However, one main disadvantage is the measurements of weight loss. There are other furnaces where the weight loss is measured throughout the process and can, therefore, study in what stage of the process the weight loss occurs. When using the sessile drop furnace the substrate and slag are weighed before and after the experiment. In Table 4.6 the mass loss of the samples before and after the experiment is seen. From this table, it can be seen that weight loss increases with increasing holding time. However, there are some problems

with these measurements, and they should not be used as definitive results. First of all, the pellets are very fragile after the experiment and some of the mass is likely lost during handling of the samples after the experiments. This applies especially for the coke pellets which is very fragile, and these can also not be investigated after the experiments as they fell apart. Another problem with the mass loss is that during the experiment there will be slag that is lost inside if the furnace. This especially happens when the slag starts to foam or create large bubbles and these bursts. When that happens some of the slag is "thrown away", i.e. it remains inside the furnace. If the mass loss was to be used in a correct and definitive matter, the mass loss would only have been from the reduction reactions of MnO and SiO_2, given in Equations 8 and 9 on page 5.

5.6 Quality of results

There is always a possibility of errors while performing experiments. One source of error is the equipment used to perform the experiments. First of all, the weights used to measure the amount of oxide used in the slag or the amount of powder used before pressing pellets and after pressing could have some error margin. In addition, there can also be a different error margin on different weights, and as a consequence of this, the same weight was used when parameters are being compared. There can also be errors from the experiment in the sessile drop furnace. As mentioned earlier, the temperature in the furnace is regulated by a thermocouple. However, the thermocouple can be worn after use, and will then deteriorate. Another source of error while performing experiments is the human source of error. This is something that always will be present and can influence the experimental work.

As was discussed in Chapter 3.1 the measurements of the pictures taken in the furnace was performed by the software ImageJ. When using this software one must analyse every frame manually which is somewhat time-consuming. For calculating the relative volume of the slag droplet, a line is drawn to divide the slag and substrate, and there is a possibility that this line is not always on the exact same place as it is drawn by hand. The measurements of the wetting angle are also done by hand, where a line is dragged along the side of the slag measuring the angle. Hence, there is here a source of error.

6 Conclusion

In this study, the reduction rate of slag from the SiMn production is investigated towards coke and charcoal as reducing agents. To see if it is the different surface of the carbon materials that affect the reduction rate or if it is the material itself, the charcoal and coke have been crushed and pelletized to try to obtain more similar surface and density properties. Coke and charcoal particles, called green materials, has also been studied. It was also investigated if the load on the press when making the pellets could influence the reactivity of the pellet. Lastly, the influence of sulfur in the slag was studied.

From the chemical analysis, it was found that the amount of MnO in the slag would decrease with increasing holding time as expected. When using coke as the substrate the amount of reduced MnO after 60 minutes is approximately the same when using both slag with sulfur and without sulfur, however, there was a lower content of MnO in the slag when it contained sulfur after 15 and 30 minutes. Hence, the reduction occurred earlier when using slag with sulfur. Furthermore, when using charcoal as the substrate there is a significant difference whether the slag contains sulfur or not. If the slag that contains sulfur is used there is a high degree of reduction early, and the amount of reduced MnO is at 90 % already at 15 minutes and the amount reduced of SiO_2 is 28.07 %, and then increases some with increasing holding time. However, when the slag without sulfur is used with charcoal there is very little reduction, where at 15 minutes only 30 % of the MnO is reduced and 47 % of the MnO is reduced at 60 minutes. Hence, the reduction rate is significantly faster when using slag with sulfur with charcoal. From this it can be concluded with that sulfur in the slag will increase the reduction rate of SiMn slag. It can also be concluded with that when using slag with sulfur charcoal has a higher reduction rate than coke, but when slag without sulfur is used coke has a higher reduction rate than charcoal.

As mentioned above, the sulfur will affect the reduction rate, however, charcoal has a much more significant difference compared to coke. This may be explained by the fact that coke has a much higher content of ash than charcoal, and then also a higher content of sulfur. When using coke, there will always be some sulfur present in the reactions regardless if there is sulfur in the slag. As there is very little sulfur in charcoal, the addition of sulfur in the slag will have a greater effect on charcoal. It could also be seen that when graphite was used as the substrate there is also a significant difference whether the slag contains sulfur or not was used where the amount of reduced MnO and is significantly higher when slag with sulfur was used. As it is for charcoal, there is also very low ash content in graphite, hence very little (or no) sulfur.

The effect of the load used when pressing the pellets have been found to have no significant effect on the reactivity of the material regarding the reduction of MnO and SiO_2. From the chemical analysis, there can be seen no clear indication whether a higher or lower load on the press should be used, which applies for both coke and charcoal. Besides, there is also very little difference in density and porosity for the pellets made with different loads. However, from the surface roughness analysis, it could be seen a trend where the roughness of the surface would decrease with increasing pressure and especially for the coke pellets, although as mentioned the load would not influence the reduction of

MnO and SiO_2.

The difference between pelletized and green particles of coke and charcoal were also investigated. When using coke there can be seen from the chemical analysis that there is more reduced MnO and SiO_2 when the pelletized coke is used. This may be from the fact that the green coke has large pores on the surface, which could influence the contact area and hence the reduction of MnO and SiO_2. Due to the pores on the green coke, there was not as much foaming or bubbling of the slag droplet since there would be gas that could escape underneath the slag because of the pores. Furthermore, when using charcoal there was no significant difference in the reduction of MnO, however, there was a higher degree of SiO_2 reduction when the pelletized charcoal was used.

The results from the chemical analysis regarding the differences between the experiments can also be seen from the measurements of relative volume, wetting angle and contact area. From the relative volume, it can be seen that the generation of gas or foaming would start soon after reaching the holding temperature for charcoal and slag with sulfur and that it would also take longer time before the foaming started for coke and slag without sulfur compared to coke with slag with sulfur. Also, there is a significant difference in the behaviour of the slag droplet from the experiments where charcoal and slag without sulfur is used compared to the other experiments. Where there is very little gas generation, hence low reduction of oxides. Regarding the experiments where the pellets were made with a different load on the press, there could not be seen any significant differences in the relative volume, wetting angle or contact area. From the relative volume for the experiments with the green particles, the behaviour of the slag was different compared to the experiments with pelletized material. However, there could be seen that there was gas generation in all experiments, in that the relative volume would oscillate, and the relative volume was approximately the same for charcoal at the end of the experiment. The pelletized coke had a somewhat lower relative volume than the green coke, although from the chemical analysis it was found that the reduction rate was higher for the pelletized coke. From the experiments with graphite, a significant difference was seen whether the slag contains sulfur or not, where there is clearly more gas generation when slag with sulfur is used. The sulfur would also affect the wettability and the contact area between the slag and the graphite substrate.

7 Bibliography

[1] European Comission. *The Sustainable Development Goals*. Nov. 2016. URL: https://ec.europa.eu/europeaid/policies/sustainable-development-goals_en (visited on 30/05/2020).

[2] United Nations. *Parisavtalen*. 2020. URL: https://www.fn.no/Om-FN/Avtaler/Miljoe-og-klima/Parisavtalen (visited on 30/05/2020).

[3] Miljødirektoratet. *Klima*. 2019. URL: https://miljostatus.miljodirektoratet.no/tema/klima/ (visited on 30/05/2020).

[4] Merete Tangstad. *Metal production in Norway*. Akademika Publishing, 2013. ISBN: 978-82-321-0241-9.

[5] Sverre E. Olsen, Merete Tangstad and Tor Lindstad. *Production of manganese ferroalloys*. Tapir Academic Press, 2007. ISBN: 978-82-519-2191-6.

[6] Merete Tangstad. 'Manganese Ferroalloys Technology'. en. In: *Handbook of Ferroalloys*. Elsevier, 2013, pp. 221–266. ISBN: 978-0-08-097753-9. DOI: 10.1016/B978-0-08-097753-9.00007-1.

[7] Sverre E. Olsen and Merete Tangstad. 'Silicomanganese Production-Process Understanding'. In: *INFACON X*. Cape Town, South Africa, Feb. 2004, pp. 231–238. ISBN: 0-9584663-5-1.

[8] Merete Tangstad. *Introduction to manganese ferroalloys production (Lecture notes)*. Norwegian University of Science, Technology, Department of Materials Science and Engineering, 2018.

[9] Caroline Oberheu. *Top 10 Wood Charcoal Producing Countries*. Apr. 2017. URL: https://www.worldatlas.com/articles/top-10-wood-charcoal-producing-countries.html (visited on 30/05/2020).

[10] Bodil Monsen, Merete Tangstad and H Midtgaard. 'Use of Charcoal in Silicomanganese Production'. In: *Tenth International Ferroalloys Congress*. Cape Town, South Africa, 2004, pp. 392–404. ISBN: 0-9584663-5-1.

[11] Jakub Kaczorowski. 'The Boudouard Reaction in Manganese Production'. PhD thesis. Trondheim: Norwegian University of Science, Technology, Faculty of Natural Sciences, Department of Materials Science and Engineering, 2006.

[12] Terkel Rosenqvist. *Principles of extractive metallurgy*. 2nd. Tapir Academic Press, 2004. ISBN: 82-519-1922-3.

[13] Inger Johanne Eikeland, Bodil Monsen and Ingunn S. Modahl. 'Reducing CO2 emissions in Norwegian ferroalloy production'. en. In: *Greenhouse Gases in the Metallurgical Industries: Policies, Abatement and Treatment, (Met. Soc. CIM), Toronto*}. Vol. 325. Toronto, Canada, 2001.

[14] Gerrit Surup et al. 'Characterization of renewable reductants and charcoal-based pellets for the use in ferroalloy industries'. In: *Energy* 167 (Jan. 2019), pp. 337–345. ISSN: 03605442. DOI: 10.1016/j.energy.2018.10.193.

[15] B Monsen et al. 'CHARCOAL FOR MANGANESE ALLOY PRODUCTION'. In: *INFACON XI*. Vol. 11. New Delhi, Feb. 2007.

[16] Sethulakshmy Jayakumari and Merete Tangstad. 'Carbon Materials for Silicomanganese reduction'. en. In: *The Fourtheenth International Ferroalloys Congress*. Kiev, Ukraine, June 2015, pp. 374–381.

[17] Gerrit Ralf Surup et al. 'Effect of operating conditions and feedstock composition on the properties of manganese oxide or quartz charcoal pellets for the use in ferroalloy industries'. In: *Energy* 193 (Feb. 2020), p. 116736. ISSN: 03605442. DOI: 10.1016/j.energy.2019.116736.

[18] Gerrit Ralf Surup et al. 'The effect of wood composition and supercritical CO2 extraction on charcoal production in ferroalloy industries'. In: *Energy* 193 (Feb. 2020). ISSN: 03605442. DOI: 10.1016/j.energy.2019.116696.

[19] Lorenzo Riva et al. 'Analysis of optimal temperature, pressure and binder quantity for the production of biocarbon pellet to be used as a substitute for coke'. en. In: *Applied Energy* 256 (Dec. 2019). ISSN: 03062619. DOI: 10.1016/j.apenergy.2019.113933.

[20] Gerrit Ralf Surup et al. 'Characterization and reactivity of charcoal from high temperature pyrolysis (800–1600 °C)'. In: *Fuel* 235 (Jan. 2019), pp. 1544–1554. ISSN: 00162361. DOI: 10.1016/j.fuel.2018.08.092.

[21] Pyunghwa Peace Kim. 'Reduction rates of SiMn slags from various raw materials'. eng. PhD thesis. Trondheim: Norwegian University of Science, Technology, Faculty of Natural Sciences, Department of Materials Science and Engineering, 2018.

[22] Kai Tang and Sverre E Olsen. 'Computer Simulation of the Equilibrium Relations Associated with the Production of Manganese Ferroalloys'. In: *INFACON X*. Cape Town, South Africa, 2004. ISBN: 0-9584663-5-1.

[23] Merete Tangstad. 'The High Carbon Ferromanganese Process - Coke Bed Relations'. PhD thesis. Trondheim: Norges Tekniske Høgskole, 1996.

[24] Weizhong Ding and Sverre E. Olsen. 'Manganese and Silicon Distribution between Slag and Metal in Silicomanganese Production.' en. In: *ISIJ International* 40.9 (2000), pp. 850–856. ISSN: 0915-1559. DOI: 10.2355/isijinternational.40.850.

[25] Oleg Ostrovski et al. 'Kinetic Modelling of MnO Reduction from Manganese Ore'. en. In: *Canadian Metallurgical Quarterly* 41.3 (Sept. 2002), pp. 309–318. ISSN: 0008-4433, 1879-1395. DOI: 10.1179/cmq.2002.41.3.309.

[26] T. Abel Engh. *Principles of Metal Refining*. Oxford University Press, 1992. ISBN: 0-19-856337-X.

[27] Vegard Olsø, Merete Tangstad and Sverre E. Olsen. 'Reduction Kinetics of MnO-Saturated Slags'. In: *INFACON 8*. China, 1998, pp. 279–283.

[28] Jafar Safarian and Merete Tangstad. 'SLAG-CARBON REACTIVITY'. In: *The Twelfth International Ferroalloys Congress*. Helsinki, Finland, June 2010, pp. 327–337.

[29] Jafar Safarian et al. 'Kinetics and Mechanism of the Simultaneous Carbothermic Reduction of FeO and MnO from High-Carbon Ferromanganese Slag'. en. In: *Metallurgical and Materials Transactions B* 40.6 (Dec. 2009), pp. 929–939. ISSN: 1073-5615, 1543-1916. DOI: 10.1007/s11663-009-9294-3.

[30] Gabriella Tranell et al. 'REDUCTION KINETICS OF MANGANESE OXIDE FROM HC FeMn SLAGS'. In: *INFACON XI*. New Delhi, 2007, pp. 231–240.

[31] Jafar Safarian and Leiv Kolbeinsen. 'Kinetic of Carbothermic Reduction of MnO from High-carbon Ferromanganese Slag by Graphite Materials'. en. In: *ISIJ International* 48.4 (2008), pp. 395–404. ISSN: 0915-1559, 1347-5460. DOI: 10.2355/isijinternational.48.395.

[32] Jafar Safarian et al. 'Reduction Kinetics of MnO from High-Carbon Ferromanganese Slags by Carbonaceous Materials in Ar and CO Atmospheres'. en. In: *Metallurgical and Materials Transactions B* 39.5 (Oct. 2008), pp. 702–712. ISSN: 1073-5615, 1543-1916. DOI: 10.1007/s11663-008-9175-1.

[33] Pyunghwa Peace Kim and Merete Tangstad. 'Kinetic Investigations of SiMn Slags From Different Mn Sources'. en. In: *Metallurgical and Materials Transactions B* 49.3 (June 2018), pp. 1185–1196. ISSN: 1073-5615, 1543-1916. DOI: 10.1007/s11663-018-1238-3.

[34] Pyunghwa Peace Kim, Trine Asklund Larssen and Merete Tangstad. 'Reduction rates of MnO and SiO2 in SiMn slags between 1500 and 1650°C'. In: *Journal of the Southern African Institute of Mining and Metallurgy* 119.5 (2019). ISSN: 22256253, 24119717. DOI: 10.17159/2411-9717/153/2019.

[35] Vincent Canaguier and Merete Tangstad. 'Kinetics of Slag Reduction in Silicomanganese Production'. In: *Metallurgical and Materials Transactions B* (Mar. 2020). ISSN: 1543-1916. DOI: 10.1007/s11663-020-01801-3. URL: https://doi.org/10.1007/s11663-020-01801-3.

[36] Kristian L. Berg and Sverre E. Olsen. *Kinetics and mechanisms fo the carbothermic reduction of MnO and SiO2 from liquid slags*. SINTEF Report STF24 A04531. Trondheim, 2004, p. 32.

[37] Vincent Canaguier. *Foaming of silicomanganese slag during carbothermic reduction (Un-published work)*. Norwegian University of Science, Technology, Department of Materials Science and Engineering, 2019.

[38] Bilal Nadir. *Mn alloys production with the use of natural gas - Understanding the kinetics of Mn alloy production*. MSc Thesis. Trondheim: Norwegian University of Science, Technology, Faculty of Natural Sciences, Department of Materials Science and Engineering, 2015.

[39] Ine Mariell F. Haugli. *Reactivity of silicomanganese slag towards carbon materials*. MSc Thesis. Trondheim: Norwegian University of Science, Technology, Faculty of Natural Sciences, Department of Materials Science and Engineering, June 2019.

[40] Benjamin Dale Hosum. *Interaction of Silicomanganese Slags with Pelletized Coke and Charcoal*. Specialization project. Norwegian University of Science, Technology, Faculty of Natural Sciences, Department of Materials Science and Engineering, 2019.

[41] Kai Tang and Merete Tangstad. 'Modelling Viscosites of Ferromanganese Slags'. In: *INFACON XI*. 2007.

[42] Shigeta Hara and Kazumi Ogino. 'Slag-foaming Phenomenon in Pyrometallurgical Processes.' en. In: *ISIJ International* 32.1 (1992), pp. 81–86. ISSN: 0915-1559. DOI: 10.2355/isijinternational.32.81.

[43] Kimihisa Ito. 'Foams and Foaming'. en. In: *Treatise on Process Metallurgy*. Vol. 2. Elsevier, 2014, pp. 197–216. ISBN: 978-0-08-096984-8. DOI: 10.1016/B978-0-08-096984-8.00003-3.

[44] Abha Kapilashrami et al. 'The fluctuations in slag foam under dynamic conditions'. en. In: *Metallurgical and Materials Transactions B* 37.1 (Feb. 2006), pp. 145–148. ISSN: 1073-5615, 1543-1916. DOI: 10.1007/s11663-006-0095-7.

[45] Kimihisa Ito and R. J. Fruehan. 'Study on the foaming of CaO-SiO2-FeO slags: Part I. Foaming parameters and experimental results'. en. In: *Metallurgical Transactions B* 20.4 (Aug. 1989), pp. 509–514. ISSN: 0360-2141, 1543-1916. DOI: 10.1007/BF02654600. URL: http://link.springer.com/10.1007/BF02654600 (visited on 31/03/2020).

[46] Xiang Li and Merete Tangstad. 'The Influence of Sulfur Content on the Carbothermal Reduction of SiMn Slag'. In: *Metallurgical and Materials Transactions B* 50.1 (Feb. 2019), pp. 136–149. ISSN: 1073-5615, 1543-1916. DOI: 10.1007/s11663-018-1373-x.

[47] Tore-Andre Skjervheim and Sverre E. Olsen. 'THE RATE AND MECHANISM FOR REDUCTION OF MANGANESE OXIDE FROM SILICATE SLAGS'. In: *INFACON 7*. Trondheim, June 1995, pp. 631–640.

[48] Marcel Escudier and Tony Atkins. *A Dictionary of Mechanical Engineering*. 2nd ed. Oxford University Press, 2019. ISBN: 978-0-19-883210-2. URL: https://%20www.oxfordreference.com/view/10.1093/acref/9780198832102.001.0001/acref-9780198832102-e-1087.

[49] R. S. Hebbar, A. M. Isloor and A. F. Ismail. 'Contact Angle Measurements'. In: *Membrane Characterization*. Ed. by Nidal Hilal et al. Elsevier, 2017, pp. 219–255. ISBN: 978-0-444-63776-5. DOI: 10.1016/B978-0-444-63776-5.00012-7.

[50] Haiping Sun et al. 'Wettability and Reduction of MnO in Slag by Carbonaceous Materials'. en. In: *ISIJ International* 50.5 (2010), pp. 639–646. ISSN: 0915-1559, 1347-5460. DOI: 10.2355/isijinternational.50.639. URL: http://joi.jlc.jst.go.jp/JST.JSTAGE/isijinternational/50.639?from=CrossRef.

[51] Gwidon W. Stachowiak and Andrew W. Batchelor. 'Fundamentals of Contact beween solids'. In: *Engineering Tribology*. 3rd. 2006, pp. 461–499. ISBN: 978-0-7506-7836-0.

[52] Hideyuki Kanai et al. 'Wetting and reaction between Si droplet and SiO2 substrate'. en. In: *Journal of Materials Science* 42.23 (Sept. 2007), pp. 9529–9535. ISSN: 0022-2461, 1573-4803. DOI: 10.1007/s10853-007-2090-z.

[53] Leif Sigurd Storlien (Ferroglobe Mangan Norge AS). *Personal communication*. 2019.

[54] Leif Sigurd Storlien. *Making carbon pellets (Un-published work)*. Norwegian University of Science, Technology, Department of Materials Science and Engineering, 2018.

[55] Hamideh Kaffash. 'Dissolution kinetics of carbon materials in FeMn'. PhD thesis. Norwegian University of Science, Technology, Faculty of Natural Sciences, Department of Materials Science and Engineering, 2019.

[56] Eli Ringdalen et al. 'Ore Melting and Reduction in Silicomanganese Production'. en. In: *Metallurgical and Materials Transactions B* 41.6 (Dec. 2010), pp. 1220–1229. ISSN: 1073-5615, 1543-1916. DOI: 10.1007/s11663-010-9350-z.

[57] Brian J. Ford, Savile Bradbury and David C. Joy. *Electron-probe microanalyzer — instrument*. en. URL: https://www.britannica.com/technology/electron-probe-microanalyzer (visited on 16/03/2020).

[58] John Goodge. *Electron probe micro-analyzer (EPMA)*. en. URL: https://serc.carleton.edu/research_education/geochemsheets/techniques/EPMA.html (visited on 16/03/2020).

[59] Jarle Hjelen. *Scanning elektron-mikroskopi*. Trondheim: SINTEF, 1989. URL: https://urn.nb.no/URN:NBN:no-nb_digibok_2013070305116 (visited on 30/05/2020).

[60] Brian J. Ford, David C. Joy and Savile Bradbury. *Scanning electron microscope — Definition, Images, Uses, Advantages, and Facts*. en. 2019. URL: https://www.britannica.com/technology/scanning-electron-microscope (visited on 16/03/2020).

Appendix

A1: Surface roughness analysis

Surface roughness analysis for pelletized charcoal made with a load of 500 kg on the press.

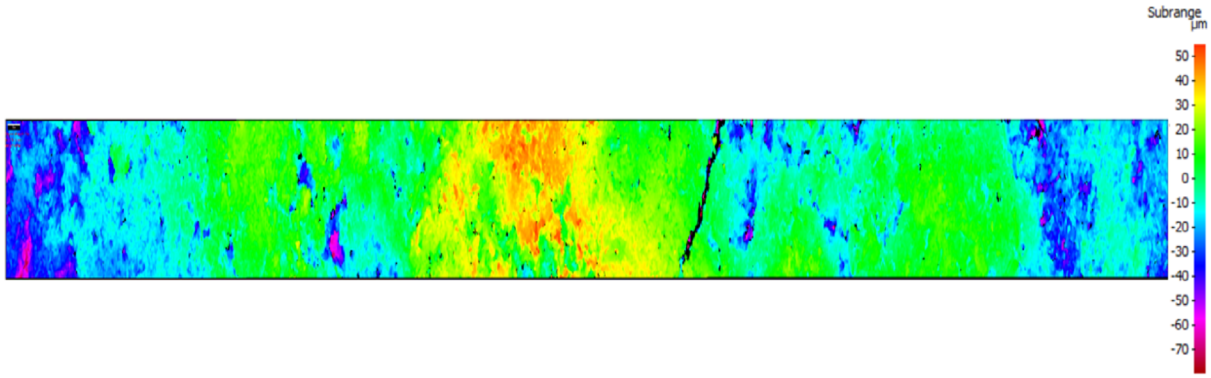

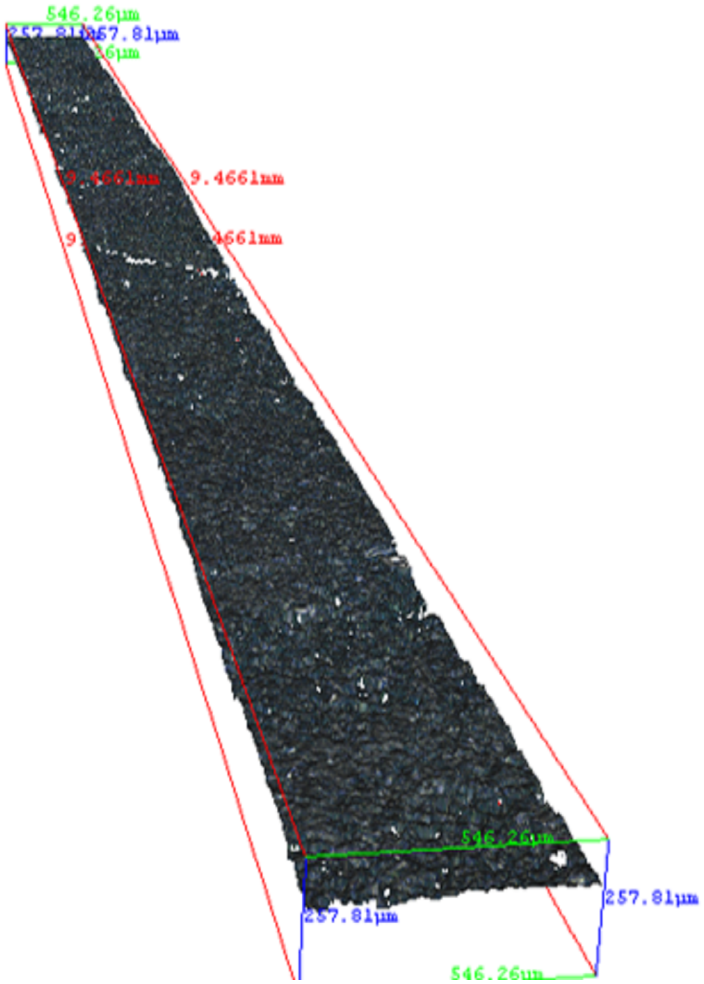

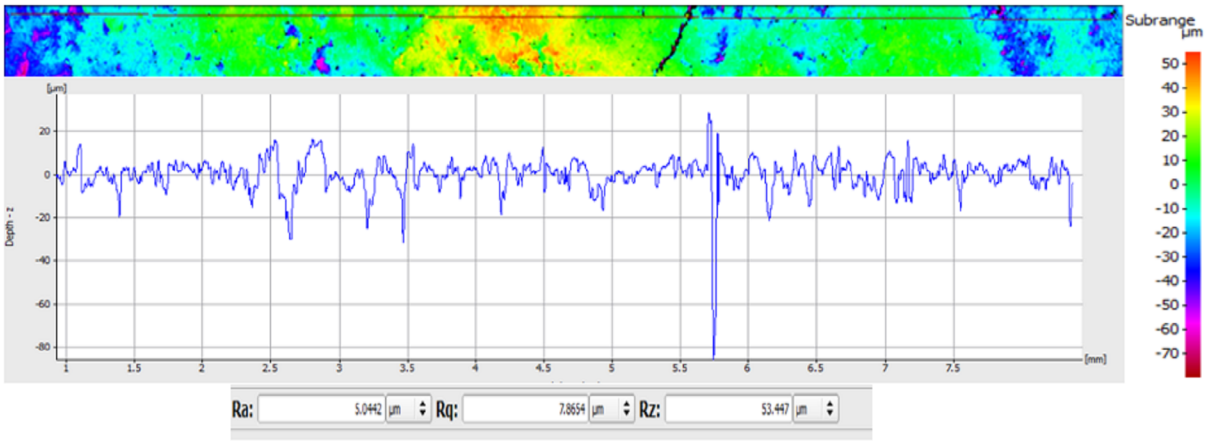
Subrange
µm
50
40
30
20
10
0
-10
-20
-30
-40
-50
-60
-70
[µm]
Depth - z
[mm]
Ra: 5.0442 µm Rq: 7.8654 µm Rz: 53.447 µm

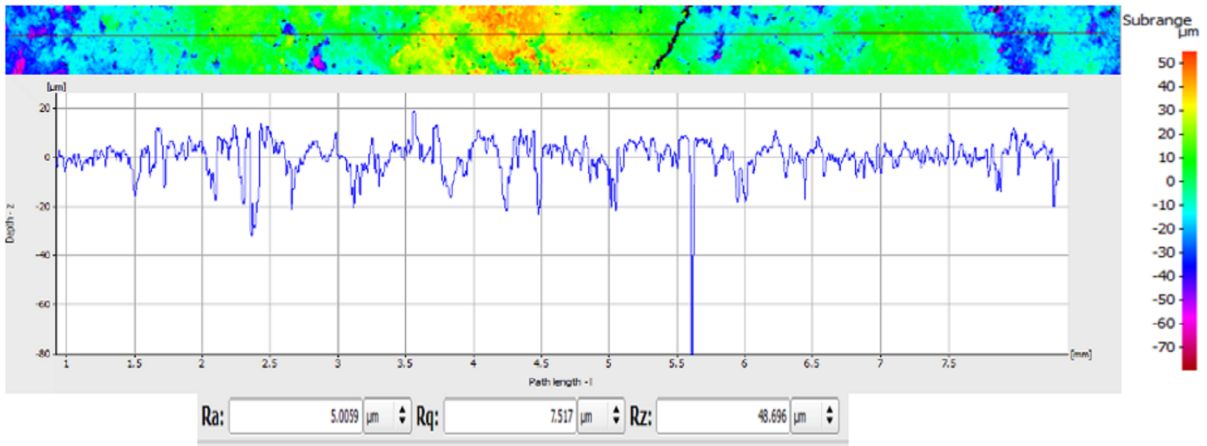
Subrange
µm
50
40
30
20
10
0
-10
-20
-30
-40
-50
-60
-70
[µm]
Depth - z
Path length - l
[mm]
Ra: 5.0059 µm Rq: 7.517 µm Rz: 48.696 µm

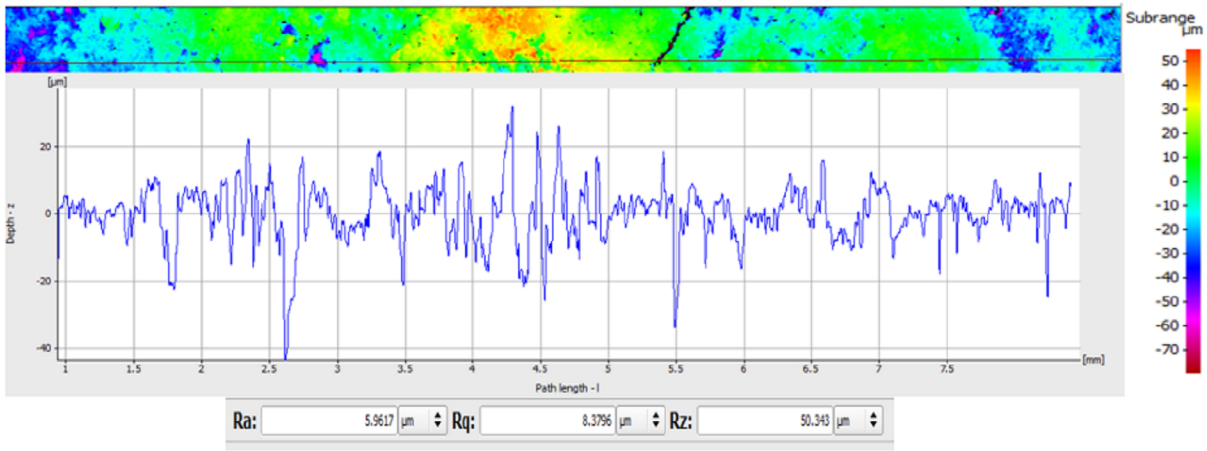
Subrange
µm
50
40
30
20
10
0
-10
-20
-30
-40
-50
-60
-70
[µm]
Depth - z
Path length - l
[mm]
Ra: 5.9617 µm Rq: 8.3796 µm Rz: 50.343 µm

Surface roughness analysis for pelletized charcoal made with a load of 1000 kg on the press

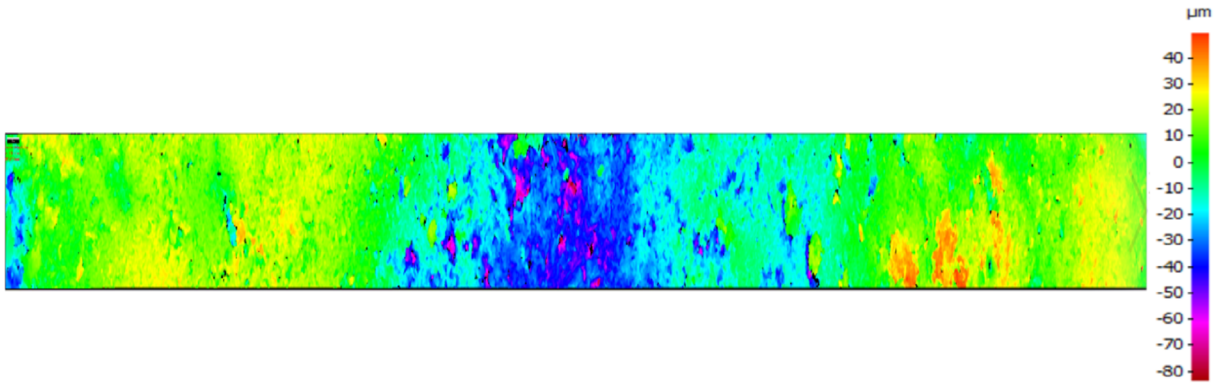

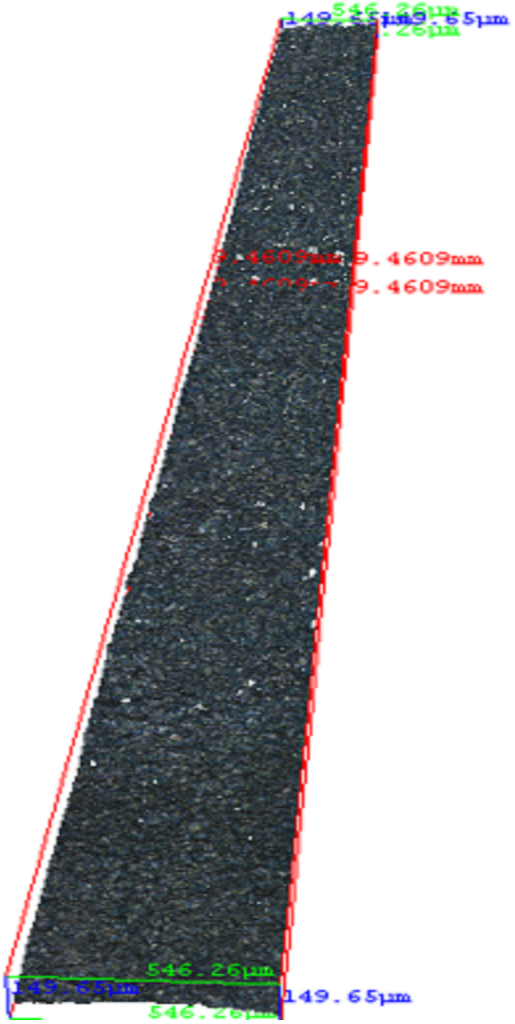

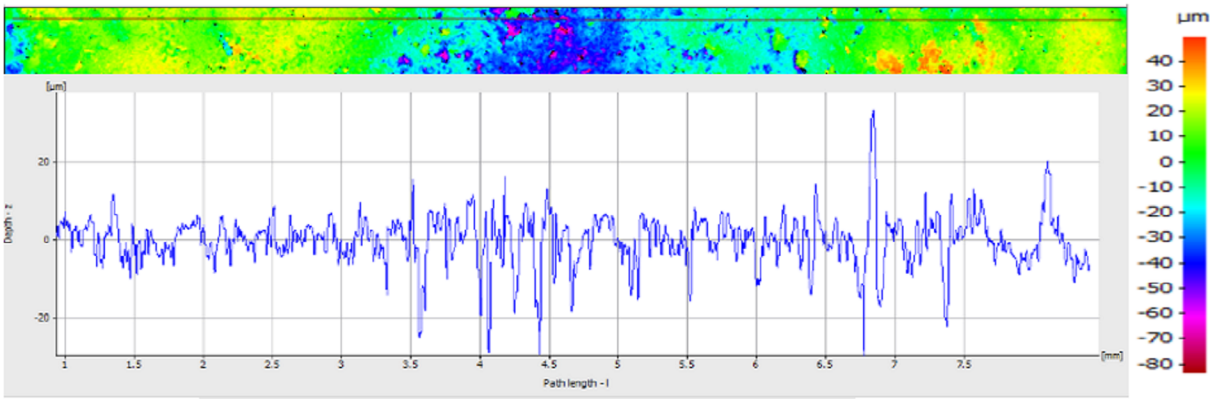
µm
40
30
20
10
0
-10
-20
-30
-40
-50
-60
-70
-80
[µm]
Depth - z
Path length - l
[mm]
Ra: 4.4819 µm Rq: 6.2789 µm Rz: 42.574 µm

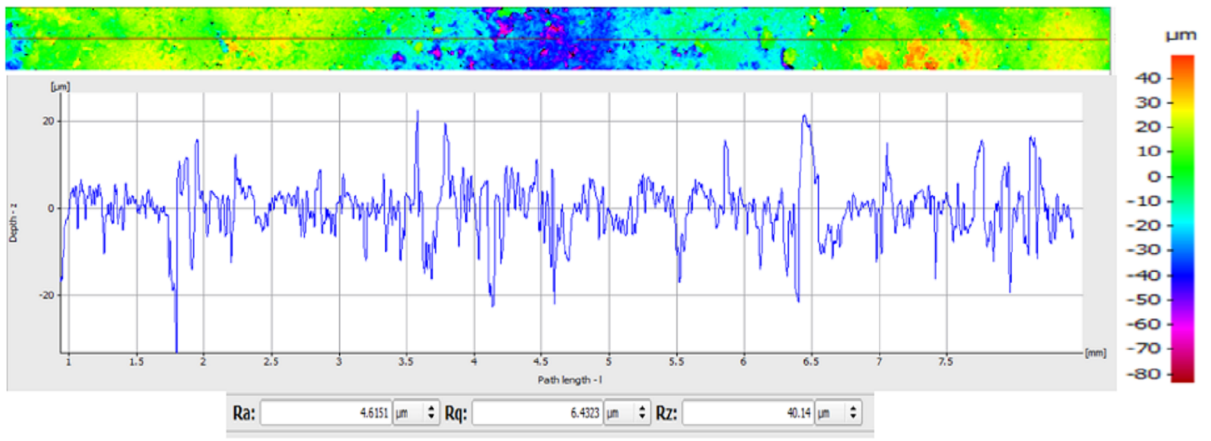
µm
40
30
20
10
0
-10
-20
-30
-40
-50
-60
-70
-80
[µm]
Depth - z
Path length - l
[mm]
Ra: 4.6151 µm Rq: 6.4323 µm Rz: 40.14 µm

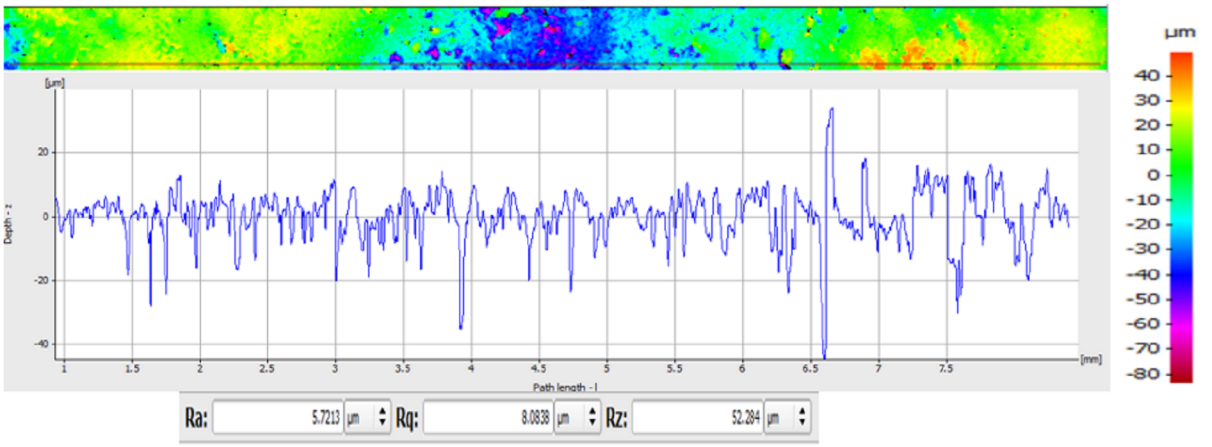
µm
40
30
20
10
0
-10
-20
-30
-40
-50
-60
-70
-80
[µm]
Depth - z
Path length - l
[mm]
Ra: 5.7213 µm Rq: 8.0838 µm Rz: 52.284 µm

Surface roughness analysis for pelletized charcoal made with a load of 2000 kg on the press

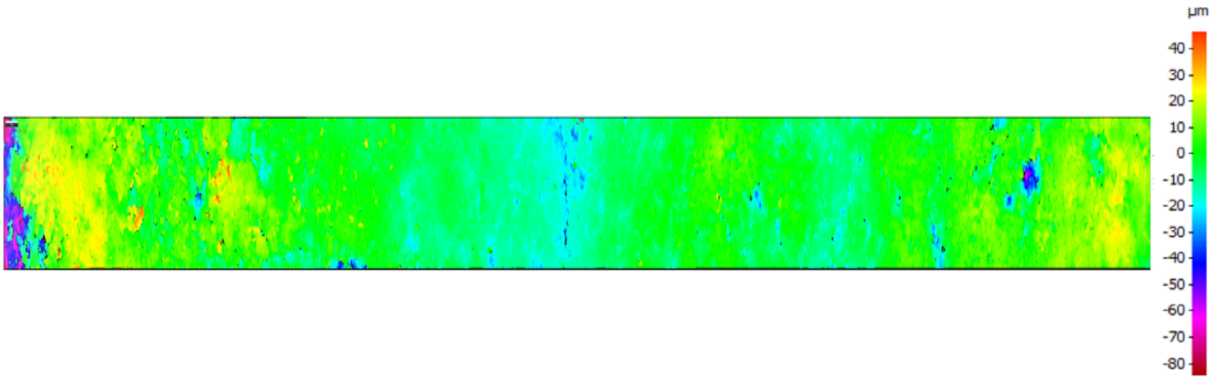

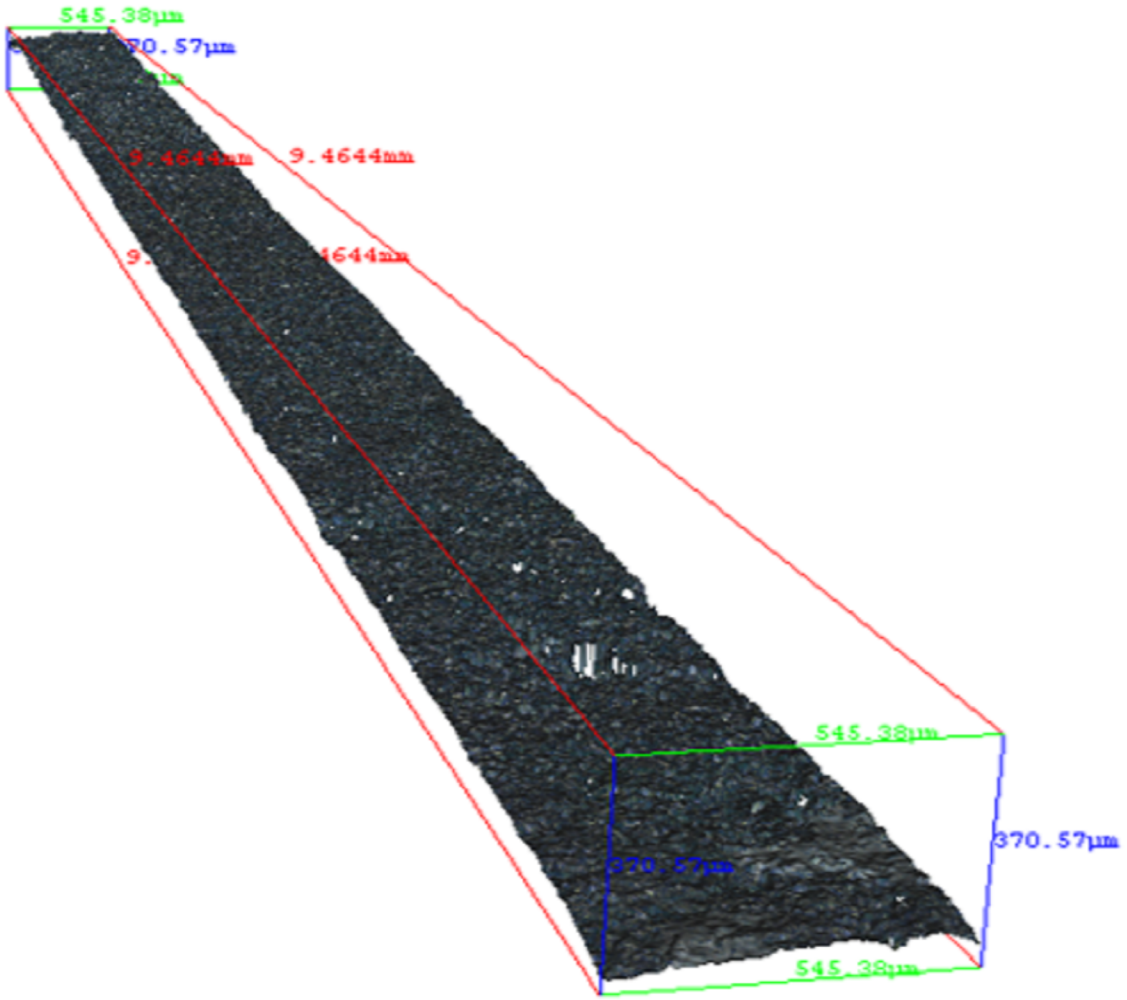

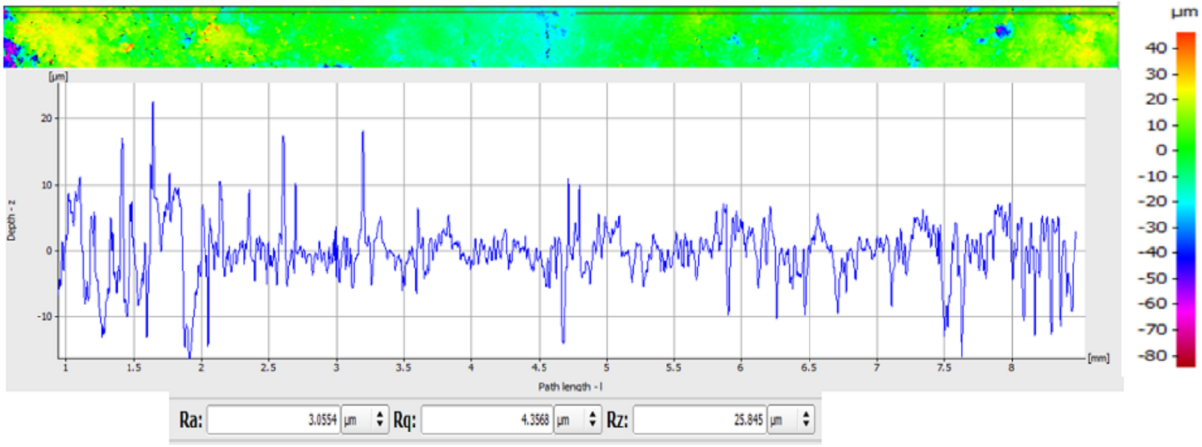
µm
40
30
20
10
0
-10
-20
-30
-40
-50
-60
-70
-80
[µm]
Depth - z
Path length - l
[mm]
Ra: 3.0554 µm Rq: 4.3568 µm Rz: 25.845 µm

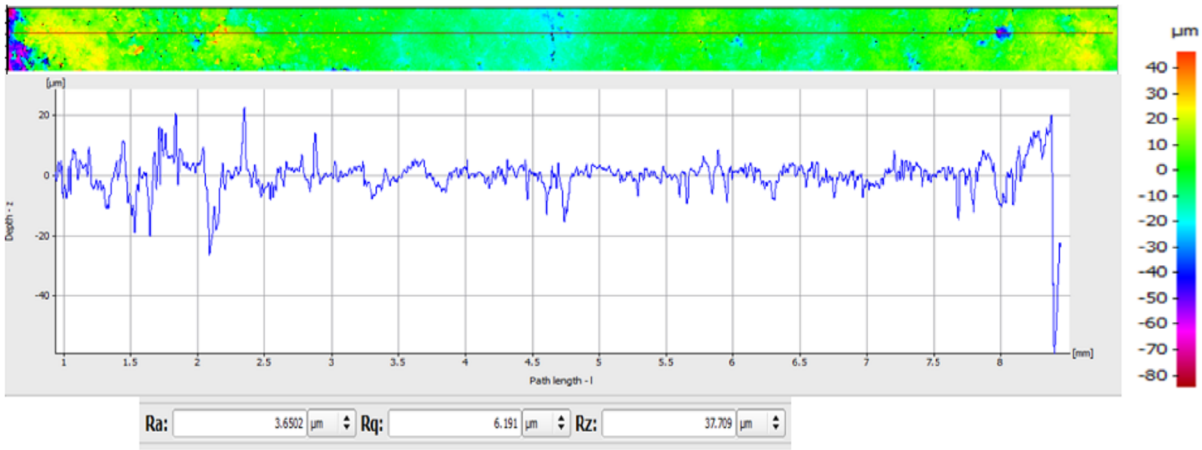
µm
40
30
20
10
0
-10
-20
-30
-40
-50
-60
-70
-80
[µm]
Depth - z
Path length - l
[mm]
Ra: 3.6502 µm Rq: 6.191 µm Rz: 37.709 µm

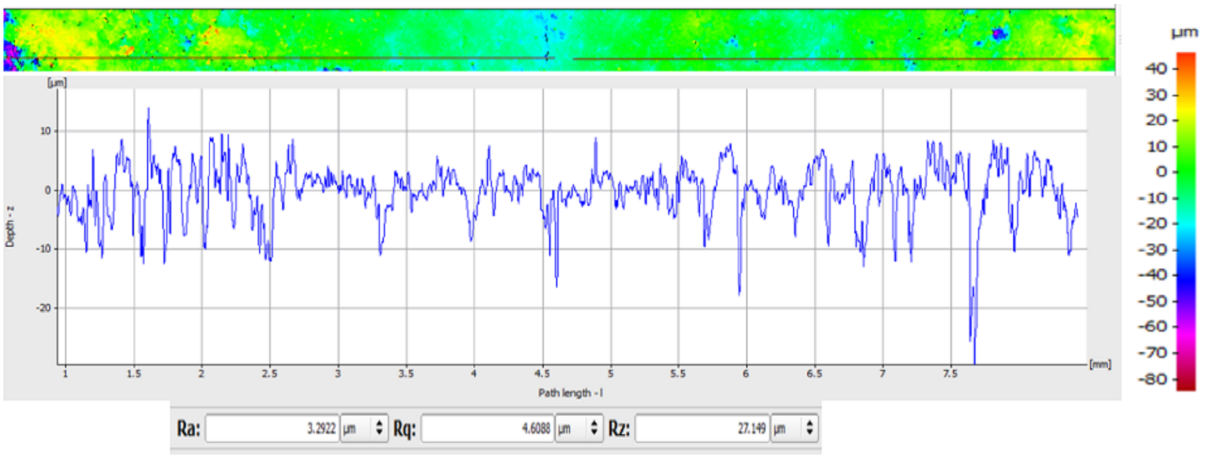
µm
40
30
20
10
0
-10
-20
-30
-40
-50
-60
-70
-80
[µm]
Depth - z
Path length - l
[mm]
Ra: 3.2922 µm Rq: 4.6088 µm Rz: 27.149 µm

Surface roughness analysis for green charcoal where the surface is along the fibres.

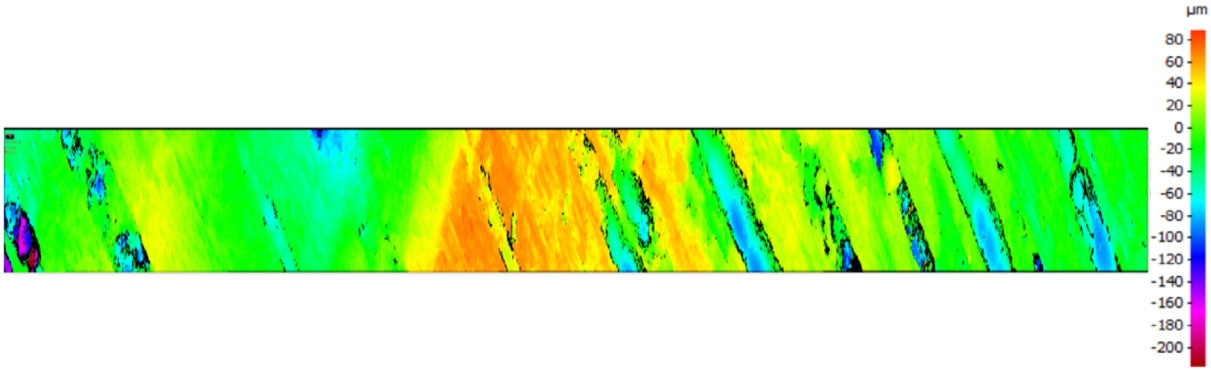

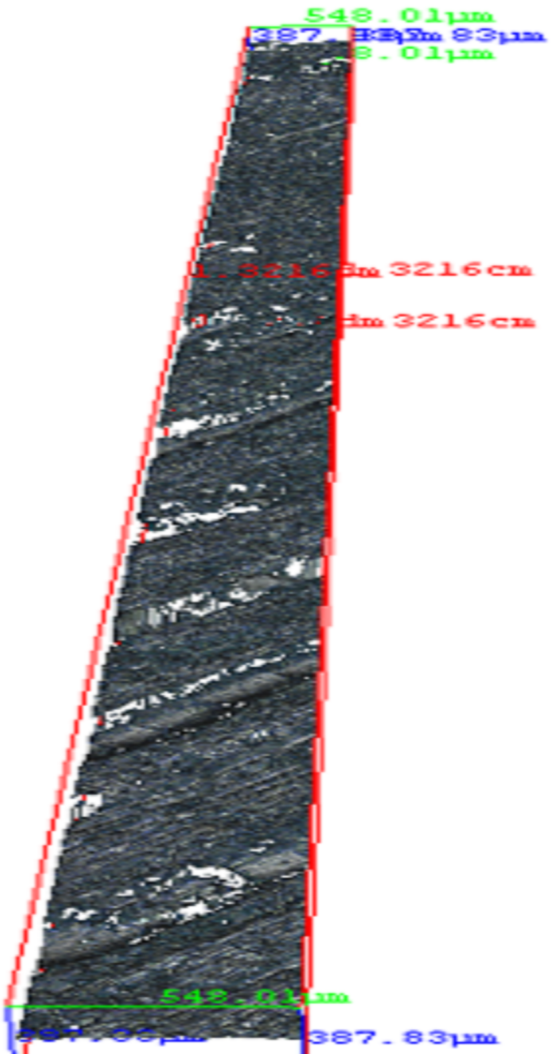

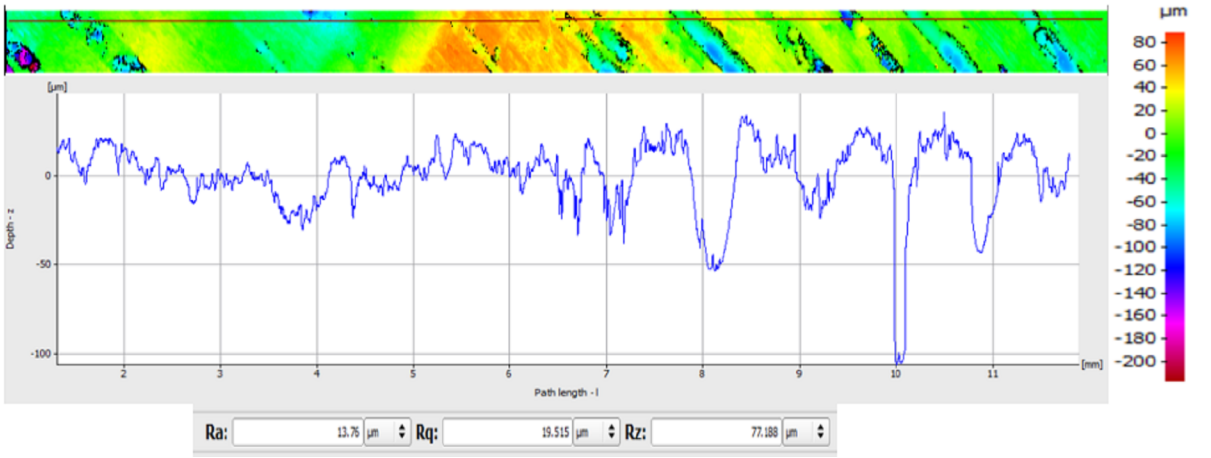
µm
80
60
40
20
0
-20
-40
-60
-80
-100
-120
-140
-160
-180
-200
[µm]
Depth - z
Path length - l
[mm]
Ra: 13.76 µm Rq: 19.515 µm Rz: 77.188 µm

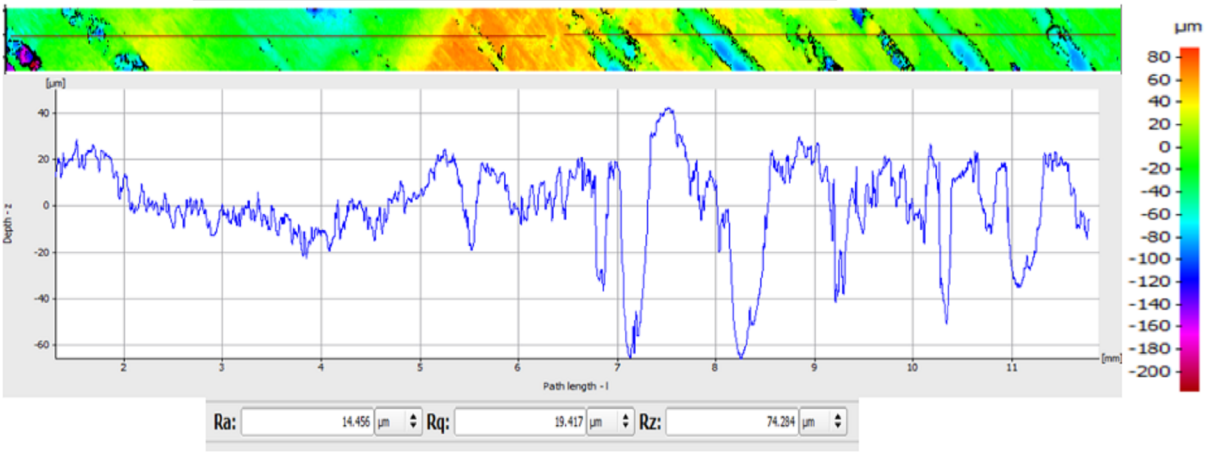
µm
80
60
40
20
0
-20
-40
-60
-80
-100
-120
-140
-160
-180
-200
[µm]
Depth - z
Path length - l
[mm]
Ra: 14.456 µm Rq: 19.417 µm Rz: 74.284 µm

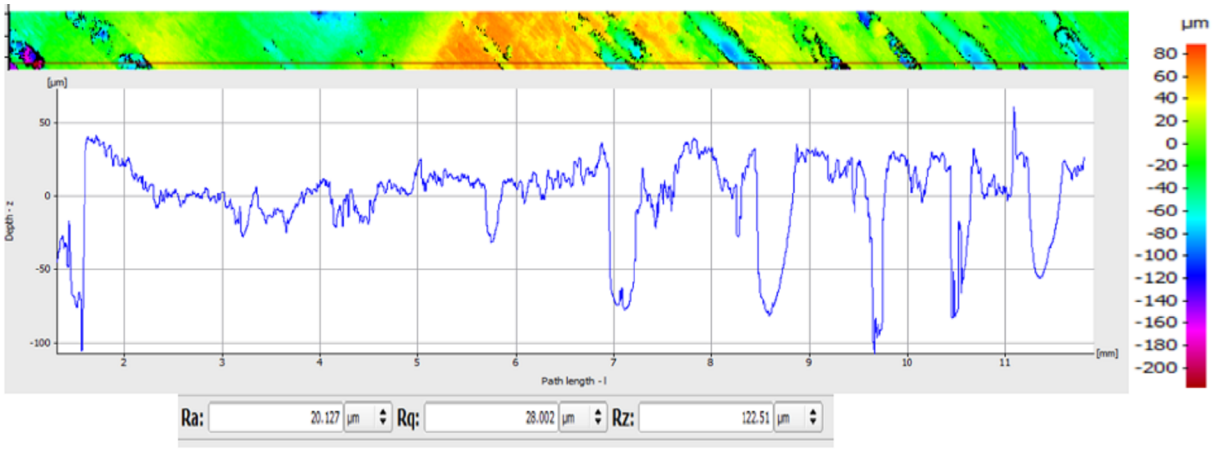
µm
80
60
40
20
0
-20
-40
-60
-80
-100
-120
-140
-160
-180
-200
[µm]
Depth - z
Path length - l
[mm]
Ra: 20.127 µm Rq: 28.002 µm Rz: 122.51 µm

Surface roughness analysis for green charcoal where the surface is on top of the fibres.

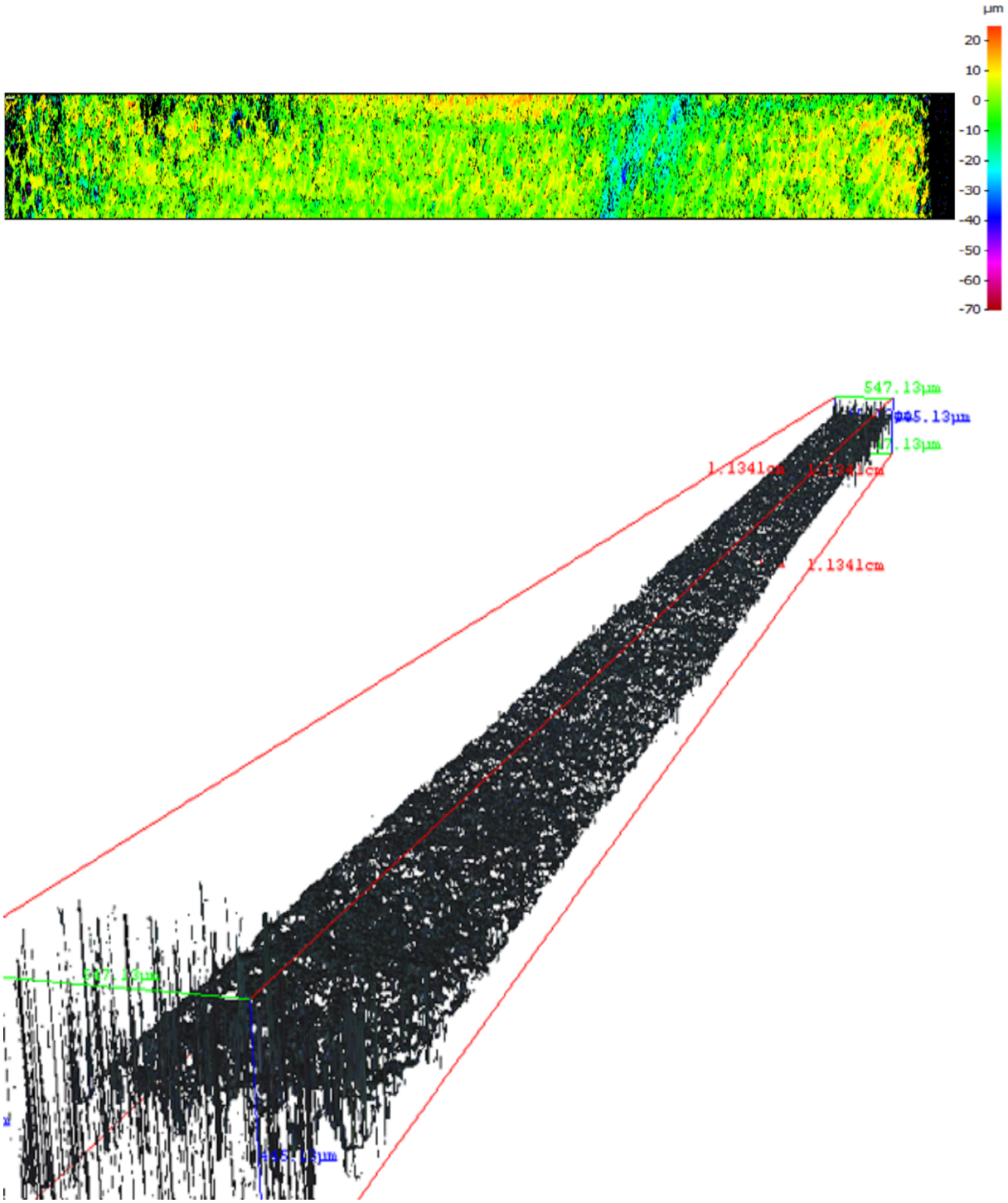

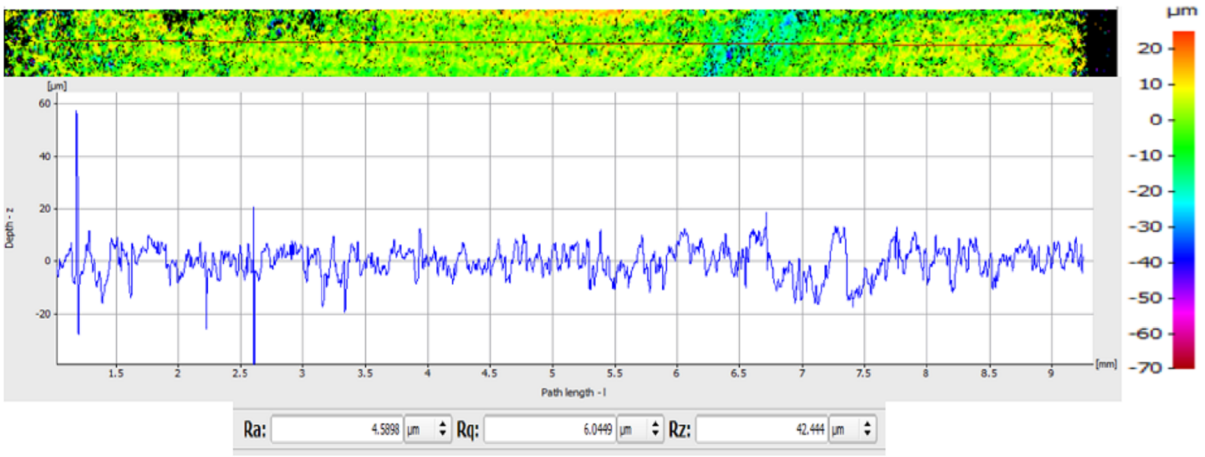
µm
20
10
0
-10
-20
-30
-40
-50
-60
-70
[µm]
60
40
20
0
-20
Depth - z
1.5
2
2.5
3
3.5
4
4.5
5
5.5
6
6.5
7
7.5
8
8.5
9
[mm]
Path length - l
Ra: 4.5898 µm
Rq: 6.0449 µm
Rz: 42.444 µm

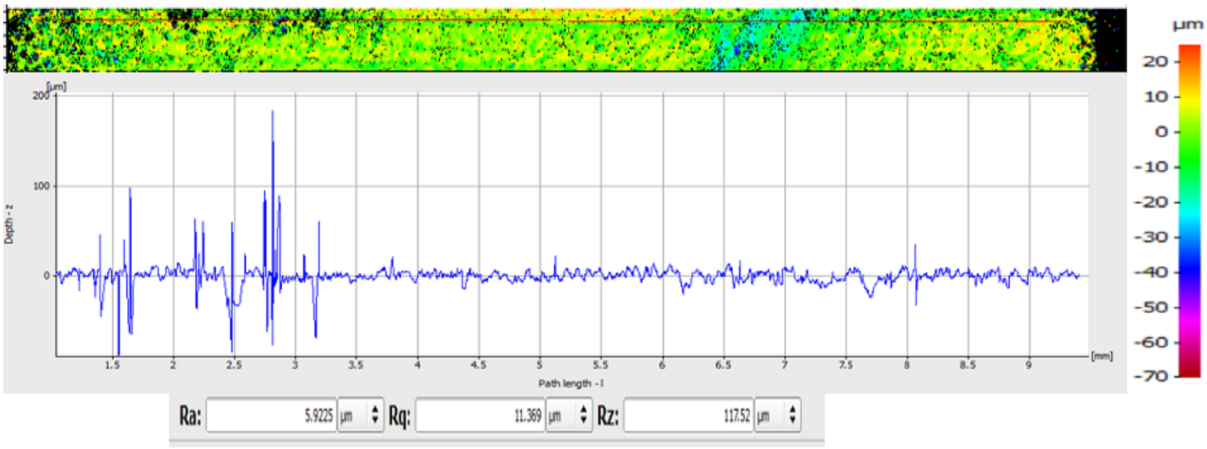
µm
20
10
0
-10
-20
-30
-40
-50
-60
-70
[µm]
200
100
0
Depth - z
1.5
2
2.5
3
3.5
4
4.5
5
5.5
6
6.5
7
7.5
8
8.5
9
[mm]
Path length - l
Ra: 5.9225 µm
Rq: 11.369 µm
Rz: 117.52 µm

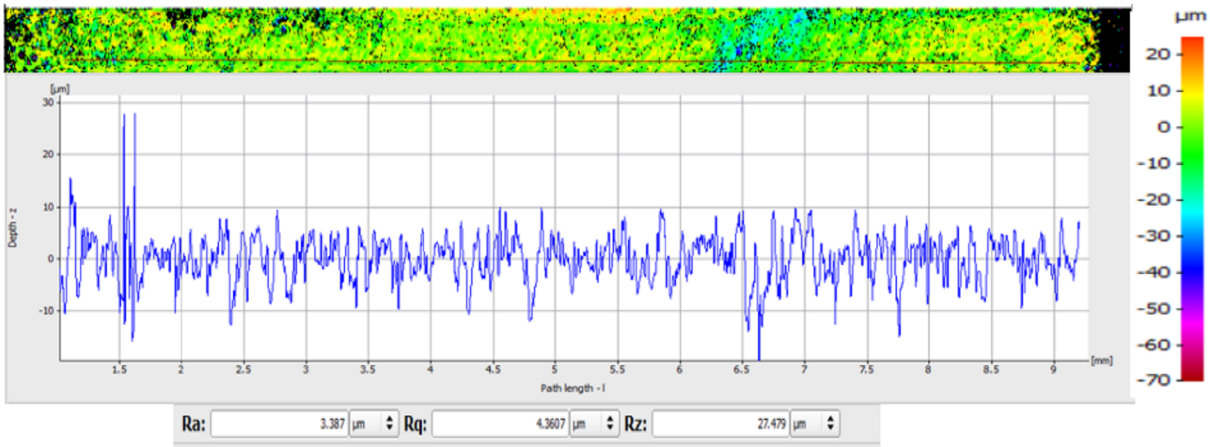
µm
20
10
0
-10
-20
-30
-40
-50
-60
-70
[µm]
30
20
10
0
-10
Depth - z
1.5
2
2.5
3
3.5
4
4.5
5
5.5
6
6.5
7
7.5
8
8.5
9
[mm]
Path length - l
Ra: 3.387 µm
Rq: 4.3607 µm
Rz: 27.479 µm

Surface roughness analysis for pelletized coke made with a load of 500 kg on the press.

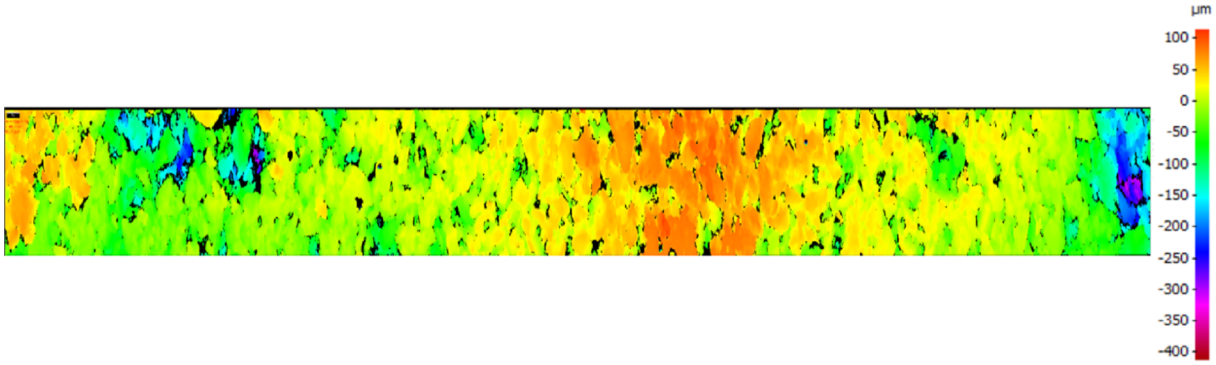

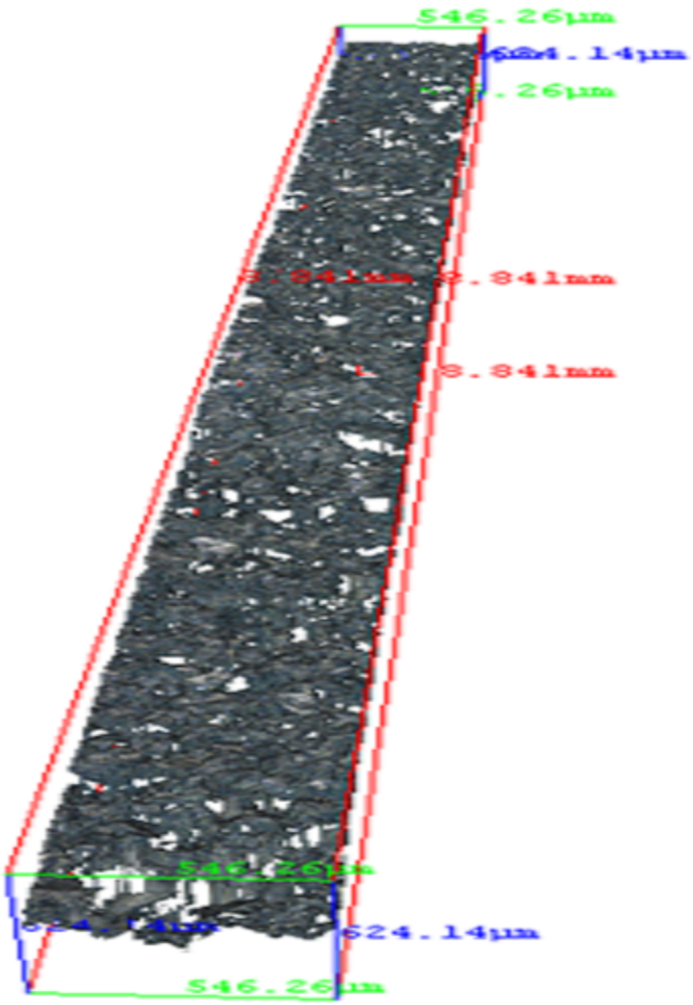

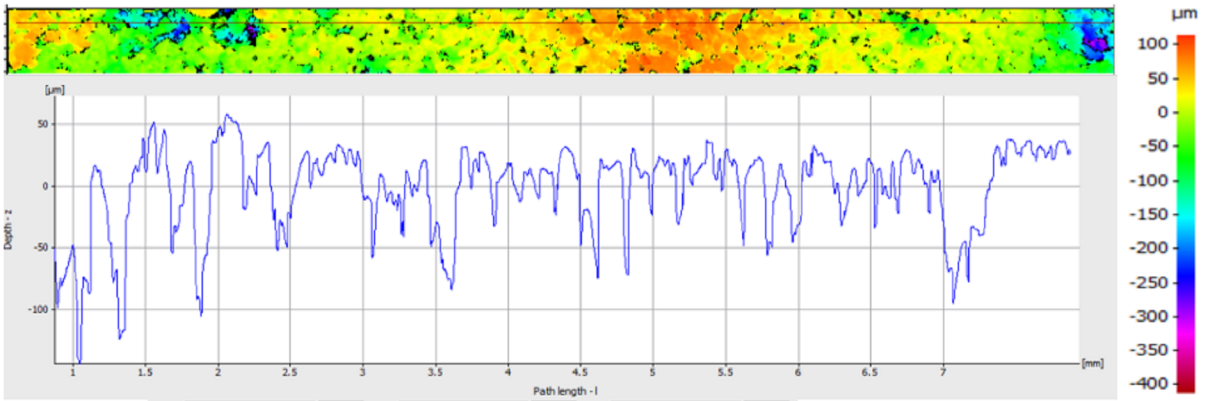
µm
100
50
0
-50
-100
-150
-200
-250
-300
-350
-400
[µm]
Depth - z
Path length - l
[mm]
Ra: 26.264 µm Rq: 34.361 µm Rz: 131.04 µm

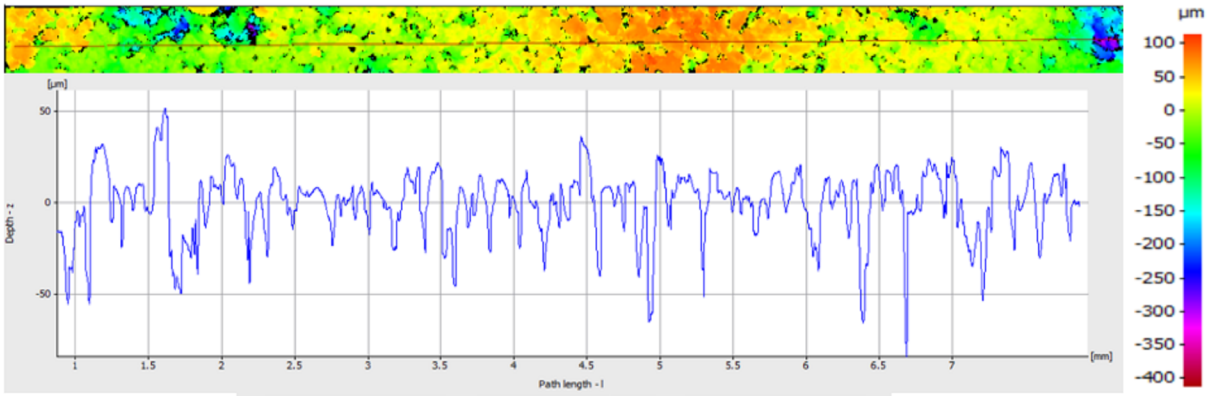
µm
100
50
0
-50
-100
-150
-200
-250
-300
-350
-400
[µm]
Depth - z
Path length - l
[mm]
Ra: 13.342 µm Rq: 17.983 µm Rz: 95.487 µm

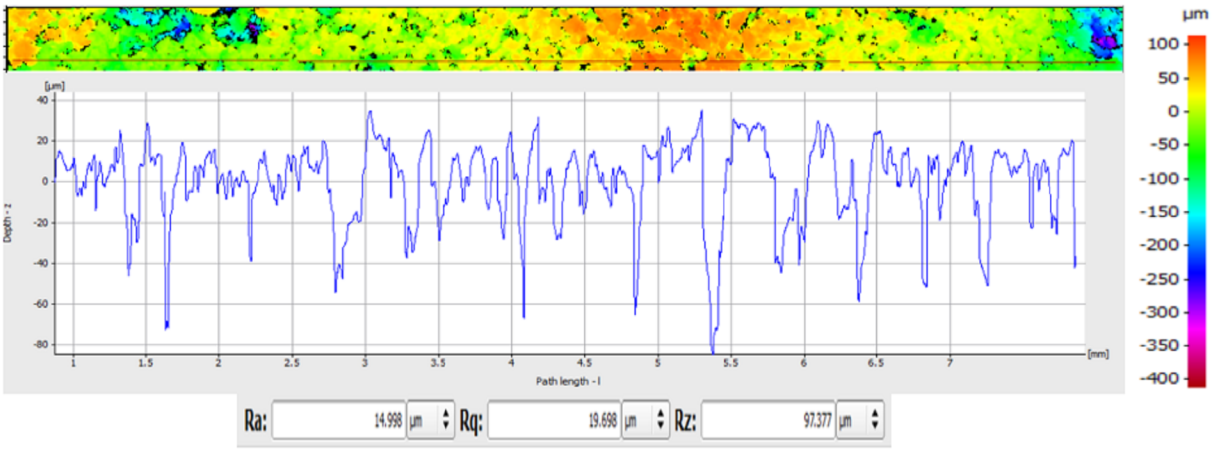
µm
100
50
0
-50
-100
-150
-200
-250
-300
-350
-400
[µm]
Depth - z
Path length - l
[mm]
Ra: 14.998 µm Rq: 19.698 µm Rz: 97.377 µm

Surface roughness analysis for pelletized coke made with a load of 1000 kg on the press.

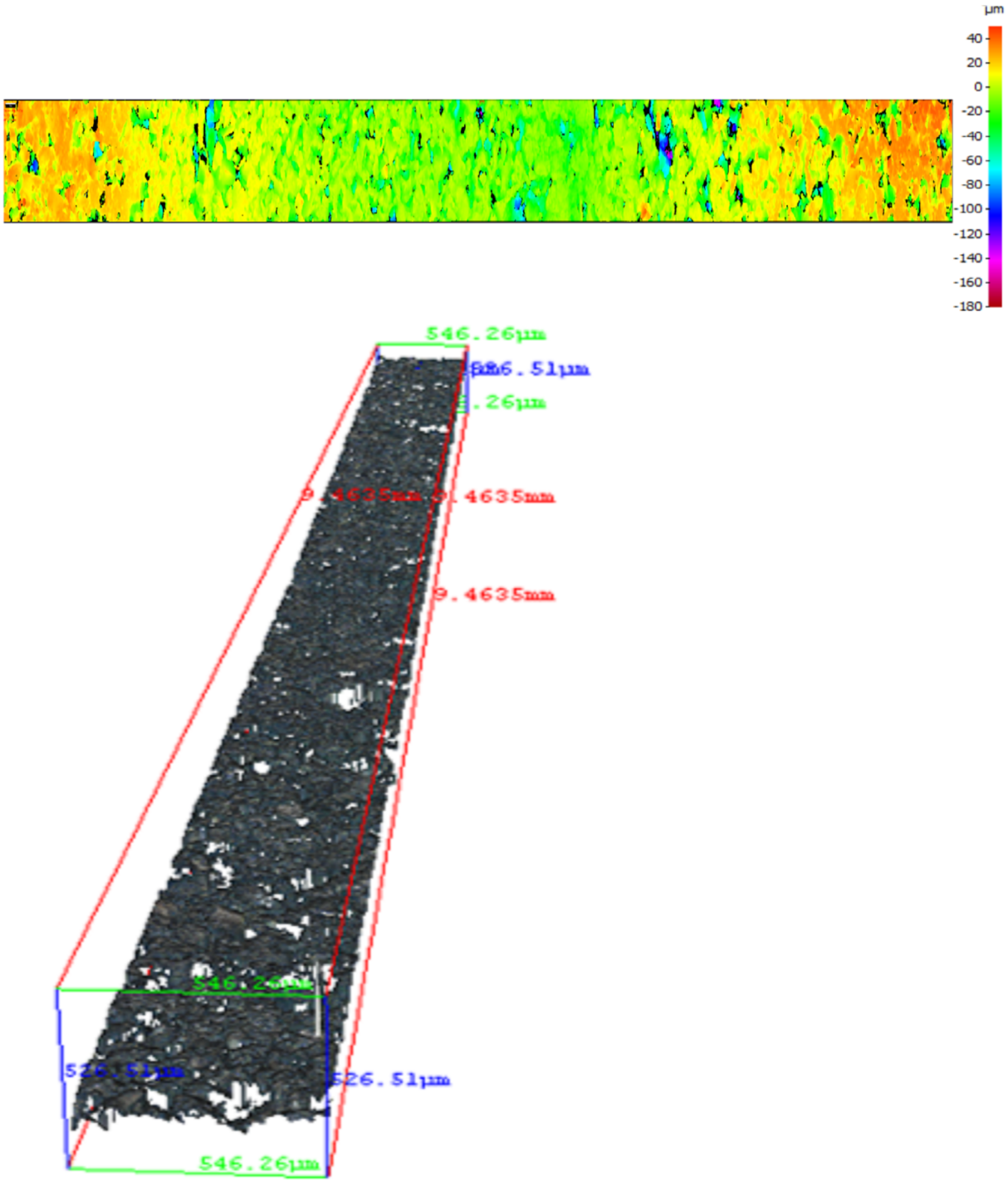

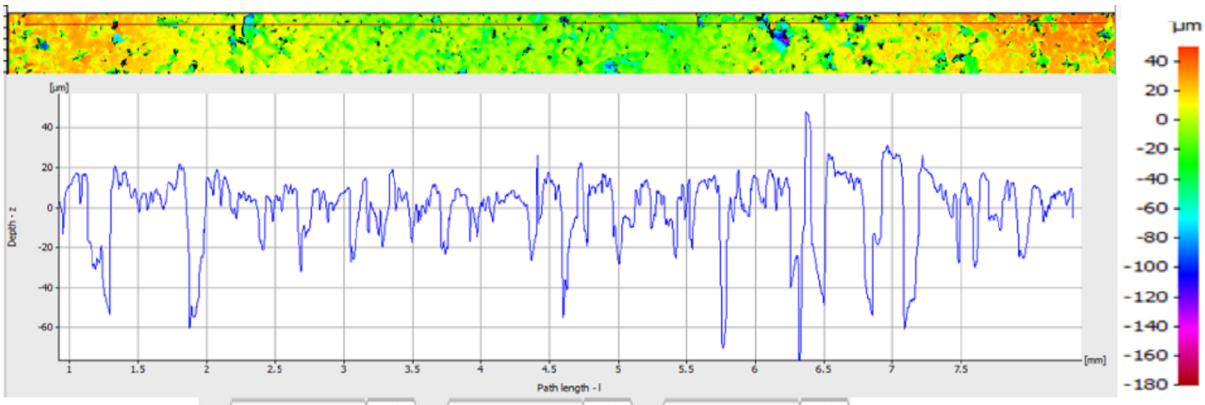
µm
40
20
0
-20
-40
-60
-80
-100
-120
-140
-160
-180
[µm]
Depth - z
Path length - l
[mm]
Ra: 12.925 µm Rq: 17.539 µm Rz: 86.092 µm

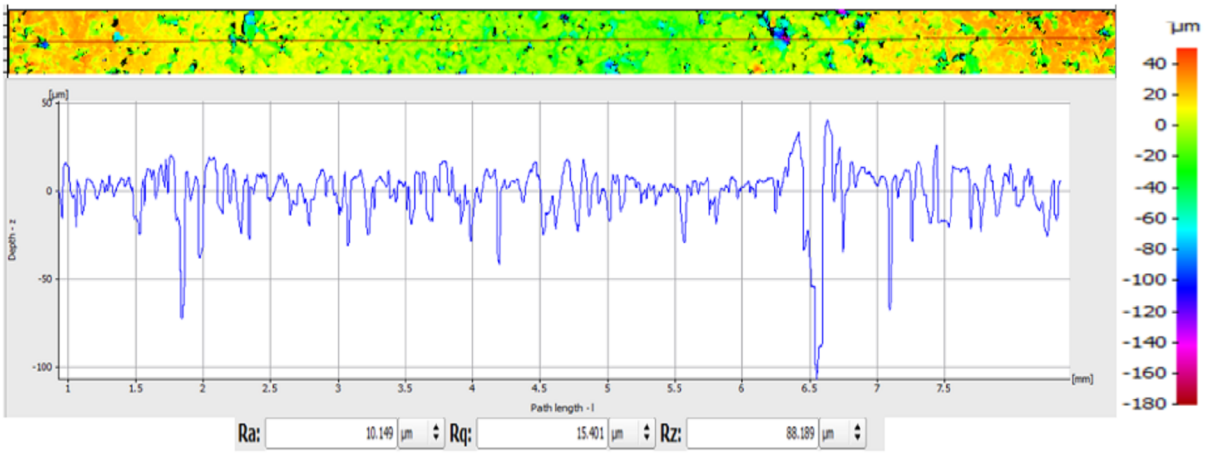
µm
40
20
0
-20
-40
-60
-80
-100
-120
-140
-160
-180
[µm]
Depth - z
Path length - l
[mm]
Ra: 10.149 µm Rq: 15.401 µm Rz: 88.189 µm

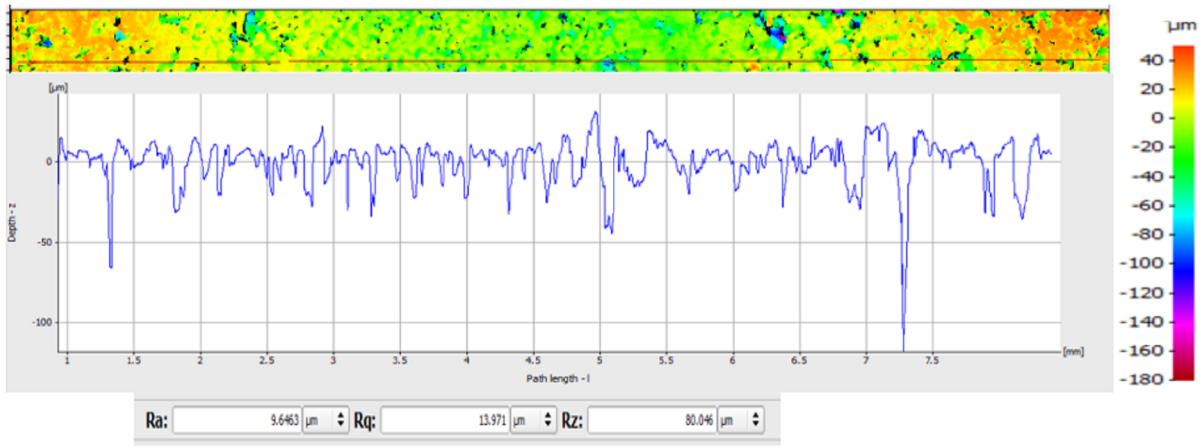
µm
40
20
0
-20
-40
-60
-80
-100
-120
-140
-160
-180
[µm]
Depth - z
Path length - l
[mm]
Ra: 9.6463 µm Rq: 13.971 µm Rz: 80.046 µm

Surface roughness analysis for pelletized coke made with a load of 2000 kg on the press.

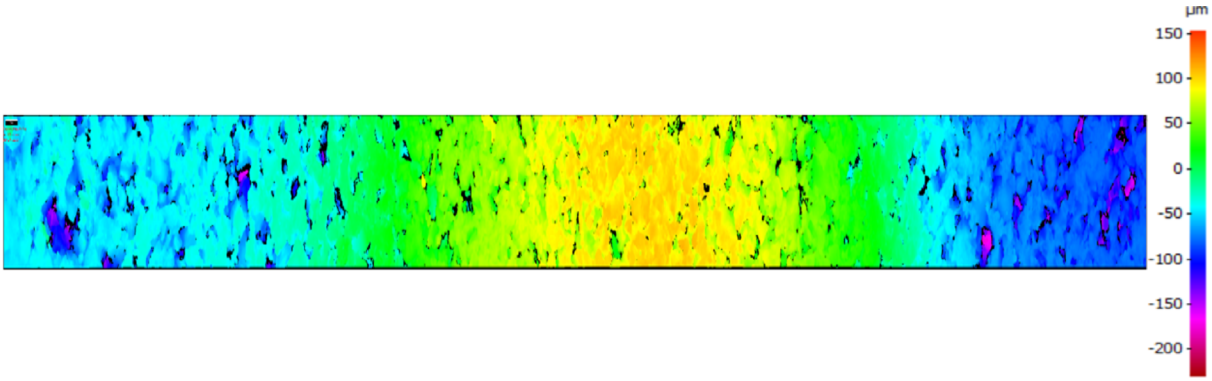

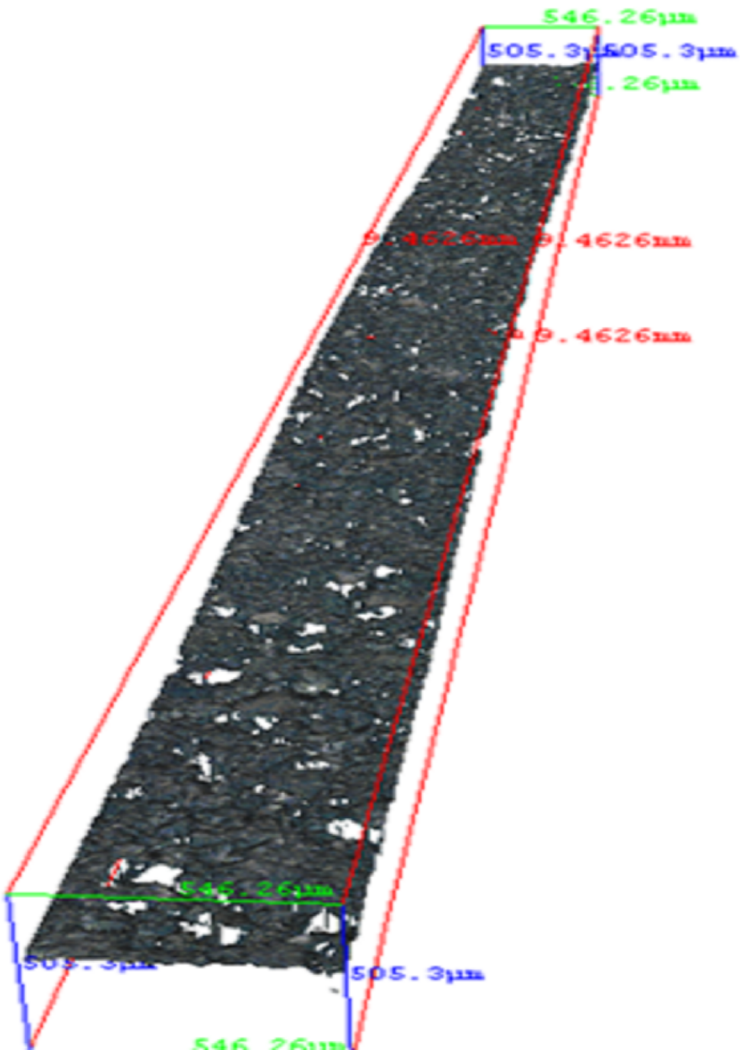

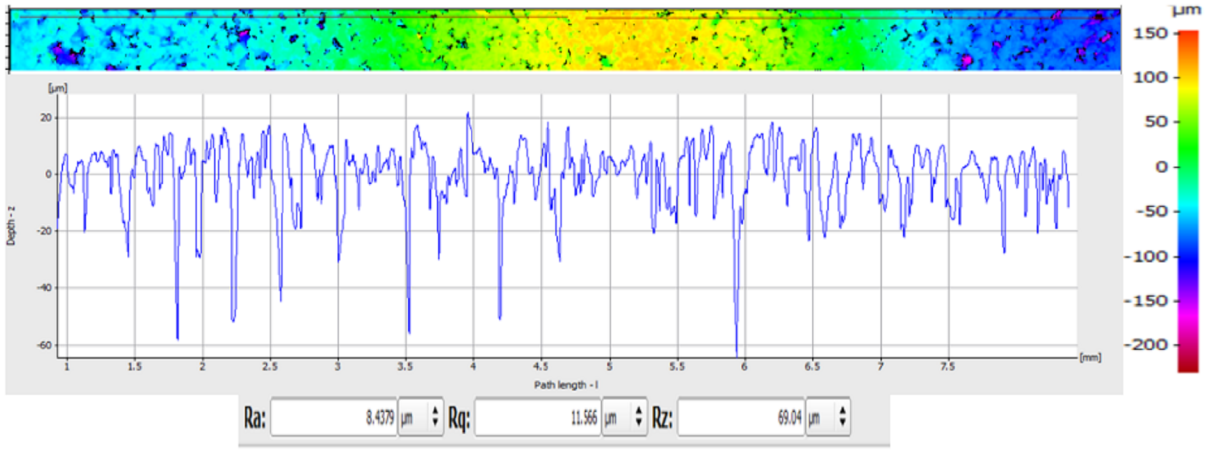
µm
150
100
50
0
-50
-100
-150
-200
[µm]
20
0
-20
-40
-60
Depth - z
1
1.5
2
2.5
3
3.5
4
4.5
5
5.5
6
6.5
7
7.5
[mm]
Path length - l
Ra: 8.4379 µm Rq: 11.566 µm Rz: 69.04 µm

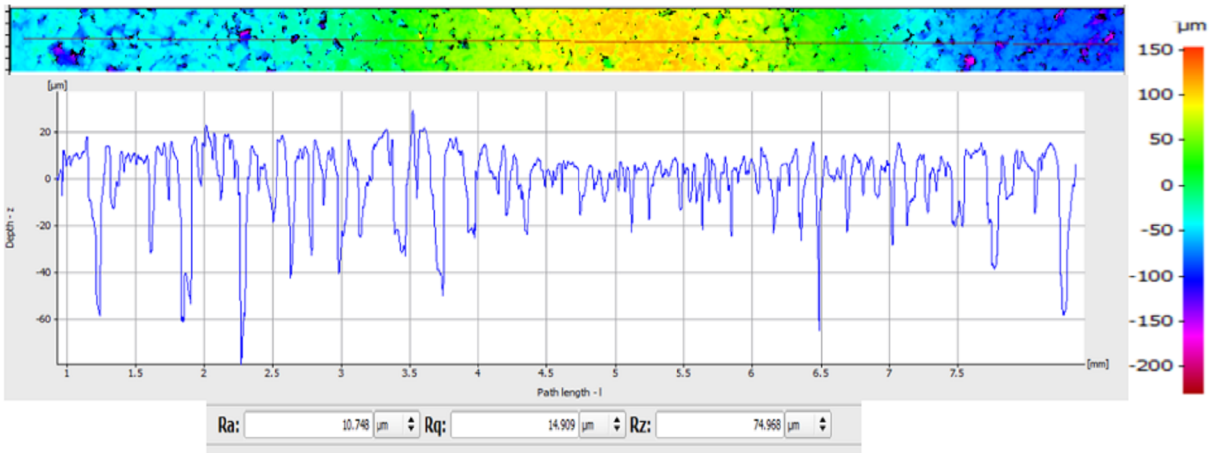
µm
150
100
50
0
-50
-100
-150
-200
[µm]
20
0
-20
-40
-60
Depth - z
1
1.5
2
2.5
3
3.5
4
4.5
5
5.5
6
6.5
7
7.5
[mm]
Path length - l
Ra: 10.748 µm Rq: 14.909 µm Rz: 74.968 µm

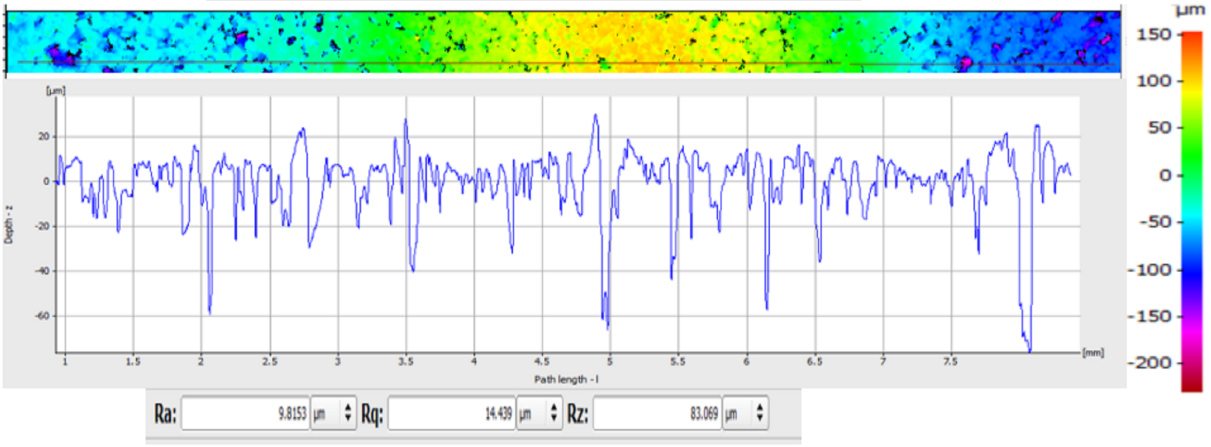
µm
150
100
50
0
-50
-100
-150
-200
[µm]
20
0
-20
-40
-60
Depth - z
1
1.5
2
2.5
3
3.5
4
4.5
5
5.5
6
6.5
7
7.5
[mm]
Path length - l
Ra: 9.8153 µm Rq: 14.439 µm Rz: 83.069 µm

Surface roughness analysis for green coke.

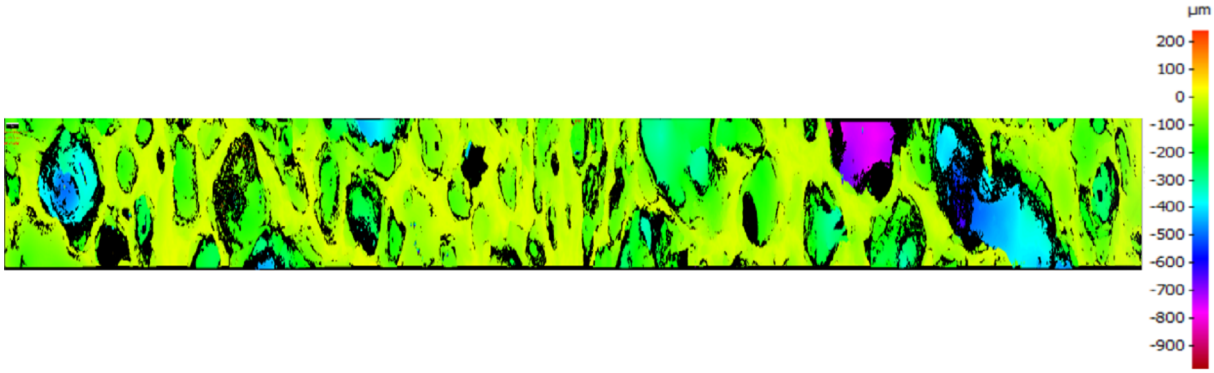

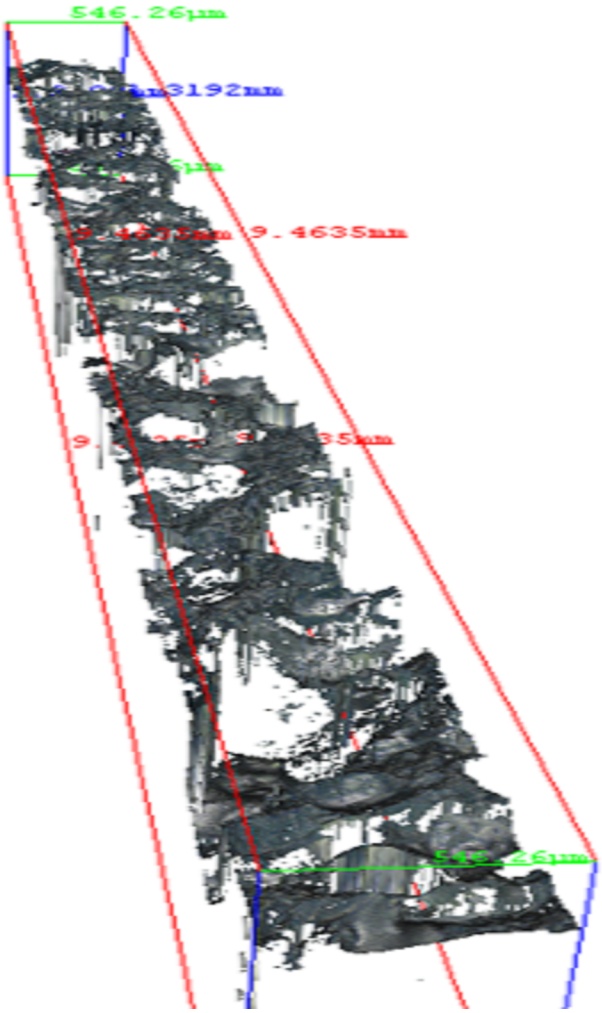

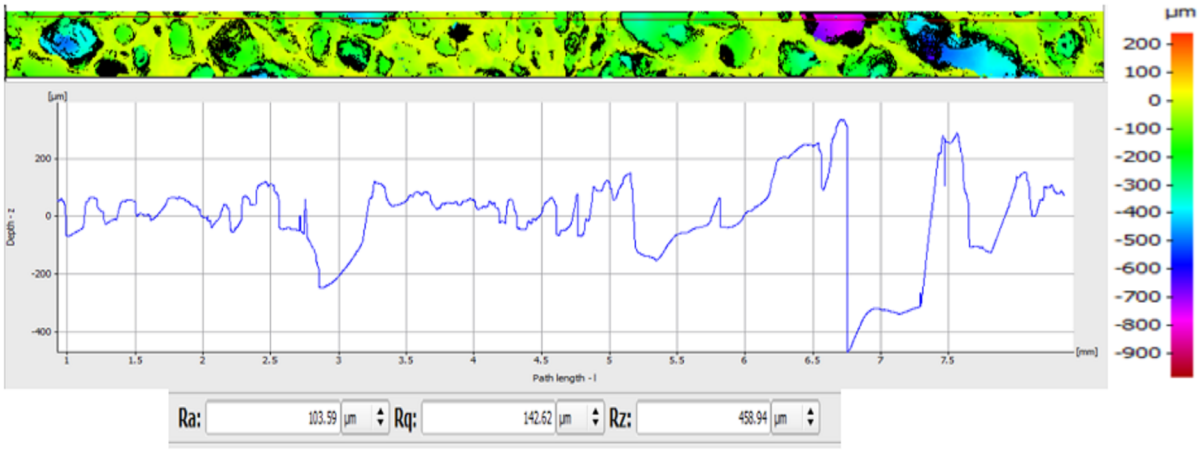
µm
200
100
0
-100
-200
-300
-400
-500
-600
-700
-800
-900
[µm]
Depth - z
Path length - l
[mm]
Ra: 103.59 µm Rq: 142.62 µm Rz: 458.94 µm

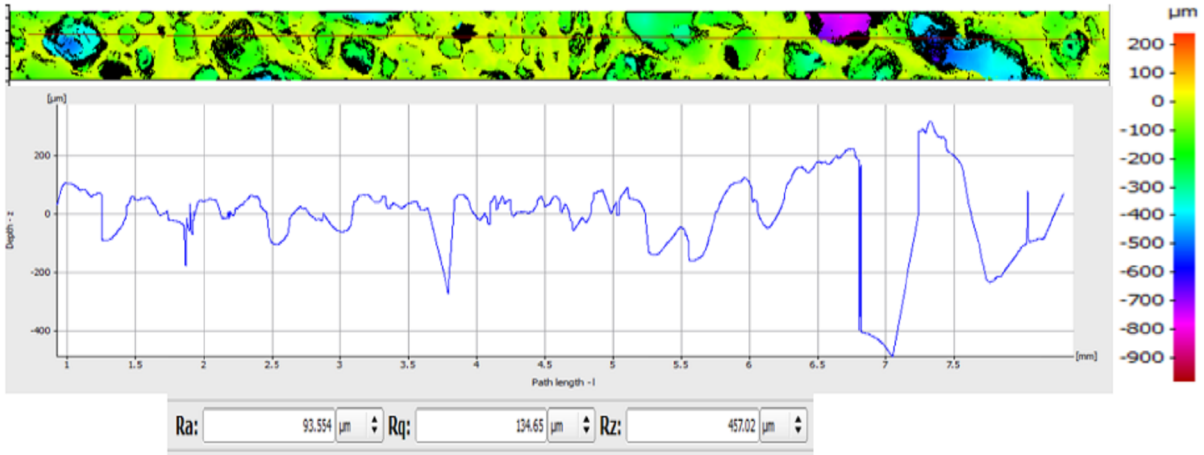
µm
200
100
0
-100
-200
-300
-400
-500
-600
-700
-800
-900
[µm]
Depth - z
Path length - l
[mm]
Ra: 93.554 µm Rq: 134.65 µm Rz: 457.02 µm

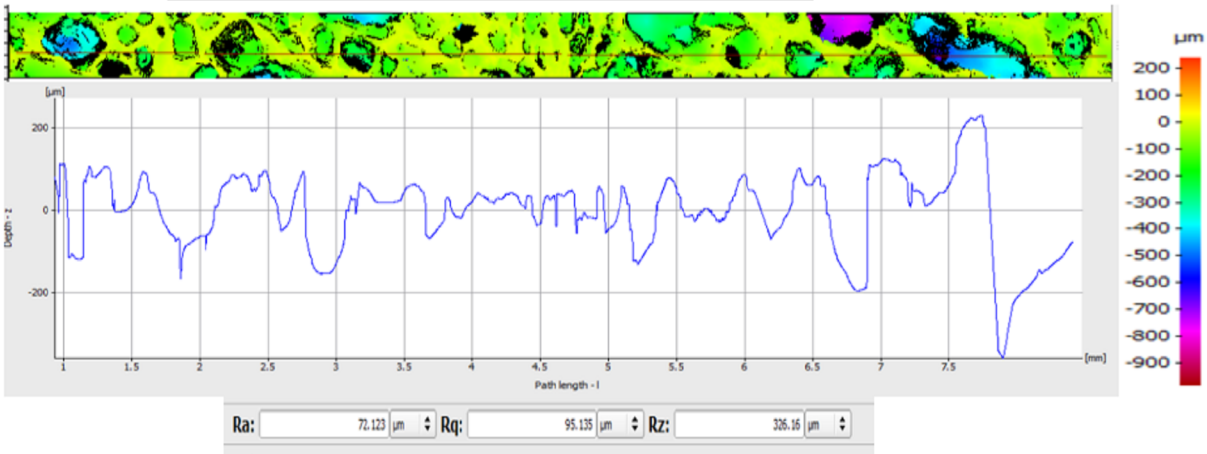
µm
200
100
0
-100
-200
-300
-400
-500
-600
-700
-800
-900
[µm]
Depth - z
Path length - l
[mm]
Ra: 72.123 µm Rq: 95.135 µm Rz: 326.16 µm

Surface roughness analysis for graphite pellet.

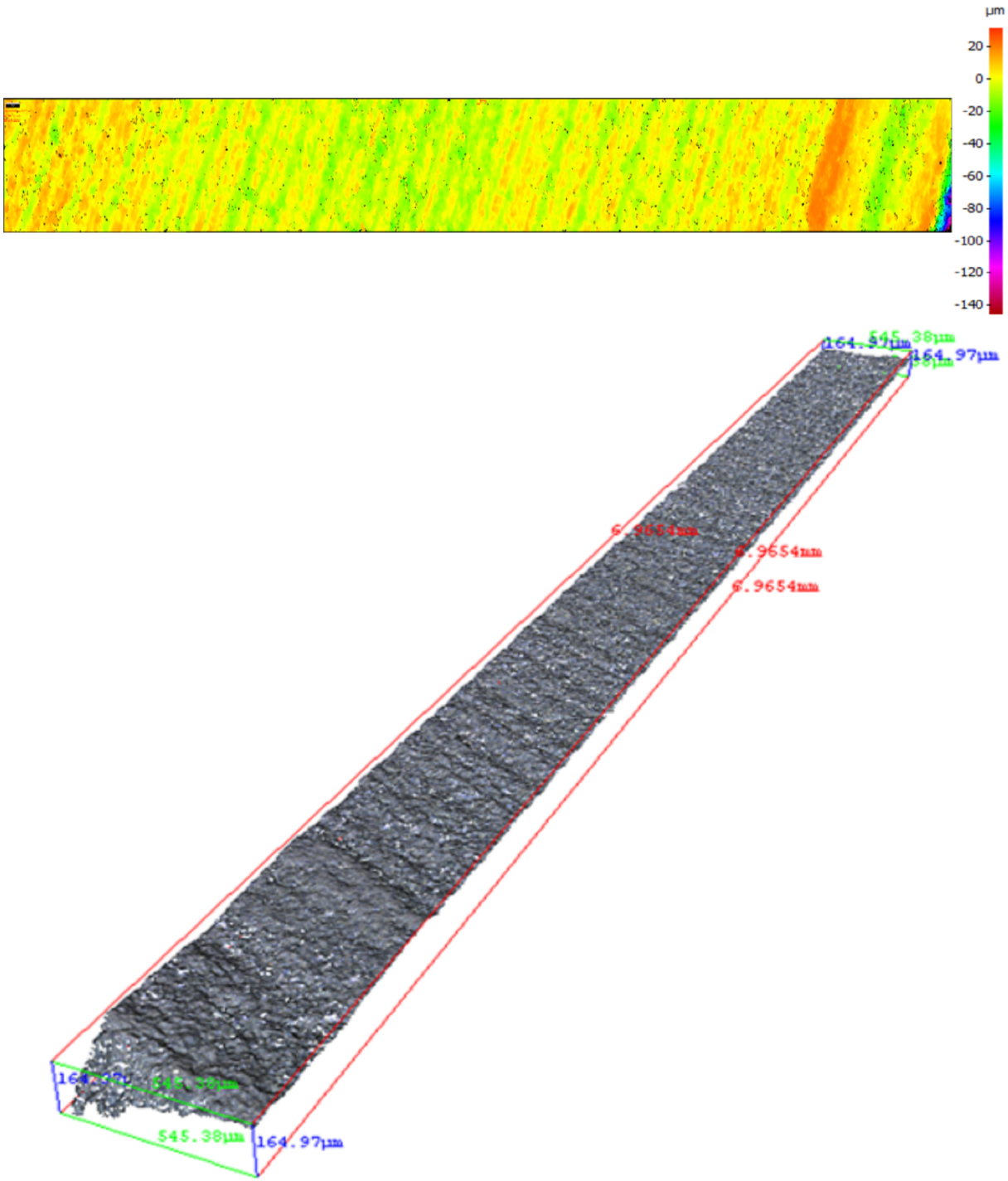

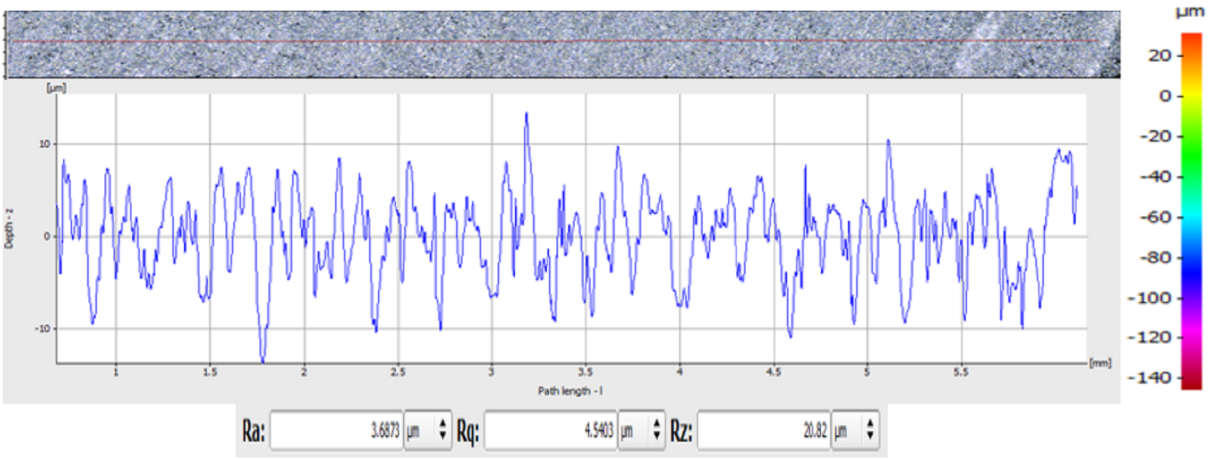
µm
20
0
-20
-40
-60
-80
-100
-120
-140
[µm]
10
0
-10
Depth - z
1
1.5
2
2.5
3
3.5
4
4.5
5
5.5
[mm]
Path length - l
Ra: 3.6873 µm
Rq: 4.5403 µm
Rz: 20.82 µm

A2: Full analysis from EPMA

In the two tables below the full analysis of the slag phase and the metal phase from the EPMA. There were chosen three random points on the surface of the slag and metal

Full analysis on the slag from EPMA

Test	Carbon	Slag	Holding time [min]	SiO_2 [%]	MgO [%]	MnO [%]	CaO [%]	Al_2O_3 [%]	FeO [%]	Total [%]
1.1	Coke	1	15	44.63	4.44	22.73	16.42	13.23	-	101.45
1.2				44.64	4.47	22.11	16.39	13.26	-	100.87
1.3				44.55	4.47	22.21	16.41	13.30	-	100.94
2.1	Coke	1	30	47.12	6.10	8.04	22.47	18.35	-	102.08
2.2				46.47	6.04	8.11	22.29	18.21	-	101.12
2.3				47.11	6.01	7.96	22.05	18.14	-	101.27
3.1	Coke	1	60	44.97	6.22	2.43	25.21	21.27	0.00	100.09
3.2				45.22	6.09	2.43	23.99	21.42	0.01	99.16
3.3				45.28	6.15	2.39	24.17	21.50	0.02	99.51
4.1	Coke	1	0	31.79	2.86	42.71	11.31	10.22	0.11	99.00
4.2				32.30	3.00	43.77	11.08	8.82	0.26	99.22
4.3				33.33	2.31	39.18	12.91	13.02	0.44	101.18
5.1	Coke	2	15	39.86	3.96	32.85	12.60	10.27	0.16	99.69
5.2				39.51	3.79	32.42	12.56	10.45	0.12	98.84
5.3				39.43	3.80	32.61	12.56	10.29	0.17	98.86
6.1	Coke	2	30	46.90	4.34	22.68	15.70	11.86	-	101.48
6.2				46.67	4.42	23.10	15.67	11.68	-	101.54
6.3				46.36	4.40	23.07	15.59	11.84	-	101.27
7.1	Coke	2	60	48.28	6.62	3.31	24.78	19.66	-	102.65
7.2				48.27	6.62	3.43	24.92	19.60	-	102.85
7.3				47.95	6.65	3.29	25.08	19.57	-	102.53
8.1	Coke	2	0	32.15	3.11	43.48	11.00	9.59	0.30	99.64
8.2				32.60	3.00	42.43	10.68	10.30	0.23	99.24
8.3				32.23	2.96	42.31	10.76	10.21	0.25	98.70
9.1	Charcoal	1	15	44.52	5.89	8.08	23.40	18.87	0.00	100.76
9.2				43.85	5.84	8.41	23.23	18.69	0.01	100.04
9.3				43.64	5.99	8.50	22.92	18.53	0.00	99.58
10.1	Charcoal	1	30	44.63	5.91	5.39	25.96	20.45	-	102.34
10.2				44.69	5.94	5.24	25.71	20.21	-	101.79
10.3				44.50	5.95	5.33	25.68	20.23	-	101.69
11.1	Charcoal	1	60	44.68	5.83	2.29	26.50	21.80	-	101.11
11.2				44.06	5.73	2.27	28.17	21.84	-	102.08
11.3				44.09	5.82	2.33	28.82	21.79	-	102.86
12.1	Charcoal	1	0	31.46	3.24	43.54	11.29	9.37	0.23	99.13
12.2				31.32	3.06	42.27	11.52	10.23	0.17	98.57
12.3				31.39	3.06	43.39	11.44	10.33	0.14	99.74

13.1	Charcoal	2	15	36.24	3.43	37.57	12.81	10.33	0.16	100.55
13.2				36.05	3.45	37.03	12.90	10.27	0.15	99.86
13.3				35.82	3.59	37.93	12.78	10.04	0.17	100.33
14.1	Charcoal	2	30	38.87	3.74	34.05	13.88	10.60	-	101.14
14.2				38.70	3.84	33.89	13.78	10.63	-	100.84
14.3				38.57	3.80	33.87	13.65	10.51	-	100.39
15.1	Charcoal	2	60	39.65	3.93	31.20	14.21	11.10	-	100.08
15.2				39.66	3.93	31.20	14.21	11.10	-	100.08
15.3				39.62	3.87	30.87	14.24	11.04	-	99.64
16.1	Charcoal	2	0	31.28	3.06	45.35	9.70	9.74	0.12	99.25
16.2				31.42	3.14	44.51	9.36	9.84	0.37	98.63
16.3				31.48	3.25	44.69	9.20	9.01	0.20	97.82
17.1	Coke	2	30	43.99	6.78	3.67	25.33	20.89	0.02	100.68
17.2				44.16	6.87	4.17	26.08	21.06	0.02	102.35
17.3				44.59	6.96	3.70	25.90	21.17	0.06	102.38
18.1	Coke	2	30	47.73	5.75	10.87	20.30	15.88	0.05	100.58
18.2				48.28	5.68	10.50	20.13	15.86	0.02	100.46
18.3				48.21	5.78	10.78	19.80	15.86	0.01	100.45
19.1	Charcoal	1	30	40.21	5.07	1.33	31.90	24.72	0.00	103.22
19.2				40.00	4.98	1.45	31.76	24.63	0.00	102.82
19.3				40.26	4.98	1.31	31.30	24.31	0.01	102.16
20.1	Charcoal	1	30	38.66	4.74	1.57	30.39	24.76	0.00	100.11
20.2				38.82	4.86	1.35	31.58	25.67	0.00	102.28
20.3				38.34	4.76	1.33	30.76	25.06	0.00	100.25
21.1	Charcoal	2	30	40.71	4.04	30.46	14.49	11.31	0.50	101.51
21.2				40.92	4.01	29.77	14.67	11.38	0.45	101.19
21.3				41.02	4.06	29.75	14.74	11.20	0.47	101.24
22.1	Charcoal	2	30	46.60	4.68	17.32	18.54	14.14	0.11	101.39
22.2				46.56	4.84	17.53	18.42	14.14	0.02	101.50
22.3				46.57	4.79	17.30	18.39	13.83	0.08	100.96
23.1	Coke	1	30	49.53	5.15	10.91	18.89	15.55	0.10	100.13
23.2				49.82	5.22	10.96	19.05	15.66	0.09	100.80
23.3				49.91	5.26	11.13	19.25	15.76	0.00	101.31
24.1	Coke	1	30	43.29	3.82	25.42	14.80	12.21	0.06	99.60
24.2				43.35	3.92	25.12	13.82	12.37	0.06	98.64
24.3				43.41	3.87	25.12	14.77	12.40	0.09	99.66
25.1	Charcoal	1	30	44.65	5.86	4.33	27.00	20.44	0.00	102.28
25.2				44.73	5.89	4.65	26.13	20.51	0.01	101.92
25.3				44.50	5.88	4.26	26.27	20.10	0.01	101.03

26.1	Charcoal	1	30	45.82	5.27	11.33	20.55	16.70	0.01	99.69
26.2				45.85	5.24	11.53	19.64	16.58	0.02	98.86
26.3				45.94	5.19	11.72	18.97	16.51	0.01	98.33
27.1	Charcoal	1	30	46.13	5.43	8.69	19.09	17.68	0.00	97.02
27.2				46.25	5.42	8.42	17.99	17.77	0.04	95.88
27.3				46.22	5.43	8.27	17.27	17.54	0.06	94.79
28.1	Graphite	1	30	43.85	4.73	17.38	18.59	15.14	0.06	99.75
28.2				43.57	4.72	16.77	18.12	15.07	0.02	98.26
28.3				43.37	4.82	16.97	18.32	15.14	0.08	98.69
29.1	Graphite	2	30	35.34	3.30	38.92	11.70	9.64	0.48	99.38
29.2				35.60	3.23	38.64	12.13	9.62	0.18	99.41
29.3				35.38	3.27	38.49	11.67	9.63	0.35	98.78
30.1	Charcoal	1	30	29.08	0.18	0.16	31.91	31.38	0.05	92.74
30.2				28.28	0.21	0.10	34.92	31.13	0.02	94.67
30.3				28.92	0.19	0.14	33.69	31.51	0.00	94.45
31.1	Charcoal	2	30	37.87	3.80	33.71	13.65	10.32	0.20	99.55
31.2				36.95	3.70	33.99	13.18	10.29	0.28	98.38
31.3				37.80	3.80	34.80	13.39	10.38	0.32	100.49

Full analysis on the metal phase from EPMA

Test	Carbon	Slag	Holding time [min]	Si [%]	Mn [%]	Fe [%]	Total [%]
1.1	Coke	1	15	6.38	39.35	55.85	101.58
1.2				6.08	38.83	57.43	102.34
1.3				5.99	37.96	58.22	102.17
2.1	Coke	1	30	16.25	87.29	3.69	107.23
2.2				17.13	87.59	3.65	108.37
2.3				17.48	87.09	3.76	108.33
3.1	Coke	1	60	16.50	32.94	54.19	103.63
3.2				17.97	34.20	50.68	102.85
3.3				18.74	34.72	50.33	103.79
4.1	Coke	1	0	0.08	16.98	80.84	97.89
4.2				0.01	16.26	82.03	98.29
4.3				0.05	16.61	81.34	98.00
5.1	Coke	2	15	1.53	34.45	63.58	99.56
5.2				1.29	35.64	62.62	99.56
5.3				1.61	34.91	63.33	99.86
6.1	Coke	2	30	5.98	33.06	62.37	101.41
6.2				5.88	33.26	61.92	101.07
6.3				6.06	33.35	62.65	102.05
7.1	Coke	2	60	10.70	9.71	79.97	100.38
7.2				11.05	8.75	81.22	101.02
7.3				11.83	8.16	80.66	100.65
8.1	Coke	2	0	-	-	-	-
9.1	Charcoal	1	15	16.06	91.30	0.67	108.02
9.2				16.11	92.35	0.73	109.19
9.3				15.89	91.01	0.75	107.66
10.1	Charcoal	1	30	15.43	45.86	44.18	105.46
10.2				14.06	44.55	45.59	104.20
10.3				13.69	49.34	42.16	105.19
11.1	Charcoal	1	60	16.67	41.91	46.10	104.67
11.2				17.86	42.85	43.88	104.59
11.3				17.40	41.34	46.65	105.39
12.1	Charcoal	1	0	-	-	-	-
13.1	Charcoal	2	15	0.22	28.87	70.80	99.89
13.2				0.23	28.24	70.44	98.91
13.3				0.30	28.56	70.18	99.03
14.1	Charcoal	2	30	-	-	-	-
15.1	Charcoal	2	60	0.04	7.10	88.39	95.53
15.2				0.08	7.06	87.98	95.13
15.3				0.10	6.74	89.08	95.91

16.1	Charcoal	2	0	0.03	20.55	77.67	98.26
16.2				0.05	21.24	76.94	98.23
16.3				0.03	20.07	78.37	98.47
17.1	Coke	2	30	18.04	53.38	33.74	105.15
17.2				11.73	55.25	38.22	105.20
17.3				18.72	53.45	34.18	106.35
18.1	Coke	2	30	13.56	43.34	47.95	104.85
18.2				13.85	43.56	47.51	104.92
18.3				13.25	45.34	45.53	104.12
19.1 (Light)	Charcoal	1	30	10.09	82.20	1.98	100.84
19.2 (Light)				9.92	82.19	2.03	100.74
19.3 (Light)				11.28	79.82	1.70	101.31
19.4 (Dark)	Charcoal	1	30	23.00	72.26	1.16	103.28
19.5 (Dark)				23.03	72.10	1.14	102.60
19.6 (Dark)				23.44	72.74	1.14	103.67
20.1	Charcoal	1	30	18.21	78.63	1.79	100.52
20.2				19.06	78.24	1.83	100.99
20.3				19.07	76.96	2.12	99.96
21.1	Charcoal	2	30	-	-	-	-
22.1	Charcoal	2	30	-	-	-	-
23.1	Coke	1	30	-	-	-	-
24.1	Coke	1	30	4.05	39.43	58.12	101.59
24.2				4.24	38.61	58.13	100.97
24.3				4.17	38.99	59.09	102.25
25.1	Charcoal	1	30	19.62	80.31	1.47	102.53
25.2				19.53	80.99	1.41	103.19
25.3				19.29	80.53	1.42	102.38
26.1	Charcoal	1	30	13.63	89.22	4.56	107.40
26.2				13.68	89.87	4.58	108.13
26.3				13.67	89.81	4.57	108.05
27.1	Charcoal	1	30	11.76	43.12	49.70	104.58
27.2				11.59	44.84	48.22	104.65
27.3				11.93	43.73	48.14	103.81
28.1	Graphite	1	30	9.77	61.74	32.91	104.42
28.2				10.36	61.57	33.21	105.14
28.3				10.58	61.59	33.41	105.58

29.1	Graphite	2	30	0.04	10.13	87.05	97.22
29.2				0.04	10.10	87.12	97.27
29.3				0.05	10.26	87.60	97.91
30.1	Charcoal	1	30	11.69	54.19	38.78	104.66
30.2				12.78	48.39	43.51	104.68
30.3				13.06	48.64	44.34	106.03
31.1	Charcoal	2	30	0.05	11.95	85.56	97.56
31.2				0.01	12.30	84.79	97.11
31.3				0.08	12.02	85.12	97.21

Benjamin Dale Hosum

Reduction Rate of SiMn Slags With Different Carbon Materials

NTNU
Norwegian University of
Science and Technology